



## **Schistosoma mansoni extracellular vesicles and their impact on the immune system: glycosylated messengers in host-pathogen communication**

Kuipers, M.E.

### **Citation**

Kuipers, M. E. (2024, September 25). *Schistosoma mansoni extracellular vesicles and their impact on the immune system: glycosylated messengers in host-pathogen communication*. Retrieved from <https://hdl.handle.net/1887/4092867>

Version: Publisher's Version

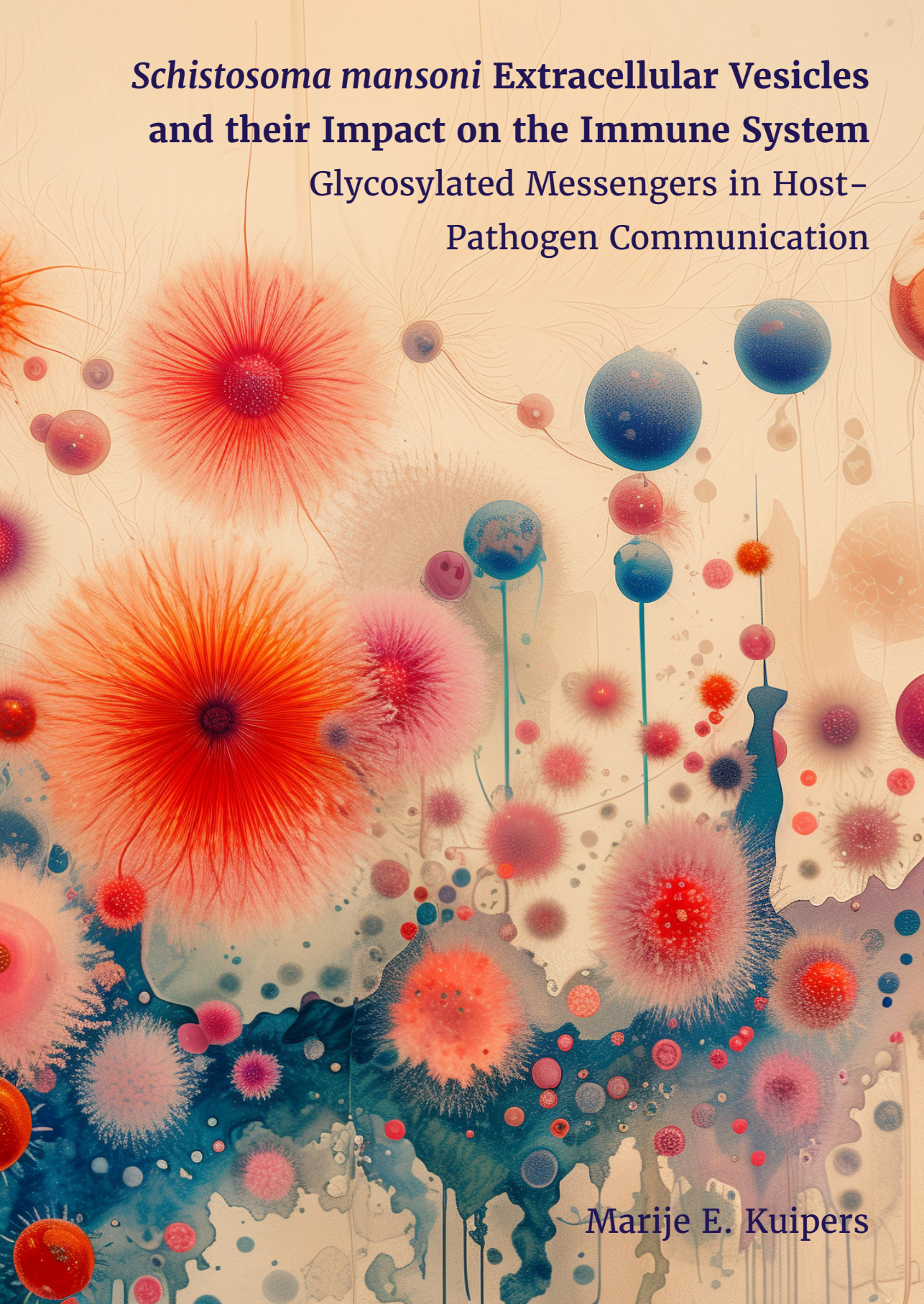
[Licence agreement concerning inclusion of doctoral thesis in the Institutional Repository of the University of Leiden](#)

License: <https://hdl.handle.net/1887/4092867>

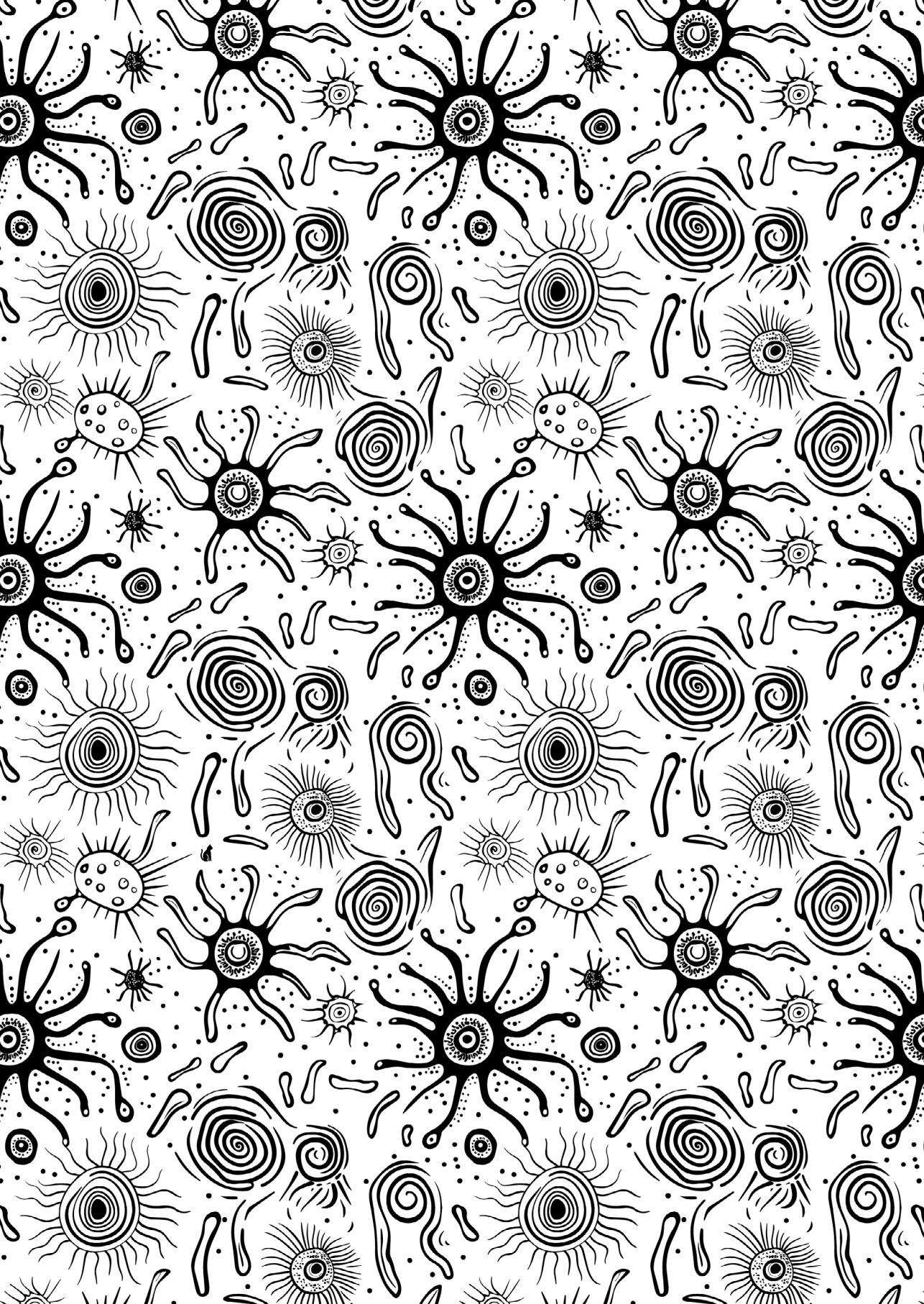
**Note:** To cite this publication please use the final published version (if applicable).

# *Schistosoma mansoni* Extracellular Vesicles and their Impact on the Immune System

## Glycosylated Messengers in Host- Pathogen Communication

The background of the poster is a detailed, abstract illustration of biological cells and extracellular vesicles. It features large, red, spiky structures resembling dandelion seeds or viruses, interspersed with smaller, blue and red spherical vesicles. Some vesicles are shown budding from larger cells, and others are suspended in the space. The overall composition is organic and dynamic, suggesting a complex biological environment.

Marije E. Kuipers



***Schistosoma mansoni* Extracellular Vesicles  
and their Impact on the Immune System:  
Glycosylated Messengers in  
Host-Pathogen Communication**

Marije E. Kuipers

ISBN: 978-94-6506-287-7  
Printing: Ridderprint | [www.ridderprint.nl](http://www.ridderprint.nl)

Cover image and chapter images were created using the Midjourney web app.  
Some figures in this thesis have been made by using Servier Medical Art, provided by Servier,  
licensed under a Creative Commons Attribution 3.0 unported license.

© Marije E. Kuipers 2024

All rights reserved. No part of this publication may be reproduced, stored in a retrieval system, or transmitted in any form or by any means, electronic, mechanical, by photocopying, recording, or otherwise, without prior written permission of the author.

The work described in this thesis was performed at the department of Parasitology (now LUCID) at the Leiden University Medical Center, Leiden, the Netherlands, and the department of Biomolecular Health Sciences at the Faculty of Veterinary Medicine at Utrecht University, Utrecht, the Netherlands. The work was supported by a grant from the Board of Directors of the Leiden University Medical Center and by the graduate program of the Dutch Research Council (NWO) (both awarded to M.E. Kuipers).

***Schistosoma mansoni* Extracellular Vesicles  
and their Impact on the Immune System:  
Glycosylated Messengers in  
Host-Pathogen Communication**

Proefschrift

ter verkrijging van  
de graad van doctor aan de Universiteit Leiden,  
op gezag van rector magnificus prof.dr.ir. H. Bijl,  
volgens besluit van het college voor promoties  
te verdedigen op woensdag 25 september 2024

klokke 10.00 uur

door

Marije Erline Kuipers  
geboren te Haarlem  
in 1986

**Promotoren:** prof.dr. C.H. Hokke  
prof.dr. H.H. Smits

**Co-promotor:** dr. E.N.M. Nolte-‘t Hoen (Utrecht University)

**Leden promotiecommissie:** prof.dr. M.J.T.H. Goumans  
prof.dr. T.H.M. Ottenhoff  
dr. A.G. van der Veen  
prof.dr. G.J.P.H. Boons (Utrecht University)  
prof.dr. K.R. Hoffmann (Aberystwyth University, UK)

voor papa



## Table of contents

Chapter 1	General introduction	9
Chapter 2	Pathogen-derived extracellular vesicle-associated molecules that affect the host immune system: an overview	23
Chapter 3	Optimized protocol for the isolation of extracellular vesicles from the parasitic worm <i>Schistosoma mansoni</i> with improved purity, concentration, and yield	49
Chapter 4	Life stage-specific glycosylation of extracellular vesicles from <i>Schistosoma mansoni</i> schistosomula and adult worms drives differential interaction with C-type lectin receptors DC-SIGN and MGL	71
Chapter 5	Extracellular vesicles from <i>Schistosoma mansoni</i> adult worms stimulate IL-10 release by B cells	101
Chapter 6	DC-SIGN mediated internalisation of glycosylated extracellular vesicles from <i>Schistosoma mansoni</i> increases activation of monocyte-derived dendritic cells	129
Chapter 7	Summarizing discussion and future perspectives	163
Appendices	Popular science summary (English & Dutch)	198
	Nederlandse samenvatting voor niet-ingewijden	199
	Curriculum Vitae	208
	List of publications	210
	Dankwoord/acknowledgements	212



"We're all here to do what we're all here to do. I'm only interested in one thing, Neo, the future. And believe me, I know – the only way to get there is together."  
- The Oracle (from The Matrix, 1999)

# Chapter 1

## General introduction

# Introduction

## ***Schistosoma* and host immune modulation**

The parasitic trematode (flatworm) *Schistosoma* (*S.*) spp. affects over 250 million people in poor, rural communities of the tropics and subtropics, especially where access to safe drinking water and adequate sanitation is lacking<sup>1</sup>. Once *S. mansoni* worms establish their residence in the blood vessels of the hepatic portal system (see Figure 1 for the full life-cycle), they can persist there for many years or even decades<sup>2</sup>. This demonstrates that schistosomes have a remarkable capacity to evade both humoral and cellular immune responses. Because parasitic worms (also called helminths) have co-evolved with humanity, they have developed evasion mechanisms alongside the maturation of human innate and adaptive immune responses, which makes them experts in immune modulation<sup>3</sup>.

The skin invasion of the cercariae, the infectious larvae of *Schistosoma*, will trigger keratinocytes to release damage-associated molecular patterns (DAMPs). Together with the pathogen-associated molecular patterns (PAMPs) of the parasite itself, these DAMPs will activate the first line of defense of the immune system. Cells such as monocytes, macrophages and dendritic cells (DCs) can recognize DAMPs and PAMPs via their pattern recognition receptors (PRRs), which include Toll-like receptors (TLRs) and C-type lectin receptors (CLRs)<sup>3</sup>. The skin penetration of the schistosomula leads to infiltration of polymorphonuclear cells (e.g. neutrophils, eosinophils) and mononuclear cells (e.g. monocytes, macrophages, DCs) and a local release of pro-inflammatory and anti-inflammatory cytokines<sup>4</sup>. This initial phase of infection (up to week 8) includes responses that characterize T helper 1 (Th1), Th2, and regulatory profiles<sup>5-7</sup>. An important manner in which the schistosomula elicit these immune responses, is via the release of excretory/secretory (ES) products<sup>8</sup>. Additional immune evasion strategies of the schistosomula includes expression of enzymes that can degrade DAMPs and compositional changes in their outer membrane to evade complement activation<sup>9</sup>.

Once matured into adult worms, the immune responses observed shift towards a dominant Th2 response. This is mostly caused by the worms' production of eggs and the egg ES components, such as omega-1<sup>10</sup>. However, single-sex infections in mice have shown that adult worms can also induce Th2 skewing before deposition of eggs<sup>11</sup>. Eventually, when the infection becomes chronic (>12 weeks), the Th2 reactivity to the parasite decreases. This Th2 dampening is suggested to be attributed by the production of anti-inflammatory cytokines by regulatory T cells (Tregs) and B (Breg) cells, and macrophages, and induced T cell anergy by alternatively activated macrophages<sup>12</sup>. Adult worm extracts are able to induce pro- and anti-inflammatory responses by immune cells isolated from chronically

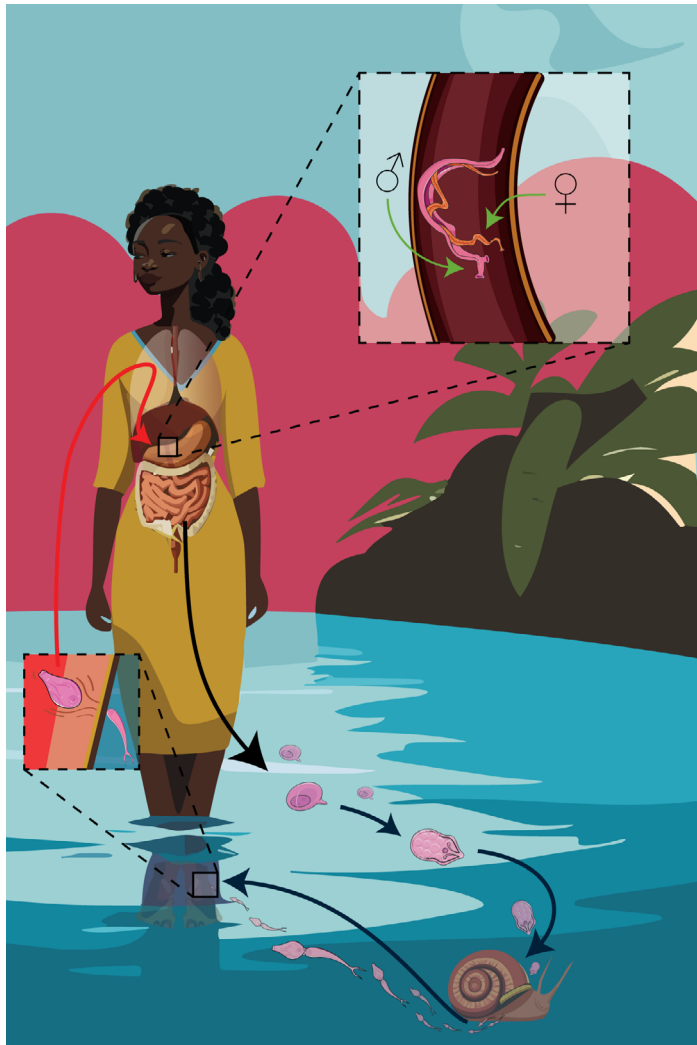


**Figure 1. Life Cycle of schistosomes.**

The intermediate host of this parasites, a freshwater snail, releases larvae (cercariae) into the water, which can infect the human host via skin penetration. Once inside, these cercariae will transform into juvenile worms that are called schistosomula. The schistosomula will migrate in the bloodstream towards the liver, where they will dwell in the hepatic portal vein and surrounding blood vessels. The eggs produced by the females of the dioecious worm pairs leave the body via the feces (*S. mansoni* and *S. japonicum*) or urine (*S. haematobium*) so that the larvae inside the egg, the miracidium, can be released upon fresh water contact and infect a snail host again. However, not all eggs find their way out, and if not, they can cause a major immunological response and organ damage, which is the basis of schistosomiasis pathology that can end up killing the host.

infected mice<sup>13</sup> and infected humans<sup>7</sup>, but there is limited data on actively released adult worm ES products that affect cytokine production by host immune cells directly<sup>14</sup>. Like the schistosomula, the adult worm ES contains many other factors to sustain life in their host by promoting anti-coagulation, reduction of oxidative stress, and complement degradation<sup>3,8</sup>.

Thus, schistosomes, like other helminth, are able to modulate immune mechanisms in the host. The alteration of pro-inflammatory responses and enhancement of the regulatory immune network can temper overreactive immunity. Notably, with the disappearance of most parasitic infections in industrialized countries, the incidence of inflammatory disorders and allergies in these countries simultaneously increased<sup>15</sup>. This observation gave rise to the “hygiene hypothesis” or “old friends hypothesis”, which suggests that altered early-life exposure to microbes and/or helminths impacts the training of the regulatory arm of the immune system<sup>16-19</sup>. Indeed, many rural helminth-endemic areas have a low incidence of allergic and auto-immune disorders, but this is not consistent in urbanized areas, suggesting the influence of yet different environmental factors<sup>17,18,20</sup>. The host may rely on parasite-induced immunomodulation for a balanced immune development, but whether this is sufficient to prevent the onset of immune-mediated diseases depends on various factors, such as the parasite species, environmental conditions, and host characteristics (e.g. genetics)<sup>21</sup>. Therefore, understanding the strategies of immune modulation by helminths on the molecular level can aid in the development of novel treatments for immunopathologies without the harmful consequences associated with parasitic infections.

To date, there is an increase in knowledge on the molecular mechanisms of immune modulation by ES components released by *Schistosoma*<sup>14</sup>. Extracellular vesicles (EVs) are constituents of the parasites’ ES and it is expected that EVs also play a role in host immune modulation, a function that has been attributed to EVs from other helminths<sup>22</sup>.

## Extracellular vesicles released by schistosomes

Almost all cells of eukaryotes and prokaryotes release EVs<sup>23</sup>. EVs are generally 50-200 nm sized vesicles enclosed by a phospholipid-bilayer membrane and contain various molecules, including (glyco)proteins, (glyco)lipids, metabolites, and nucleic acids. There are two major EV biogenesis pathways: they can be formed by inward budding of multivesicular bodies (MVBs) inside the cell and released after fusion of the MVB with the plasma membrane; and EVs can be released into the extracellular space by budding off the plasma membrane itself (Figure 2, left panel)<sup>24</sup>. Their molecular composition is highly heterogenous, differs per cell type,

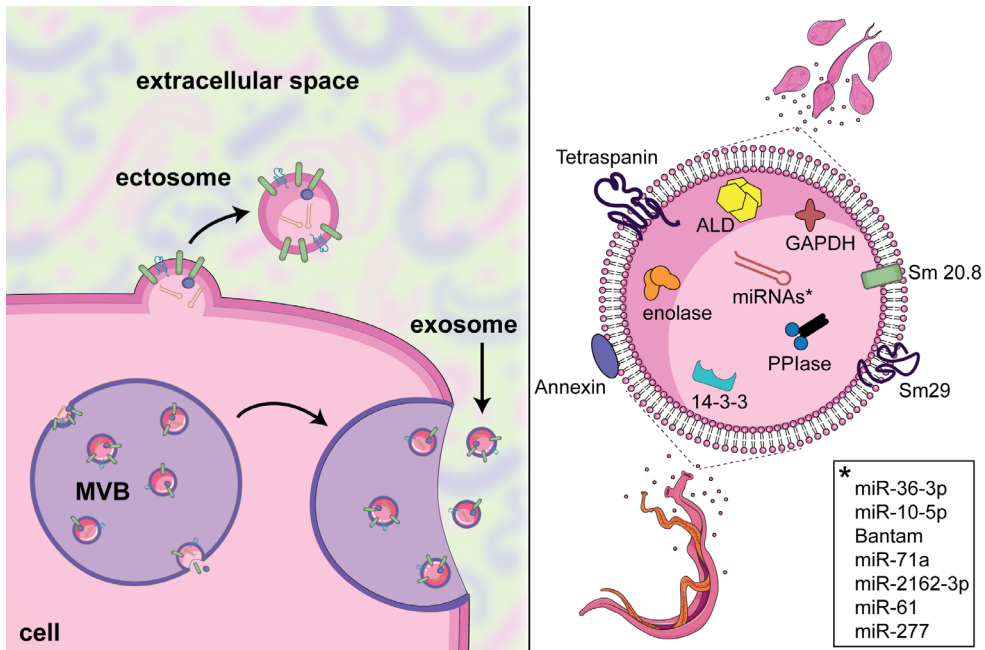


**Figure 2. Release of EVs from *S. mansoni* schistosomula and adult worms.**

Left panel: schematic overview of EV release by a cell. Exosomes are formed by inward budding of a multivesicular body (MVB) inside the cell and are released after fusion of the MVB with the plasma membrane. Ectosomes or microvesicles are released into the extracellular space by budding off the plasma membrane. EVs is an umbrella term for all vesicles released in the extracellular space.

Right panel: Selection of most frequent reported proteins and RNAs associated with EVs released by *S. mansoni* schistosomula and adult worms<sup>30–33,62</sup>. ALD, Fructose-bisphosphate aldolase; GAPDH, Glyceraldehyde-3-phosphate dehydrogenase; PPIase, Peptidyl-prolyl cis-trans isomerase.

and depends on the current status (e.g. cell cycle stage, environmental conditions, stress) of the EV-releasing cell. This heterogeneity and their small size makes EVs technically challenging to study. Thus far, many efforts have been made in the mammalian EV field to optimize EV isolation protocols to separate them from equally sized lipoprotein particles and non-EV particles, such as large protein complexes<sup>23</sup>. The three most commonly used EV isolation/separation techniques are differential centrifugation followed by ultra centrifugation with speeds above  $100,000 \times g$ , size exclusion chromatography (SEC), and density gradients<sup>25</sup>. In general, obtaining a highly pure EV population requires multiple steps that result in a low EV yield, which will limit following applications to study EV characteristics

1

and/or function. Yet, there is no golden standard and overall each EV population of interest and research question might require different technical approaches<sup>23</sup>.

EVs play a role in cell-to-cell communication by transferring their contents to other cells on both local and systemic levels<sup>26</sup>. In mammals, EVs are involved in many processes and have the ability of regulating immune responses<sup>27</sup>. In the last decade, EVs have emerged as a compelling communication mechanism between parasites and their host<sup>28,29</sup>. Thus far, proteome and transcriptome studies have been reported of EVs released by *S. mansoni* schistosomula<sup>30</sup> and adult worms<sup>31-33</sup> (Figure 2, right panel), *S. japonicum* adult worms<sup>34-37</sup> and eggs<sup>38</sup>, and *S. haematobium* adult worms<sup>39</sup>. In addition, one lectin microarray study showed that adult worm EVs from *S. mansoni* contain glycans<sup>40</sup>. Yet, there is little literature on the direct effect of schistosome EVs on immune cells<sup>22</sup>. Thus far, crude EV pellets of *S. japonicum* adult worm EVs skewed macrophages towards an M1 phenotype<sup>34</sup> and interacted with peripheral blood derived monocytes and T cells<sup>36</sup>. For *S. mansoni*, adult worm derived EVs are shown to be taken up by a monocyte cell line, but there is no report on subsequent immune responses<sup>41</sup>. *S. mansoni* EVs and EV-associated molecules are also explored *in vivo* as vaccination strategy against schistosomes<sup>42,43</sup>. There currently is no effective vaccine to prevent schistosomiasis and utilization of EVs may reveal additional insights<sup>44</sup>. Thus far, immunization of mice with *S. mansoni* egg EVs was shown to reduce worm and egg burden after challenge with cercariae<sup>45</sup>. In addition, vaccination with recombinant Tetraspanin (TSPs) proteins, abundant proteins in adult worm EVs<sup>31,33</sup>, reduced egg burden in mice after challenge<sup>39</sup>. These studies provide evidence that schistosome EVs influence host immunity, but the exact mechanisms or cells involved remain unknown.

### ***S. mansoni* glycoconjugates and lectin receptors**

An important part of the immune modulation by schistosomes is *via* their ligation of glycosylated ES products to CLRs or other glycan-binding proteins (lectins). CLRs constitute a large family of proteins that have a carbohydrate recognition domain (CRD) which predominantly depends on calcium ( $\text{Ca}^{2+}$ ) for binding their glycan ligand<sup>46</sup>. The ligands for lectins can be N-linked (carbohydrate chain is attached to Asn) or O-linked (carbohydrate chain is attached to Ser/Thr) glycans of glycoproteins, or glyco(sphingo)lipids (glycan attached to ceramide). CLRs are often expressed on antigen presenting cells (APCs), such as DCs, to discriminate between non-self, altered self (e.g. tumors) and self<sup>47</sup>. On these APCs, CLR activation by PAMPs can influence adaptive immunity *via* direct activation of signaling pathways or through crosstalk with other PRRs, in which activated signaling pathways can be glycan-specific<sup>48</sup>. Furthermore, CLRs can mediate endocytosis and internalize (glycosylated) molecules for processing towards the

antigen loading machinery<sup>49</sup>. CLRs may recognize glycans that are pathogen specific but can also bind to glycan structures found in both pathogens and mammalian cells<sup>50</sup>.

Schistosomes have a conserved glycosylation machinery that is similar to other multicellular organisms<sup>51</sup>. Their glycans are constructed from the same monosaccharides as their mammalian host, with the exception of sialic acids, which are abundant in mammalian, but lacking from helminth glycans<sup>52</sup>. Schistosome-derived glycans include both motifs that are rarely observed within mammals (e.g. fucosylation of terminal GalNAc $\beta$ 1-4GlcNAc (LacDiNAc or LDN) and/or unusual core modifications that are common in plants<sup>52</sup>) or that are expressed in their mammalian host more commonly, but in specific organs or cells (e.g. Gal $\beta$ 1-4(Fuc $\alpha$ 1-3)GlcNAc (Lewis X or Le $X$ ))<sup>47</sup>. Detailed mass spectrometry analyses have revealed the glycan motifs expressed in each life stage of *S. mansoni*<sup>53</sup>. However, most studies on schistosome-CLR interaction have been performed with egg-derived soluble antigens (SEA), which contain many glycosylated proteins<sup>54</sup>. For example, egg-derived glycoprotein omega-1 is internalized by monocyte-derived DCs (moDCs) via the mannose receptor (MR)<sup>55</sup>. Previous reports have illustrated that glycans on ES components released by cercariae/schistosomula can bind to the MR<sup>56</sup> and DC-SIGN<sup>57</sup> (Figure 3). Adult worm-derived glycans, mainly structures containing a terminal LDN motif, have been shown to bind to macrophage galactose-type lectin (MGL)<sup>58</sup>, soluble Galectin-3<sup>59</sup>, and the mouse homologue of DC-SIGN<sup>60</sup>. Still, in most of these studies on adult worm- and schistosomula-derived glycans, subsequent immune responses upon CLR binding were not investigated.

## Glycosylation of schistosome EVs and their interaction with immune cells: the knowledge gap and thesis outline

Helminth released EVs form a relatively young field of research<sup>28</sup>, as well as EV glycosylation<sup>61</sup>. Schistosomes release EVs, but there is limited to no knowledge on their glycosylation<sup>40</sup>, their interaction with immune cells<sup>22</sup>, and how host immune cells respond to this interaction. In this thesis, we aim to elucidate the glycosylation of EVs released by *S. mansoni* schistosomula and adult worms. Additionally, we explore the interaction of these EVs with CLRs. Subsequently, we study the effects these EVs have on host immune cells and their cytokine responses. To investigate EV-associated glycans and their functionality, we also had to overcome methodological challenges in EV isolation.

Chapter 2 is a narrative review, outlining the current understanding of immune modulation by pathogen EV-associated molecules, including EVs from parasites, bacteria, and fungi. In Chapter 3, we set out experiments to optimize the protocol

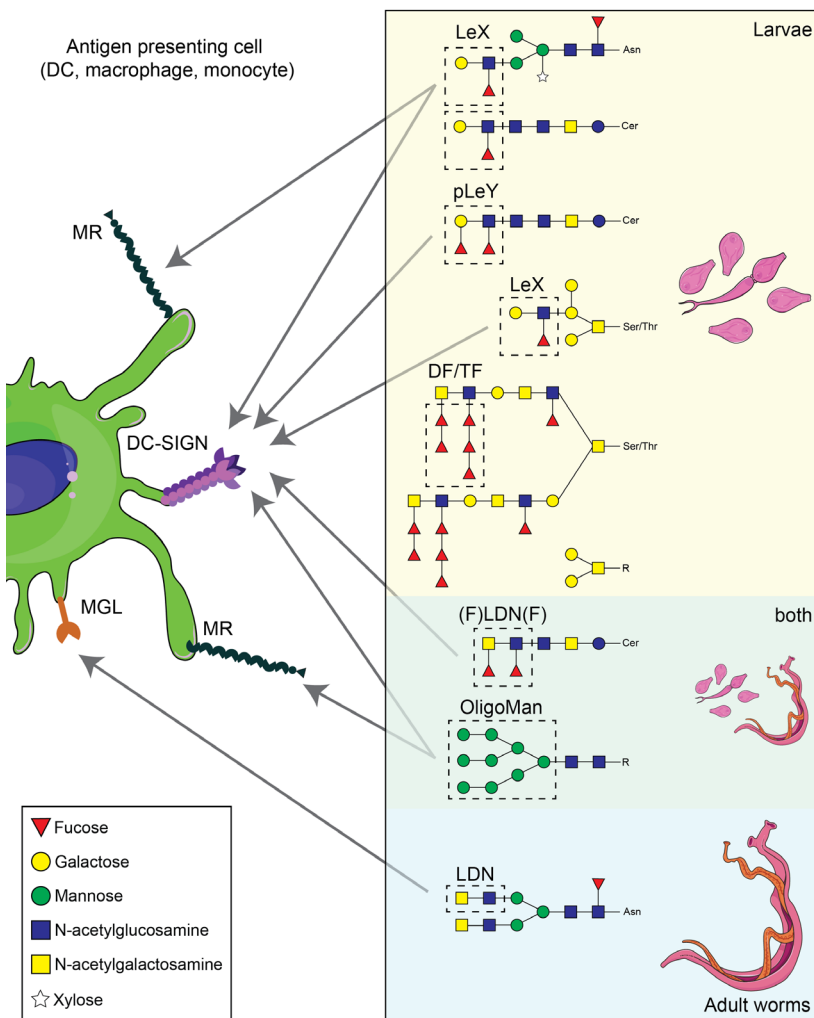


**Figure 3 – Examples of major glycan motifs found in larvae (cercariae/ schistosomula) and adult worms and possible interactions of these structures with host C-type lectin receptors on human antigen presenting cells.**

Le<sup>X</sup> (Lewis X, Gal $\beta$ 1-4(Fuc $\alpha$ 1-3)GlcNAc-), pLe<sup>Y</sup> (pseudo Lewis Y, Fuc $\alpha$ 1-3Gal $\beta$ 1-4(Fuc $\alpha$ 1-3)GlcNAc-), F-LDN-F (Fuc $\alpha$ 1-3GalNAc $\beta$ 1-4(Fuc $\alpha$ 1-3)GlcNAc $\beta$ 1-), and OligoMan (Oligomannoside, Man<sub>9</sub>GlcNAc<sub>2</sub>) motifs can be recognized by DC-SIGN<sup>48,63,64</sup>. Oligomannoside and LeX (less strongly) can bind to the MR<sup>56</sup>. LDN (LacDiNAc, GalNAc $\beta$ 1-4GlcNAc $\beta$ 1-) is a ligand for the MGL<sup>58</sup>. Glycan overview adapted from Hokke & van Diepen<sup>52</sup>. DF/TF; Fuc $\alpha$ 1-2Fuc $\alpha$ 1-3-/ Fuc $\alpha$ 1-2Fuc $\alpha$ 1-2Fuc $\alpha$ 1-3-; DC, dendritic cell; MR, mannose receptor; DC-SIGN, dendritic cell-specific intercellular adhesion molecule-3-grabbing non-integrin; MGL, macrophage galactose-type lectin.

for the isolation and purification of EVs from *Schistosoma* adult worms, using density gradients as opposed to SEC. In the context of a limited availability of parasites, we also study the influence of density gradient volume on the overall amount of isolated EVs. Next, in **Chapter 4**, we characterize the glycan profile of adult worm EVs in detail by mass spectrometry. We compare the adult worm EV-associated glycans to the glycan motifs associated with schistosomula EVs. In addition, we investigate whether differences in glycosylation between adult worm and schistosomula EVs have consequences for the interaction of these EVs with CLRs MGL and DC-SIGN. In **Chapter 5** we explore the effect of adult worm ES and EVs on the induction of cytokine release (i.e. both IL-10 and IL-6) by B cells *in vitro*. This study includes both mouse splenic B cells as well as human peripheral blood B cells. The direct interaction of EVs with the B cells is investigated by microscopy using an EV-associated *Schistosoma* tetraspanin protein. Finally, **Chapter 6** addresses the ability of schistosomula EVs to activate human moDCs. In addition, this chapter describes mass spectrometry characterization of schistosomula EV-associated protein and lipid glycans. We furthermore investigate the role of EV-associated glycans on schistosomula EVs in the interaction with the C-type lectin receptor DC-SIGN on moDCs. In conclusion, **Chapter 7** summarizes and discusses the main findings of this thesis and includes suggestions for future research on *Schistosoma* EVs to elucidate EV-mediated pathogen-host communication.

## References

1. Schistosomiasis. <https://www.who.int/news-room/fact-sheets/detail/schistosomiasis>.
2. Wilson, R. A. & Jones, M. K. Fifty years of the schistosome tegument: discoveries, controversies, and outstanding questions. *International Journal for Parasitology* **51**, 1213–1232 (2021).
3. Maizels, R. M., Smits, H. H. & McSorley, H. J. Modulation of Host Immunity by Helminths: The Expanding Repertoire of Parasite Effector Molecules. *Immunity* **49**, 801–818 (2018).
4. Jenkins, S. J., Hewitson, J. P., Jenkins, G. R. & Mountford, A. P. Modulation of the host's immune response by schistosome larvae. *Parasite Immunol* (2005).
5. Pearce, E. J. & MacDonald, A. S. The immunobiology of schistosomiasis. *Nat Rev Immunol* **2**, 499–511 (2002).
6. Langenberg, M. C. C. *et al.* A controlled human *Schistosoma mansoni* infection model to advance novel drugs, vaccines and diagnostics. *Nat Med* **26**, 326–332 (2020).
7. Koopman, J. P. R. *et al.* Safety and infectivity of female cercariae in *Schistosoma*-naïve, healthy participants: a controlled human *Schistosoma mansoni* infection study. *eBioMedicine* **97**, (2023).
8. Skelly, P. J. & Da'dara, A. A. Schistosome secretomes. *Acta Trop* **236**, 106676 (2022).
9. Hambrook, J. R. & Hanington, P. C. Immune Evasion Strategies of Schistosomes. *Front Immunol* **11**, 624178 (2020).
10. Everts, B. *et al.* Omega-1, a glycoprotein secreted by *Schistosoma mansoni* eggs, drives Th2 responses. *J Exp Med* **206**, 1673–1680 (2009).
11. de Oliveira Fraga, L. A., Torrero, M. N., Tocheva, A. S., Mitre, E. & Davies, S. J. Induction of Type 2 Responses by Schistosome Worms during Prepatent Infection. *The Journal of Infectious Diseases* **201**, 464–472 (2010).
12. Fairfax, K., Nascimento, M., Huang, S. C.-C., Everts, B. & Pearce, E. J. Th2 responses in schistosomiasis. *Semin Immunopathol* **34**, 863–871 (2012).
13. Sombetzki, M. *et al.* A one-year unisexual *Schistosoma mansoni* infection causes pathologic organ alterations and persistent non-polarized T cell-mediated inflammation in mice. *Frontiers in Immunology* **13**, (2022).
14. Acharya, S., Da'dara, A. A. & Skelly, P. J. Schistosome immunomodulators. *PLoS Pathog* **17**, e1010064 (2021).
15. Maizels, R. M. Regulation of immunity and allergy by helminth parasites. *Allergy* **75**, 524–534 (2020).
16. Maizels, R. M., McSorley, H. J. & Smyth, D. J. Helminths in the hygiene hypothesis: sooner or later? *Clin Exp Immunol* **177**, 38–46 (2014).
17. Liu, A. H. Revisiting the hygiene hypothesis for allergy and asthma. *Journal of Allergy and Clinical Immunology* **136**, 860–865 (2015).
18. Versini, M. *et al.* Unraveling the Hygiene Hypothesis of helminthes and autoimmunity: origins, pathophysiology, and clinical applications. *BMC Medicine* **13**, 81 (2015).
19. Apostol, A. C., Jensen, K. D. C. & Beaudin, A. E. Training the Fetal Immune System Through Maternal Inflammation—A Layered Hygiene Hypothesis. *Frontiers in Immunology* **11**, (2020).

20. Santiago, H. C. & Nutman, T. B. Human Helminths and Allergic Disease: The Hygiene Hypothesis and Beyond. *Am J Trop Med Hyg* **95**, 746–753 (2016).
21. McSorley, H. J., Chayé, M. A. M. & Smits, H. H. Worms: Pernicious parasites or allies against allergies? *Parasite Immunology* **41**, e12574 (2019).
22. Drurey, C. & Maizels, R. M. Helminth extracellular vesicles: Interactions with the host immune system. *Mol Immunol* **137**, 124–133 (2021).
23. Théry, C. et al. Minimal information for studies of extracellular vesicles 2018 (MISEV2018): a position statement of the International Society for Extracellular Vesicles and update of the MISEV2014 guidelines. <https://doi.org/10.1080/20013078.2018.1535750> **7**, (2018).
24. van Niel, G., D'Angelo, G. & Raposo, G. Shedding light on the cell biology of extracellular vesicles. *Nat Rev Mol Cell Biol* **19**, 213–228 (2018).
25. Royo, F., Théry, C., Falcón-Pérez, J. M., Nieuwland, R. & Witwer, K. W. Methods for Separation and Characterization of Extracellular Vesicles: Results of a Worldwide Survey Performed by the ISEV Rigor and Standardization Subcommittee. *Cells* **9**, 1955 (2020).
26. Kalluri, R. & LeBleu, V. S. The biology, function, and biomedical applications of exosomes. *Science* **367**, eaau6977 (2020).
27. Robbins, P. D. & Morelli, A. E. Regulation of immune responses by extracellular vesicles. *Nat Rev Immunol* **14**, 195–208 (2014).
28. White, R. et al. Special considerations for studies of extracellular vesicles from parasitic helminths: A community-led roadmap to increase rigour and reproducibility. *J Extracell Vesicles* **12**, e12298 (2023).
29. Fernandez-Becerra, C. et al. Guidelines for the purification and characterization of extracellular vesicles of parasites. *Journal of Extracellular Biology* **2**, e117 (2023).
30. Nowacki, F. C. et al. Protein and small non-coding RNA-enriched extracellular vesicles are released by the pathogenic blood fluke *Schistosoma mansoni*. *J Extracell Vesicles* **4**, 28665 (2015).
31. Sotillo, J. et al. Extracellular vesicles secreted by *Schistosoma mansoni* contain protein vaccine candidates. *Int J Parasitol* **46**, 1–5 (2016).
32. Samoil, V. et al. Vesicle-based secretion in schistosomes: Analysis of protein and microRNA (miRNA) content of exosome-like vesicles derived from *Schistosoma mansoni*. *Sci Rep* **8**, 3286 (2018).
33. Kifle, D. W. et al. Proteomic analysis of two populations of *Schistosoma mansoni*-derived extracellular vesicles: 15k pellet and 120k pellet vesicles. *Mol Biochem Parasitol* **236**, 111264 (2020).
34. Wang, L. et al. Exosome-like vesicles derived by *Schistosoma japonicum* adult worms mediates M1 type immune-activity of macrophage. *Parasitol Res* **114**, 1865–1873 (2015).
35. Zhu, L. et al. Molecular characterization of *S. japonicum* exosome-like vesicles reveals their regulatory roles in parasite-host interactions. *Sci Rep* **6**, 25885 (2016).
36. Liu, J. et al. *Schistosoma japonicum* extracellular vesicle miRNA cargo regulates host macrophage functions facilitating parasitism. *PLoS Pathog* **15**, e1007817 (2019).
37. Du, P. et al. Proteomic and deep sequencing analysis of extracellular vesicles isolated from adult male and female *Schistosoma japonicum*. *PLOS Neglected Tropical Diseases* **14**, e0008618 (2020).

1

38. Zhu, S. *et al.* Release of extracellular vesicles containing small RNAs from the eggs of *Schistosoma japonicum*. *Parasit Vectors* **9**, 574 (2016).
39. Mekonnen, G. G. *et al.* *Schistosoma haematobium* Extracellular Vesicle Proteins Confer Protection in a Heterologous Model of Schistosomiasis. *Vaccines (Basel)* **8**, (2020).
40. Dagenais, M. *et al.* Analysis of *schistosoma mansoni* extracellular vesicles surface glycans reveals potential immune evasion mechanism and new insights on their origins of biogenesis. *Pathogens* **10**, (2021).
41. Kifle, D. W. *et al.* Uptake of *Schistosoma mansoni* extracellular vesicles by human endothelial and monocytic cell lines and impact on vascular endothelial cell gene expression. *Int J Parasitol* **50**, 685–696 (2020).
42. Jia, X. *et al.* Solution structure, membrane interactions, and protein binding partners of the tetraspanin Sm-TSP-2, a vaccine antigen from the human blood fluke *Schistosoma mansoni*. *J Biol Chem* **289**, 7151–7163 (2014).
43. Siddiqui, A. J. *et al.* A Critical Review on Human Malaria and Schistosomiasis Vaccines: Current State, Recent Advancements, and Developments. *Vaccines* **11**, 792 (2023).
44. Egesa, M., Hoffmann, K. F., Hokke, C. H., Yazdanbakhsh, M. & Cose, S. Rethinking Schistosomiasis Vaccine Development: Synthetic Vesicles. *Trends in Parasitology* **33**, 918–921 (2017).
45. Mossallam, S. F., Abou-El-naga, I. F., Bary, A. A., Elmorsy, E. A. & Diab, R. G. Schistosoma mansoni egg-derived extracellular vesicles: A promising vaccine candidate against murine schistosomiasis. *PLoS neglected tropical diseases* **15**, (2021).
46. Dibo, N., Liu, X., Chang, Y., Huang, S. & Wu, X. Pattern recognition receptor signaling and innate immune responses to schistosome infection. *Front Cell Infect Microbiol* **12**, 1040270 (2022).
47. Rabinovich, G. A., van Kooyk, Y. & Cobb, B. A. Glycobiology of immune responses. *Annals of the New York Academy of Sciences* **1253**, 1–15 (2012).
48. Geijtenbeek, T. B. H. & Gringhuis, S. I. Signalling through C-type lectin receptors: shaping immune responses. *Nat Rev Immunol* **9**, 465–479 (2009).
49. van Vliet, S. J., García-Vallejo, J. J. & van Kooyk, Y. Dendritic cells and C-type lectin receptors: coupling innate to adaptive immune responses. *Immunology & Cell Biology* **86**, 580–587 (2008).
50. van Kooyk, Y. & Rabinovich, G. A. Protein–glycan interactions in the control of innate and adaptive immune responses. *Nat Immunol* **9**, 593–601 (2008).
51. Schnaar, R. L. Glycobiology simplified: diverse roles of glycan recognition in inflammation. *Journal of Leukocyte Biology* **99**, 825–838 (2016).
52. Hokke, C. H. & van Diepen, A. Helminth glycomics – glycan repertoires and host–parasite interactions. *Mol Biochem Parasitol* **215**, 47–57 (2017).
53. Smit, C. H. *et al.* Glycomic Analysis of Life Stages of the Human Parasite *Schistosoma mansoni* Reveals Developmental Expression Profiles of Functional and Antigenic Glycan Motifs. *Mol Cell Proteomics* **14**, 1750–1769 (2015).
54. Vázquez-Mendoza, A., Carrero, J. C. & Rodriguez-Sosa, M. Parasitic Infections: A Role for C-Type Lectins Receptors. *BioMed Research International* **2013**, e456352 (2013).

55. Everts, B. *et al.* Schistosome-derived omega-1 drives Th2 polarization by suppressing protein synthesis following internalization by the mannose receptor. *J Exp Med* **209**, 1753–67, S1 (2012).
56. Paveley, R. A. *et al.* The Mannose Receptor (CD206) is an important pattern recognition receptor (PRR) in the detection of the infective stage of the helminth *Schistosoma mansoni* and modulates IFNgamma production. *Int J Parasitol* **41**, 1335–1345 (2011).
57. Meyer, S. *et al.* DC-SIGN mediates binding of dendritic cells to authentic pseudo-LewisY glycolipids of *Schistosoma mansoni* cercariae, the first parasite-specific ligand of DC-SIGN. *J Biol Chem* **280**, 37349–37359 (2005).
58. van Vliet, S. J. *et al.* Carbohydrate profiling reveals a distinctive role for the C-type lectin MGL in the recognition of helminth parasites and tumor antigens by dendritic cells. *Int Immunol* **17**, 661–669 (2005).
59. van den Berg, T. K. *et al.* LacdiNAc-Glycans Constitute a Parasite Pattern for Galectin-3-Mediated Immune Recognition1. *The Journal of Immunology* **173**, 1902–1907 (2004).
60. Saunders, S. P. *et al.* The C-Type Lectin SIGNR1 Binds *Schistosoma mansoni* Antigens In Vitro, but SIGNR1-Deficient Mice Have Normal Responses during Schistosome Infection. *Infect Immun* **77**, 399–404 (2008).
61. Gerlach, J. Q. & Griffin, M. D. Getting to know the extracellular vesicle glycome. *Mol Biosyst* **12**, 1071–1081 (2016).
62. Avni, D. & Avni, O. Extracellular Vesicles: Schistosomal Long-Range Precise Weapon to Manipulate the Immune Response. *Frontiers in Cellular and Infection Microbiology* **11**, (2021).
63. Geijtenbeek, T. B. & Gringhuis, S. I. C-type lectin receptors in the control of T helper cell differentiation. *Nat Rev Immunol* **16**, 433–448 (2016).
64. Prasanphanich, N. S., Mickum, M. L., Heimburg-Molinaro, J. & Cummings, R. D. Glycoconjugates in host-helminth interactions. *Front Immunol* **4**, 240 (2013).



## Chapter 2

# Pathogen-derived extracellular vesicle-associated molecules that affect the host immune system: an overview

Marije E. Kuipers, Cornelis H. Hokke, Hermelijn

H. Smits, Esther N. M. Nolte-’t Hoen

**Frontiers in Microbiology, 2018**

**PMID: 30258429**

**DOI: [10.3389/fmicb.2018.02182](https://doi.org/10.3389/fmicb.2018.02182)**

## Abstract

Recently, the interest in extracellular vesicles (EVs) released by pathogens like bacteria, fungi, and parasites has rapidly increased. Many of these pathogens actively modulate the immune responses of their host and there is accumulating evidence that pathogen-derived EV contribute to this process. The effects of pathogen-derived EV on the host immune system have been attributed to proteins, lipids, nucleic acids, and glycans contained in, or present on these EV. For example, toxins in bacterial EV can modulate pathogen clearance and antigen presentation, while EV-associated polysaccharides are potential vaccine targets because they induce protective immune responses. Furthermore, parasite EV-associated microRNA may increase parasite survival via host gene repression, and the lipid A moiety of LPS in bacteria-derived EV induces strong pro-inflammatory responses. Research on pathogen EV-associated molecules may pave new avenues to combat infectious diseases by immune intervention. This review provides an overview of the current knowledge of EV-associated molecules released by extracellular pathogens and their effects on the host immune system. The current focus and future hotspots of this rapidly expanding field will be highlighted and discussed.

## Introduction

An increasing number of studies documenting the molecular characteristics and the function of pathogen-derived extracellular vesicles (EVs) suggest that pathogen EV play important roles in the activation and modulation of the host immune system. However, only few reports assign EV-mediated effects to specific EV-associated molecules or molecular principles. Here, we focus on defined pathogen-derived EV-associated molecules, their immunomodulatory effects, and the implications for host-pathogen interactions. We first briefly discuss pathogen-host communication via EV and EV biogenesis. Next, various classes of molecules in pathogen-derived EV—proteins, lipids, glycans (carbohydrate chains), and nucleic acids—will be addressed with respect to molecular identity and function. With this approach we aim to outline the current understanding of molecular principles through which pathogen EV modulate immune responses of their hosts.

## Pathogen–host communication: sending messages via extracellular vesicles

Many pathogens, including bacteria, fungi and parasites, have evolved to survive and reproduce in their host environment. For their success, modulation of the host immune system is often crucial. Simultaneously, the mammalian innate immune system has evolved to recognize and respond to the invading pathogens in order to eliminate them. Various pathogen-associated molecular patterns (PAMPs)—such as proteins, lipids, glycans, and nucleic acids—can bind to different families of pattern recognition receptors (PRRs), including Toll-like receptors (TLRs), C-type lectin receptors (CLRs), and NOD-like receptors (NLRs), expressed by both immune and non-immune cells in the host. While the activation of PRRs by PAMPs is essential for immunity and host defense, pathogens have developed several modulatory mechanisms to interfere in PRR binding and signaling<sup>1–3</sup>. In addition to PAMPs, pathogens can employ other molecules to increase their survival. For instance, cytotoxic proteins that induce apoptosis, enzymes targeting intracellular signaling pathways, or host gene regulating micro(mi)RNAs<sup>4,5</sup>. Classically, PAMPs and other pathogen-derived immunomodulatory molecules are found on the surface of pathogens or they are released as secretory biomolecules. Recently, however, it has become clear that PAMPs and other immunomodulatory molecules can also be released into the extracellular space as part of EV.

Extracellular vesicles are a collective term for exosomes, microvesicles, and other cell-derived membrane-enclosed vesicles. These vesicles transport various molecules, including proteins, lipids, and nucleic acids between cells within one organism or between organisms, such as in host-pathogen cross-talk.

Mammalian EV contain a mix of endosomal and plasma membrane proteins, including tetraspanins and major histocompatibility complex (MHC) molecules, and cytosolic proteins such as cytoskeletal proteins and heat shock proteins<sup>6</sup>. Lipids are essential for the formation and structure of the EV bilayer and EV are mainly enriched in cholesterol, sphingomyelin, phosphatidylserine, and glycosphingolipids. In addition, mammalian EV can transfer bioactive lipids and lipid-related enzymes between cells, such as prostaglandin E2 and phospholipase A2, respectively<sup>7</sup>. The most abundant nucleic acids in EV are small RNA species (<200 nucleotides)<sup>8</sup>, but mRNA, long non-coding RNA, and DNA have also been detected<sup>6</sup>. A lot of research has been dedicated to the characterization of EV-derived miRNA because of their well-known capacity to modulate gene expression. Additionally, EV contain glycans<sup>9</sup> that are present as part of larger glycoconjugates, such as glycolipids and proteoglycans, or as post-translational modification of proteins. Given that the variation and heterogeneity in glycoconjugates is very high, EV-associated glycans may serve multiple and dedicated roles in both the biogenesis and function of EV<sup>10</sup>. The molecular composition of mammalian- and pathogen-derived EV is highly dynamic and depends on the type of EV-producing cell/organism, the developmental/physiological status of that cell/organism, and environmental conditions<sup>6</sup>. Therefore, the functional behavior of these EV and their effects on recipient cells are probably 'donor' cell/organism- and niche/context-specific<sup>8</sup>. The immunological imprinting by EV has been spearheaded by previous studies on EV derived from mammalian immune cells (reviewed in <sup>8,11,12</sup>), tumor cells (reviewed in <sup>13,14</sup>) and mesenchymal stromal/stem cells (reviewed in <sup>15-17</sup>).

The release of pathogen-derived vesicles was observed 40–50 years ago in gram-negative bacteria, *Vibrio cholerae*<sup>18</sup> and *Neisseria meningitidis*<sup>19</sup>, the fungus *Cryptococcus neoformans*<sup>20</sup>, and the parasites *Schistosoma mansoni* and *Fasciola hepatica*<sup>21,22</sup>. These vesicles were initially regarded as artifacts, until decades later, studies on gram-negative bacteria showed that their released outer membrane vesicles supported bacterial survival. Indeed, bacterial vesicles contributed to biofilm formation<sup>23</sup> and were able to transfer DNA to other bacteria, thereby sharing genes involved in, for example, antibiotic resistance<sup>24,25</sup>. In the past decade, evidence was also provided for release of EV by gram-positive bacteria<sup>26</sup>, fungi<sup>27</sup>, parasites<sup>28</sup>, parasite-infected cells, like *Plasmodium falciparum*-infected red blood cells<sup>29</sup>, and the pathogenic protozoa *Acanthamoeba castellanii*<sup>30</sup>. The description of EV released by pathogen-infected cells is beyond the scope of this review and has been extensively described elsewhere<sup>31-34</sup>. In this review, we focus on EV released by extracellular pathogens and their direct effects on the host.

## Extracellular vesicle biogenesis in mammals and pathogens

Despite growing numbers of studies on EV biogenesis in mammalian cells, full details of the molecular pathways involved are not yet resolved<sup>35</sup>. So far, it is known that various sorting machineries are involved in clustering membrane-associated proteins and lipids destined for secretion via EV. This clustering occurs within membrane microdomains found on the limited membrane of the multivesicular endosome (MVE, also called multivesicular body) and on the plasma membrane (Figure 1). Although the biogenesis of vesicles within the MVE is better understood than vesicle biogenesis at the plasma membrane, both routes share molecular machineries for EV generation, such as 'Endosomal Sorting Complex Required for Transport' (ESCRT) proteins and tetraspanins. Both ESCRT-dependent and independent mechanisms have been implicated in clustering of cargo for biogenesis of EV<sup>36</sup>. The microdomain-associated molecules have also been suggested to participate in recruiting soluble proteins and ribonucleoprotein complexes from the cytosol into the vesicles. Budding of EV from the plasma membrane or into the lumen of MVE is often ESCRT dependent. The type of recruited sorting machinery likely determines whether the MVE will fuse with the plasma membrane or with lysosomes<sup>37</sup>. Upon fusion of the MVE with the plasma membrane, the intraluminal vesicles (ILVs) are released into the extracellular space and then referred to as exosomes. EV budding from the plasma membrane are often called microvesicles. A schematic overview of EV biogenesis pathways is shown in Figure 1 (top). For further details on the biogenesis of mammalian EV, we refer to a recently published comprehensive review on this topic<sup>35</sup>.

With regard to pathogen-derived EV, the release of EV by parasites shows most similarities with EV release by mammalian cells. Transmission electron microscopic (TEM) analysis of multicellular parasites, such as *F. hepatica*<sup>38</sup>, and unicellular protozoan parasites, such as *Trypanosoma cruzi*<sup>39</sup>, indicated budding of microvesicles from the plasma membrane and the presence of ILVs in MVEs. Interestingly, a third secretion route was described for *T. cruzi* and *Leishmania* spp. where vesicles are released from an organelle involved in protein endocytosis and exocytosis called the flagellar pocket<sup>39–41</sup>. However, whether these flagellar membrane-derived EV differ in molecular content compared to the EV released via the other two routes remains unknown<sup>34</sup>. In addition, proteomic studies on EV from many different parasite species (excluding the strictly intracellular parasites) have indicated the presence of molecular orthologs of proteins involved in EV biogenesis, including ESCRT components, the tetraspanin CD63, and vacuolar protein sorting-associated protein 4 (VPS4)<sup>38,42</sup>. These findings suggest that EV formation is highly conserved in eukaryotes. It is less clear how fungi-derived

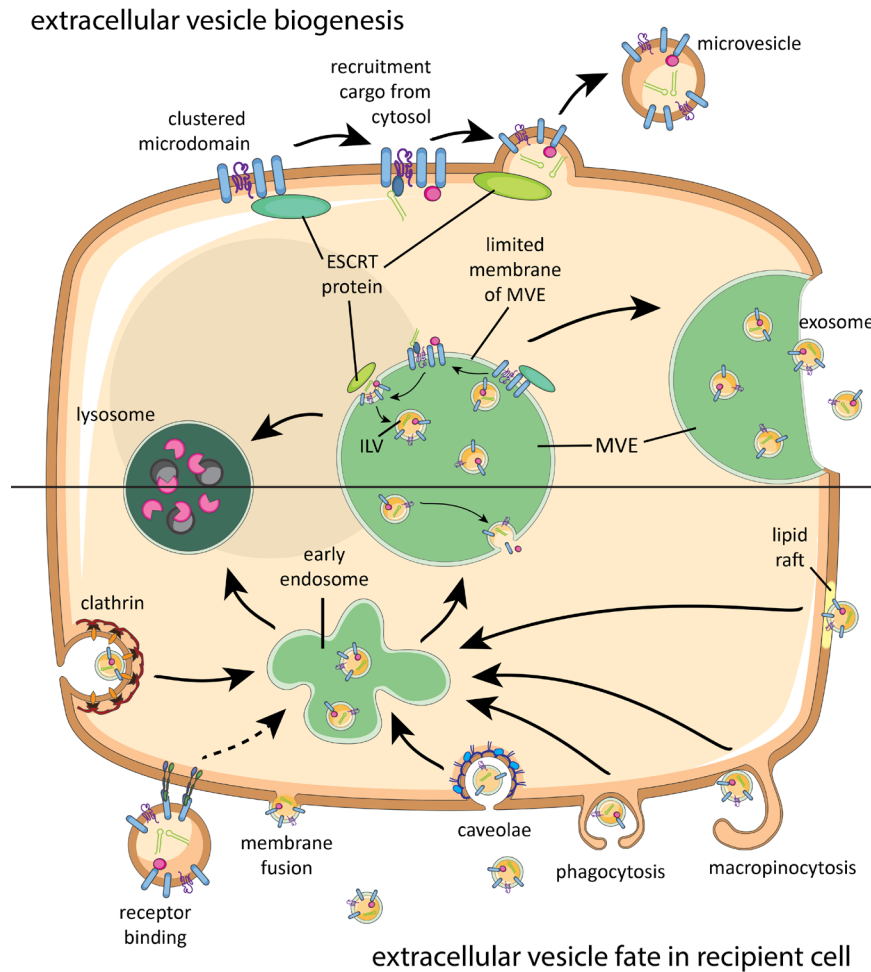


**Figure 1. Brief schematic summary of known mammalian extracellular vesicle biogenesis and their fate in recipient cells.**

Proteins, lipids, and sorting machineries cluster in microdomains of the plasma membrane or limited membrane of the multivesicular endosome (MVE) and can recruit molecules from the cytosol (top). Furthermore, components of the sorting machinery contribute to microvesicle or intraluminal vesicle (ILV) formation. Microvesicles bud off the plasma membrane, while ILVs are released as exosomes once the MVE fuses with the plasma membrane. Released extracellular vesicles can interact with a recipient cell via receptor binding, fusion, or various internalization routes (bottom). After endocytosis, extracellular vesicles will be either degraded in lysosomes or end up in MVEs with endogenous ILVs. Intraluminal cargo can only be released into the cytosol of the recipient cell upon fusion of EV with the plasma membrane or MVE membrane. ESCRT: Endosomal Sorting Complex Required for Transport.

vesicles are formed. TEM of *C. neoformans* showed MVE-like structures and ESCRT proteins have been detected in EV from *Saccharomyces cerevisiae*. ESCRT proteins were not required for EV release in *S. cerevisiae*, but played a role in determining the protein composition of EV<sup>43</sup>. Furthermore, it is not known how fungal EV traverse the complex fungal cell wall. For fungi and other thick-walled microorganisms, such as mycobacteria and gram-positive bacteria, it has been suggested that EV traverse the wall by (1) mechanical pressure that forces EV through small pores in the cell wall; (2) passage through protein channels in the cell wall; and (3) remodeling/degradation of the wall by EV-associated enzymes (detected in proteomic analyses)<sup>44</sup>. Different models have also been proposed to explain the biogenesis of gram-negative bacteria-derived outer membrane vesicles (reviewed in <sup>45,46</sup>). For this class of bacteria, it remains to be elucidated whether outer membrane vesicles originate from the inner and/or outer membrane, or both<sup>46</sup>. Since the subcellular origin of vesicles released by pathogens is generally unknown, we will here refer to all types of pathogen-derived vesicles as EV.

## EV-associated molecules and targeting to recipient cells

There is limited knowledge on the mechanisms through which EV can interact with cell surfaces and transfer their (intraluminal) cargo to the recipient cell. In general, membrane-bound (glyco)proteins and (glyco)lipids drive the initial interaction with the recipient cell. First, the EV needs to dock at the recipient plasma membrane where it can subsequently remain bound to the surface, be internalized, or fuse with the cell membrane. Receptors on the target cell plasma membrane, such as integrins, can recognize the exterior cargo of the EV, which can lead to activation of signaling cascades within the cell<sup>35</sup>. Receptor binding may also facilitate endocytosis of the EV, a route that targets the EV to endosomes and often further to degradation in lysosomes. In addition to receptor-mediated internalization, mammalian EV can also be endocytosed via non-specific macropinocytosis, clathrin-mediated endocytosis, and endocytosis via lipid rafts or caveolae<sup>35</sup>. EV need to fuse with the limited membrane of the endosome or with the plasma membrane in order to deliver their intraluminal cargo such as nucleic acids, eicosanoids, and soluble proteins to the cytosol of recipient cells. A simplified overview of EV interaction with recipient cells can be found in Figure 1 (bottom).

Pathogen-derived EV can interact with host cells in various ways. For example, EV from gram-negative bacteria were shown to either fuse with the membrane of the recipient cells or internalize via all previous mentioned routes of endocytosis<sup>47</sup>. Additionally, defined molecules on the surface of pathogen-derived EV may drive their targeting to specific cells or organs in the host to create a niche

for infection and survival. Since PAMPs are abundantly present on the surface of pathogens<sup>48</sup>, EV that bud off these membranes likely interact with PRRs on recipient cells, as was demonstrated for bacteria-derived EV<sup>45,49,50</sup>. The presence of pathogen-specific enzymes, toxins, or PAMP-containing molecules distinguishes pathogen-derived EV from those released by mammalian cells and may explain differences in their uptake and function. Pathogen-derived molecules in or on EV may therefore be exploited in biomarker research and therapeutic applications. Examples include the detection of parasite-derived EV-associated miRNA in host serum as diagnostic marker for schistosome infections and the exploration of new drugs that target the fusion of *Trypanosome* EV to erythrocytes for prevention of anemia<sup>51</sup>.

## Effects of pathogen EV-associated molecules on the immune system

Below, we give an overview of immunomodulatory effects induced by components of pathogen-derived EV, subdivided per major class of biological macromolecules (proteins, lipids, glycans, and nucleic acids). In this way, we aim to assess whether there are similarities in how different pathogens use EV-associated molecules to affect host cells. This overview is restricted to studies in which clear evidence was provided for the association of a pathogen-specific molecule in/on EV and the direct involvement of this molecule in the EV-induced effects. A total overview of the selected papers, the reported EV-associated molecules, the observed effects on the host immune system, and the methodological approaches applied in these studies can be found in Table 1.

### Pathogen EV-associated proteins with immunomodulatory activities

Proteins form the largest group of known pathogen EV-associated molecules (Figure 2A). These EV proteins have been shown to affect immune responses or the survival rates of the host or pathogen (Figure 2B). Below, we distinguish and describe pathogen EV-associated proteins that cause cytotoxicity, increase pathogen survival, or induce pro-inflammatory responses.

#### Cytotoxic proteins associated to pathogen EV

Thus far, only EV-associated proteins derived from bacteria have shown to compromise immune defenses by inducing apoptosis of host cells. For example, EV from the gram-negative bacterium *N. gonorrhoeae* contained a porin protein, PorB, that was shuttled to mitochondria in host macrophages<sup>52</sup>. Here, the voltage gated pore induced loss of mitochondria membrane potential and cytochrome c

release leading to activation of the caspase pathway and apoptosis. As such, PorB promoted immune evasion and survival of this sexually transmitted infection. Importantly, it was shown that *N. gonorrhoeae* depends on EV for the delivery of PorB, suggesting a role for bacteria-derived EV and associated proteins in increased virulence. In addition, various cytotoxic proteins were found in EV derived from a highly virulent *Escherichia coli* strain<sup>53</sup>. The authors demonstrated the association of Shiga toxin 2a (Stx2a) and Shigella enterotoxin 1 with the EV. Stx2a was shown to cause cytotoxicity after EV uptake by various human intestinal epithelial cell lines via activation of caspase-9 and caspase-3. This effect could not be reduced by preincubating the EV with a Stx2a-neutralizing antibody, confirming the intravesicular localization of Stx2a<sup>53</sup>.

Extracellular vesicle released by the gram-positive bacteria *Bacillus anthracis* were also shown to contain cytotoxic molecules<sup>54</sup>. The anthrax toxins released by this bacterium have lethal consequences for its host during infection. Both EV-associated anthrolysin (a cholesterol-dependent pore-forming protein) and an anthrax toxin polypeptide induced toxicity in macrophages. Additional effects of these EV-associated toxins were shown in immunized mice. Immunization with isolated EV from *B. anthracis* increased the survival of mice after bacterial re-challenge and led to an increase in IgM titers against *B. anthracis* toxins in mouse sera. This differed from immunization with purified, non-EV associated toxins, which mainly induced IgG production<sup>54</sup>.

### **EV-associated proteins promoting survival of pathogens**

Bacteria-derived toxins transported by EV can also modulate immune cell functions to promote pathogen survival. For example, cytotoxic necrotizing factor type 1 (CNF1) in EV from an uropathogenic *E. coli* was shown to reduce antimicrobial activity and chemotactic responses in neutrophils<sup>55</sup>. Another example has been provided for the Cif toxin derived from the gram-negative bacterium *Pseudomonas aeruginosa*<sup>56,57</sup>. EV-associated Cif increased the bacterial pathogenesis of *P. aeruginosa* by reducing the abundance of the cystic fibrosis transmembrane conductance regulator (CFTR) in human airway epithelial cells. CFTR facilitates chloride secretion by epithelial cells needed for mucociliary clearance of the pathogen in the lungs<sup>56</sup>. In a follow-up paper, it was suggested that Cif may also increase the severity and duration of infections in the airways by reducing the 'transporter associated with antigen processing 1' (TAP1). This leads to reduced antigen transport to MHC class I molecules and inhibition of antigen presentation, including antigens from other pathogens such as viruses<sup>57</sup>. These studies suggest that Cif can contribute to pathogen survival in various ways. Another human respiratory pathogen, *Moraxella catarrhalis*, was shown to release

Table 1. Pathogen EV-associated molecules and their effect on host immunity<sup>#</sup>

Microbe / genus	Species (strain)	EV-associated molecule	Effect on host	Methodological approaches used <sup>#</sup>	Reference
<b>Bacteria</b>					
<b>gram-negative</b>					
<b>Escherichia</b>	<i>coli</i> (CP9)	CNF1 toxin	Attenuates antimicrobial function and chemotaxis of murine neutrophils.	density gradient, proteinase K, mutant strain,	Davis et al., 2006 <sup>55</sup>
	<i>coli</i> (LB226692)	Shiga toxin 2a	Activates caspase- 9 and caspase-3 in human intestinal epithelial cells resulting in apoptosis.	density gradient, proteinase K, electron microscopy, mutant strain, blocking control, internalization	Kunsmann et al., 2015 <sup>53</sup>
		H4 flagellin	Induces IL-8 secretion by human intestinal epithelial cells.	electron microscopy <sup>a</sup> , mutant strain <sup>b</sup> , blocking control <sup>a</sup> , liposomes <sup>b</sup> , internalization <sup>a,b</sup>	<sup>a</sup> Vanaja et al., 2016 <sup>65</sup> , <sup>b</sup> Santos et al., 2018 <sup>66</sup>
<i>coli</i> (BL21)		LPS (lipid A)	EV target LPS to cytosol and induce IL1-β release via caspase-11 activation in murine cells <i>in vitro</i> and <i>in vivo</i> .	electron microscopy, mutant strain	Stevenson et al., 2018 <sup>74</sup>
		less acetylated PNAG polysaccharide	Immunized mice show protective immune responses after challenge with unrelated bacteria.	electron microscopy, mutant strain	
<b>Francisella</b>	<i>t. polaris</i> (ΔS)	FtA lipase protein	Facilitates adhesion to and internalization of bacteria by murine macrophages.	density gradient, proteinase K, mutant strain	Chen et al., 2017 <sup>59</sup>
<b>Helicobacter</b>	<i>pylori</i> (251)	peptidoglycan (PGN)	Promotes inflammation <i>in vitro</i> and <i>in vivo</i> via NOD1-dependent mechanism.	density gradient, proteinase K, DNase, mutant strain	Kaparakis et al., 2010 <sup>75</sup>
<b>Moraxella</b>	<i>catarrhalis</i> (BH18)	Moraxella IgD-binding protein	B cell receptor binding and vesicle internalization via B cell receptor.	electron microscopy, DNase, mutant strain, blocking control	Vidakovics et al., 2010 <sup>63</sup>
		DNA	Increases IL-6 and IgM secretion via TLR9 activation in human tonsillar B cells.	mutant strain	Schaar et al., 2011 <sup>58</sup>
		Ubiquitous surface proteins A1/A2	Downregulation of pro-inflammatory response in epithelial cells.		

<b>Neisseria</b>	<i>gonorrhoeae</i> (MS11-A)	PorB porin protein	Targets mitochondrial to activate the caspase pathway and apoptosis in murine macrophages.	density gradient, electron microscopy, mutant strain, internalization	Deo et al., 2018 <sup>52</sup>
	<i>meningitidis</i> (H44/76)	LPS (lipid A)	Activation of innate immunity <i>in vitro</i> .	mutant strain	Zariri et al., 2016 <sup>68</sup>
<b>Pseudomonas</b>	<i>aeruginosa</i> (PA14)	Cif toxin	Reduces deubiquitination of CFTR and TAP in airway epithelial cells leading to reduction of pathogen clearance and antigen presentation, respectively.	density gradient, mutant strain, internalization	Bomberger et al., 2011 <sup>56</sup> , 2014 <sup>57</sup>
		tRNA fragment	Reduces LPS- and EV-induced IL-8 release by human airway epithelial cells. Reduces neutrophil infiltration in mouse lung.	density gradient, RNase, mutant strain, molecule control, internalization	Koeppen et al., 2016 <sup>81</sup>
<b>gram-positive</b>					
<b>Bacillus</b>	<i>anthracis</i> (34F2)	anthrolysin toxin polypeptide	Contribute to cytotoxicity in murine macrophages and induces IgM responses <i>in vivo</i> .	electron microscopy, mutant strain, blocking control, molecule control	Rivera et al., 2010 <sup>64</sup>
<b>Streptococcus</b>	<i>pneumoniae</i>	PspA surface protein	PspA specific IgG responses and increased survival in EV immunized mice.	density gradient, proteinase K, mutant strain, molecule control	Muraliath et al., 2011 <sup>64</sup>

\*Brief description of abbreviated methodological approaches: **density gradient**, density gradient isolation for purification of EV, often combined with Western Blot detection of the EV-associated molecule; **proteinase K**, DNase, RNase, proteinase K, DNase, or RNase treatment of EV, often combined with a detergent or enzyme inhibitor to investigate the topology of the EV-associated molecule; **electron microscopy**, electron microscopy immunogold staining to show association of the molecule with EV; **lipophilic dye**, staining of EV membrane or EV-depleted control samples with lipophilic dye for binding/uptake assays; **mutant strain**, EV from mutant strains lacking the (functional) molecule; **blocking control**, using a control to inhibit the EV-associated molecule with either a neutralizing antibody or compound; **liposomes**, mimicking EV by synthesis of liposomes containing only the molecule of interest; **molecule control**, using (a synthetic form of) the molecule as a soluble protein control to confirm the importance of EV association; **internalization**, confirmed intracellular detection of the molecule in recipient cells incubated with the EV.

EV that reduced TLR2-induced IL-8 production by human alveolar epithelial cells, via the activity of EV-associated Ubiquitous surface protein (Usp)A1. UspA1 can bind to carcinoembryonic antigen-related cell adhesion molecule-1 (CEACAM-1) on epithelial cells and subsequently reduce TLR2-activated IL-8 production<sup>58</sup>. As IL-8 is a key player to attract other cells, mainly neutrophils, to the site of infection, UspA1-dependent reduction of IL-8 could increase bacterial survival in the lungs.

Extracellular vesicle from zoonotic *Francisella tularensis*, the gram-negative bacterium that can cause fatal pneumonic tularemia in humans, contain a protein with lipolytic activity named FtlA. Since this bacterium primarily replicates inside alveolar macrophages and epithelial cells, the success of invasion into host cells determines its virulence. *FtlA* mutant bacteria showed significantly reduced lipolytic activity and virulence and reduced inflammatory cell infiltrations in a lung infection model<sup>59</sup>. Interestingly, it was shown that FtlA is absent from the surface of the bacterium but present on the surface of EV from *F. tularensis*. By adding EV from the wild type strain to *ftlA* mutant bacteria *in vitro*, bacterial infiltration increased significantly, suggesting a role for the EV-associated lipase protein in bacterial adhesion and cell invasion<sup>59</sup>.

In addition to gram-negative bacteria, parasites also release EV that promote survival in the host. This was shown for EV containing Glycoprotein (GP)63 released by the protozoan parasite *L. major*<sup>60</sup>. GP63 is a zinc-dependent metalloprotease that is expressed on the surface of the infectious *Leishmania* life stage. Parasite-derived GP63 is known to modulate signaling pathways (such as tyrosine phosphatases) within macrophages such that it inhibits inflammatory responses leading to increased parasite survival. Although this is an intracellular parasite, the authors used isolated EV from *in vitro* extracellular parasite cultures. *In vivo* administration of EV from GP63-/- *L. major* parasites resulted in stronger pro-inflammatory effects, such as increased neutrophil and eosinophil recruitment, compared to wild type *L. major*. This suggests that EV-associated GP63 could dampen immune responses and may support the establishment of *Leishmania* infection in the host. However, these effects could also be due to other EV-associated proteins, since it was shown that GP63 additionally affects the proteomic content of EV<sup>60</sup>. Furthermore, EV-associated GP63 was shown to affect liver cell function. GP63-containing EV released by *L. donovani* reduced the activity of miRNA miR-122 in a human liver cell line, likely by affecting DICER1-mediated cleavage of this miRNA<sup>61</sup>. These results were confirmed *in vivo* by administering liposomes containing purified GP63 or *Leishmania*-derived EV to mice. The GP63-induced reduction in DICER1 and miR-122 expression in hepatocytes resulted in metabolic changes in these cells and lower serum cholesterol levels. This may favor parasite

infection, as a high serum cholesterol is associated with reduced parasite burden in the liver<sup>61</sup>.

### Pro-inflammatory responses induced by EV-associated proteins

In addition to their cytotoxic and survival-promoting effects, pathogen-derived EV have also been implicated in raising host immune responses against the pathogens. EV from the liver fluke (flatworm) *Opisthorchis viverrini*, for example, were shown to induce IL-6 production by human cholangiocytes, an effect that could be blocked by antibodies against the EV-associated tetraspanin TSP-1<sup>62</sup>. This suggested a role for TSP-1 carrying EV in the chronic inflammatory environment observed in host tissues during infection with *O. viverrini*. Also EV-associated proteins from bacteria can induce pro-inflammatory responses in the host. This has been shown for virulent *E. coli*-derived EV-associated H4 flagellin, which triggered TLR5 signaling and subsequent IL-8 release by EV-targeted intestinal cells<sup>53</sup>. An additional way in which pro-inflammatory responses are induced by EV was shown for *M. catarrhalis*. *Moraxella* IgD-binding (MID) protein on the EV of this gram-negative bacterium was essential for EV uptake by human tonsillar B lymphocytes via the B cell receptor and induced IL-6 production by these cells<sup>63</sup>. Interestingly, IgM production was increased after B cell uptake of EV, but these antibodies were not specific for *Moraxella* bacteria. The authors therefore suggested that the non-specific IgM production induced by MID-associated EV is rather a survival strategy to divert the B cell antibody production away from the bacterial infection<sup>63</sup>. These results suggest that one EV-associated protein may induce multiple effects that could benefit both the host and the pathogen.

Overall, these findings indicate that a wide variety of pathogen-derived EV-associated proteins can modulate host immune responses. The pro-inflammatory properties of pathogen-derived EV may be used for EV-based vaccination strategies. This has been investigated for PspA, a surface protein expressed by all strains of the gram-positive *Streptococcus pneumoniae*. PspA was introduced into a gram-negative *Salmonella enterica* strain<sup>64</sup>, after which EV released by these bacteria were used for intranasal immunization of mice. These EV induced a PspA-specific IgG responses and increased mouse survival after *S. pneumoniae* challenge. This was not observed when administrating EV from a similar *Salmonella* strain without PspA or when PspA was administered as purified antigen<sup>64</sup>.

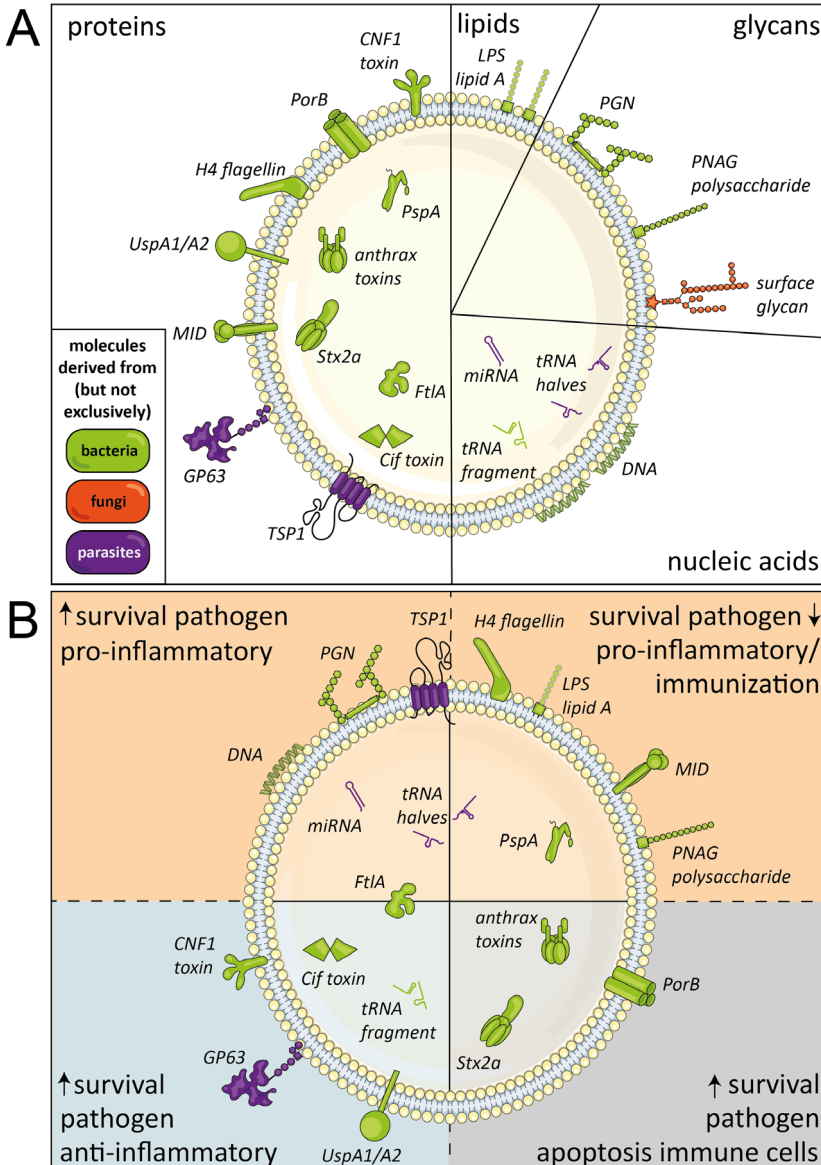


**Figure 2. Immunomodulatory molecules in pathogen-derived EV.**

(A) Schematic summary of pathogen-derived EV-associated molecules with immunomodulatory effects released by bacteria (green), fungi (orange), and parasites (purple), subdivided in proteins, lipids, glycans, and nucleic acids. The suggested topology of the molecules, i.e. inside the EV or in its lipid membrane facing the exterior, is also shown. (B) Defined EV-associated molecules released by pathogens arranged based on immunomodulatory effects, i.e. pathogen survival, inflammatory response, and immune cell apoptosis.

## EV-associated lipids

Bacterial LPS is the most intensely investigated pathogen-derived (glyco)lipid associated with EV. LPS is known to bind to TLR4, but can also be recognized in the cytosol by the murine receptor protease caspase-11, and in humans by caspase-4 and caspase-5. EV from gram-negative bacteria were shown to deliver LPS to the cytosol, thereby inducing an inflammatory form of programmed cell death (pyroptosis) and increased IL-1 $\beta$  expression in a caspase-11-dependent manner<sup>65</sup>. These effects were reduced when LPS on EV was neutralized, when EV from an *E. coli* mutant lacking a functional lipid A (an essential component of LPS) were used, or when cells were incubated with EV from gram-positive bacteria lacking LPS. The pro-inflammatory effects were also reduced when using bacteria from a *E. coli* strain which released less EV due to mutations in EV biogenesis. These data suggest a role for EV in delivering LPS into the cytosol and subsequent activation of innate immune responses during an infection with gram-negative bacteria<sup>65</sup>. A more recent study confirmed these findings by mimicking the EV structure of gram-negative bacteria by incorporation of LPS in liposomes<sup>66</sup>. When stimulating murine macrophages with these liposomes, cell death and IL-1 $\beta$  release were induced in a caspase-11-dependent fashion. In addition, a role for guanylate-binding proteins (GBPs) in this process was observed. GBPs can destroy the membrane of pathogens in the cytosol. It was suggested that EV-associated LPS recruits GBPs, which then engage in a membrane-disrupting activity leading to either LPS release from the EV or providing direct access of caspase-11 to the lipid A moiety of LPS, both resulting in caspase-11 activation<sup>66</sup>. Lipid A was indeed shown to be essential for GBP-dependent cell death. Additionally, injection of LPS-containing *E. coli*-derived EV into wild type mice caused lethality, while GBP-/- mice showed increased survival and caspase-11 deficient mice showed complete survival. This suggests a role for EV-associated LPS in EV-induced endotoxic shock.

Extracellular vesicle-associated lipids are also gaining attention in the development of EV-based vaccines<sup>16</sup>. EV derived from the gram-negative bacterium *N. meningitidis* are already used in a vaccine against meningococcal disease in children<sup>67</sup>. Research has been performed on how different types and modifications of LPS in EV from gram-negative bacteria contribute to immunogenicity or (endo)toxicity<sup>65</sup>. Lipid A modifications in *N. meningitidis* mutants, for example, were shown to reduce EV-induced innate immune responses *in vitro*, which could indicate these EV are less endotoxic and thus probably safer to use in vaccines<sup>68</sup>.

Thus far, only the above described studies gave strong proof of the presence of biologically active (glyco)lipids in pathogen-derived EV (see Figure 2A). Considering the increasing interest in EV and continuous improvement of EV

isolation and characterization technologies, it is suspected that additional biological effects of pathogen-derived EV-associated lipids may be elucidated in the near future. For example, mass spectrometry indicated that EV from the parasitic worm *Heligmosomoides polygyrus* differed in lipid composition from murine cell-derived EV and were enriched in ether glycerophospholipids called plasmalogens. The authors created artificial vesicles and observed that increasing the plasmalogen content of the vesicles increased the efficiency with which they fused with cells<sup>69</sup>. However, it remains to be elucidated whether plasmalogens influence the immunomodulatory property of these EV.

## Glycans associated to EV

Several lines of evidence indicate that glycans are present on EV from bacteria, parasites, and fungi. Pathogen glycans can bind to and signal via different host cell receptors, which may lead to modification of host cell function. For example, using mammalian lectin microarrays, it was shown that surface glycans on EV of the fungi *Paracoccidioides brasiliensis* and *P. lutzii* were recognized by human DC-SIGN<sup>70</sup>. In addition, analysis of the proteomes of parasite-derived EV has indicated the presence of many (putative) glycoproteins<sup>71-73</sup>. Whether or how these components truly interact with host cells and modify their function it is not yet known.

While no data are available on potential immunomodulatory effects of glycans associated to fungi- or parasite-derived EV, several studies addressed the function of glycans on bacteria-derived EV. Mice immunized with EV from a genetically engineered *E. coli* with decreased acetylation of poly-*N*-acetyl-D-glucosamine (PNAG) showed higher protective immune responses after bacterial challenge compared to their highly acetylated counterparts<sup>74</sup>. PNAG is a surface polysaccharide present in many different pathogen species, suggesting that these engineered EV as immunization strategy may be broadly effective. Indeed, immunized mice were protected against lethal doses of *Staphylococcus aureus* and *F. tularensis*. In another study, EV from *Helicobacter pylori* were shown to induce NF- $\kappa$ B activity and subsequent IL-8 production in human epithelial cell lines in an NOD1-dependent fashion<sup>75</sup>. Cytosolic NOD1 is known to specifically recognize peptidoglycan, a component of the bacterial cell wall. The authors indeed showed that EV-associated peptidoglycan from gram-negative bacteria could activate NOD1. Interestingly, feeding of mice with EV from *H. pylori* increased gastric gene expression of the chemokine *Cxcl2*, which was shown to be dependent on NOD1 and independent of TLR activation<sup>75</sup>. However, it remains to be determined whether association of peptidoglycan with EV is required to mediate these effects.

Thus far, only a handful of studies have investigated the glycome of EV,

none of which addressed pathogen EV (reviewed by <sup>9,76</sup>), partly due to the technical limitations dictated by the scale and purity of EV preparations. The importance of analyzing the glycomic profiles of EV has been demonstrated for mammalian EV. In different pathological conditions, such as cancer or metabolic diseases, differences were observed in the EV glycomic profile<sup>77-79</sup>, suggesting the physiological importance of EV glycosylation. Studying glycomic profiles of pathogen-derived EV could improve our understanding of EV biogenesis and interaction with recipient cells, and elucidate whether glycosylation of proteins and lipids plays a role in (immune) modulation by these EV<sup>76</sup>.

## EV-associated nucleic acids

The nucleic acid content of pathogen-derived EV consists of different RNA classes and DNA. Depending on the type of nucleic acid and its localization in the EV these molecules can either regulate host mRNA or trigger RNA or DNA sensing receptors. The latter was observed for EV of the gram-negative bacterium *M. catarrhalis*<sup>63</sup>. These vesicles were shown to induce the proliferation of human tonsillar B cells and activate TLR9 via its EV-associated DNA that contained CpG-motifs. Furthermore, it was observed that the increase in B cell proliferation was significantly reduced when EV were treated with DNase, suggesting that the DNA is on the outside surface of *M. catarrhalis*-released EV<sup>63</sup>.

There is an increasing number of studies that report on the composition of the small RNA repertoires in vesicles from bacteria<sup>80,81</sup>, fungi<sup>82</sup>, and parasites<sup>72,83-88</sup>. However, so far, only few studies provided evidence that EV-associated RNA is responsible for the modulation of host cells. For example, uptake of EV from the gastrointestinal parasitic worm *H. polygyrus* by mouse epithelial cells led to decreased expression of the *Dusp1* gene while uptake of EV from mouse intestinal cells had no effect<sup>84</sup>. This effect is likely caused by the EV-associated miRNAs, since transfection of host cells with synthetic analogs of these parasite miRNAs also showed reduction of *Dusp1* expression. DUSP1 is a regulator of mitogen-activated protein kinase (MAPK) signaling and favors a reduction in IL-6 and an increase in macrophage arginase expression. As IL-6 enhances host susceptibility to *H. polygyrus* and arginase is a mediator of killing this parasite in mice, repression of DUSP1 may be a parasite-driven mechanism to enhance its survival in the host. This is a very interesting example of cross-organism communication in which a parasite EV-associated miRNA functions due to complementarity to the host target gene.

Immunomodulatory effects induced by other EV-associated small non-coding RNAs have been described for both parasites and bacteria. The parasite *T. cruzi* releases EV containing transfer RNA-derived small RNAs (tsRNA), that could

be visualized inside HeLa cells after uptake of these EV<sup>85</sup>. This led to several alterations in gene expression levels, including increased mRNA levels for pro-inflammatory *il-6* and *cxcl2*. Part of this effect, such as increased *cxcl2* expression, was also observed when HeLa cells were transfected with a synthetic form of the most abundant EV-associated tsRNAs<sup>85</sup>. However, the mechanism by which tsRNA derived from parasite influences host mRNA transcription remains to be elucidated. EV-associated tRNA-derived fragments (from different isoacceptor tRNAs) were also detected in EV from the opportunistic bacterium *P. aeruginosa*<sup>81</sup>. One specific tsRNA (sRNA52320) present in isolated EV could be detected inside EV-treated primary human bronchial epithelial cells. Both EV-mediated transfer of sRNA52320 and direct transfection of cells with synthetic sRNA52320 led to reduction of LPS-induced IL-8 production. This provided indirect evidence that EV-enclosed tRNAs mediated these effects. Also *in vivo*, *P. aeruginosa*-derived EV significantly reduced the mouse homolog of IL-8 in bronchoalveolar lavage fluid and lowered lung neutrophil infiltration, which was sRNA52320 dependent<sup>81</sup>. However, whether the EV-associated tsRNA contributes to persistence of *P. aeruginosa* infections is yet to be determined.

## Conclusion and outlook

The observed effects of EV released by pathogens underline that intercellular communication via EV is a conserved mechanism that most likely benefits pathogen survival in co-evolution with its host. Immunomodulatory components of pathogen-derived EV are represented in all molecular subclasses—proteins, lipids, glycans, and nucleic acids (Figure 2A)—and can modify host cell function or induce host cell apoptosis. Although the field of research on pathogen-derived EV is still in its infancy, many advanced studies have already been performed on EV released by bacteria. The generation of mutant bacterial strains has provided great opportunities to study the function of specific EV-derived molecules. From these studies, we learned that many, if not all, gram-negative bacteria release LPS-containing EV that are well-capable of inducing pro-inflammatory reactions. Despite gaps in our understanding of the broad group of pathogen-derived EV, the currently available data indicate that pathogen EV-associated molecules can promote survival and spreading of pathogens, but can also facilitate the induction of host-immune responses (Figure 2B). The exact role of pathogen-derived EV in host-pathogen interaction likely depends on pathogen life stage, environmental, and/or tissue specific conditions.

The current overview does not show us yet whether EV from different pathogens contain conserved classes of molecules or act via similar principles. This is probably due to the limited number of publications on EV-associated

immunomodulatory molecules from pathogens that is available at this early stage. In addition, inter-study comparability of data on both mammalian and pathogen EV is currently hampered by the use of a wide range of different techniques to isolate and characterize EV. Different EV isolation methods, for example, yield EV of different purity and can bias toward isolating certain EV subtypes<sup>89</sup>. This urges the need to adhere to guidelines stated in the “minimal information for studies of EV (MISEV)”<sup>90</sup>, of which an update is currently under development. Increasing the reproducibility of EV research also requires that all experimental details relating to EV isolation and characterization are reported in scientific publications. This is facilitated by EV-TRACK, which is a crowdsourcing knowledgebase to centralize experimental parameters of EV publications<sup>91</sup>. Optimization and standardization of experimental methods will help to unravel effects of specific EV-associated molecules from pathogens and is particularly important for the design of, e.g., EV-based vaccines. Additionally, a more standardized approach will allow the comparison of similar molecules or immune responses induced by different pathogen-derived EV.

A promising method to allow pathogen-overarching comparisons of pathogen-derived EV-associated molecules is the use of bioinformatics<sup>92</sup>. The increasing number of publications on molecular characterization of pathogen-derived EV will generate large databases, such as EVpedia<sup>93</sup>, with a wide range of omics data ready to be investigated *in silico*. Computer-based models can search all available pathogen specific EV-associated molecules for family members with immunomodulatory potential that are conserved between different pathogens, and directly point toward interesting molecules for further functional studies. Increasing the knowledge on pathogen-derived EV-associated molecules and their effects on the host immune system will certainly shed further light on the importance of EV molecules in infection biology.

## Author contributions

MK wrote the manuscript. EN-‘tH, CH, and HS initiated and edited the manuscript. All authors read and approved the final manuscript.

## Funding

This work was supported by grants from NWO Graduate School Program 022.006.010 (to MK); ZonMW-Vidi 20972 (to HS); the European Research Council under the European Union’s Seventh Framework Programme [FP/2007–2013]/ERC Grant Agreement No. 337581 (to EN-‘tH).

## References

1. Takeuchi, O. & Akira, S. Pattern recognition receptors and inflammation. *Cell* **140**, 805–820 (2010).
2. Kumar, H., Kawai, T. & Akira, S. Pathogen recognition by the innate immune system. *Int Rev Immunol* **30**, 16–34 (2011).
3. Blander, J. M. & Sander, L. E. Beyond pattern recognition: five immune checkpoints for scaling the microbial threat. *Nat Rev Immunol* **12**, 215–225 (2012).
4. Santos, A. S. & Finlay, B. B. Bringing down the host: enteropathogenic and enterohaemorrhagic *Escherichia coli* effector-mediated subversion of host innate immune pathways. *Cell Microbiol* **17**, 318–332 (2015).
5. Poole, J., Day, C. J., von Itzstein, M., Paton, J. C. & Jennings, M. P. Glycointeractions in bacterial pathogenesis. *Nat Rev Microbiol* **16**, 440–452 (2018).
6. Yanez-Mo, M. *et al.* Biological properties of extracellular vesicles and their physiological functions. *J Extracell Vesicles* **4**, 27066 (2015).
7. Record, M., Carayon, K., Poirot, M. & Silvente-Poirot, S. Exosomes as new vesicular lipid transporters involved in cell-cell communication and various pathophysiologies. *Biochim Biophys Acta* **1841**, 108–120 (2014).
8. Nolte-’t Hoen, E. N. & Wauben, M. H. Immune cell-derived vesicles: modulators and mediators of inflammation. *Curr Pharm Des* **18**, 2357–2368 (2012).
9. Gerlach, J. Q. & Griffin, M. D. Getting to know the extracellular vesicle glycome. *Mol Biosyst* **12**, 1071–1081 (2016).
10. Costa, J. Glycoconjugates from extracellular vesicles: Structures, functions and emerging potential as cancer biomarkers. *Biochim Biophys Acta Rev Cancer* **1868**, 157–166 (2017).
11. Thery, C., Ostrowski, M. & Segura, E. Membrane vesicles as conveyors of immune responses. *Nature Reviews Immunology* **9**, 581–593 (2009).
12. Robbins, P. D. & Morelli, A. E. Regulation of immune responses by extracellular vesicles. *Nat Rev Immunol* **14**, 195–208 (2014).
13. Tkach, M. & Thery, C. Communication by Extracellular Vesicles: Where We Are and Where We Need to Go. *Cell* **164**, 1226–1232 (2016).
14. Wendler, F. *et al.* Extracellular vesicles swarm the cancer microenvironment: from tumor–stroma communication to drug intervention. *Oncogene* **36**, 877–884 (2017).
15. Bruno, S., Deregibus, M. C. & Camussi, G. The secretome of mesenchymal stromal cells: Role of extracellular vesicles in immunomodulation. *Immunol Lett* **168**, 154–158 (2015).
16. Lener, T. *et al.* Applying extracellular vesicles based therapeutics in clinical trials – an ISEV position paper. *J Extracell Vesicles* **4**, 30087 (2015).
17. Stephen, J. *et al.* Mesenchymal stromal cells as multifunctional cellular therapeutics – a potential role for extracellular vesicles. *Transfus Apher Sci* **55**, 62–69 (2016).
18. Chatterjee, S. N. & Das, J. Electron microscopic observations on the excretion of cell-wall material by *Vibrio cholerae*. *J Gen Microbiol* **49**, 1–11 (1967).

19. Devoe, I. W. & Gilchrist, J. E. Release of endotoxin in the form of cell wall blebs during in vitro growth of *Neisseria meningitidis*. *J Exp Med* **138**, 1156–1167 (1973).

20. Takeo, K., Uesaka, I., Uehira, K. & Nishiura, M. Fine structure of *Cryptococcus neoformans* grown in vivo as observed by freeze-etching. *J Bacteriol* **113**, 1449–1454 (1973).

21. Senft, A. W., Philpott, D. E. & Pelofsky, A. H. Electron microscope observations of the integument, flame cells, and gut of *Schistosoma mansoni*. *J Parasitol* **47**, 217–229 (1961).

22. Threadgold, L. T. The ultrastructure of the ‘cuticle’ of *Fasciola hepatica*. *Exp Cell Res* **30**, 238–242 (1963).

23. Schooling, S. R. & Beveridge, T. J. Membrane vesicles: an overlooked component of the matrices of biofilms. *J Bacteriol* **188**, 5945–5957 (2006).

24. Renelli, M., Matias, V., Lo, R. Y. & Beveridge, T. J. DNA-containing membrane vesicles of *Pseudomonas aeruginosa* PAO1 and their genetic transformation potential. *Microbiology* **150**, 2161–2169 (2004).

25. Mashburn-Warren, L. M. & Whiteley, M. Special delivery: vesicle trafficking in prokaryotes. *Mol Microbiol* **61**, 839–846 (2006).

26. Dorward, D. W. & Garon, C. F. DNA Is Packaged within Membrane-Derived Vesicles of Gram-Negative but Not Gram-Positive Bacteria. *Appl Environ Microbiol* **56**, 1960–1962 (1990).

27. Rodrigues, M. L. *et al.* Vesicular polysaccharide export in *Cryptococcus neoformans* is a eukaryotic solution to the problem of fungal trans-cell wall transport. *Eukaryot Cell* **6**, 48–59 (2007).

28. Silverman, J. M. *et al.* An exosome-based secretion pathway is responsible for protein export from *Leishmania* and communication with macrophages. *J Cell Sci* **123**, 842–852 (2010).

29. Mantel, P. Y. *et al.* Malaria-infected erythrocyte-derived microvesicles mediate cellular communication within the parasite population and with the host immune system. *Cell Host Microbe* **13**, 521–534 (2013).

30. Goncalves, D. D. *et al.* Extracellular vesicles and vesicle-free secretome of the protozoa *Acanthamoeba castellanii* under homeostasis and nutritional stress and their damaging potential to host cells. *Virulence* **9**, 818–836 (2018).

31. Schwab, A. *et al.* Extracellular vesicles from infected cells: potential for direct pathogenesis. *Front Microbiol* **6**, 1132 (2015).

32. Nolte-’t Hoen, E., Cremer, T., Gallo, R. C. & Margolis, L. B. Extracellular vesicles and viruses: Are they close relatives? *Proc Natl Acad Sci U S A* **113**, 9155–9161 (2016).

33. Rodriguez, G. M. & Prados-Rosales, R. Functions and importance of mycobacterial extracellular vesicles. *Appl Microbiol Biotechnol* **100**, 3887–3892 (2016).

34. Szempruch, A. J., Dennison, L., Kieft, R., Harrington, J. M. & Hajduk, S. L. Sending a message: extracellular vesicles of pathogenic protozoan parasites. *Nat Rev Microbiol* **14**, 669–675 (2016).

35. van Niel, G., D’Angelo, G. & Raposo, G. Shedding light on the cell biology of extracellular vesicles. *Nat Rev Mol Cell Biol* **19**, 213–228 (2018).

36. Colombo, M., Raposo, G. & Thery, C. Biogenesis, secretion, and intercellular interactions of exosomes and other extracellular vesicles. *Annu Rev Cell Dev Biol* **30**, 255–289 (2014).

37. Ostrowski, M. *et al.* Rab27a and Rab27b control different steps of the exosome secretion pathway. *Nat Cell Biol* **12**, 13–19 (2010).

2

38. de la Torre-Escudero, E., Bennett, A. P. S., Clarke, A., Brennan, G. P. & Robinson, M. W. Extracellular Vesicle Biogenesis in Helminths: More than One Route to the Surface? *Trends Parasitol* **32**, 921–929 (2016).
39. Bayer-Santos, E. *et al.* Proteomic analysis of *Trypanosoma cruzi* secretome: characterization of two populations of extracellular vesicles and soluble proteins. *J Proteome Res* **12**, 883–897 (2013).
40. Silverman, J. M. *et al.* Proteomic analysis of the secretome of *Leishmania donovani*. *Genome Biol* **9**, R35 (2008).
41. Atayde, V. D. *et al.* Exosome Secretion by the Parasitic Protozoan *Leishmania* within the Sand Fly Midgut. *Cell Rep* **13**, 957–967 (2015).
42. Mantel, P. Y. & Marti, M. The role of extracellular vesicles in *Plasmodium* and other protozoan parasites. *Cell Microbiol* **16**, 344–354 (2014).
43. Rodrigues, M. L., Godinho, R. M. C., Zamith-Miranda, D. & Nimrichter, L. Traveling into Outer Space: Unanswered Questions about Fungal Extracellular Vesicles. *PLoS Pathog* **11**, e1005240 (2015).
44. Brown, L., Wolf, J. M., Prados-Rosales, R. & Casadevall, A. Through the wall: extracellular vesicles in Gram-positive bacteria, mycobacteria and fungi. *Nat Rev Microbiol* **13**, 620–630 (2015).
45. Pathirana, R. D. & Kaparakis-Liaskos, M. Bacterial membrane vesicles: Biogenesis, immune regulation and pathogenesis. *Cell Microbiol* **18**, 1518–1524 (2016).
46. Jain, S. & Pillai, J. Bacterial membrane vesicles as novel nanosystems for drug delivery. *Int J Nanomedicine* **12**, 6329–6341 (2017).
47. O'Donoghue, E. J. & Krachler, A. M. Mechanisms of outer membrane vesicle entry into host cells. *Cell Microbiol* **18**, 1508–1517 (2016).
48. Broz, P. & Monack, D. M. Newly described pattern recognition receptors team up against intracellular pathogens. *Nat Rev Immunol* **13**, 551–565 (2013).
49. Hashimoto, M. *et al.* Characterization of outer membrane vesicles of *Acetobacter pasteurianus* NBRC3283. *J Biosci Bioeng* **125**, 425–431 (2018).
50. Canas, M. A., Fabrega, M. J., Gimenez, R., Badia, J. & Baldoma, L. Outer Membrane Vesicles From Probiotic and Commensal *Escherichia coli* Activate NOD1-Mediated Immune Responses in Intestinal Epithelial Cells. *Front Microbiol* **9**, 498 (2018).
51. Zhang, H. *et al.* Identification of distinct nanoparticles and subsets of extracellular vesicles by asymmetric flow field-flow fractionation. *Nat Cell Biol* **20**, 332–343 (2018).
52. Deo, P. *et al.* Outer membrane vesicles from *Neisseria gonorrhoeae* target PorB to mitochondria and induce apoptosis. *PLoS Pathog* **14**, e1006945 (2018).
53. Kunsmann, L. *et al.* Virulence from vesicles: Novel mechanisms of host cell injury by *Escherichia coli* O104:H4 outbreak strain. *Scientific Reports* **5**, 13252 (2015).
54. Rivera, J. *et al.* *Bacillus anthracis* produces membrane-derived vesicles containing biologically active toxins. *Proc Natl Acad Sci U S A* **107**, 19002–19007 (2010).
55. Davis, J. M., Carvalho, H. M., Rasmussen, S. B. & O'Brien, A. D. Cytotoxic necrotizing factor type 1 delivered by outer membrane vesicles of uropathogenic *Escherichia coli* attenuates polymorphonuclear leukocyte antimicrobial activity and chemotaxis. *Infect Immun* **74**, 4401–4408 (2006).

56. Bomberger, J. M. *et al.* A *Pseudomonas aeruginosa* toxin that hijacks the host ubiquitin proteolytic system. *PLoS Pathog* **7**, e1001325 (2011).

57. Bomberger, J. M. *et al.* *Pseudomonas aeruginosa* Cif protein enhances the ubiquitination and proteasomal degradation of the transporter associated with antigen processing (TAP) and reduces major histocompatibility complex (MHC) class I antigen presentation. *J Biol Chem* **289**, 152–162 (2014).

58. Schaar, V. *et al.* Multicomponent *Moraxella catarrhalis* outer membrane vesicles induce an inflammatory response and are internalized by human epithelial cells. *Cell Microbiol* **13**, 432–449 (2011).

59. Chen, F. *et al.* Outer membrane vesicle-associated lipase FtlA enhances cellular invasion and virulence in *Francisella tularensis* LVS. *Emerg Microbes Infect* **6**, e66 (2017).

60. Hassani, K., Shio, M. T., Martel, C., Faubert, D. & Olivier, M. Absence of metalloprotease GP63 alters the protein content of *Leishmania* exosomes. *PLoS One* **9**, e95007 (2014).

61. Ghosh, J., Bose, M., Roy, S. & Bhattacharyya, S. N. *Leishmania donovani* targets Dicer1 to downregulate miR-122, lower serum cholesterol, and facilitate murine liver infection. *Cell Host Microbe* **13**, 277–288 (2013).

62. Chaiyadet, S. *et al.* Carcinogenic Liver Fluke Secretes Extracellular Vesicles That Promote Cholangiocytes to Adopt a Tumorigenic Phenotype. *J Infect Dis* **212**, 1636–1645 (2015).

63. Vidakovics, M. L. *et al.* B cell activation by outer membrane vesicles—a novel virulence mechanism. *PLoS Pathog* **6**, e1000724 (2010).

64. Muralinath, M., Kuehn, M. J., Roland, K. L. & Curtiss 3rd, R. Immunization with *Salmonella enterica* serovar Typhimurium-derived outer membrane vesicles delivering the pneumococcal protein PspA confers protection against challenge with *Streptococcus pneumoniae*. *Infect Immun* **79**, 887–894 (2011).

65. Vanaja, S. K. *et al.* Bacterial Outer Membrane Vesicles Mediate Cytosolic Localization of LPS and Caspase-11 Activation. *Cell* **165**, 1106–1119 (2016).

66. Santos, J. C. *et al.* LPS targets host guanylate-binding proteins to the bacterial outer membrane for non-canonical inflammasome activation. *EMBO J* **37**, (2018).

67. Acevedo, R. *et al.* Bacterial outer membrane vesicles and vaccine applications. *Front Immunol* **5**, 121 (2014).

68. Zariri, A. *et al.* Meningococcal Outer Membrane Vesicle Composition-Dependent Activation of the Innate Immune Response. *Infect Immun* **84**, 3024–3033 (2016).

69. Simbari, F. *et al.* Plasmalogen enrichment in exosomes secreted by a nematode parasite versus those derived from its mouse host: implications for exosome stability and biology. *J Extracell Vesicles* **5**, 30741 (2016).

70. Peres da Silva, R. *et al.* Extracellular vesicles from *Paracoccidioides* pathogenic species transport polysaccharide and expose ligands for DC-SIGN receptors. *Sci Rep* **5**, 14213 (2015).

71. Twu, O. *et al.* *Trichomonas vaginalis* exosomes deliver cargo to host cells and mediate host-parasite interactions. *PLoS Pathog* **9**, e1003482 (2013).

2

72. Nowacki, F. C. *et al.* Protein and small non-coding RNA-enriched extracellular vesicles are released by the pathogenic blood fluke *Schistosoma mansoni*. *J Extracell Vesicles* **4**, 28665 (2015).
73. Samoil, V. *et al.* Vesicle-based secretion in schistosomes: Analysis of protein and microRNA (miRNA) content of exosome-like vesicles derived from *Schistosoma mansoni*. *Sci Rep* **8**, 3286 (2018).
74. Stevenson, T. C. *et al.* Immunization with outer membrane vesicles displaying conserved surface polysaccharide antigen elicits broadly antimicrobial antibodies. *Proc Natl Acad Sci U S A* **115**, E3106–E3115 (2018).
75. Kaparakis, M. *et al.* Bacterial membrane vesicles deliver peptidoglycan to NOD1 in epithelial cells. *Cell Microbiol* **12**, 372–385 (2010).
76. Williams, C. *et al.* Glycosylation of extracellular vesicles: current knowledge, tools and clinical perspectives. *J Extracell Vesicles* **7**, 1442985 (2018).
77. Escrevente, C., Keller, S., Altevogt, P. & Costa, J. Interaction and uptake of exosomes by ovarian cancer cells. *BMC Cancer* **11**, 108 (2011).
78. Staubach, S., Schadewaldt, P., Wendel, U., Nohroudi, K. & Hanisch, F. G. Differential glycomics of epithelial membrane glycoproteins from urinary exovesicles reveals shifts toward complex-type N-glycosylation in classical galactosemia. *J Proteome Res* **11**, 906–916 (2012).
79. Gerlach, J. Q. *et al.* Surface glycosylation profiles of urine extracellular vesicles. *PLoS One* **8**, e74801 (2013).
80. Blenkiron, C. *et al.* Uropathogenic *Escherichia coli* Releases Extracellular Vesicles That Are Associated with RNA. *PLoS One* **11**, e0160440 (2016).
81. Koeppen, K. *et al.* A Novel Mechanism of Host-Pathogen Interaction through sRNA in Bacterial Outer Membrane Vesicles. *PLoS Pathog* **12**, e1005672 (2016).
82. Peres da Silva, R. *et al.* Extracellular vesicle-mediated export of fungal RNA. *Scientific Reports* **5**, 7763 (2015).
83. Bernal, D. *et al.* Surface analysis of *Dicrocoelium dendriticum*. The molecular characterization of exosomes reveals the presence of miRNAs. *J Proteomics* **105**, 232–241 (2014).
84. Buck, A. H. *et al.* Exosomes secreted by nematode parasites transfer small RNAs to mammalian cells and modulate innate immunity. *Nat Commun* **5**, 5488 (2014).
85. Garcia-Silva, M. R. *et al.* Gene expression changes induced by *Trypanosoma cruzi* shed microvesicles in mammalian host cells: relevance of tRNA-derived halves. *Biomed Res Int* **2014**, 305239 (2014).
86. Hansen, E. P., Kringel, H., Williams, A. R. & Nejsum, P. Secretion of RNA-Containing Extracellular Vesicles by the Porcine Whipworm, *Trichuris suis*. *J Parasitol* **101**, 336–340 (2015).
87. Zamanian, M. *et al.* Release of Small RNA-containing Exosome-like Vesicles from the Human Filarial Parasite *Brugia malayi*. *PLoS Negl Trop Dis* **9**, e0004069 (2015).
88. Zhu, L. *et al.* Molecular characterization of *S. japonicum* exosome-like vesicles reveals their regulatory roles in parasite-host interactions. *Sci Rep* **6**, 25885 (2016).
89. Mateescu, B. *et al.* Obstacles and opportunities in the functional analysis of extracellular vesicle RNA – an ISEV position paper. *J Extracell Vesicles* **6**, 1286095 (2017).

90. Lotvall, J. *et al.* Minimal experimental requirements for definition of extracellular vesicles and their functions: a position statement from the International Society for Extracellular Vesicles. *J Extracell Vesicles* **3**, 26913 (2014).

91. Van Deun, J. *et al.* EV-TRACK: transparent reporting and centralizing knowledge in extracellular vesicle research. *Nat Methods* **14**, 228–232 (2017).

92. Bryant, W. A. *et al.* In Silico Analysis of the Small Molecule Content of Outer Membrane Vesicles Produced by *Bacteroides thetaiotaomicron* Indicates an Extensive Metabolic Link between Microbe and Host. *Front Microbiol* **8**, 2440 (2017).

93. Kim, D.-K. *et al.* EVpedia: an integrated database of high-throughput data for systemic analyses of extracellular vesicles. *J Extracell Vesicles* **2**, (2013)



## Chapter 3

# Optimized protocol for the isolation of extracellular vesicles from the parasitic worm *Schistosoma mansoni* with improved purity, concentration and yield

Marije E. Kuipers, Roman I. Koning, Erik Bos, Cornelis H. Hokke, Hermelijn H. Smits, Esther N. M. Nolte-’t Hoen

Journal of Immunology Research, 2022

PMID: 35434142

DOI: [10.1155/2022/5473763](https://doi.org/10.1155/2022/5473763)

## Abstract

In the past decade, the interest in helminth-derived extracellular vesicles (EVs) increased owing to their role in pathogen-host communication. However, the availability of EVs from these parasitic worms is often limited due to the restricted occurrence and culturing possibilities of these organisms. *Schistosoma mansoni* is one of several helminths that have been shown to release EVs affecting the immune response of their host. Further investigation of mechanisms underlying these EV-induced effects warrants separation of EVs from other components of the helminth excretory/secretory products. However, isolation of high-purity EVs often come to the expense of reduced EV yield. We therefore aimed to develop an optimized protocol for isolation of EVs from *S. mansoni* schistosomula and adult worms with respect to purity, concentration and yield. We tested the use of small (1.7 ml) iodixanol density gradients and demonstrated that this enabled western blot-based analysis of the EV marker protein tetraspanin-2 (TSP-2) in gradient fractions without additional concentration steps. Moreover, the concentration and yield of EVs obtained with small iodixanol gradients were higher compared to medium-sized (4.3 ml) or conventional large-sized (12 ml) gradients. Additionally, we provide evidence that iodixanol is preferred over sucrose as medium for the small density gradients, because EVs in iodixanol gradients reached equilibrium much faster (2 hours) and iodixanol but not sucrose was suitable for purification of schistosomula EVs. Finally, we demonstrate that the small iodixanol gradients were able to separate adult worm EVs from non-EV contaminants such as the blood digestion product hemozoin. Our optimized small iodixanol density gradient allows to simultaneously separate and concentrate EVs while reducing handling time and EV loss, and can be applied for EVs from helminths and other limited EV sources.

## Introduction

Extracellular vesicles (EVs) are nanosized, lipid bilayer-enclosed particles containing (glycosylated)proteins, lipids and RNAs that are released into the extracellular space by virtually all cells and organisms. EVs are widely investigated for their role in communication between cells in various diseases<sup>1-3</sup>, in host-pathogen interactions<sup>4,5</sup>, and for their biomarker or therapeutic potential<sup>6-8</sup>. EVs from parasitic worms have emerged as important players in host-pathogen interactions and their role in parasitic diseases warrants extensive investigations<sup>9</sup>. Research on such EVs faces many technical challenges<sup>9-11</sup>.

To characterize their molecular composition and function, EVs need to be isolated from biological fluids and separated from large molecular (lipo)protein complexes that overlap in size and/or buoyant density<sup>12</sup>. These purification steps generally reduce EV yield<sup>13,14</sup> and it has been shown that adsorption of EVs to plastic surfaces, e.g. from (ultra)centrifugation tubes, results in EV loss over time<sup>15</sup>. This loss of EVs could be compensated by increasing the starting material, but this poses an extra challenge when working with limited material, such as parasites. Additionally, the complex life cycle of helminths poses a technical challenge for EV research in this area. The life cycles of many helminths depend on mammalian and intermediate hosts and one of these helminths is *Schistosoma mansoni*. Obtaining the different schistosome life stages for culture and subsequent EV isolation is challenging due to limited availability of larvae and the restricted amount of parasites obtained from sacrificed infected animals<sup>16</sup>. The schistosomula are transformed cercarial larvae that can only be obtained from an infected intermediate snail host. Adult worms are obtained from perfusion of the portal venous system of mice or hamsters infected with cercarial larvae, and eggs can be isolated from enzymatically digested liver and gut tissue from the infected animals. EVs are released by all three life stages as part of the complex excretory/secretory (ES) products released by *S. mansoni*<sup>17-19</sup>. Studying their EVs requires separation from other proteins and lipids in these ES products. ES from blood feeding parasites, amongst which is *S. mansoni*, also contains digestion products of blood that the adult worms regurgitate when they are cultured *ex vivo* in serum-free medium<sup>20,21</sup>. One of these products is hemozoin, a non-toxic, insoluble and crystallized form of the otherwise toxic heme.

The discovery of (glyco)proteins and RNAs that are specifically enriched in schistosome EVs will accelerate research on how these EVs interact with and manipulate their hosts and on the biomarker potential of these EVs. This kind of research, however, demands the acquisition of sufficient amounts of highly purified EVs. We aimed to develop an optimized method for separating adult worm and schistosomula EVs from non-EV contaminants while keeping the EV yield as

high as possible. We propose the use of small sized iodixanol density gradients to increase concentration and yield of obtained EV isolates while reducing handling time.

## Materials and methods

### Parasite culture

The life cycle of *S. mansoni* (Puerto Rican strain) was maintained in golden Syrian hamsters (HsdHan-Aura) and *Biomphalaria glabrata* snails as previously described<sup>22</sup>. All hamster experiments were performed in accordance with the Guide for the Care and Use of Laboratory Animals of the Institute for Laboratory Animal Research and have received approval from the university Ethical Review Board (Leiden University Medical Center, Leiden, The Netherlands). Cercariae from shed snails were washed with >25 ml cold DMEM (high glucose with L-glutamine, Lonza, Basel, Switzerland) supplemented with Antibiotic Antimycotic Solution (ABAM, Sigma-Aldrich, St. Louis, MO, USA) in a 30 µm pluriStrainer (pluriSelect, Leipzig, Germany) and subsequently resuspended in 12 ml warm medium (37 °C) and transformed to schistosomula by pipetting with a 10 ml serological pipet and incubation at 37 °C for 20 minutes. Schistosomula (cercariae without tails) were collected using an orbital shaker and cultured at 37 °C and 5% CO<sub>2</sub> for three days in DMEM+ABAM at 7,500 schistosomula/ml in 25 cm<sup>2</sup> polystyrene flasks (Greiner Bio-One, Alphen a/d Rijn, The Netherlands).

Obtained adult worms (mixed sex) from perfused hamsters were washed five times or more with >25 ml DMEM+ABAM supplemented with 10 mM HEPES (pH7.4). Residual hair and tissue, blot clots, and dead worms were removed. Worms were cultured in DMEM+ABAM+HEPES for two days at 37 °C and 5% CO<sub>2</sub> and at 10 worms/ml in 75 cm<sup>2</sup> polystyrene flasks (Corning, Sigma-Aldrich) with a maximum of 40 ml/flask. Viability of the worms was ensured during and after culture by visual inspection of worm movement and attachment of the worms' sucker to the flask bottom.

### Differential ultracentrifugation (dUC)

Culture medium of the schistosomula and adult worms was collected in 15 ml tubes and 50 ml tubes (Greiner Bio-One), respectively, and centrifuged twice at 200 × *g* and twice at 500 × *g*, all for 10 minutes and at 4 °C with low brake (SX4750A rotor and an Allegra X-15R centrifuge) (Beckman Coulter, Brea, CA, USA). After each centrifugation step, supernatants were transferred to a new tube using a serological pipet. The 500 × *g* supernatants were centrifuged (all in 15 ml tubes) 30 minutes at 5,000 × *g* (SX4750A rotor) and 4 °C (max brake). The 5,000 ×

*g* supernatants were stored at -80 °C till further use.

The frozen 5,000  $\times$  *g* supernatants (11–66 mL) were thawed overnight at 4 °C, transferred to polypropylene tubes and ultracentrifuged for 65 minutes 4 °C, at 28,000 rpm (~100,000  $\times$  *g*, k-factor 265) in an XE-90 centrifuge using an SW 41 Ti rotor (Beckman Coulter). Subsequently, supernatant was aspirated until the liquid surface reached the conical part of the tube. If this was the final spin, the rest of the supernatant was decanted after which the walls of the tube were wiped dry with a tissue while holding the tube upside down. When a washing step was performed, pellets were resuspended in supernatant remaining in the conical part of the tube, pooled to one tube, topped up with cold PBS (B. Braun, Melsungen, Germany) and spun as before. This washing step was then repeated once more followed by the steps for the final spin. Final EV-enriched pellets were resuspended in PBS or PBS supplemented with 0.2% BSA (Sigma-Aldrich), which was made from a 5% BSA in PBS stock that was cleared from protein aggregates by overnight ultracentrifugation at 100,000  $\times$  *g*. Washed UC pellets for cryo electron microscopy of schistosomula were prepared as described in<sup>23</sup>.

### Size Exclusion Chromatography (SEC)

The SEC column (qEVoriginal, 70 nm, IZON Science LTD, Christchurch, Aotearoa-New Zealand) was washed with 10 ml PBS at room temperature. Subsequently, 170  $\mu$ l of ultra-filtrated adult worm culture ES, corresponding to material from ~100 worms, was loaded onto the column followed by addition of 10 ml PBS, after which 25 consecutive eluted fractions of 500  $\mu$ l were collected. Fractions were stored at -20 °C till preparation for SDS-PAGE.

### Density gradient ultracentrifugation

UC pellets from 11–30 ml adult worm or 40 ml schistosomula culture supernatants were resuspended in a final volume of 70  $\mu$ l PBS+0.2% BSA. For bottom-up iodixanol gradient centrifugation, the resuspended EV pellet was mixed gently with 60% iodixanol (Optiprep, Axis-Shield PoC AS, Oslo, Norway) and blocks of 40%, 30% and 10% were carefully layered on top using a plastic Pasteur pipet. The volumes used for small, medium and large gradients are displayed in Table 1. Iodixanol dilutions were made from a 50% dilution and PBS. For the sucrose gradients, a 2.5 M D(+)-Sucrose (Biochemica, PanReac AppliChem, Darmstadt, Germany) stock solution was prepared and from that 2 M and 0.4 M dilutions were made to prepare 14 linear dilutions as described previously<sup>24</sup>. 70  $\mu$ l of EV pellet was mixed gently with 320  $\mu$ l 2.5 M sucrose within the small UC tube. Subsequently, 14 fractions with decreasing sucrose densities (from 1.886 M to 0.4 M sucrose) of 105  $\mu$ l were carefully added. For top-down centrifugation, the

**Table 1. Iodixanol gradient volumes and centrifugation details**

		Gradient build (iodixanol)				
		EV sample ( $\mu$ L)	60% ( $\mu$ L)	40% ( $\mu$ L)	30% ( $\mu$ L)	10% ( $\mu$ L)
large	SW 41 Ti	70	3,200	1,600	1,600	5,500
medium	SW 55 Ti	70	1,100	550	550	1,980
small	TLS-55	70	440	220	220	792

rotor type	rpm	average g-force	k-factor	Centrifugation time (h)	total gradient volume ( $\mu$ L)	fraction volume ( $\mu$ L) (12x)
SW 41 Ti	37,000	169,044	152	>16	11,970	997
SW 55 Ti	42,000	169,639	82	>15	4,250	354
TLS-55	50,000	166,180	60	2	1,742	145

gradients were built with equal iodixanol or sucrose volumes first after which 70  $\mu$ L EVs suspensions were carefully added on top of the 10% iodixanol or 0.4 M sucrose.

Centrifugation times of large (SW 41 Ti), medium (SW 55 Ti) and small (TLS-55) gradients can be found in Table 1. Centrifugation time for the small sucrose gradients was either two or 13.5 hours on similar speed as the iodixanol small gradient. All were centrifuged in thin-wall polypropylene tubes, at 4 °C with slow acceleration and slow deceleration. SW 41 Ti and SW 55 Ti rotors were used in an XE-90 ultracentrifuge and the TLS-55 rotor in an Optima TLX (Beckman Coulter). Volumes of collected fractions of the iodixanol gradients are mentioned in Table 1. The volume of sucrose gradient fractions was 155  $\mu$ L. Collected fractions were kept on ice, vortexed, and 15  $\mu$ L per fraction was used to measure their refractive index (RI) by a CETI refractometer (Medline Scientific, Chalgrove, UK). Densities were calculated with the formulas  $(3,35 \times (RI)) - 3,4665$  and  $(2,6448 \times (RI)) - 2,5263$  for iodixanol and sucrose, respectively.

When comparing the different tube sizes, culture medium of the same worm culture was used and EV pellets were pooled and split evenly before building the gradients and each gradient consisted of EV material from 11 ml medium. For the washing of iodixanol density gradient fractions, two fractions were pooled: 400  $\mu$ L per pool for the medium gradient and 1,650  $\mu$ L per pool for the large gradient in SW41 and SW32 sized polypropylene tubes, respectively. Tubes were topped up with cold PBS (diluting the gradient fractions ~22 $\times$ ) supplemented with 0.1% BSA (from 5% BSA stock) or with plain PBS. Samples were centrifuged for 65 minutes, 4 °C, at 32,000 rpm in an XE-90 centrifuge (average  $126,444 \times g$  and k-factor 203 for SW 41 Ti and average  $125,755 \times g$  and k-factor 204 for SW 32 Ti) after which

the obtained pellets were resuspended in a volume of 1× sample buffer equal to the pooled small gradient fractions. Samples were stored at -20 °C until SDS-PAGE.

### Ultra-filtration

Adult worm culture medium from ~1,100 worms was centrifuged once at 200 × *g* and the supernatant was concentrated in 3 or 10 kDa filter tubes (Amicon Ultra, Millipore, Merck, Darmstadt, Germany) according to the manufacturer's protocol. ES in the filters was washed 3 times with PBS and finally concentrated to a volume of 1,870 µl, of which aliquots were stored at -80 °C till further use.

Fractions 5–8 with a density 1.21–1.07 g/ml of bottom-up small iodixanol density gradient isolated adult worm EVs (from ~660 worms) were pooled, diluted 1:1 with PBS, and transferred into an 0.5 ml 10 kDa centrifugal filter unit (Amicon Ultra, Millipore, Merck) that was pre-coated with 20 µg trypsin-digested BSA. Iodixanol was removed in 5 centrifugation steps of 10 minutes at 14,000 × *g*, by which the sample was fully loaded after three steps followed by two additional washing steps with 300–400 µl PBS. The sample was concentrated to 50 µl by a final centrifugation step of 20 minutes. This final sample was collected by brief reverse centrifugation of the filter and directly used for cryo electron microscopy (EM).

### Cryo Electron Microscopy (cryo-EM)

300 mesh EM grids (Quantifoil R2/2, Jena, Germany) were glow-discharged by 0.2 mbar air for two minutes using the glow discharger unit of an EMITECH K950X. Three µl of sample was applied per glow-discharged grid and the grid was vitrified using an EMGP (Leica, Wetzlar, Germany) at room temperature and 100% humidity. For vitrification, excess sample was removed by blotting for one second to Whatman #1 filter paper directly followed by plunging the grid into liquid ethane (-183 °C) after which the grid was stored under liquid nitrogen till further use. Cryo-EM imaging was performed at 120 kV on a Tecnai 12 electron microscope (Thermo Fisher Scientific, Waltham, MA, USA) after mounting the grid in a Gatan 626 cryo-holder. A 4k×4k Eagle camera (Thermo Fisher Scientific) was used to record images with focus between 5–10 µm and an 18,000 × magnification (pixel size 1.2 nm).

### Trichloroacetic acid (TCA) precipitation

Iodixanol density fractions were mixed with 2% (w/v) Na-deoxycholate (added 1:117) and proteins were precipitated by mixing each fraction with cold 100% (w/v) trichloroacetic acid (TCA) (added 1:10) and a 15 minutes incubation on ice. Eppendorf tubes were centrifuged at maximum speed (16,100 × *g*) for 10 minutes

at 4 °C and supernatant was discarded. Eppendorf tubes were spun briefly again to allow removal of all remaining supernatant. Protein pellets were subsequently mixed with 100% ice cold acetone (similar volume as original gradient fraction) and incubated for >10 minutes at -20 °C and centrifuged as before. This acetone washing step was repeated after which the samples were dried at room temperature for 5 minutes. Fractions were mixed with 200 µl (large gradient fractions) or 100 µl (medium and small gradient fractions) 1× unreduced sample buffer.

## Western Blotting

SEC fractions were thawed and vortexed before mixing with 4× Laemmli sample buffer under non-reducing conditions. Iodixanol and sucrose density fractions were either directly mixed with 4× sample buffer or after pooling and washing by UC. All samples were incubated 3 min 100 °C directly after mixing with sample buffer, stored at -20 °C, and incubated again at 100 °C before loading on the SDS-PAGE gel. All samples were loaded 15 µl per lane, with an exception for the TCA samples of the small and medium gradient fractions, which were loaded 2 µl per lane. Samples and 1.5 µl of ladder (PageRuler Plus, Thermo Fisher Scientific) were separated on 12.5% gels, which were subsequently blotted onto methanol activated PVDF membranes. Membranes were blocked with PBS supplemented with 0.1% (v/v) Tween-20 and 0.2% (w/v) gelatin from cold water fish skin (Sigma-Aldrich) and overnight incubated with TSP2-2D6 (mouse IgG, 1:2,000) (kind gift from prof. Alex Loukas, James Cook University, Australia) monoclonal antibody. Incubated blots were washed several times with blocking buffer and incubated 45 minutes with Goat- $\alpha$ Mouse-IgG-HRP (1:10,000, Promega, Leiden, The Netherlands) and washed again extensively. Chemiluminescence substrate (SuperSignal West Pico PLUS, Thermo Fisher Scientific) was applied and Alliance Q9 (UVITEC, Cambridge, UK) imaged blots were analyzed and signals quantified in Fiji/ImageJ<sup>25</sup>.

## Results

### Worm EV isolates obtained by differential ultracentrifugation and size exclusion chromatography contain non-EV contaminants

We first tested two size-based separation methods, differential (ultra) centrifugation (dUC) and size exclusion chromatography (SEC), for isolation of EVs released by *Schistosoma* adult worms. As an indicator for the presence of EVs we used western blot analysis for *S. mansoni* tetraspanin-2 (TSP-2), which is one of the most abundant proteins identified in adult worm EVs<sup>26,27</sup>. Both in the EV-enriched 100,000  $\times$  g pellet obtained by dUC and in the EV-enriched

SEC fractions, we confirmed the presence of TSP-2 containing schistosome EVs (Figures 1a, 1c). However, we observed brown coloring of both the UC pellet and the EV-containing SEC fractions (Figures 1b, 1d). We suspected that this was due to contamination with the blood digestion product hemozoin, which is pigmented and colors the worm gut dark and culture medium light brown. We confirmed the presence of hemozoin crystals in  $100,000 \times g$  EV pellets by cryo electron microscopy (cryo-EM) and observed that these crystals overlapped in size with the adult worm EV (Figure 1e). This suggests that small hemozoin crystals, and possibly also other non-EV particles<sup>21</sup>, sedimented at similar  $g$ -forces as the worm EVs and could not be separated from EVs based on size differences. The hemozoin contamination was specific for adult worm EV isolates, as EV-enriched dUC pellets from schistosomula did not contain hemozoin (Figure 1f). This was expected because schistosomula are transformed from larvae released by snails and cultures of these worms do not contain blood-digestion products. These data indicate that for the design of a protocol that allows purification of EVs from both schistosome life stages, size-based separation methods do not suffice and should be combined with density gradient centrifugation.

## The use of small density gradients increases EV concentration and yield

When separation based on size is insufficient, EVs can be further purified using density gradient centrifugation<sup>12,14,28</sup>. An unwanted consequence of conventional density gradient separation, however, is the dilution of EVs in relatively large volumes of gradient medium. As a consequence, additional concentrating steps are required for further analysis of the EVs. This can be achieved by ultracentrifugation, after pooling the EV-containing density gradient fractions in a larger UC tube, dilution with PBS, and re-pelleting by UC<sup>28</sup>. This step can cause loss of EVs via adsorption to tube walls and handling time, though the addition of BSA to the PBS may reduce some of the loss<sup>15</sup>. Because loss of EVs is particularly undesirable when working with limited worm-derived material, we aimed to optimize density gradient based EV isolation for low-input material. We hypothesized that using a small volume density gradient in a small tube will reduce EV loss by decreasing the plastic surface area to which EVs may be adsorbed<sup>15</sup>. In addition, the shorter centrifugation time needed for EVs to reach their equilibrium density in these small tubes reduces exposure time of EVs to the plastic surfaces. Finally, a small gradient introduces a concentrating factor of the EVs as fraction volumes will be smaller. We compared EV isolation efficiency in conventional large-sized (12 ml) and medium-sized (4.3 ml) gradients to a small-sized (1.7 ml) gradient. All three iodixanol gradients were built according to a similar set-up (see Table 1)

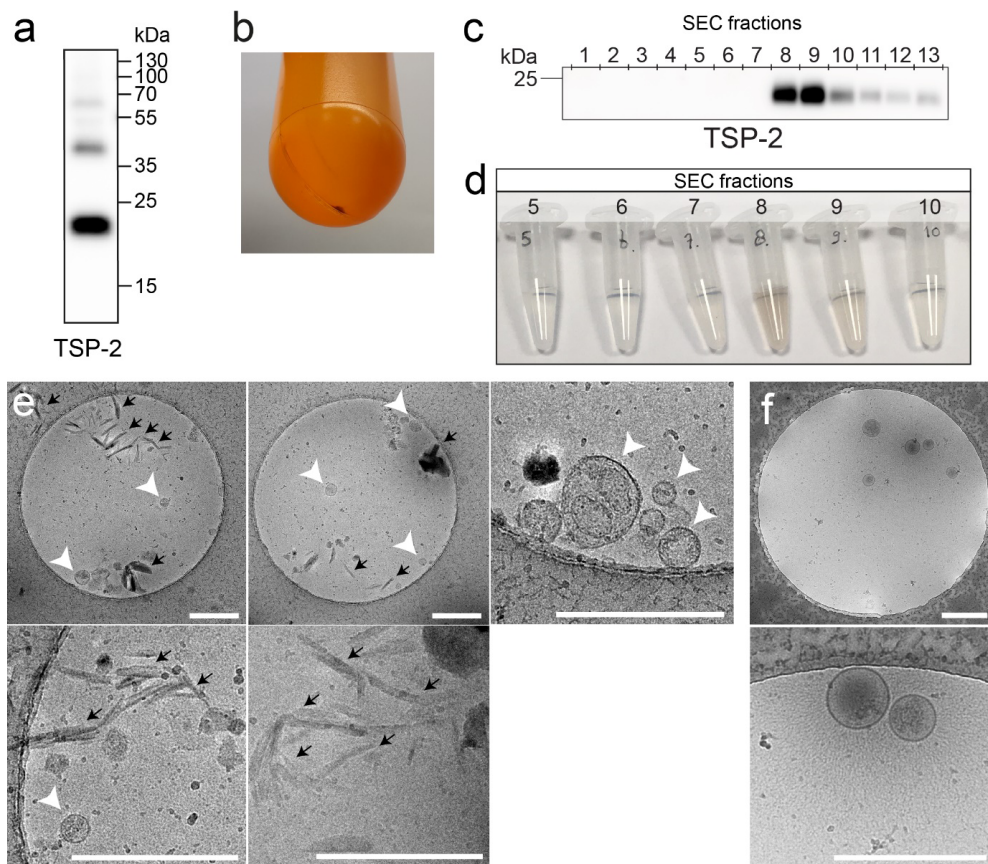


**Figure 1. Adult worm EV isolates prepared by differential (ultra)centrifugation (dUC) or size exclusion chromatography (SEC) are contaminated by hemozoin**

Culture supernatant of adult worms was subjected to dUC (a, b, e) or SEC (c, d). (a) Western blot detection of the schistosome EV marker tetraspanin-2 (TSP-2) in 100,000  $\times g$  pelleted adult worm EVs. (b) Black 100,000  $\times g$  pellet of adult worm EVs indicates the presence of hemozoin. Collected SEC fractions from adult worm ES released by ~100 worms shows similar fractions containing TSP-2 (c) and hemozoin (brown fractions in d). (e) Cryo-EM analysis of washed 100,000  $\times g$  pellet from 22 ml adult worm culture shows EVs (white arrowheads) and co-isolated hemozoin crystals (black arrows). (f) Cryo-EM analysis shows that pelleted schistosomula EVs from 15 ml culture medium, with characteristic 'hair-like' filaments on their surface, do not contain hemozoin crystals. Scale bars (e, f) are 500 nm.

but the large and medium gradients were centrifuged for >16 hours<sup>28</sup> and the small gradient was centrifuged for two hours<sup>29</sup>. These centrifugation times were sufficient for EVs to float to the ~1.07–1.10 g/ml density fractions, as based on western blot detection of schistosome TSP-2 (Figure 2a).

Next, we assessed whether the smaller gradient size reduced adult worm EV loss and enabled western blot-based analysis of EV proteins in gradient fractions without additional concentration steps. To be able to accurately compare EV concentrations within the gradient fractions, adult worm EVs from the same worm culture were equally divided over the three differently sized gradients. After centrifugation, 12 equal volume fractions were collected from each gradient and two consecutive fractions were pooled to allow all EV containing fractions (F5–F10) from the three different gradients to be loaded on the same SDS-page gel. First, the pools of gradient fractions were directly mixed with sample buffer, subjected to SDS-PAGE, and analyzed by western blotting for the presence of TSP-2 (Figure 2b). We observed that the concentration in the fractions of the medium and large sized gradients was 41–56% and 90–94% lower compared to the small gradients, respectively (Figure 2c). Thus, the small gradient allows western blot analysis of EV proteins without the need to concentrate the density fractions before gel loading.

Next, we tested the effect of concentration steps on EV recovery from fractions of the medium and large gradients. Based on previous indications that this loss could be reduced in the presence of BSA, the EV containing density fractions were diluted in PBS or PBS supplemented with BSA prior to re-pelleting of EVs by UC. EV pellets were resuspended in the same volume as the pooled fractions from the small gradient. Western blotting of TSP-2 showed that concentrating the pooled fractions in the presence of BSA resulted in 8–20% lower concentration of EVs from the medium gradient and 24–73% lower concentration for the EVs from the large gradient, as compared to the small gradient fractions (Figure 2d). Concentration in the absence of BSA led to an almost complete loss of EVs. Thus, the small gradient is superior over the other sized gradients in EV concentration and yield while the handling time is reduced.

### Iodixanol but not sucrose density gradients are suitable for purification of adult worm and schistosomula EVs

We aimed to optimize an EV purification protocol suitable for EVs of both adult worms and schistosomula. To verify whether both types of EVs reached equilibrium density within 2 hours of centrifugation in these small gradients, we compared loading the gradients on top of the EV-enriched pellets (EVs floating ‘bottom-up’) to loading the EVs on top of the gradients (EVs floating ‘top-down’). TSP-2

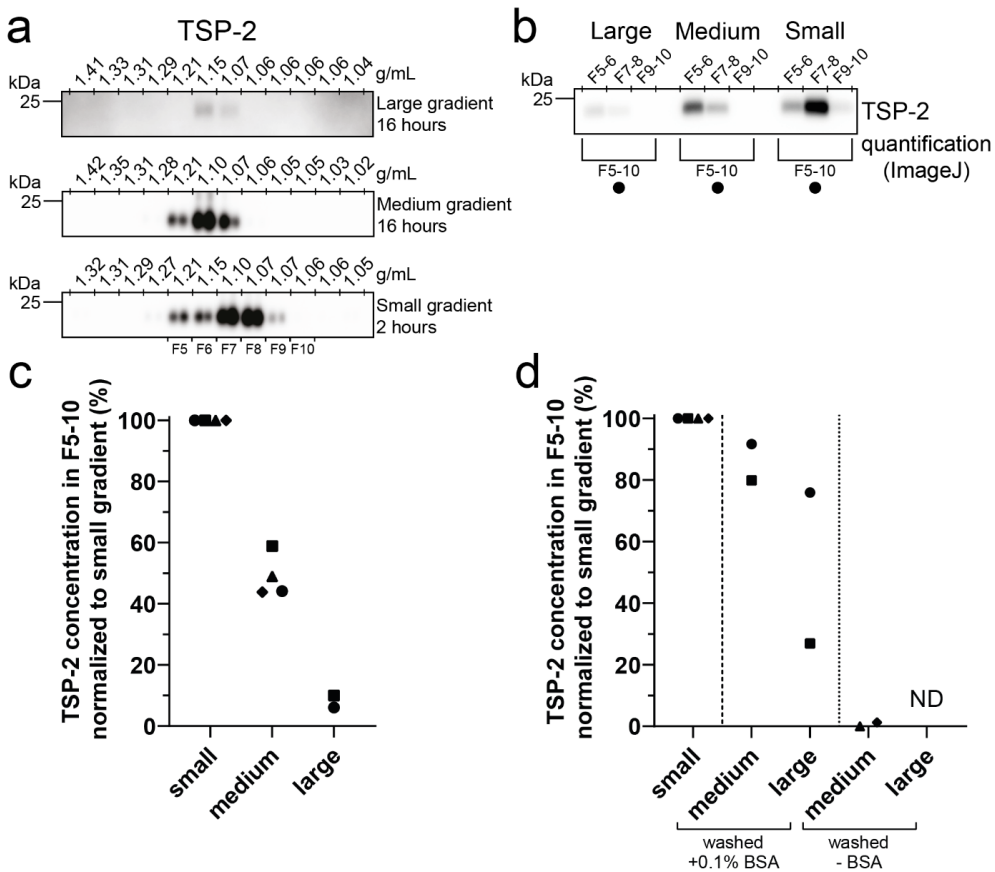


**Figure 2. Comparative detection of adult worm EVs isolated with three different sizes iodixanol density gradients**

(a) Western blot detection of tetraspanin-2 (TSP-2) in TCA precipitated protein isolates of fractions from adult worm EVs floated bottom-up into large (12 ml), medium (4.3 ml) or small (1.7 ml) iodixanol gradients. (b) Equal  $100,000 \times g$  EV-enriched pellets of the same adult worm cultures were loaded in the three differently sized gradients. EV-containing fractions were pooled and directly mixed with sample buffer for SDS-PAGE to compare TSP-2 detection by western blot. (c) Quantification of TSP-2 band intensities of western blots in (b). (d) EVs in pooled fractions of medium and large gradients were diluted in PBS with or without 0.1%BSA, re-pelleted by UC, and concentrated to equal volumes as the small gradient fractions. TSP-2 levels in concentrated EV isolates from medium- and large-sized gradients were compared to EV isolates taken directly from the small density gradient. TSP-2 western blot and quantification were performed as in b. Data in a and b is representative for 2-4 independent experiments. Each symbol in c and d corresponds to an independent experiment.

detection in collected fractions showed that both schistosomula and adult worm EVs concentrated in fractions with densities characteristic for EVs (1.08–1.16 g/ml) and that this was similar in bottom-up or top-down loaded gradients (Figure 3a, b), indicating that equilibrium densities were reached.

Another widely used density gradient medium is sucrose and we additionally tested whether EVs from both schistosome life stages could also be isolated by a small sucrose gradient. However, two hours of centrifugation was not sufficient for the adult worm EVs to reach equilibrium density in bottom-up sucrose gradients (Figure 3c). Under these conditions, part of the TSP-2 remained in the fractions with higher densities, suggesting that the EVs needed more time to reach the lower densities. Indeed, 13.5 hours centrifugation of the bottom-up gradient was needed for the adult worm EVs to reach the 1.12–1.16 g/ml density fractions (Figure 3c). In contrast to the EVs from the adult worms, sucrose gradients were less effective in purification of schistosomula EVs. In both bottom-up and top-down sucrose gradients, the schistosomula EVs ended up in fractions with higher densities (between 1.21 and 1.28 g/ml) compared to iodixanol gradients (Figure 3d). This is undesirable, since various non-EV contaminants also remain in the bottom fractions of gradients. These data suggest that the small iodixanol gradients are most optimal and time-efficient for purifying EVs from both life stages of *S. mansoni*.

### **Small iodixanol density gradients separate EVs from non-EV contaminants**

Finally, we verified whether the small iodixanol gradients allowed separation of EVs from non-EV contaminants (Figure 1). We selected hemozoin as detectable example for non-EV contaminants, since markers for other protein contaminants are currently lacking for *Schistosoma* spp. UC pellets of adult worm culture supernatant were overlaid with the optimized small iodixanol density gradient. After two hours centrifugation we observed a black substance in the bottom of the gradient, suggesting the presence of hemozoin (Figure 4a). Cryo-EM analysis of EV containing fractions (1.07–1.21 g/ml) confirmed the absence of hemozoin among the high number of adult worm EVs in these gradient fractions (Figure 4b). These data indicate that the small iodixanol density gradient allowed successful separation of EVs from non-EV particles such as hemozoin. We propose that small-sized (1.7 ml) iodixanol density gradients can be used to simultaneously separate and concentrate EVs from limited sources, such as helminths, to increase EV yield while reducing handling time.

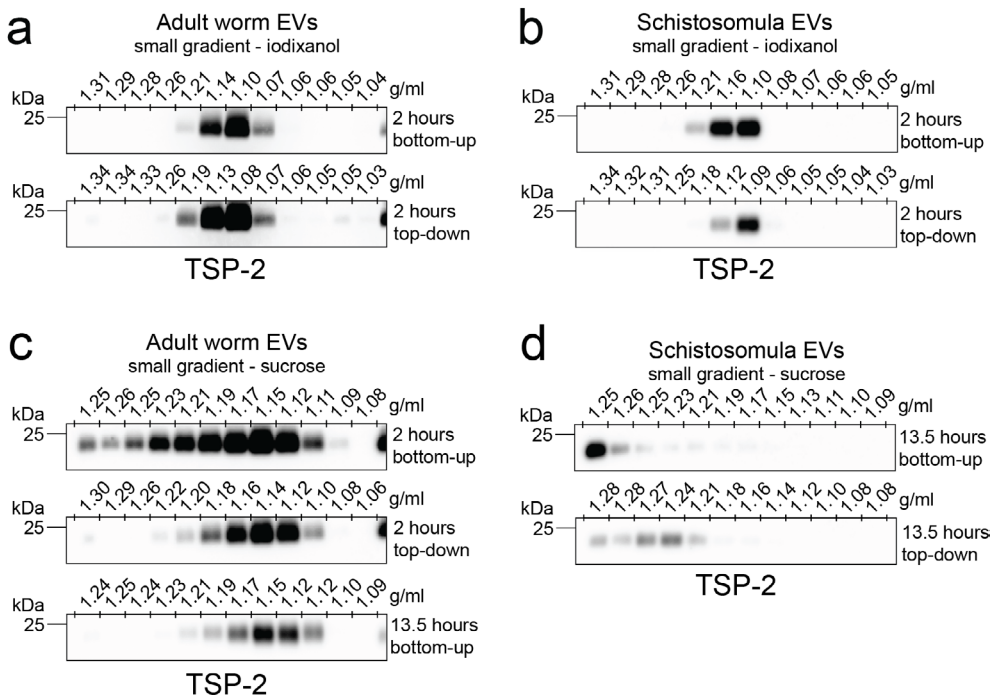


**Figure 3. Iodixanol gradients are preferred over sucrose gradients for purification of adult worm and schistosomula EVs**

EV-enriched UC pellets of adult worm EVs (a) or schistosomula EVs (b) were loaded at the bottom (bottom-up) or on top (top-down) of a small iodixanol density gradient and centrifuged for two hours. Western blot analysis of collected density fractions for the EV marker TSP-2 shows that both EV types reached equilibrium densities in the small gradients. (c) Adult worm EVs were loaded at the bottom or top of small sucrose density gradients. Shown are western blot detections of TSP-2 in fractions collected from two and 13.5 hours centrifuged sucrose density gradients. (d) Top-down and bottom-up sucrose gradients were used to purify schistosomula EVs. Shown are western blot detections of TSP-2 in fractions collected from 13.5 hours centrifuged gradients. Gradients were loaded with material from 11 or 10 ml culture medium from the adult worms or schistosomula, respectively. Western blots shown are representative for 2-3 independent experiments.

## Discussion

Each EV source has its own challenge for obtaining a high quality EV preparation with sufficient material for downstream analysis and these challenges often include the separation of EVs from non-EV contaminants<sup>30</sup>. For *Schistosoma mansoni* parasites, these non-EV contaminants include many released ES

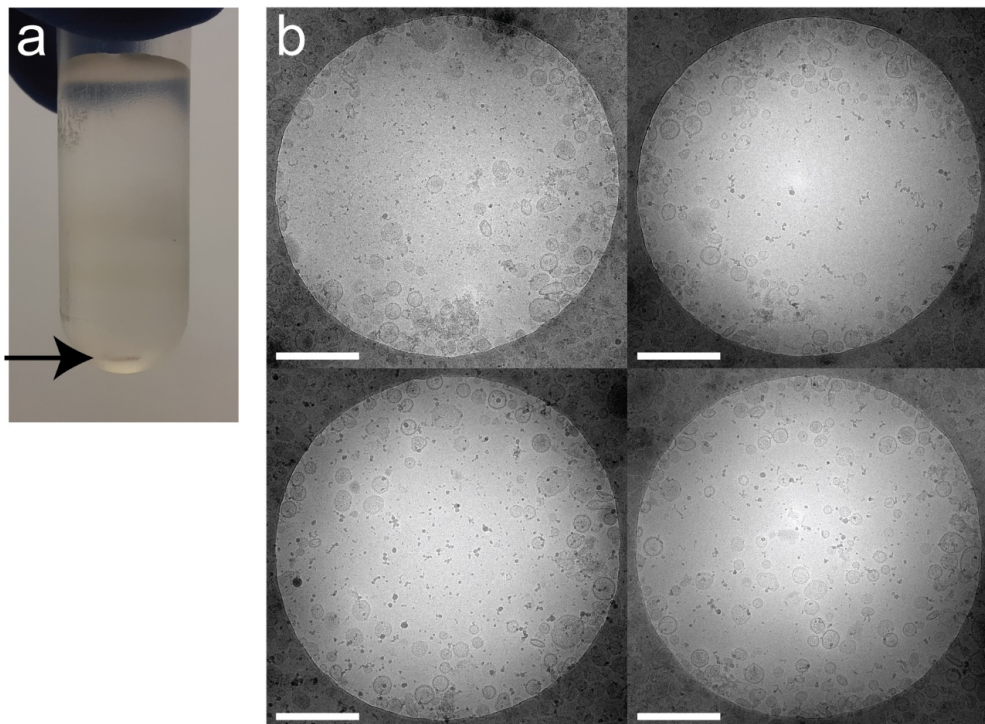


**Figure 4. Small iodixanol gradient separates adult worm EVs from non-EV contaminants**  
Adult worm EV-enriched UC pellets were overlaid with a small (1.7 ml) iodixanol density gradient and centrifuged for two hours. (a) The gradient after centrifugation shows hemozoin (black arrow) in the bottom of the tube. (b) Cryo-EM analysis of washed iodixanol gradient fractions with density 1.07–1.21 g/ml shows that EV-enriched fractions of the small gradients are devoid of hemozoin crystals. Scale bars are 500 nm.

components<sup>17,18</sup> and for adult worms also the blood-digestion product hemozoin<sup>31</sup>. Both non-EV ES components and hemozoin are unwanted in EV-preparations, especially when studying host-pathogen interactions as they can affect host immune responses<sup>32,33</sup>. Additional challenges for studying EVs from *S. mansoni* are imposed by the complex life cycle of this parasite. Not only do the different life stages of the parasite release EVs with different characteristics (Figure 1e-f and<sup>23</sup>), there is also limited availability of each life stage, thus restricting the material to isolate EVs from. This latter restriction makes any loss of EVs during the isolation process highly undesirable. Here, we propose the use of small iodixanol density gradients to increase EV yield compared to larger sized gradients for separating EVs from non-EV contaminants. This protocol is applicable to EVs from the different *S. mansoni* life stages and EVs from other limited sources.

Methods that separate structures based on size, such as dUC and SEC, were not sufficient to separate adult worm EVs from contaminating particles such as hemozoin crystals (Figure 1). Previously, SEC was proposed as a promising method for helminth EVs<sup>11</sup>. In that study, dUC and SEC were compared for isolation of EVs from *Fasciola hepatica*. Since *F. hepatica* lives in the bile duct and consumes local cells and bile instead of red blood cells for survival, there will be no hemozoin among the non-EV contaminants. However, SEC often dilutes the sample and EVs may be lost upon subsequent concentration steps, which would be unwanted for limited EV sources. Furthermore, a combination of size- and density-based separation methods is preferred to prepare EV populations to the highest purity<sup>14,28,30,34</sup>.

Both sucrose and iodixanol are used as gradient media for density-based isolation of EVs. Studies comparing iodixanol and sucrose density gradients for isolation of mammalian EVs showed no clear differences in densities the EVs ended up in<sup>35,36</sup>. We here provide evidence that the type of gradient medium can strongly influence in which density fraction the *S. mansoni* EVs are concentrated and that this differs between EVs from the different parasite life stages. Our data show that the EVs from schistosomula, in contrast to EVs from adult worms, did not float to the characteristic EV density fractions (~1.10–1.17 g/ml) in sucrose gradients (Figure 3d). Yet, these two types of EVs floated to similar density fractions in the iodixanol gradients. The preferential localization of schistosomula EVs in high sucrose densities may possibly be linked to the unique filamentous structures on the schistosomula EV surface of which the actual molecular structure remains unknown<sup>23</sup>. We speculate that these structures contain glycans and/or mucins that interact with the sucrose, thereby influencing their localization in the gradient. There are several advantages of iodixanol over sucrose gradients for the purification of EVs. Iodixanol is isosmotic and isotonic, which is better to preserve EV structure and function. Moreover, iodixanol is far less toxic to cells than sucrose and therefore more suitable to study EV function. Our data substantiates the advantages of iodixanol over sucrose since iodixanol gradients allowed purification of EVs released by both *S. mansoni* life stages and allowed EVs to reach equilibrium density within shorter centrifugation times.

To our knowledge, this is the first report on utilizing small gradients for EV isolation, even though such gradients have been used for isolation of (multi)-protein complexes<sup>29,37,38</sup>. In these smaller gradients, EVs reach their equilibrium density after shorter centrifugation times than in conventional large volume gradients, which reduces handling time. Moreover, EVs are concentrated in a smaller volume, which makes it more feasible to directly subject density fractions to western blot analysis without additional concentration steps that may cause EV loss<sup>15</sup>. Another possible benefit of concentrated EV in small volume iodixanol density fractions

is that these fractions could be directly added to cells, but this has not yet been studied. Though iodixanol is non-toxic, potential side-effects on cell functions would need to be controlled for. Of note, our proposed small iodixanol gradient was optimized for isolation of schistosome EVs. The exact construction of the gradient may need to be adjusted for optimal separation of EVs from other sources. Therefore, we highly encourage researchers to adjust their own established gradients to smaller sized tubes.

EV research in the last decade taught us that choosing an appropriate EV isolation method is guided by both the research question and the type of source material. Our optimized protocol increases the concentration and yield of highly purified EVs from *S. mansoni* life stages. This may accelerate research and discoveries in the field including EV-induced immune modulatory mechanisms and EV-associated biomarkers.

## EV-TRACK

We have submitted all relevant data of our experiments to the EV-TRACK knowledgebase (EV-TRACK ID: EV220119)<sup>39</sup>.

## Acknowledgements

The authors would like to thank Jan de Best and the rest of the life-cycle team for maintaining the availability of *S. mansoni* parasites, Professor Alex Loukas from James Cook University, Queensland (Australia) for providing the TSP-2-targeting antibodies, Sjaak van Voorden and the rest of the Medical Microbiology department (LUMC) for using their refractometer, Uvitec Alliance, ultracentrifuges and rotors, and Dr George MC Janssen of the Center for Proteomics and Metabolomics of the LUMC for providing trypsin-digested BSA.

## Funding

This work was supported by grants from Nederlandse Organisatie voor Wetenschappelijk Onderzoek (NWO) Graduate School Program[022.006.010] (to M.E.K.); the European Research Council under the European Union's Seventh Framework Programme [FP/2007–2013]/ERC Grant Agreement[No. 337581] (to E.N.-‘tH.).

## Author's contributions

M.E.K. contributed to conceiving the study, designed experiments, performed the parasite cultures, EV isolations and western blots, data analysis and drafting of the manuscript. R.I.K. and E.B. performed the cryo-EM imaging and provided feedback on the manuscript. H.H.S. and C.H.H. both contributed to conceiving

the study, interpretation of results and correcting the manuscript. E.N.-'tH. contributed to conceiving the study, designed experiments, interpretation of the results and drafting of the manuscript. All authors read and approved the final manuscript.

## References

1. Nolte-'t Hoen, E. N. & Wauben, M. H. Immune cell-derived vesicles: modulators and mediators of inflammation. *Curr Pharm Des* **18**, 2357–2368 (2012).
2. Tkach, M. & Thery, C. Communication by Extracellular Vesicles: Where We Are and Where We Need to Go. *Cell* **164**, 1226–1232 (2016).
3. Urabe, F., Patil, K., Ramm, G. A., Ochiya, T. & Soekmadji, C. Extracellular vesicles in the development of organ-specific metastasis. *Journal of Extracellular Vesicles* **10**, (2021).
4. Kuipers, M. E., Hokke, C. H., Smits, H. H. & Hoene, E. N. M. N. ' Pathogen-Derived Extracellular Vesicle-Associated Molecules That Affect the Host Immune System: An Overview. *Frontiers in Microbiology* **9**, 2182 (2018).
5. Saad, M. H., Badierah, R., Redwan, E. M. & El-Fakharany, E. M. A comprehensive insight into the role of exosomes in viral infection: Dual faces bearing different functions. *Pharmaceutics* **13**, 1405 (2021).
6. Hoshino, A. *et al.* Extracellular Vesicle and Particle Biomarkers Define Multiple Human Cancers. *Cell* **182**, 1044–1061.e18 (2020).
7. Driedonks, T. A. P. *et al.* Y-RNA subtype ratios in plasma extracellular vesicles are cell type- specific and are candidate biomarkers for inflammatory diseases. *Journal of Extracellular Vesicles* **9**, (2020).
8. Elsharkasy, O. M. *et al.* Extracellular vesicles as drug delivery systems: Why and how? *Advanced Drug Delivery Reviews* **159**, 332–343 (2020).
9. Sánchez-López, C. M., Treliis, M., Bernal, D. & Marcilla, A. Overview of the interaction of helminth extracellular vesicles with the host and their potential functions and biological applications. *Molecular Immunology* **134**, 228–235 (2021).
10. Zakeri, A., Hansen, E. P., Andersen, S. D., Williams, A. R. & Nejsum, P. Immunomodulation by Helminths: Intracellular Pathways and Extracellular Vesicles. *Front Immunol* **9**, 2349 (2018).
11. Davis, C. N. *et al.* The importance of extracellular vesicle purification for downstream analysis: A comparison of differential centrifugation and size exclusion chromatography for helminth pathogens. *PLoS neglected tropical diseases* **13**, (2019).
12. Arab, T. *et al.* Proteomic characterisation of leech microglia extracellular vesicles (EVs): comparison between differential ultracentrifugation and Optiprep™ density gradient isolation. <https://doi.org/10.1080/20013078.2019.1603048> **8**, (2019).
13. Cvjetkovic, A., Lötvall, J. & Lässer, C. The influence of rotor type and centrifugation time on the yield and purity of extracellular vesicles. *Journal of Extracellular Vesicles* **3**, (2014).
14. Onódi, Z. *et al.* Isolation of high-purity extracellular vesicles by the combination of iodixanol density gradient ultracentrifugation and bind-elute chromatography from blood plasma. *Frontiers in Physiology* **9**, (2018).
15. Evtushenko, E. G., Bagrov, D. V., Lazarev, V. N., Livshits, M. A. & Khomyakova, E. Adsorption of extracellular vesicles onto the tube walls during storage in solution. *PLoS ONE* **15**, (2020).
16. Lombardo, F. C., Pasche, V., Panic, G., Endriss, Y. & Keiser, J. Life cycle maintenance and drug-sensitivity assays for early drug discovery in *Schistosoma mansoni*. *Nature Protocols* **14**, 461–481 (2019).

3

17. Maizels, R. M., Smits, H. H. & McSorley, H. J. Modulation of Host Immunity by Helminths: The Expanding Repertoire of Parasite Effector Molecules. *Immunity* **49**, 801–818 (2018).
18. Giera, M. et al. The *Schistosoma mansoni* lipidome: Leads for immunomodulation. *Analytica Chimica Acta* **1037**, 107–118 (2018).
19. Mossallam, S. F., Abou-El-naga, I. F., Bary, A. A., Elmorsy, E. A. & Diab, R. G. *Schistosoma mansoni* egg-derived extracellular vesicles: A promising vaccine candidate against murine schistosomiasis. *PLoS neglected tropical diseases* **15**, (2021).
20. Skelly, P. J., Da'dara, A. A., Li, X. H., Castro-Borges, W. & Wilson, R. A. Schistosome Feeding and Regurgitation. *PLoS Pathogens* **10**, e1004246 (2014).
21. Hall, S. L. et al. Insights into blood feeding by schistosomes from a proteomic analysis of worm vomitus. *Molecular and Biochemical Parasitology* **179**, 18–29 (2011).
22. Van Dam, G. J., Bogitsh, B. J., Van Zeyl, R. J. M., Rotmans, J. P. & Deelder, A. M. *Schistosoma mansoni*: In vitro and in vivo excretion of CAA and CCA by developing schistosomula and adult worms. *Journal of Parasitology* **82**, 557–564 (1996).
23. Kuipers, M. E. et al. DC-SIGN mediated internalisation of glycosylated extracellular vesicles from *Schistosoma mansoni* increases activation of monocyte-derived dendritic cells. *J Extracell Vesicles* **9**, 1753420 (2020).
24. van der Vlist, E. J., Nolte-'t Hoen, E. N., Stoorvogel, W., Arkesteijn, G. J. & Wauben, M. H. Fluorescent labeling of nano-sized vesicles released by cells and subsequent quantitative and qualitative analysis by high-resolution flow cytometry. *Nat Protoc* **7**, 1311–1326 (2012).
25. Schindelin, J. et al. Fiji: an open-source platform for biological-image analysis. *Nat Methods* **9**, 676–682 (2012).
26. Sotillo, J. et al. Extracellular vesicles secreted by *Schistosoma mansoni* contain protein vaccine candidates. *Int J Parasitol* **46**, 1–5 (2016).
27. Kifle, D. W. et al. Proteomic analysis of two populations of *Schistosoma mansoni*-derived extracellular vesicles: 15k pellet and 120k pellet vesicles. *Mol Biochem Parasitol* **236**, 111264 (2020).
28. Brennan, K. et al. A comparison of methods for the isolation and separation of extracellular vesicles from protein and lipid particles in human serum. *Scientific Reports* **2020 10:1** **10**, 1–13 (2020).
29. Aibara, S., Andréll, J., Singh, V. & Amunts, A. Rapid Isolation of the Mitoribosome from HEK Cells. *Journal of visualized experiments: JoVE* (2018) doi:10.3791/57877.
30. Théry, C. et al. Minimal information for studies of extracellular vesicles 2018 (MISEV2018): a position statement of the International Society for Extracellular Vesicles and update of the MISEV2014 guidelines. <https://doi.org/10.1080/20013078.2018.1535750> **7**, (2018).
31. Xiao, S. hua & Sun, J. *Schistosoma* hemozoin and its possible roles. *International Journal for Parasitology* **47**, 171–183 (2017).
32. Truscott, M., Evans, D. A., Gunn, M. & Hoffmann, K. F. *Schistosoma mansoni* hemozoin modulates alternative activation of macrophages via specific suppression of Retnla expression and secretion. *Infection and Immunity* **81**, 133–142 (2013).

33. Coakley, G., Buck, A. H. & Maizels, R. M. Host parasite communications—Messages from helminths for the immune system: Parasite communication and cell–cell interactions. *Mol Biochem Parasitol* **208**, 33–40 (2016).

34. Vergauwen, G. *et al.* Robust sequential biophysical fractionation of blood plasma to study variations in the biomolecular landscape of systemically circulating extracellular vesicles across clinical conditions. *Journal of extracellular vesicles* **10**, (2021).

35. Krishn, S. R. *et al.* Prostate cancer sheds the  $\alpha v\beta 3$  integrin in vivo through exosomes. *Matrix biology: journal of the International Society for Matrix Biology* **77**, 41–57 (2019).

36. Paolini, L. *et al.* Residual matrix from different separation techniques impacts exosome biological activity. *Scientific reports* **6**, (2016).

37. Tanese, N. Small-scale density gradient sedimentation to separate and analyze multiprotein complexes. *Methods: A Companion to Methods in Enzymology* **12**, 224–234 (1997).

38. Bagnat, M., Keränen, S., Shevchenko, A., Shevchenko, A. & Simons, K. Lipid rafts function in biosynthetic delivery of proteins to the cell surface in yeast. *Proceedings of the National Academy of Sciences* **97**, 3254–3259 (2000).

39. Van Deun, J. *et al.* EV-TRACK: transparent reporting and centralizing knowledge in extracellular vesicle research. *Nat Methods* **14**, 228–232 (2017).



## Chapter 4

# Life stage-specific glycosylation of extracellular vesicles from *Schistosoma mansoni* schistosomula and adult worms drives differential interaction with C-type lectin receptors DC-SIGN and MGL

Marije E. Kuipers, D. Linh Nguyen, Angela van Diepen,

Lynn Mes, Erik Bos, Roman I. Koning, Esther N.M.

Nolte-'t Hoen, Hermelijn H. Smits\*, Cornelis H. Hokke\*

\*These authors contributed equally to this study

Frontiers in Molecular Biosciences, 2023

PMID: 37006612

DOI : [10.3389/fmolb.2023.1125438](https://doi.org/10.3389/fmolb.2023.1125438)

## Abstract

Schistosomes can survive in mammalian hosts for many years, and this is facilitated by released parasite products that modulate the host's immune system. Many of these products are glycosylated and interact with host cells via C-type lectin receptors (CLRs). We previously reported on specific fucose-containing glycans present on extracellular vesicles (EVs) released by schistosomula, the early juvenile life stage of the schistosome, and the interaction of these EVs with the C-type lectin receptor Dendritic Cell-Specific Intercellular adhesion molecule-3-Grabbing Non-integrin (DC-SIGN or CD209). EVs are membrane vesicles with a size range between 30–1,000 nm that play a role in intercellular and interspecies communication. Here, we studied the glycosylation of EVs released by the adult schistosome worms. Mass spectrometric analysis showed that GalNAc $\beta$ 1–4GlcNAc (LacDiNAc or LDN) containing N-glycans were the dominant glycan type present on adult worm EVs. Using glycan-specific antibodies, we confirmed that EVs from adult worms were predominantly associated with LDN, while schistosomula EVs displayed a highly fucosylated glycan profile. In contrast to schistosomula EV that bind to DC-SIGN, adult worm EVs are recognized by macrophage galactose-type lectin (MGL or CD301), and not by DC-SIGN, on CLR expressing cell lines. The different glycosylation profiles of adult worm- and schistosomula-derived EVs match with the characteristic glycan profiles of the corresponding life stages and support their distinct roles in schistosome life-stage specific interactions with the host.

## Introduction

Parasitic *Schistosoma* worms infect over 200 million people in Africa alone, and many millions more are infected in tropical areas of the Americas, Eastern Mediterranean, and Western Pacific<sup>1</sup>. Infection takes place when cercariae, present in infected water, penetrate the skin and develop into egg producing adult worm pairs. Schistosomiasis is treatable with anti-helminthics but reinfection rates are high in endemic areas and there is no vaccine available yet. One of the reasons that *Schistosoma* infections are chronic if untreated and that effective immunity does not develop, is due to the immune modulatory strategies of the parasite that inhibit the generation of adequate protective immune responses<sup>2</sup>. Studying the interaction of this 'master regulator of the immune system' with its host can lead to new treatment strategies against schistosome infections. Additionally, the identification of immune regulatory mechanisms utilized by schistosomes may help to identify new treatment opportunities for inflammatory disorders<sup>3</sup>.

During each of their life stages schistosomes employ various mechanisms to evade and control host immune responses during an infection. Most of the parasites' immunomodulatory effects are attributed to excretory/secretory (ES) products, including glycosylated proteins and lipids. Via specific glycan motifs, these glycoconjugates are known to interact with a range of C-type lectin receptors (CLRs) mainly present on antigen presenting cells of the host. For example, the glycoprotein omega-1 derived from *S. mansoni* eggs enters monocyte-derived dendritic cells (moDCs) via binding of Gal $\beta$ 1-4(Fuc $\alpha$ 1-3)GlcNAc (Lewis X, Le $x$ ) motifs to the mannose receptor (MR)<sup>4</sup>. Schistosomula ES products have also been shown to interact with various other CLRs such as DCIR and DC-SIGN<sup>5</sup>, which bind to various fucosylated and mannosylated glycans. The schistosome glycan repertoire also includes GalNAc $\beta$ 1-4GlcNAc (LacDiNAc or LDN)-motifs, which can be recognized by the macrophage galactose-type lectin (MGL)<sup>6,7</sup>. Since schistosome glycosylation varies between the different life stages and their ES products, it is likely that differential glycosylation contributes to the differences observed in immune responses induced by schistosomula, adult worms, or eggs.

Recently, we found that the ES products of *S. mansoni* schistosomula contain extracellular vesicles (EVs) that play a role in pathogen-host interaction via uptake by dendritic cells<sup>8</sup>. EVs are lipid membrane vesicles released into the extracellular space by nearly all cells and organisms, including multicellular helminth parasites<sup>9</sup>. Generally, EVs are 30–1,000 nm in diameter with an average between 50–150 nm and can contain proteins, lipids, and nucleic acids, which can induce or affect responses by recipient cells. We showed that schistosomula EVs contain both protein- and lipid-linked glycans<sup>8</sup>, corresponding largely to the overall glycan profile of schistosomula<sup>6</sup>. Many of these glycans were highly fucosylated and a

relatively large proportion carried the  $\text{Le}^x$  trisaccharide, a well-known DC-SIGN ligand. We showed that these glycans mediated schistosomula EV uptake by moDCs mainly via interaction with DC-SIGN, leading to augmented cytokine release by the cells. A role for helminth EV-associated glycans in cellular uptake has also been described for *Fasciola hepatica*-derived EVs that displayed a glycosylation-dependent interaction with monocytes<sup>10</sup>. Similarly, roles for EV glycans in cancer biology are starting to become apparent<sup>11,12</sup>, including their diagnostic potential<sup>13</sup>. However, studies on the role of EV glycosylation in parasite-host interaction and detailed studies of EV glycan structures remain limited<sup>14-16</sup>.

It is known that the overall glycan repertoire of *S. mansoni* differs between larvae and adult worms<sup>6</sup>. To address whether glycosylation of schistosome-derived EVs is also life-stage dependent, we here elucidated the glycan structures of EVs released by *S. mansoni* adult worms using a mass spectrometry (MS) based approach. The differences in EV-associated glycans between adult worms and schistosomula were confirmed using glycan-targeted monoclonal antibodies (moAbs). Finally, we showed that EV surface glycans significantly influence the interaction of EVs with the MGL or DC-SIGN in CLR expressing cell lines. Our findings suggest that life stage-specific glycosylation of EVs by schistosomal larvae and adult worms influences the interaction of these EVs with host cells and subsequent cellular responses.

## Materials and Methods

### Parasite culture

Male and female adult worms from the Puerto Rican-strain of *S. mansoni* were obtained through liver perfusion of golden Syrian hamsters (HsdHan-Aura) 7 weeks post infection, in accordance with the Guide for the Care and Use of Laboratory Animals of the Institute for Laboratory Animal Research and have received approval from the university Ethical Review Board (Leiden University Medical Center, Leiden, The Netherlands). Collected worms were gently washed at least 5 times with 25–40 ml DMEM (high glucose with L-glutamine, Lonza, Basel, Switzerland) supplemented with Antibiotic Antimycotic Solution (Sigma-Aldrich, St. Louis, MO, USA) and 10 mM HEPES pH 7.4. Dead worms, residual hair or tissue and blot clots were removed. 200–400 worms were cultured in polystyrene culture flasks (75 cm<sup>2</sup>) (Corning, Sigma-Aldrich) in a concentration of 10 worms/ml. After 48 hours of culture at 37 °C 5% CO<sub>2</sub>, worms were confirmed being viable by microscope and ES was subsequently collected in 50 ml tubes. The collected ES was centrifuged twice at 200 × g followed by two times at 500 × g (all 10 minutes, 4 °C, slow brake, in an SX4750A rotor in an Allegra X-15 R centrifuge)

(Beckman Coulter, Brea, CA, USA). The final  $500 \times g$  supernatant was transferred to 15 ml tubes and centrifuged 30 minutes at  $5,000 \times g$  ( $4^{\circ}\text{C}$ , max brake) after which the  $5,000 \times g$  supernatant was transferred to new tubes and stored at  $-80^{\circ}\text{C}$  till further use. Cercariae were transformed to schistosomula and cultured as described previously<sup>8</sup>. The ES from 3 day cultured schistosomula was processed and stored similar as the adult worm ES using 15 ml tubes in all steps. As a control, supplemented DMEM without parasites was cultured and processed similarly. A summary of ES processing before EV isolation can be found in Figure 1 (top).

## EV isolation and staining

Figure 1 (bottom) shows a schematic overview of the EV isolation steps described in more detail hereafter. The  $5,000 \times g$  supernatants were thawed overnight at  $4^{\circ}\text{C}$  and transferred to polypropylene tubes (Beckman Coulter). Tubes were centrifuged for 65 minutes in an SW41 Ti rotor at 28,000 rpm (average  $96,808 \times g$ , k-factor 265) at  $4^{\circ}\text{C}$  in an XE90 centrifuge (Beckman Coulter). For one adult worm EV or schistosomula EV isolation, 60 ml (equal to material from 600 worms) or 20 ml (equal to material from 150,000 schistosomula) of  $5,000 \times g$  supernatant was used, respectively. The EV-enriched pellets were resuspended and pooled in 20–60  $\mu\text{l}$  PBS/0.2% BSA (made from 5% BSA in PBS, top 2/3 supernatant from >16 hours centrifuged at 28,000 rpm ( $96,589 \times g$ , k-factor 266) in an SW32 rotor) and transferred to a TLS-55 polypropylene tube. Diluent C was added to the resuspended EV pellet to obtain a total volume of 100  $\mu\text{l}$ , to which 93  $\mu\text{l}$  diluted PKH26 (Sigma-Aldrich) (1.5  $\mu\text{l}$  in 100  $\mu\text{l}$  Diluent C) was added. After 3 minutes, the staining reaction was quenched by the addition of 100  $\mu\text{l}$  RPMI/10% EV depleted

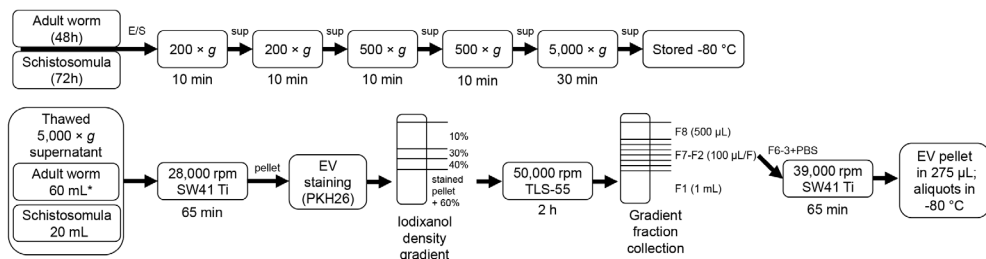


**Figure 1. Schematic overview of ES processing and EV isolation**

Summary of the processing of adult worm and schistosomula ES (top) and subsequent EV isolation (bottom). \*additional details on EV isolation for glycan release and western blotting can be found in the corresponding methods sections. ES, excretory/secretory products; sup, supernatant; min, minutes; h, hours

FCS (top 2/3 supernatant from RPMI/30% FCS centrifuged >16 hours at 28,000 rpm in SW32 rotor). Stained pellets (293  $\mu$ l) were gently mixed with 660  $\mu$ l 60% iodixanol (Optiprep, Axis-Shield PoC AS, Oslo, Norway) and a gradient was built on top with 220  $\mu$ l 40%, 220  $\mu$ l 30%, and 720  $\mu$ l 10% iodixanol. Gradients were centrifuged in an Optima TLX centrifuge (Beckman Coulter) for 2 hours at 50,000 rpm (average  $166,180 \times g$ , k-factor 60) (slow acceleration and deceleration) and 4 °C in a TLS-55 rotor. Fractions were collected from the gradient from top to bottom by pipetting one time 500  $\mu$ l (F8) followed by six times 100  $\mu$ l (F7-2) and a remaining 1 ml bottom fraction (F1). The refractive index (RI) of the fractions were measured with a CETI refractometer (Medline Scientific, Chalgrove, UK) (15  $\mu$ l per fraction) and densities were calculated with the formula  $(3,35 \times (RI)) - 3,4665$ . F6-3 were pooled in an SW41 tube and topped up with cold PBS. The tube was covered with parafilm and decanted for 10 times after which the tube was spun at 39,000 rpm (average  $187,813 \times g$ , k-factor 136) in an SW41 Ti rotor for 65 minutes (4 °C). The purified EV pellet was resuspended in 275  $\mu$ l PBS and aliquots were stored at -80 °C. Medium control was processed similarly as control for unbound dye.

Protein concentration of a thawed aliquot of purified EV was measured according to the manufacturers protocol for microBCA (Pierce, Thermo Fisher Scientific, Waltham, MA, USA). For nanoparticle tracking analysis (NTA), aliquots were thawed from -80 °C and 100 times diluted in PBS directly before NTA measurement. Each sample was recorded three times 30 seconds on camera level 12, 14, and 16 on a NanoSight NS500 (Malvern Panalytical, Malvern, UK) equipped with an sCMOS camera. The analysis and average particle concentration calculation was performed as previously described<sup>8</sup>. All relevant data of our experiments have been submitted to the EV-TRACK knowledgebase (EV-TRACK ID: EV220409)<sup>17</sup>.

## Cryo electron microscopy

EVs were purified on a density gradient as described above. The EV containing fractions with a density between 1.21-1.07 g/ml were pooled (total volume of 580  $\mu$ l) and washed with PBS on a 0.5 ml 10 kDa centrifugal filter (Amicon, Merck KGaA, Darmstadt, Germany) as described<sup>18</sup>. The sample (3  $\mu$ l) was subsequently applied on a 300 mesh EM grid (Quantifoil R2/2, Jena, Germany) that was previously glow-discharged (2 minutes in 0.2 mbar air using a EMITECH K950X with glow discharger unit) and vitrified using an EMGP (Leica, Wetzlar, Germany) at room temperature and 100% humidity. Excess sample was removed by blotting once for 1 second with filter paper (Whatman #1). The blotted grid was plunged into liquid ethane (-183 °C). After vitrification, the grid was stored under liquid nitrogen until further use. The grid was mounted in a Gatan 626 cryo-holder for cryo-EM imaging. Cryo-EM imaging was performed on a Tecnai 12 electron microscope

(FEI Company, Eindhoven, The Netherlands) operated at 120 kV. Images were recorded on a 4k×4k Eagle camera (FEI Company) at 18,000 × magnification (pixel size 1.2 nm) between 5 and 10 µm under focus.

### Glycan release

Iodixanol purified EVs from 600 adult worms were used for the release of total N-glycans as previously described<sup>6</sup>. Briefly, lyophilized EVs were sonicated and denatured before 24 hours N-glycosidase (PNGase) F (4 U/100 µl, Roche Diagnostics, Almere, The Netherlands) treatment. Released N-glycans were isolated and purified using reversed phase (RP) C18-cartridges (JT Baker, Phillipsburg, NJ, USA) loaded with the PNGase F treated sample followed by loading the flow through on carbon cartridges (Supelclean ENVI-carb SPE, Sigma-Aldrich) as described<sup>19</sup>. Additionally, intact purified EVs without prior denaturation were treated with PNGase F for 24 hours at 37 °C, after which the EVs were resuspended with PBS in a TLS-55 tube and spun for 65 min (4 °C) at 42,000 rpm (average 117,553 × g, k-factor 87) in an Optima TLX centrifuge. N-glycans released in this way from the EV surface were isolated from the supernatant and the EV pellet was resuspended and treated as above to obtain the remaining EV associated glycans that were not released by PNGase F. To obtain glycolipid derived glycans, purified as well as enriched adult worm EVs were treated with endo-glycoceramidase as described previously<sup>8</sup>. All isolated glycans were labelled with 2-aminobenzoic acid as described<sup>19</sup>.

### Glycan analysis

Isolated glycans were analyzed using Matrix Assisted Laser Desorption/ Ionisation – Time of flight mass spectrometry (MALDI-TOF-MS) using a Bruker Daltonics UltrafileXtreme® mass spectrometer equipped with a 1 kHz Smartbeam II laser and controlled by the software FlexControl 3.4 Build 119, as previously reported<sup>19</sup>. 2-AA labelled glycans solubilized in MQ were mixed onto a 384-well polished steel target plate with 2,5-dihydroxybenzoic acid (DHB) matrix (#8201346, Bruker Daltonics, 20 mg/ml in 30% ACN) while products of exoglycosidase digestions were directly eluted onto the plate in 50% ACN, 0.1% TFA mixed with DHB (10 mg/ml) at the end of the enzyme removal with C18 Millipore® Zip-Tips. All spectra were obtained in the negative-ion reflectron mode using Bruker® peptide calibration mix (#8206195, Bruker Daltonics) for external calibration. Spectra were obtained over a mass window of  $m/z$  700 – 3500 with ion suppression below  $m/z$  700 for a minimum of 20,000 shots (2000 Hz) obtained by manual selection of “sweet spots”. The software FlexAnalysis (Version 3.4 Build 50) was used for data processing including smoothing of the spectra (Savitzky Golay algorithm, peak

width: *m/z* 0.06, 1 cycle), baseline subtraction (Tophat algorithm) and manual peak picking. Peaks with a signal-to-noise ratio below 3 were excluded as well as known non-glycan peaks or contaminating glucose polymers. Deprotonated masses of the selected peaks were assigned using the GlycoPeakfinder® tool of the free software GlycoWorkBench (Version 3, 29 June 2007)<sup>20</sup>. The 2-AA label was taken into account as a fixed reducing-end modification and possible glycan composition was set up based on available schistosome glycosylation data in the literature<sup>6</sup>. A deviation of 300 ppm was allowed for initial assignment of compositions. Spectral assignments were aided by additional MS/MS measurements, exoglycosidase sequencing, and available published structural data<sup>6</sup>. MS/MS was performed for structural elucidation via fragmentation ion analysis by MALDI-TOF/TOF on selected ions using the UltrafleXtreme® mass spectrometer in negative-ion mode. Confirmation of structures was also aided by treatments of N-glycans with  $\beta$ -N-acetylglucosaminidase from *Streptococcus pneumoniae* and  $\beta$ -N-acetylhexosaminidase from *Streptomyces plicatus* (New England Biolabs, Ipswich, MA, USA; P744, P721, respectively). Enzymatic digestions were performed by digesting 1-2  $\mu$ L of 2-AA labelled glycan overnight at 37 °C in recommended buffer in 10  $\mu$ L total reaction volumes.

## 4

### Western and lectin blotting

EV-enriched pellets from adult worm ES (per gradient from 300-600 worms) or schistosomula ES (per gradient from 110,000-220,000 schistosomula) were resuspended in 73  $\mu$ L PBS/0.2% BSA, transferred to TLS-55 tubes, and gently mixed with 440  $\mu$ L 60% iodixanol. The gradient was built by carefully loading 220  $\mu$ L 40%, 220  $\mu$ L 30%, and 792  $\mu$ L 10% iodixanol on top and spun as described above. After centrifugation, 12 equal fractions of 145  $\mu$ L were collected from top to bottom, 15  $\mu$ L was used for determining the refractive index, and 125  $\mu$ L was directly mixed with 42  $\mu$ L 4 $\times$  non-reducing sample buffer (0.2 M TrisHCl pH 6.8, 8% SDS, 40% glycerol, and Bromophenol blue). In addition, the 96,589  $\times$  *g* EV-depleted supernatant of the ES was concentrated in 10 kDa filter tubes (Amicon) to 300.9  $\mu$ L to which 100.2  $\mu$ L 4 $\times$  non-reducing sample buffer was added. This mix was 5 times diluted in sample buffer to load an equal end volume compared to all the fractions of one gradient. All samples were heated at 98 °C for 3 minutes and stored at -20 °C till SDS-PAGE.

15  $\mu$ L of sample or 1.5  $\mu$ L of marker (PageRuler Plus, Thermo Fisher Scientific) was run into a 12.5% gel, blotted onto PVDF membranes and blocked with blocking buffer consisting of PBS supplemented with 0.1% Tween-20 and 0.2% gelatin from cold water fish skin (Sigma-Aldrich). Blots were incubated overnight with antibodies (1:200-1:2000) in blocking buffer. Antibodies used included: TSP2-2D6

(kind gift from prof. Alex Loukas, James Cook University, Australia) and monoclonal antibodies generated in house at LUMC<sup>21</sup>: 100-4G11<sup>22</sup>, 114-4D12, 128-1E7, 258-3E3, 273-3F2, 290-2E6, and 291-5D5. Bands were visualized with chemiluminescence substrate (SuperSignal West Pico PLUS, Thermo Fisher Scientific) in an Alliance Q9 (UVITEC, Cambridge, UK) and analysed with Fiji/ImageJ<sup>23</sup>.

For the lectin blots, 260  $\mu$ l of EV enriched pellets from 1200 adult worms was split equally (130  $\mu$ l) and incubated with or without PNGase F (4 U/100  $\mu$ l) for 24 hours at 37 °C. EVs were subsequently purified with an iodixanol gradient and fractions 4-7 (1.08-1.20 g/ml) were pooled and washed as described above. Final pellets were resuspended in 70  $\mu$ l PBS and mixed with 2x non-reducing sample buffer, heated, and stored as described. Similar SDS-PAGE and blotting was performed as above. Blocking buffer for the lectin blots consisted of TBS supplemented with 5% BSA and 0.1% Tween-20. Blots were blocked overnight and subsequently incubated for 1 hour with 5  $\mu$ g/mL biotinylated SBA (*Glycine max* (soybean) agglutinin) or DBA (*Dolichos biflorus* agglutinin) (Vector laboratories, Burlingame, CA, USA). Visualization was done as described above after 30 minutes of Streptavidin poly-HRP (Sanquin, Amsterdam, The Netherlands) incubation and several washing steps.

### **PNGase F treatment of EVs for cell experiments**

EV-enriched pellets, obtained as described above from 120 ml adult worm (material from 1200 worms) or 40 ml schistosomula (from 300,000 schistosomula) 5,000  $\times$  g supernatant, were resuspended in a total volume of 150  $\mu$ l or 100  $\mu$ l PBS with 0.2% BSA (as above), respectively. Pellets were then split in two separate Eppendorf tubes and 4  $\mu$ l PNGase F (4 U) was added to one of these two tubes. All samples were incubated for 20 hours at 37 °C after which the EV were stained with PKH26 and isolated via a iodixanol density gradient as described above. The final purified EV pellets were resuspended in 175  $\mu$ l PBS and stored at -80 °C till further use.

### **C-type lectin receptor cell lines**

CHO and CHO-MGL (kind gift from dr. ing. S.J. van Vliet<sup>24</sup>) cells were maintained in RPMI supplemented with 10% FCS, L-glutamine (20  $\mu$ M), penicillin (100 U/ml), and streptomycin (100 U/ml). K562 and K562-DC-SIGN cells (kind gift from prof. dr. C.G. Figdor<sup>25</sup>) were maintained in DMEM with 10% FCS, L-glutamine, pyruvate (20  $\mu$ M), penicillin, and streptomycin. Geneticin (0.6 mg/mL) (G418, Roche Diagnostics) was added to the CHO-MGL and K562-DC-SIGN cultures to select for cells with the CLR expressing vector. Cells (400,000/ml) rested for 2 hours (37 °C, 5% CO<sub>2</sub>) after harvest before addition of PKH26 labelled EVs or dye control with or without 30 minutes EGTA (10 mM) pre-incubation. After 18

hours incubation, cells were placed on ice, harvested, stained with Aqua live/dead staining (Invitrogen, Thermo Fisher Scientific), and measured on a FACSCanto II (BD Bioscience, Franklin Lakes, NJ, USA). Receptor expression was measured by staining cells with  $\alpha$ CD209-V450 (clone DCN46, BD Biosciences),  $\alpha$ CD301-APC (clone H037G3, Biolegend, San Diego, CA, USA),  $\alpha$ FcgammaR-binding inhibitor (eBioscience, Invitrogen, Thermo Fisher Scientific), and 7AAD viability dye (eBioscience).

Data was statistically analyzed in GraphPad Prism 8.0 (GraphPad Software Inc., La Jolla, CA, USA) using a repeated measure One-way ANOVA with Dunnett's Multiple Comparison Test. *P* values  $<0.05$  were considered significant.

## Results

### Characterization of adult worm EVs by cryo-EM and NTA

*S. mansoni* adult worm EVs were isolated from ES collected following a 48 hour culture of adult worms using sequential (ultra)centrifugation and density gradient purification to separate EVs from non-EV particles. EV preparations were visualized by cryo-EM and showed the presence of 30–180 nm vesicles (Figure 2A). Part of these EVs had small structures extruding from their surface (Figure 2A, arrows and bottom panel). NTA of the adult worm EVs showed a size-range between 30 and 250 nm with the majority of the EVs to be around 90 nm in size (Figure 2B). The small peaks of particles observed in the medium control (similarly processed culture medium without parasites) and in PBS alone, were considered background noise of the NTA. The average number of particles measured was equal to 6.85E<sup>9</sup> per 100 adult worms with an average of 4.89  $\mu$ g protein from EVs of 100 adult worms.

### EV surface contains glycan motifs prevalent in adult worms

To study glycosylation of adult worm EVs, the isolated N-glycans and glycolipid-derived glycans were analyzed by mass spectrometry. Glycan structures were assigned to each of the observed molecular ions using the previously published whole adult worm glycan profiles as reference library<sup>6</sup>. The N-glycan composition of the adult worm EVs (Figure 3A) revealed a similar complex glycan profile as described for 6-week old adult worms<sup>6</sup>. The two major ion peaks in the spectrum represented core( $\alpha$ 6)-fucosylated di-antennary structures containing the LDN motif on either one or both antennae. Less abundant N-glycans observed in the spectrum were oligomannosidic structures (3–9 mannoses), glycans with one or two antennae consisting of Gal $\beta$ 1–4GlcNAc (LacNAc, LN), or an LN and LDN combination, and two minor peaks with structures containing an LN and

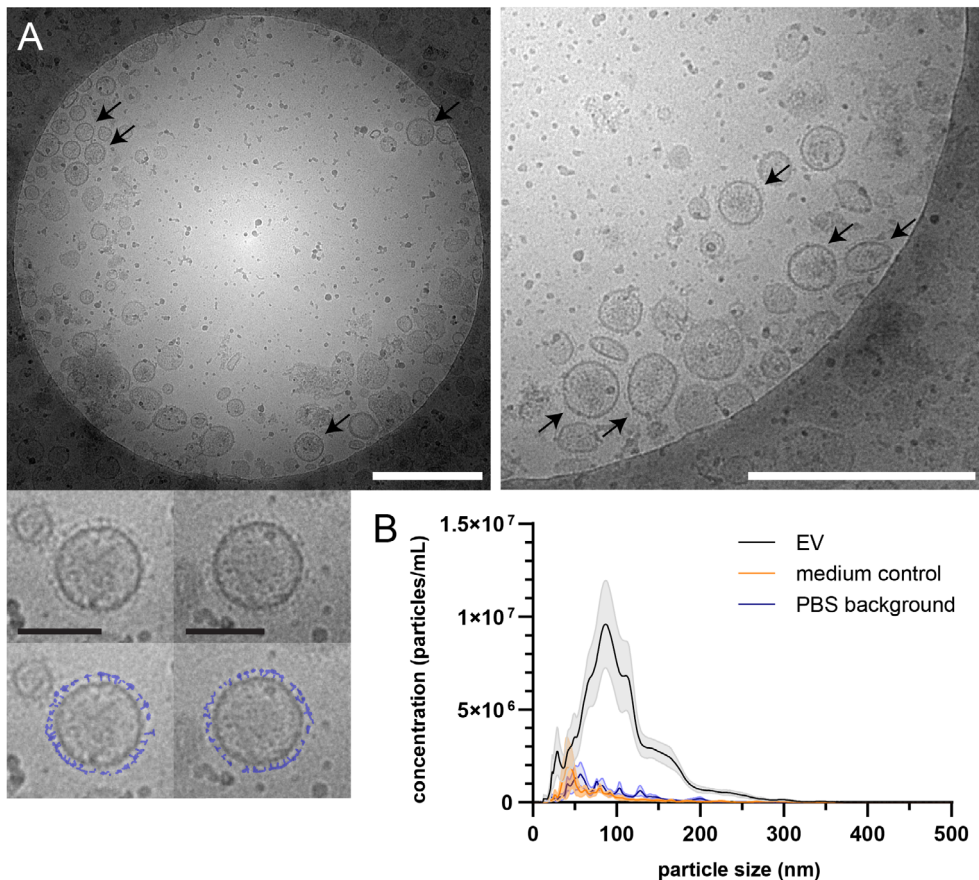
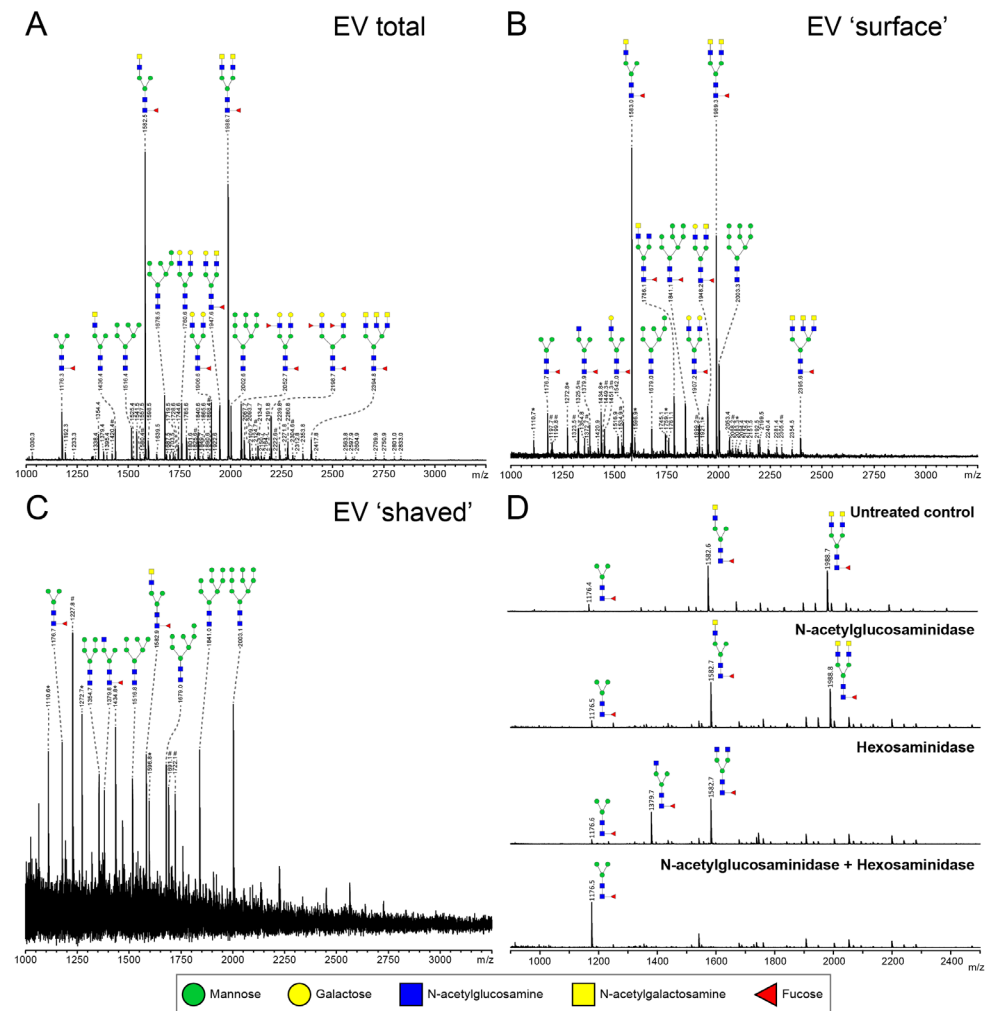


**Figure 2. Isolated EVs from *Schistosoma* adult worms visualized by cryo-EM and measured by NTA**

Purified EVs were visualized by cryo-EM (A) showing surface structures (corona) on part of the EVs (arrows). The bottom panel shows two individual EVs with a copy in which the surface structure is drawn in blue. White scale bars are 500 nm, black scale bars are 100 nm. NTA was performed on purified adult worm EVs from eight biological replicates of which the average is shown (black line) with SEM (grey area) (B). In addition, four medium controls (orange) and four samples PBS (background) in which the EVs were resuspended (blue) are shown.

Le<sup>x</sup> or two Le<sup>x</sup> motifs. Each of these N-glycans were previously confirmed to be present in whole adult worm extracts<sup>6</sup>. In all repeated analyses, glycolipids were not detectable in the adult worm EVs (data not shown).



Glycans present on the EV surface can form ligands for host lectins that play a role in the activation and modulation of immune responses<sup>4,22,26</sup>. To identify these surface glycans, intact purified adult worm EVs were first treated with PNGase F to release and collect EV surface N-glycans. The remaining 'shaved' EVs were re-pelleted, disrupted by sonication and denaturing, and then again treated with PNGase F to release the N-glycans present on the inside of the shaved EVs. The most abundant N-glycans at the EV surface (Figure 3B) were the same LDN-containing structures that were most abundant in the total EV N-glycan profile. The minor peaks observed also represented similar structures with LN or LN-LDN antennae as observed in the total spectrum. In the shaved EV

← **Figure 3. Most relative abundant complex N-glycans on adult worm EVs contain LDN-motif**

N-glycans released by PNGase F of total (A), intact ('surface' N-glycans accessible to the enzyme) (B), and PNGase F treated ('shaved', N-glycans on surface or inside EV that PNGase F cannot access) (C) adult worm EVs were measured by MALDI-TOF-MS. To confirm the presence of GalNAc $\beta$ 1-4GlcNAc (LDN) antennae in glycans released from EV surface in B, AA-labeled N-glycans were treated with either  $\beta$ -N-acetylglucosaminidase,  $\beta$ -hexosaminidase, or both.  $\beta$ -N-acetylglucosaminidase removes GlcNAc residues only after they become accessible by  $\beta$ -hexosaminidase digestion to remove the terminal  $\beta$ -linked GalNAc residues. Peaks are labelled with their monoisotopic masses. The structural assignments are putative and were deduced from the masses (which includes the 2-AA label) and previously published data<sup>6</sup>. These are representative spectra for three biological replicates. Green circle, mannose; yellow circle, galactose; blue square, N-acetylglucosamine; yellow square, N-acetylgalactosamine; red triangle, fucose. \*, signals corresponding to hexose oligomer of unknown origin; #, non-glycan signals

however, oligomannosidic structures (3-9 mannoses) were the most abundant, and complex-type N-glycans were not detected (Figure 3C). The occurrence of a single LDN antenna rather than two separate GlcNAc terminating branches in the N-glycan species observed at  $m/z$  1582.6, and occurrence of two LDN antenna in the  $m/z$  1988.7 structure, were confirmed by treatments with N-acetylglucosaminidase and N-acetylhexosaminidase (Figure 3D) and by MS/MS fragmentation analysis (Supplementary Figure S1). These results indicate that *S. mansoni* adult worm EVs expose N-glycans with one or two terminal LDN motifs.

**Difference in EV-associated glycoconjugates between adult worms and schistosomula**

To confirm the glycan data obtained by mass spectrometry (Figure 3 and Kuipers *et al.*<sup>8</sup>), and make a direct comparison with schistosomula EVs we investigated glycosylation of both adult worm and schistosomula EVs by western blotting. Monoclonal antibodies (mAbs) directed against various glycan motifs including LDN, the unsubstituted tri-mannosyl core motif, and fucosylated (F)-GlcNAc (Supplementary Figure S2) were used to visualize glycoproteins with these motifs in their N-glycans, as well as in O-glycans possibly present but undetected by our MS approach. An overview of the detected glycans in EVs and EV-depleted supernatant of both life stages (as analyzed in Supplementary Figure S2A) is provided in Table 1. The presence of the EV marker Tetraspanin-2 (TSP2) confirmed that the majority of the EVs from adult worms and schistosomula were present in

fractions with a density of iodixanol between 1.07 and 1.16 g/ml (Figure 4). For the adult worms, minute amounts of TSP2 were also detected in the bottom fraction and top fractions and in the EV-depleted supernatant.

The most abundant glycan motifs detected in the adult worm EVs were LDN, the tri-mannosyl motif, and LDN with a GlcNAc-linked fucose (GalNAc $\beta$ 1-4(Fuc $\alpha$ 1-3)GlcNAc, LDN-F) (Table 1). These same motifs were also detected in the EV-depleted supernatant, however, with a different band pattern (Supplementary Figure S2B), suggesting that the EVs and EV-depleted supernatant contain different glycoprotein subsets. Mabs targeting fucosylated GalNAc, such as Fuc $\alpha$ 1-3GalNAc $\beta$ 1-4(Fuc $\alpha$ 1-3)GlcNAc (F-LDN-F), or fucosylated GlcNAc (Fuc $\alpha$ 1-3GlcNAc, F-GlcNAc) were not reactive in western blots of adult worm EV samples. The diverse glycosylation of schistosomula EVs, previously characterized by mass spectrometry<sup>8</sup>, was illustrated using western blotting by the substantial recognition of F-LDN, LDN-F, and F-GlcNAc motifs (Table 1). In accordance with the previous findings, unsubstituted LDN was not detected in schistosomula EV. Interestingly, the tri-mannosyl was abundantly detected in the schistosomula EV-depleted supernatant (Supplementary Figure S2B). Other glycan specific band patterns in the EV-depleted supernatant were also distinct from the patterns observed in the EV fractions. Together, these findings suggest

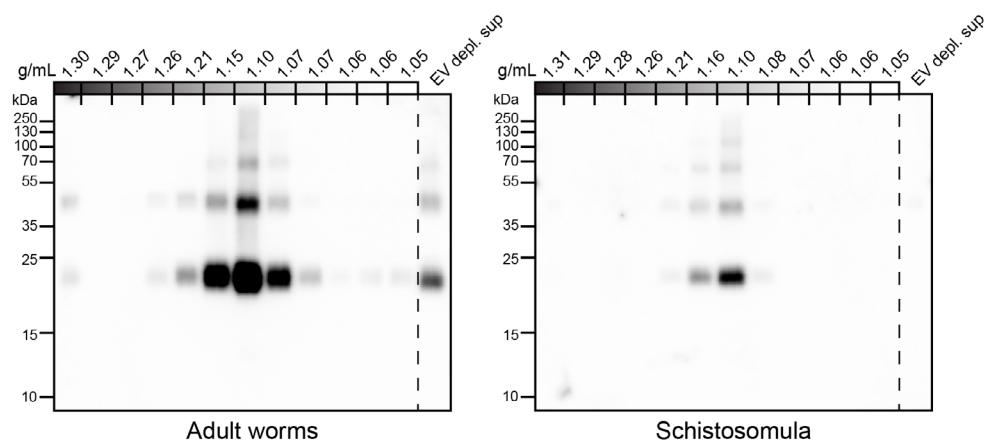


**Figure 4. Tetraspanin-2 containing EV fractions in iodixanol gradient.**

EV enriched pellets were floated upwards into iodixanol density gradients. Twelve equal fractions were obtained, mixed with sample buffer and loaded on an SDS-PAGE gel followed by western blot targeting *Schistosoma* Tetraspanin-2 (TSP2). EV depl. sup = EV depleted supernatant ( $100,000 \times g$  supernatant that was concentrated to equal volume of the full density gradient).

that EVs contain glycoproteins distinct from those in non-EV ES products. Moreover, the western blot data confirm along with the mass spectrometry data that schistosomula and adult worm EVs are differentially glycosylated, in line with the overall differential glycosylation of these schistosome life stages<sup>6</sup>.

## Adult worm EVs interact with MGL receptor

Previously, we found that *S. mansoni* schistosomula EVs interact with DC-SIGN, but not with MR or DCIR, which was in line with the clear presence of DC-SIGN ligands on the schistosomula EV surface<sup>8</sup>. Since the most abundant N-glycans on the surface of the adult worm EVs contained LDN (Figure 3C), we reasoned that adult worm EV could bind to MGL rather than DC-SIGN. MGL is a CLR expressed on monocyte-derived DCs and macrophages, capable of binding LDN- and GalNAc-containing glycoconjugates present in helminths and tumors<sup>27</sup>.

**Table 1.** Glycan motifs in EV or EV-depleted supernatant from adult worms and schistosomula detected with western Blot. – : not detected; + : 1–50,000; ++ : 50,000–200,000; +++ : >200,000 area under the curve measured in ImageJ. Data based on blots in Supplementary Figure 2B. LDN, GalNAc $\beta$ 1–4GlcNAc $\beta$ 1–; LDN-F, GalNAc $\beta$ 1–4(Fuc $\alpha$ 1–3)GlcNAc $\beta$ 1–; F-GlcNAc, Fuc $\alpha$ 1–3GlcNAc $\beta$ 1–; F-LDN, Fuc $\alpha$ 1–3GalNAc $\beta$ 1–4GlcNAc $\beta$ 1–; F-LDN-F, Fuc $\alpha$ 1–3GalNAc $\beta$ 1–4(Fuc $\alpha$ 1–3)GlcNAc $\beta$ 1–; DF-GlcNAc, Fuc $\alpha$ 1–2Fuc $\alpha$ 1–3GlcNAc $\beta$ 1–; TF-GlcNAc, Fuc $\alpha$ 1–2Fuc $\alpha$ 1–2Fuc $\alpha$ 1–3GlcNAc $\beta$ 1–

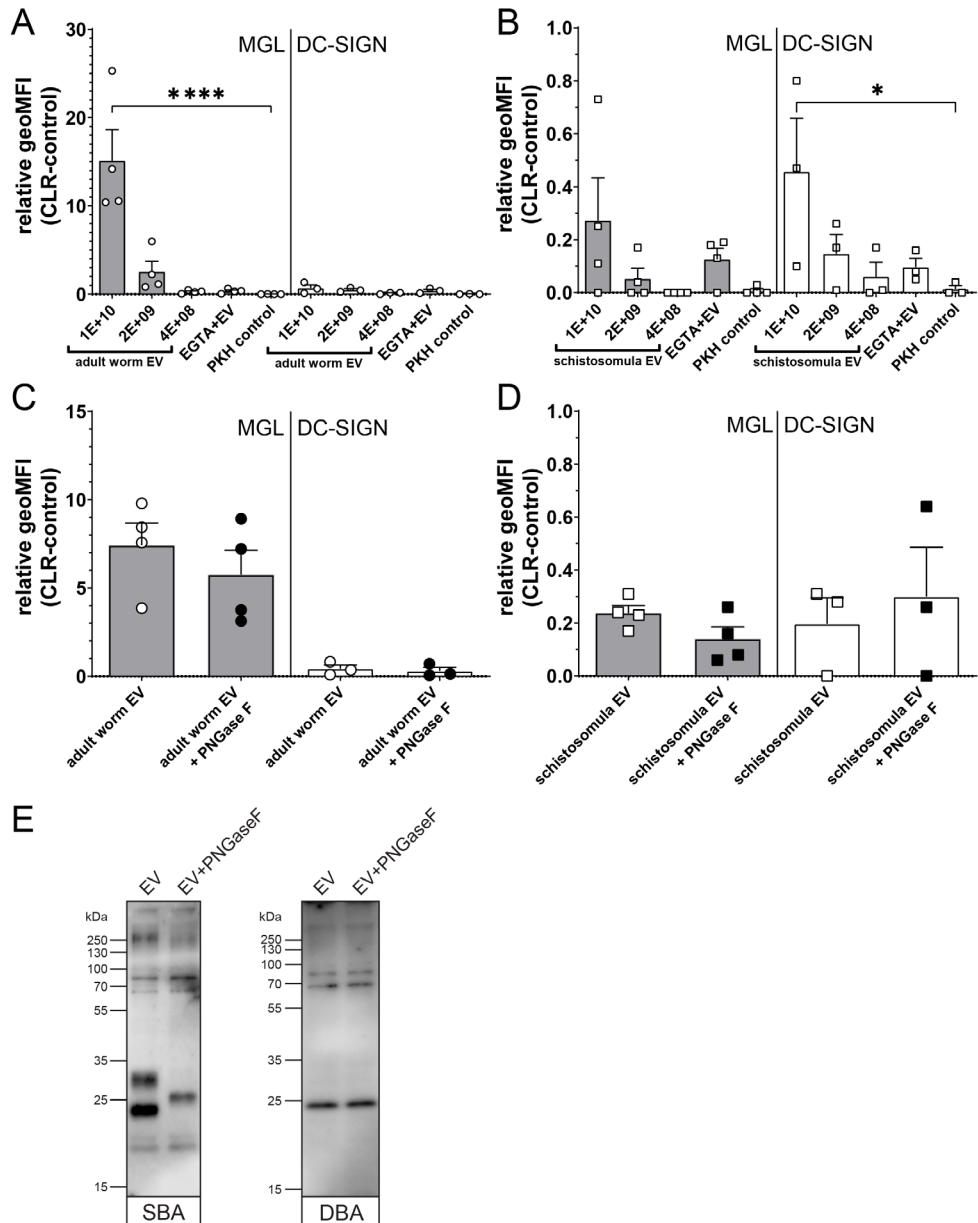
	LDN	tri-manno-syl core	LDN-F	F-LDN	F-LDN-F	F-GlcNAc	TF-GlcNAc	F-LDN	F-LDN-F
Adult worm EV	+	+	++	–	–	–	–	–	–
Adult worm EV-depleted supernatant	+	+	+	–	–	–	–	–	–
Schistosomula EV	–	–	+	++	++	+++	++	–	–
Schistosomula EV-depleted supernatant	–	++	+	+	+	+	+	+++	+++

Indeed, flow cytometric measurements of cell lines overexpressing the MGL or DC-SIGN receptor (Supplementary Figure S3) showed a significant interaction of MGL with fluorescently labelled adult worm EVs, while these EVs did not interact with DC-SIGN expressing cells (Figure 5A). The opposite was observed for the schistosomula EVs, which were strongly interacting with DC-SIGN but less with MGL (Figure 5B). These EV-CLR interactions were confirmed to be glycan-dependent, as the pre-incubation of EGTA disabling the  $\text{Ca}^{2+}$  dependent glycan binding domain of CLR, reduced the binding or uptake of EVs.

Since we observed that the LDN-containing N-glycans on the surface of the adult worm EVs could be removed by PNGase F (Figure 3D), we studied the effect of PNGase F treatment of EVs on MGL-dependent binding. Surprisingly, PNGase F treatment had no significant effect on adult worm EVs binding or uptake by the CLR expressing cells (Figure 5C). Similarly, PNGase F treatment did not affect schistosomula EVs binding to DC-SIGN (Figure 5D), which we attributed earlier to the presence of additional and abundant DC-SIGN ligands within the schistosomula EV-associated glycolipids<sup>8</sup>. We did not detect any glycolipids in the adult worm EVs, however, to possibly explain the MGL affinity remaining after removal of LDN-containing N-glycans. Therefore, we investigated by lectin blotting whether PNGase F treatment resulted in complete LDN removal as expected (Figure 3C) and whether the adult worm EVs might also contain other MGL ligands such as Tn antigens. The Tn antigen is an O-linked  $\alpha$ -GalNAc residue often occurring in mucin domains and a known MGL ligand produced by various organisms, including mammals and helminths<sup>24</sup>. Lectin blotting with SBA, which recognizes both  $\alpha$ -GalNAc (as in Tn) and  $\beta$ -GalNAc (as in LDN), showed that PNGase F treatment did indeed affect N-glycan contained LDN reactivity. The band around

→ **Figure 5. Interaction Schistosoma EVs with MGL or DC-SIGN expressing cell lines suggest multiple MGL ligands on adult worm EVs**

Fluorescently labelled EVs from adult worms (A) or schistosomula (B) or dye (PKH) control were incubated with MGL or DC-SIGN expressing cell lines and measured for fluorescence by flow cytometry. The geometric mean fluorescent intensity (geoMFI) of similar cell lines without CLR expressing vector incubated with EVs (control) was subtracted from the geoMFI of the cells with the CLR. Similar experiment was performed with EVs treated with PNGase F before density gradient isolation (C-D). Adult worm EVs treated with or without PNGase F were loaded on SDS-PAGE followed by western blot for detection of LDN (SBA lectin) and Tn antigen (DBA lectin) (E). EV concentrations are given in EV/ml. Data from 3-4 independent experiments. Mean $\pm$ SEM \* $p < 0.05$ , \*\*\* $p < 0.0001$ , using repeated measures ANOVA with Dunnett's Multiple Comparison Test compared to PKH control.



23 kDa was absent in the PNGase F treated EV lane, and the band at ~30 kDa disappeared while a new band showed at ~26 kDa (Figure 5E), likely due to removal of N-glycans resulting in a mass shift. The remaining SBA binding after PNGase F treatment suggests that other SBA ligands than N-glycan LDN, such as O-linked glycans with the LDN motive or the Tn antigen are present. Application of DBA, which binds only  $\alpha$ -GalNAc, confirmed that glycoproteins of adult worm EVs indeed contain Tn antigen, and that these are not affected by PNGase F treatment. These findings suggest that the interaction of PNGase F treated, N-glycan shaved, adult worm EVs with MGL are most likely due to the presence of O-linked GalNAc residues exposed on the EVs.

## Discussion

4

Helminth parasites, including *S. mansoni*, release EVs that can interact with host cells. There are multiple publications reporting about the proteome and transcriptome of adult schistosome<sup>28-31</sup>. However, the glycans associated with these worm EVs remain largely undescribed and their role has been almost completely unexplored so far<sup>8,32</sup>. Here we found that EV released by adult worms contained complex N-glycans with LDN motifs, which were almost exclusively present on the EV surface. The observed EV-glycan profile corresponds with the glycan profile of entire adult worms<sup>6</sup>. This similarity between the overall glycan profile of a life stage and the glycan profile of their released EVs has been previously observed for schistosomula as well<sup>8</sup>. This indicates that the previously observed differences in overall N-glycan profile between the two life stages<sup>6</sup> are reflected in their released EVs (Figure 3A and Kuipers *et al.*<sup>8</sup>), where adult worm EV N-glycans mainly contain LDN, but not highly fucosylated glycans as observed for schistosomula EVs. This was confirmed by both mass spectrometry (Figure 3) and glycan-targeting antibodies in a western blot analysis (Table 1, Supplementary Figure S2). In contrast to a recent publication on *S. mansoni* adult worm EVs that were analyzed by lectin microarrays<sup>32</sup>, we did not detect sialylated host-derived glycans in our EV preparations (Figure 3). We did not use FCS in worm culture medium and applied multiple washing steps before EV analysis to exclude the presence of host material. Helminths, such as *S. mansoni*, lack the molecular machinery for the biosynthesis of sialylated glycans<sup>33</sup>. Although our data shows that schistosomes in an *ex vivo* culture do not release EVs with sialylated glycan motifs, it could be possible that host glycoproteins are incorporated into schistosome EVs *in vivo*, or that host-derived sialic acids get incorporated into schistosome products otherwise<sup>34</sup>.

The majority of the EV-associated glycoprotein glycans we detected have previously been reported to be present in whole adult worm extracts. We could,

however, not detect glycolipids known to be abundantly present in adult worms<sup>6</sup> in the purified worm EVs. In contrast, glycolipids are ample and diverse in the case of schistosomula-derived EVs<sup>8</sup>. Furthermore, the unique long filamentous 'hair-like' structures previously observed on the surface of schistosomula EVs<sup>8</sup> were not present on adult worm EVs (Figure 2A). These observations could suggest a difference between schistosomula and adult worms in cellular source and pathways from which the EVs derive. There is evidence that schistosomula EVs are released from their pre-acetabular glands<sup>35</sup>, although they may also origin from the cercarial glycocalyx, as their long surface filaments resemble the glycocalyx morphology<sup>36</sup>. The source of adult worm EVs is largely unknown but we suggest that the adult worm gut and tegument are likely candidates as a high abundance of LDN structures has been reported for both locations using lectin staining<sup>37</sup>. In addition, the EV marker TSP2 has been found abundantly on the adult worm tegument<sup>38</sup>. Both tegument and gut-derived EVs have been observed or suggested to occur for other helminths<sup>39</sup>, but the exact adult *S. mansoni* worm EV source or sources remain(s) to be elucidated. The corona structure on adult worm EVs (Figure 2A) appears to be a unique feature. The EV (protein) corona gained more interest just recently<sup>40</sup> and to our current knowledge the structures observed on the adult worm EV surface have not been imaged/reported as such on the surface of naturally released mammalian EVs in the absence of blood plasma. Since we did not detect host-derived sialic acids in our measurements, it is also unlikely that the worm EV corona observed consists of host material, yet the exact composition remains to be elucidated. These coronas do resemble the surface structures seen on EVs from transfected mammalian cells enriched in nematode or viral membrane proteins<sup>41</sup>. Furthermore, coated EVs have been reported for other helminths<sup>42</sup>, fungi<sup>43</sup>, and bacteria<sup>44,45</sup>. It is therefore tempting to suggest that these membrane structures are a hallmark of pathogen-derived EVs and may be involved in pathogen-host interaction.

The finding that adult worm EVs interacted more significantly with MGL compared to DC-SIGN, while for the schistosomula EV the opposite was found (Figure 5) indicates that the glycosylation of *S. mansoni* EVs drives their interaction with host cells. Both receptors are selectively present on DCs and macrophages but rarely coincide on the same cell *in vivo* and have only been found together on some cells in the small intestine<sup>7</sup>, suggesting distinct immunological functions. DC-SIGN can bind glycoconjugates containing either mannose or fucose structures which, in specific molecular context and with additional TLR activation, can promote Th1 and Th2 responses, respectively<sup>46</sup>. For *Schistosoma* larvae, it has been suggested that their fucosylated glycolipids are recognized by DCs in the skin<sup>47</sup>. These DCs react to the parasite with pro-inflammatory responses, yet the

DC-SIGN activation induces an increase of anti-inflammatory cytokine IL-10. This increase in IL-10 prevents the generation of full adaptive responses which allows successful reinfection of the host<sup>48</sup>. Similar responses have been observed in moDC for the DC-SIGN binding schistosomula EVs that contain ample fucosylated glycolipids<sup>8</sup>. Glycolipids are insensitive to PNGase F treatment and we indeed still observed schistosomula EV-DC-SIGN interaction with the CLR-expressing cell lines after enzymatically removing the N-glycans (Figure 5D), similar to what we previously found for moDCs<sup>8</sup>.

Although mouse MGL1 can recognize Le<sup>x</sup> motifs, the human MGL cannot<sup>7</sup>, and the observed interaction of schistosomula EVs with the human MGL in our experiments might be through the interaction of terminal GalNAc residues of the LDN-F epitopes present in schistosomula EV glycans (Table 1)<sup>7</sup>. The binding capacity of schistosomula EVs to MGL is limited, in contrast to the interaction of the adult worm EVs with this receptor (Figure 5). This finding is corroborated by the high abundance in adult worm EV of LDN motifs and the Tn antigen (Figure 5E), which are the two major ligands of the MGL<sup>27</sup>. The MGL is mainly associated with tolerogenic DCs and macrophages and MGL stimulation by the Tn antigen strongly increases IL-10 release<sup>49</sup>. MGL is superior to DC-SIGN in the ability to generate IL-10 producing regulatory T cells after DCs stimulation<sup>50</sup> and is mainly investigated for its role in tumor immunology<sup>51</sup>. Tumor cells are known to have altered glycosylation and the presence of the Tn antigen has been correlated to poor clinical outcome<sup>52</sup>. Although it has been shown that helminths such as *S. mansoni* stimulate the generation of regulatory cells<sup>53</sup>, an exact role for the MGL during helminth infection has not been elucidated so far<sup>27</sup>. We therefore hypothesize that the adult worms release EVs to stimulate immune tolerance via interaction with the MGL. For example, human monocytes increase their MGL expression in the presence of IL-4<sup>54</sup>, a Th2 cytokine that accumulates in the granuloma induced by eggs trapped in the liver, which in turn links to the increased presence of alternatively activated macrophages (M2). It is therefore possible that adult worm EVs contribute to protecting the host from egg-derived toxins via MGL-induced tolerance<sup>55</sup>. Interestingly, also schistosome egg-derived glycoprotein kappa-5 contains the LDN motif, as well as LDN-F. However, in addition to MGL, kappa-5 has been shown to interact with DC-SIGN and MR on the basis of the fucosylated LDN variant<sup>56</sup>. Another observation for possible adult worm EV-induced tolerance comes from vaccination studies. Whereas recombinant *Schistosoma* TSP2 is a potential vaccine candidate against schistosomiasis<sup>57</sup>, initial vaccine studies with complete adult worm EVs showed no clear protection thus far<sup>58</sup>. This low efficacy of TSP2-containing worm EVs might be due to tolerogenic properties induced by

EV glycosylation.

There are profound differences between the *Schistosoma* life stages. The schistosomulum has to find a way via the skin to the lungs and fight off the first line of defense of the host immune system while establishing infection and maturing into adult worms. Once developed into adult worms, the parasites reside in the veins near the liver and the gut where they need to establish a chronic infection and stay alive for years if untreated. Hence, the adult worms utilize different strategies than the larvae to evade or limit host responses. These differences are not only reflected in the morphology and glycosylation of the adult worms and schistosomula themselves, but also their released EVs. Furthermore, we found that glycosylation patterns differ between EVs and EV-depleted ES (Table 1). This suggests that EVs from these parasites have a distinct contribution to infection and survival within their host. Studying the interactions of schistosome EVs with host CLRs not only increases our understanding of the roles of CLRs during helminth infections, it can also tell us how we could target these CLRs to either generate immune activation to fight infections and tumors or to induce immunotolerance to dampen unwanted inflammations.

4

## Conflict of Interest

The authors declare that the research was conducted in the absence of any commercial or financial relationships that could be construed as a potential conflict of interest.

## Author Contributions

MEK performed the majority of the experiments. DLN and AvD performed the glycan characterizations and assisted with the analysis of the spectra. LM contributed to the CLR experiments. EB and RIK generated the cryo-EM images. MEK, ENMH, HHS and CHH conceived the project and contributed to the design of experiments and interpretation of the results. MEK and CHH wrote the manuscript. All authors revised the manuscript. All authors read and approved the final manuscript.

## Funding

This work was supported by the Nederlandse Organisatie voor Wetenschappelijk Onderzoek (NWO) Graduate School Program[022.006.010] (to MEK) and the Dutch Lung Foundation AWWA Consortium [5.1.15.015] (to HHS).

## Acknowledgments

The authors would like to thank Jan de Best and the rest of the life-cycle team for maintaining the availability of the parasites, Professor Alex Loukas from James Cook

University, Queensland (Australia), for providing the TSP-2-targeting antibodies, Sjaak van Voorden and the rest of the Medical Microbiology department (LUMC) for using their refractometer, Uvitec Alliance, ultracentrifuges, and rotors, and Dr. ing. Sandra van Vliet from the AmsterdamUMC and Professor Carl Figdor from RadboudUMC, Nijmegen (The Netherlands), for providing the CLR-expressing cell lines.

## References

1. Colley, D. G., Bustinduy, A. L., Secor, W. E. & King, C. H. Human schistosomiasis. *The Lancet* **383**, 2253–2264 (2014).
2. Jenkins, S. J., Hewitson, J. P., Jenkins, G. R. & Mountford, A. P. Modulation of the host's immune response by schistosome larvae. *Parasite Immunol* (2005).
3. Maizels, R. M., Smits, H. H. & McSorley, H. J. Modulation of Host Immunity by Helminths: The Expanding Repertoire of Parasite Effector Molecules. *Immunity* **49**, 801–818 (2018).
4. Everts, B. *et al.* Schistosome-derived omega-1 drives Th2 polarization by suppressing protein synthesis following internalization by the mannose receptor. *J Exp Med* **209**, 1753–67, S1 (2012).
5. Bloem, K. *et al.* DCIR interacts with ligands from both endogenous and pathogenic origin. *Immunol Lett* **158**, 33–41 (2014).
6. Smit, C. H. *et al.* Glycomic Analysis of Life Stages of the Human Parasite *Schistosoma mansoni* Reveals Developmental Expression Profiles of Functional and Antigenic Glycan Motifs. *Mol Cell Proteomics* **14**, 1750–1769 (2015).
7. van Vliet, S. J., Saeland, E. & van Kooyk, Y. Sweet preferences of MGL: carbohydrate specificity and function. *Trends in Immunology* **29**, 83–90 (2008).
8. Kuipers, M. E. *et al.* DC-SIGN mediated internalisation of glycosylated extracellular vesicles from *Schistosoma mansoni* increases activation of monocyte-derived dendritic cells. *J Extracell Vesicles* **9**, 1753420 (2020).
9. Sánchez-López, C. M., Trelis, M., Bernal, D. & Marcilla, A. Overview of the interaction of helminth extracellular vesicles with the host and their potential functions and biological applications. *Molecular Immunology* **134**, 228–235 (2021).
10. de la Torre-Escudero, E. *et al.* Surface molecules of extracellular vesicles secreted by the helminth pathogen *Fasciola hepatica* direct their internalisation by host cells. *PLoS Negl Trop Dis* **13**, e0007087 (2019).
11. Dusoswa, S. A. *et al.* Glycan modification of glioblastoma-derived extracellular vesicles enhances receptor-mediated targeting of dendritic cells. *J Extracell Vesicles* **8**, 1648995 (2019).
12. Nishida-Aoki, N., Tominaga, N., Kosaka, N. & Ochiya, T. Altered biodistribution of deglycosylated extracellular vesicles through enhanced cellular uptake. *Journal of Extracellular Vesicles* **9**, (2020).
13. Martins, Á. M., Ramos, C. C., Freitas, D. & Reis, C. A. Glycosylation of Cancer Extracellular Vesicles: Capture Strategies, Functional Roles and Potential Clinical Applications. *Cells* **10**, (2021).
14. Kuipers, M. E., Hokke, C. H., Smits, H. H. & Hoene, E. N. M. N. ' . Pathogen-Derived Extracellular Vesicle-Associated Molecules That Affect the Host Immune System: An Overview. *Frontiers in Microbiology* **9**, 2182 (2018).
15. Whitehead, B., Boysen, A. T., Mardahl, M. & Nejsum, P. Unique glycan and lipid composition of helminth-derived extracellular vesicles may reveal novel roles in host-parasite interactions. *International Journal for Parasitology* **50**, 647–654 (2020).

4

16. Macedo-da-Silva, J., Santiago, V. F., Rosa-Fernandes, L., Marinho, C. R. F. & Palmisano, G. Protein glycosylation in extracellular vesicles: Structural characterization and biological functions. *Mol Immunol* **135**, 226–246 (2021).
17. Van Deun, J. *et al.* EV-TRACK: transparent reporting and centralizing knowledge in extracellular vesicle research. *Nat Methods* **14**, 228–232 (2017).
18. Kuipers, M. E. *et al.* Optimized Protocol for the Isolation of Extracellular Vesicles from the Parasitic Worm *Schistosoma mansoni* with Improved Purity, Concentration, and Yield. *J Immunol Res* **2022**, 5473763 (2022).
19. Petralia, L. M. C. *et al.* Mass Spectrometric and Glycan Microarray-Based Characterization of the Filarial Nematode *Brugia malayi* Glycome Reveals Anionic and Zwitterionic Glycan Antigens. *Mol Cell Proteomics* **21**, 100201 (2022).
20. Ceroni, A. *et al.* GlycoWorkbench: a tool for the computer-assisted annotation of mass spectra of glycans. *J Proteome Res* **7**, 1650–1659 (2008).
21. Smit, C. H. *et al.* Surface expression patterns of defined glycan antigens change during *Schistosoma mansoni* cercarial transformation and development of schistosomula. *Glycobiology* **25**, 1465–1479 (2015).
22. van Remoortere, A. *et al.* *Schistosoma mansoni*-infected mice produce antibodies that cross-react with plant, insect, and mammalian glycoproteins and recognize the truncated biantennary N-glycan Man3GlcNAc2-R. *Glycobiology* **13**, 217–225 (2003).
23. Schindelin, J. *et al.* Fiji: an open-source platform for biological-image analysis. *Nat Methods* **9**, 676–682 (2012).
24. van Vliet, S. J. *et al.* Carbohydrate profiling reveals a distinctive role for the C-type lectin MGL in the recognition of helminth parasites and tumor antigens by dendritic cells. *Int Immunol* **17**, 661–669 (2005).
25. Geijtenbeek, T. B. H. *et al.* Identification of DC-SIGN, a novel dendritic cell-specific ICAM-3 receptor that supports primary immune responses. *Cell* **100**, 575–585 (2000).
26. van Die, I. *et al.* The dendritic cell-specific C-type lectin DC-SIGN is a receptor for *Schistosoma mansoni* egg antigens and recognizes the glycan antigen Lewis x. *Glycobiology* **13**, 471–478 (2003).
27. van Kooyk, Y., Ilarregui, J. M. & van Vliet, S. J. Novel insights into the immunomodulatory role of the dendritic cell and macrophage-expressed C-type lectin MGL. *Immunobiology* **220**, 185–192 (2015).
28. Sotillo, J. *et al.* Extracellular vesicles secreted by *Schistosoma mansoni* contain protein vaccine candidates. *Int J Parasitol* **46**, 1–5 (2016).
29. Samoil, V. *et al.* Vesicle-based secretion in schistosomes: Analysis of protein and microRNA (miRNA) content of exosome-like vesicles derived from *Schistosoma mansoni*. *Sci Rep* **8**, 3286 (2018).
30. Meningher, T. *et al.* Schistosomal MicroRNAs Isolated From Extracellular Vesicles in Sera of Infected Patients: A New Tool for Diagnosis and Follow-up of Human Schistosomiasis. *J Infect Dis* **215**, 378–386 (2017).
31. Kifle, D. W. *et al.* Proteomic analysis of two populations of *Schistosoma mansoni*-derived extracellular vesicles: 15k pellet and 120k pellet vesicles. *Mol Biochem Parasitol* **236**, 111264 (2020).

32. Dagenais, M. *et al.* Analysis of schistosoma mansoni extracellular vesicles surface glycans reveals potential immune evasion mechanism and new insights on their origins of biogenesis. *Pathogens* **10**, (2021).

33. Hokke, C. H. & van Diepen, A. Helminth glycomics – glycan repertoires and host–parasite interactions. *Mol Biochem Parasitol* **215**, 47–57 (2017).

34. Dagenais, M., Gerlach, J. Q., Geary, T. G. & Long, T. Sugar Coating: Utilisation of Host Serum Sialoglycoproteins by Schistosoma mansoni as a Potential Immune Evasion Mechanism. *Pathogens* **11**, 426 (2022).

35. Gasan, T. A. *et al.* Schistosoma mansoni Larval Extracellular Vesicle protein 1 (SmLEV1) is an immunogenic antigen found in EVs released from pre-acetabular glands of invading cercariae. *PLOS Neglected Tropical Diseases* **15**, e0009981 (2021).

36. Samuelson, J. C. & Caulfield, J. P. The cercarial glycocalyx of Schistosoma mansoni. *J Cell Biol* **100**, 1423–1434 (1985).

37. Schmidt, J. Glycans with N-acetyllactosamine type 2-like residues covering adult Schistosoma mansoni, and glycomimesis as a putative mechanism of immune evasion. *Parasitology* **111** ( Pt 3, 325–336 (1995).

38. Tran, M. H. *et al.* Tetraspanins on the surface of Schistosoma mansoni are protective antigens against schistosomiasis. *Nat Med* **12**, 835–840 (2006).

39. Drurey, C., Coakley, G. & Maizels, R. M. Extracellular vesicles: new targets for vaccines against helminth parasites. *Int J Parasitol* **50**, 623–633 (2020).

40. Buzas, E. I. Opportunities and challenges in studying the extracellular vesicle corona. *Nat Cell Biol* **24**, 1322–1325 (2022).

41. Zeev-Ben-Mordehai, T., Vasishtan, D., Siebert, C. A., Whittle, C. & Grunewald, K. Extracellular Vesicles: A Platform for the Structure Determination of Membrane Proteins by Cryo-EM. *Structure* **22**, 1687–1692 (2014).

42. Sánchez-López, C. M. *et al.* Diversity of extracellular vesicles from different developmental stages of *Fasciola hepatica*. *Int J Parasitol* **50**, 663–669 (2020).

43. Rizzo, J. *et al.* Revisiting Cryptococcus extracellular vesicles properties and their use as vaccine platforms. *bioRxiv* 2020.08.17.253716 (2021) doi:10.1101/2020.08.17.253716.

44. Gui, M. J., Dashper, S. G., Slakeski, N., Chen, Y. Y. & Reynolds, E. C. Spheres of influence: *Porphyromonas gingivalis* outer membrane vesicles. *Molecular Oral Microbiology* **31**, 365–378 (2016).

45. Cecil, J. D. *et al.* Outer Membrane Vesicle–Host Cell Interactions. *Microbiology Spectrum* **7**, 7.1.06 (2019).

46. Geijtenbeek, T. B. & Gringhuis, S. I. C-type lectin receptors in the control of T helper cell differentiation. *Nat Rev Immunol* **16**, 433–448 (2016).

47. Figliuolo da Paz, V. R., Figueiredo-Vanzan, D. & Dos Santos Pyrrho, A. Interaction and involvement of cellular adhesion molecules in the pathogenesis of Schistosomiasis mansoni. *Immunol Lett* **206**, 11–18 (2019).

48. Mountford, A. P. & Trottein, F. Schistosomes in the skin: a balance between immune priming and regulation. *Trends Parasitol* **20**, 221–226 (2004).

49. van Vliet, S. J. *et al.* MGL signaling augments TLR2-mediated responses for enhanced IL-10 and TNF- $\alpha$  secretion. *J Leukoc Biol* **94**, 315–323 (2013).

50. Hirata, Y., Ihara, S. & Koike, K. Targeting the complex interactions between microbiota, host epithelial and immune cells in inflammatory bowel disease. *Pharmacol Res* **113**, 574–584 (2016).

51. Valverde, P., Martínez, J. D., Cañada, F. J., Ardá, A. & Jiménez-Barbero, J. Molecular Recognition in C-Type Lectins: The Cases of DC-SIGN, Langerin, MGL, and L-Sectin. *Chembiochem* **21**, 2999–3025 (2020).

52. Brockhausen, I. Mucin-type O-glycans in human colon and breast cancer: glycodynamics and functions. *EMBO Rep* **7**, 599–604 (2006).

53. Maizels, R. M. & McSorley, H. J. Regulation of the host immune system by helminth parasites. *Journal of Allergy and Clinical Immunology* **138**, 666–675 (2016).

54. Raes, G. *et al.* Macrophage galactose-type C-type lectins as novel markers for alternatively activated macrophages elicited by parasitic infections and allergic airway inflammation. *J Leukoc Biol* **77**, 321–327 (2005).

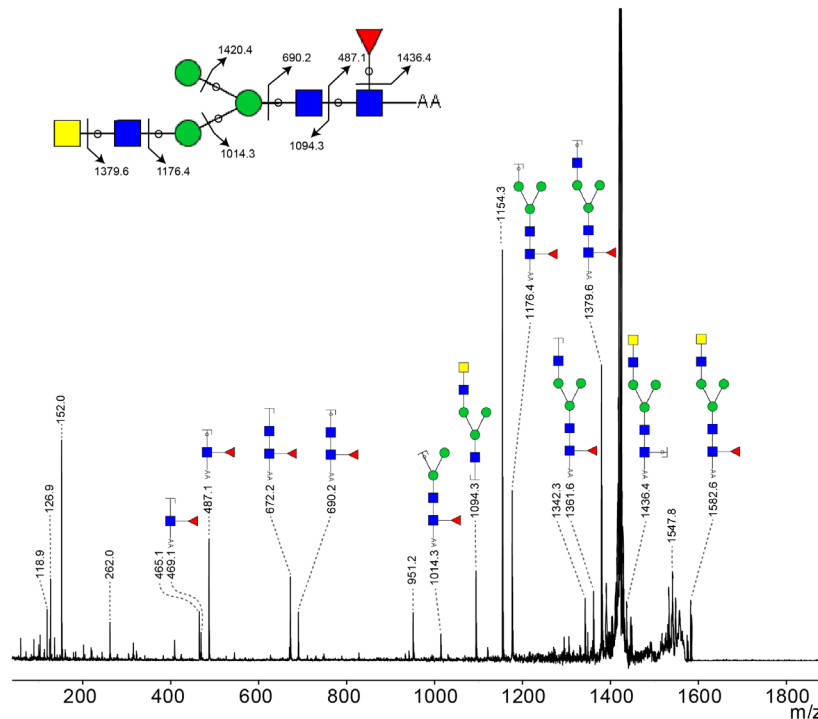
55. Costain, A. H., MacDonald, A. S. & Smits, H. H. Schistosome Egg Migration: Mechanisms, Pathogenesis and Host Immune Responses. *Front Immunol* **9**, 3042 (2018).

56. Meevissen, M. H. J. *et al.* Specific glycan elements determine differential binding of individual egg glycoproteins of the human parasite *Schistosoma mansoni* by host C-type lectin receptors. *Int J Parasitol* **42**, 269–277 (2012).

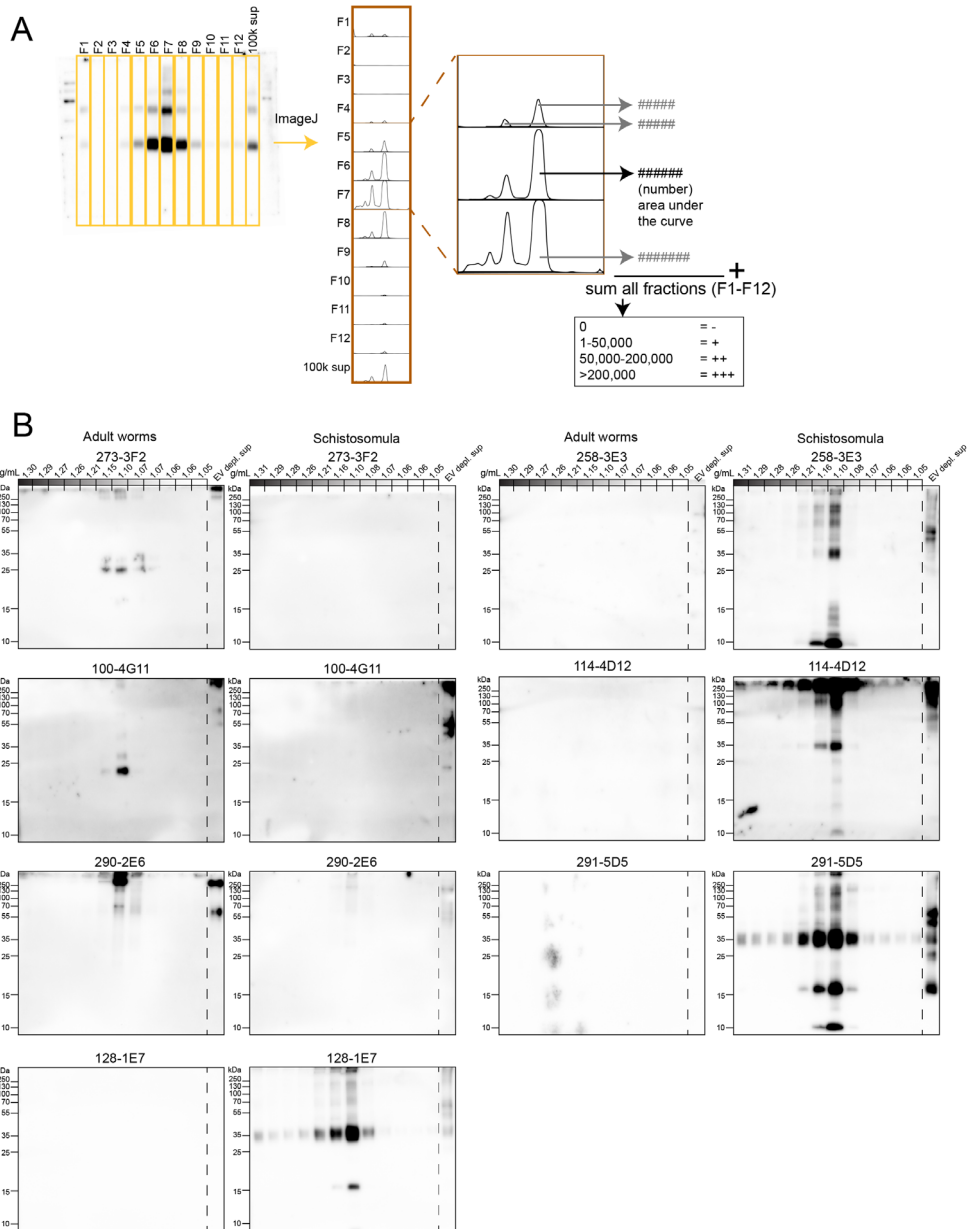
57. Mekonnen, G. G. *et al.* *Schistosoma haematobium* Extracellular Vesicle Proteins Confer Protection in a Heterologous Model of Schistosomiasis. *Vaccines (Basel)* **8**, (2020).

58. Kifle, D. W. (2020). Schistosoma mansoni extracellular vesicles: immunobiology and vaccine efficacy. [Dissertation Thesis] [Queensland, Australia]: James Cook University, *College of Public Health, Medical and Veterinary Sciences Centre for Molecular Therapeutics Australian Institute of Tropical Health and Medicine* doi: 10.25903/fhzh-2h14.

## Supplementary Figures

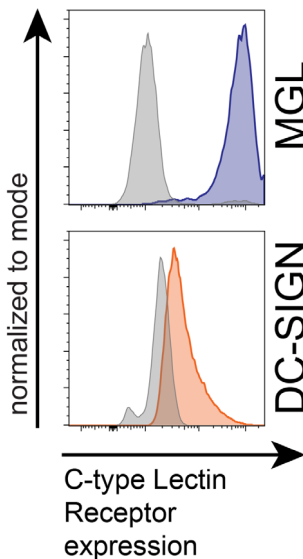


**Supplementary Figure S1. MS/MS fragmentation of 1582 m/z to confirm LDN antenna**  
MS/MS fragmentation of 1582 m/z by MALDI-TOF/TOF of PNGase F released and AA-labeled N-glycans of adult worm EVs to confirm the presence of a single LDN antenna. Peaks are labelled with their monoisotopic masses. Green circle, mannose; yellow circle, galactose; blue square, N-acetylglucosamine; yellow square, N-acetylgalactosamine; red triangle, fucose.



← **Supplementary Figure S2. Western blots of EV-associated glycoconjugates and their analysis by ImageJ.**

Analysis workflow of measured blots in ImageJ (A). Area under the curve of the 12 gradient fractions were added together to form one number, EV-depleted (100k sup) supernatant had its own number. Full western blots of each antibody and life stage (B). Blots are representative for 2-3 biological replicates. 273-3F2 detects LDN; 100-4G11 detects tri-mannosyl core; 290-2E6 detects LDN-F; 128-1E7 detects F-GlcNAc, F-LDN, and F-LDN-F; 258-3E3 detects F-GlcNAc; 114-4D12 detects DF-GlcNAc and TF-GlcNAc; 291-5D5 detects F-LDN and F-LDN-F. Full description of these glycans and their linkage can be found in the legend of table 1.



**Supplementary Figure S3. MGL and DC-SIGN receptor expression on CLR expressing cell lines.**

CHO (MGL) and K562 (DC-SIGN) without the CLR vector are shown in grey.



# Chapter 5

## **Extracellular vesicles from *Schistosoma mansoni* adult worms stimulate IL-10 release by B-cells**

Marije E. Kuipers, Simone Haeberlein, Arifa Ozir-Fazalalikhan, Nicole N. Driessen, Clarize M. de Korne, Lynn Mes, Paul Hensbergen, Esther N.M. Nolte-‘t Hoen, Cornelis H. Hokke, Hermelijn H. Smits

**Submitted to International Journal for Parasitology**

## Abstract

Schistosome parasites are known to modulate host immune responses, which is achieved in part through the release of excretory/secretory (ES) products, including extracellular vesicles (EVs). During chronic schistosomiasis, increased regulatory responses are found, which includes enhanced IL-10 production by B (Breg) cells. ES products from schistosome eggs are able to induce IL-10 production by B cells. However, since infection with male worms only (without egg production) also promotes IL-10 producing B cells, we here studied the stimulatory effects of adult worm ES and EVs on murine and human B cells. Worm ES increased IL-10 release by mouse splenic B cells; this activity was concentrated in defined size-separated fractions of adult worm ES. Interestingly, mass spectrometry of the fractions that induced the highest IL-10 response revealed an enrichment of EV-associated proteins. Indeed, highly purified adult worm EVs could interact with mouse splenic B cells, visualized by binding of a schistosome-specific tetraspanin (TSP2) targeting antibody. Furthermore, purified adult worm EVs induced IL-10 release in both mouse splenic and human peripheral blood B cells, suggesting that adult worm EVs can play a role in immune regulatory processes within their host.

## Introduction

*Schistosoma* spp. are endemic in tropical areas and globally affect over 250 million people<sup>1</sup>. These parasites are known to regulate host immune responses enabling the adult worms to survive in their human host for many years, despite being exposed to the full army of immune defenses present in the blood<sup>2</sup>. Enhanced knowledge of how schistosomes can avoid and attenuate immune responses contributes to our understanding of immunity against schistosomes and aids the development of vaccines. Furthermore, understanding parasite–host interactions can reveal new mechanisms to dampen immune responses, which we can implement in novel strategies to treat inflammatory disorders<sup>3</sup>.

Schistosomes can modulate both innate and adaptive immune responses of their hosts. One crucial mechanism for increased survival of both the parasites and their host is the dampening of immune responses via stimulation of the regulatory arm of the immune system<sup>4</sup>. This regulatory arm consists of both innate (e.g. dendritic cells and macrophages) and adaptive (e.g. T and B cells) cells and involves the release of regulatory cytokines such as TGF- $\beta$  and IL-10 by these cells. Stimulation of regulatory responses by helminths, including schistosomes, is often studied by exposing immune cells to soluble antigen extracts of the parasites, released excretory/secretory (ES) products, and/or single antigen/ES components<sup>5</sup>. A previously overlooked component that is studied among the ES products are extracellular vesicles (EVs)<sup>6</sup>. EVs are released by cells of almost every organism and are generally 50–200 nm in size with a lipid-bilayer membrane and diverse cargo (e.g. (glyco)proteins, lipids, and RNAs)<sup>7</sup>. Although, several studies have investigated the composition of schistosome-derived EVs<sup>8–14</sup>, information regarding their role in modulating the host immune system is limited<sup>15,16</sup>.

Regulatory B (Breg) cells is a collective name for a heterogenous group of B cells with anti-inflammatory activity, which are relatively new to the framework of regulatory immune cells. They can suppress pro-inflammatory responses via the release of anti-inflammatory cytokines such as IL-10, IL-35 and/or TGF- $\beta$ , or via cell-contact dependent mechanisms. Breg cells can drive effector T cell suppression and induce regulatory T cells, but they can also inhibit cytokine production by antigen-presenting cells or drive T cell apoptosis<sup>17</sup>. IL-10 producing Breg cells are induced during schistosome infections<sup>18,19</sup>. Additionally, *in vivo* and *in vitro* studies with *S. mansoni* soluble egg antigens (SEA), without the context of a full infection, showed that SEA can induce IL-10 production in both mouse and human B cells, respectively<sup>20,21</sup>. However, during an *S. mansoni* infection, IL-10 producing Breg cells are not exclusively induced by schistosome egg-derived components. Intriguingly, infections with male worms only, and thus in the absence of eggs, could still protect mice against experimental anaphylaxis in a B

cell- and IL-10-dependent manner<sup>22</sup>. So far, it is unknown whether ES products or other components of adult worms influenced B(reg) cell function in this model.

Hence, we investigated the effect of *S. mansoni* adult worm ES on mouse and human B cell cytokine release. Adult worm ES induced IL-10 release by mouse splenic B cells. Interestingly, proteomics on IL-10 inducing ES-fractions, generated by size exclusion chromatography, revealed an enrichment in EV-related proteins. Indeed, stimulation with highly purified EVs from adult worms could increase IL-10 release by naïve mouse splenic B cells and by human peripheral blood B cells. This suggests that adult worm EVs harbor immune suppressive potential when exposed to B cells.

## Methods

### Ethical statement

All animal experiments were in accordance with the Guide for the Care and Use of Laboratory Animals of the Institute for Laboratory Animal Research and have received approval from the university Ethical Review Board (Leiden University Medical Center, Leiden, Netherlands) which is registered with the number AVD1160020171067 (for hamsters) and AVD1160020173525 (for mice).

### Worm culture and ES collection

*S. mansoni* adult worms (mixed sex) were collected from perfused Syrian hamsters, washed multiple times, and cultured ~10–20 worms/ml DMEM (high glucose with L-glutamine, Lonza, Basel, Switzerland) supplemented with Antibiotic Antimycotic Solution (ABAM, Sigma-Aldrich, St. Louis, MO, United States) and 10 mM HEPES for two days as previously described in detail<sup>14</sup>. Collected ES was centrifuged at 300 × g for 5 minutes to remove worms and debris and the supernatant was stored at -20 °C till further use. Collected ES for subsequent EV isolation was centrifuged twice on 200 × g and twice on 500 × g, all for 10 minutes and on 4 °C. The final supernatant was stored at -80 °C till further use. For the experiments with total ES and ES fractionation, worms were cultured two days in M199 medium (Gibco, Thermo Fischer Scientific, Waltham, MA, USA) supplemented with 1.5 mM glutamine, 10 mM HEPES, and ABAM. Generation of SEA from *S. mansoni* eggs has been described elsewhere<sup>20</sup>. Protein concentration of ES was determined by BCA (Pierce, Thermo Fisher Scientific).

### FPLC fractionation

Thawed worm ES from 310–502 ml was centrifuged at 1,800 × g for 10 minutes (4 °C) and the supernatant was concentrated in 10 kDa centrifugal filters (Amicon,

Merck KGaA, Darmstadt, Germany) with three additional PBS washing till a volume of 1-2 ml. The concentrated ES was centrifuged twice in Eppendorf tubes on  $17,000 \times g$ . For each FPLC run, 0.8-1 ml of the final supernatant was applied to a Sephadryl S-300 HR column (Pharmacia, Stockholm, Sweden) and eluted with PBS using an ÄKTA FPLC system (Pharmacia). Fractions of 1 ml were collected and stored at  $-20^{\circ}\text{C}$  till further use. A chromatogram of a representative run can be found in Supplementary Figure S1A. For the B cell stimulations, collected matching fractions from 3 runs were pooled and the protein concentration was determined by NanoDrop (Thermo Fischer Scientific).

### SDS-PAGE and mass spectrometry

Pooled FPLC fractions were mixed with non-reducing sample buffer before loading 20  $\mu\text{l}$  onto an 10% SDS-PAGE gel followed by Coomassie staining. The gel was kept in MilliQ and cut in selected pieces (Supplementary Figure S1B). Proteins in sliced gel bands were digested with trypsin (12.5 ng/ $\mu\text{l}$  in 25 mM  $\text{NH}_4\text{HCO}_3$ , sequencing-grade modified trypsin; Promega, Madison, WI, USA) after reduction and alkylation with dithiothreitol (10 mM) and iodoacetamide (55 mM), respectively. Tryptic peptides were then analyzed by LC-MS/MS using an Ultimate 3000 RSLCnano system (Thermo Fisher Scientific) coupled to an ion trap mass spectrometer (amaZon ETD (Bruker, Billerica, MA, USA)). The RAW data has been submitted to ProteomeExchange and is currently being processed.

For peptide identification, mass spectrometry data were converted to Mascot Generic Files (MGF) and searched against the Uniprot *Schistosoma mansoni* database (Downloaded Nov 19, 2020, 15910 protein entries) with the Mascot search algorithm (Mascot 2.2.07, Matrix Science, London, UK). A MS tolerance of 0.3 Da and a MS/MS tolerance of 0.5 Da were used. Trypsin was selected for enzyme specificity, and up to 2 missed cleavage sites were allowed. Carbamidomethyl cysteine was selected as a fixed modification, and oxidation of methionine and acetylation at the protein N-terminus as variable modifications. All searches and subsequent data analysis, including Percolator<sup>23</sup>, were performed using Proteome Discoverer 2.5 (Thermo Fischer Scientific). Peptide-spectrum matches were adjusted to a 1% FDR. Proteins with only 1 detected peptide were excluded from further analysis. For comparing our proteome to published EV proteomes, we combined three publications on *S. mansoni* adult worm EVs<sup>9,11,12</sup> and one publication on *S. mansoni* schistosomula EVs<sup>8</sup>. Since previously published proteomes were annotated with smp accession numbers, these entries were IDmapped to Uniprot entries via the Uniprot website (uniprot.org, consulted in Augustus 2022). 60 entries could not be mapped (see Supplementary Data Sheet) and were therefore not included in the comparison.

## ES preparation and EV isolation

An overview of the steps for EV isolation from the adult worm ES can be found in Figure 1. Thawed  $500 \times g$  supernatant from multiple worm cultures (160 ml total) were pooled and equally split in two. One half (80 ml) was concentrated for ES in 15 ml 10 kDa centrifugal filters (Amicon) and washed several times with PBS until the flow-through was clear. The final ES volume of 3 ml was aliquoted and stored at  $-80^{\circ}\text{C}$ . The final flow-through was also collected, aliquoted and stored to be used later as 'PBS control'. The other half (80 ml) was processed for EV isolation, which has been described in full detail previously<sup>14</sup>. Briefly, the  $500 \times g$  supernatant was centrifuged 30 minutes at  $5,000 \times g$  after which the  $5,000 \times g$  supernatant was ultracentrifuged at  $100,000 \times g$  for 65 minutes (k-factor 265, SW41 Ti rotor, Beckman Coulter, Brea, CA, United States). All centrifugation steps were performed at  $4^{\circ}\text{C}$ . The  $100,000 \times g$  supernatant ('EV-depleted ES') was collected, pooled and split equally in two parts again. One half was concentrated similarly as the ES described above to a volume of 1.5 ml. The other half was transferred to SW41 tubes and centrifuged at  $200,000 \times g$  (40,000 rpm, k-factor 130) for 65 minutes. The  $100,000 \times g$  pellets were resuspended in a total of 260  $\mu\text{L}$  PBS+0.2% BSA and divided over two TLS55 tubes (130  $\mu\text{l}$ /tube) and iodixanol (Optiprep, Axis-Shield PoC AS, Oslo, Norway) gradients were built on top. After two hours ultracentrifugation at 50,000 rpm (k-factor 60), eight fractions were

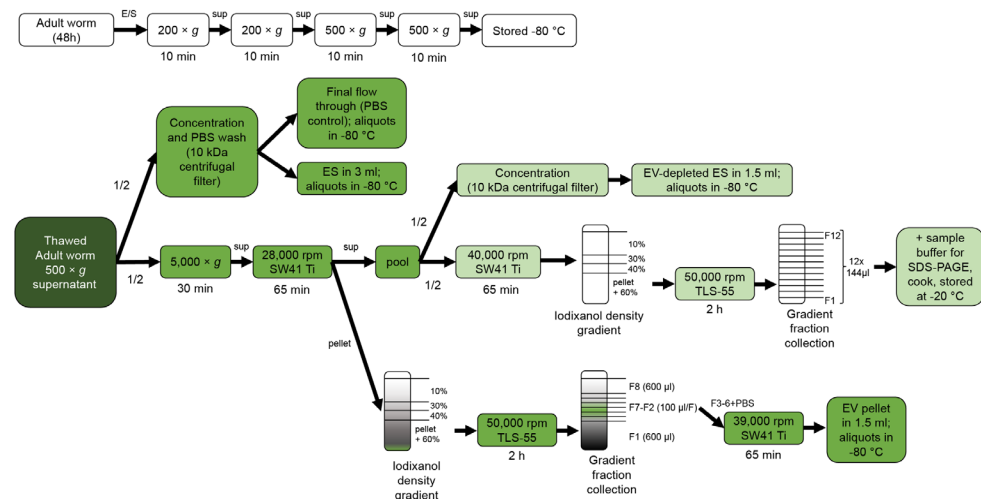


**Figure 1. Schematic overview of procedures for preparation of adult worm ES, EV-depleted ES and purified EVs used for B cell stimulations**

ES, excretory/secretory products; sup, supernatant; min, minutes; h, hours; rpm, rotations per minute

collected from top to bottom: 600  $\mu$ l (F1), six times 100  $\mu$ l (F2-7), and one left over (F8) fraction. Fractions 3-6 were transferred to an SW41 tube and mixed with cold PBS. EVs were pelleted at 39,000 rpm (k-factor 136) for 65 minutes and resuspended in 1.5 ml PBS. The final resuspended EV pellet was deliberately half of the ES volume to compensate for estimated loss of EVs along the density gradient isolation process<sup>24</sup> (Supplementary Figure S1C). All samples were only thawed once and directly used to stimulate cells. BCA was performed to determine the protein concentration of the ES.

The 200,000  $\times$  g pellet was resuspended and transferred to a TLS55 tube. An iodixanol gradient was built on top and spun as above. Twelve equal fractions were collected from the gradient, which were directly mixed with non-reducing sample buffer, cooked, and stored at -20 °C till SDS-PAGE and TSP2 western blotting as described in Kuipers *et al.*<sup>24</sup>.

We have submitted all relevant data of our experiments to the EV-TRACK knowledgebase (EV-TRACK ID: EV230956)<sup>25</sup>.

## Mouse splenic B cell isolation and stimulation

Spleens of C57/Bl6 mice (SC1300012, purchased by Envigo RMS B.V., Horst, The Netherlands) between 7 and 15 weeks of age were harvested and made into a single cell suspension using a 100  $\mu$ m cell strainer (BD Biosciences, Franklin Lakes, NJ, United States). B cells were isolated from the splenocytes with CD19 targeting microbeads (Miltenyi Biotec, Bergisch Gladbach, Germany) or CD19 targeting MojoSort nanobeads (BioLegend, San Diego, CA, USA) according to the manufacturer's instructions. Purity was >96%, which was determined by flow cytometry detecting B220 (Invitrogen, clone RA3-6B2).

B cells were resuspended in RPMI 1640 glutamax (Gibco) supplemented with 5% FCS (Bodinco BV, Alkmaar, The Netherlands), 100 U/mL penicillin, 100  $\mu$ g/mL streptomycin, and 50  $\mu$ M 2-mercaptoethanol (Sigma-Aldrich). 500,000 B cells per well (96-wells plate, U bottom) were stimulated for 2 or 3 days with SEA (20  $\mu$ g/ml), adult worm ES (12.5, 25, 50, 100  $\mu$ g/ml), adult worm ES FPLC fractions (50  $\mu$ g/ml), adult worm EVs (equal volume as adult worm ES), adult worm EV-depleted ES (equal volume as adult worm ES), or PBS control (ES flow through, equal volume as highest concentration ES), in the presence or absence of co-stimulatory rat- $\alpha$ -mouse CD40 (0.5, 1, 2  $\mu$ g/ml; clone 1C10, BioLegend) as indicated in the figure legends. After stimulation, the supernatants were collected and stored at -20 °C.

## Staining of murine B cells for confocal microscopy and flow cytometry

Murine splenic B cells isolated as above were seeded at 375,000 B cells per well (96 well U-bottom plate) and stimulated adult worm ES, EVs, and PBS control. An equal volume of EV and PBS-control was used as calculated for the ES to get an ES concentration of 50  $\mu$ g/ml. After 18 hours incubation, B cells were transferred to a V-bottom plate and washed twice with PBS. For confocal microscopy, cells were fixed with PFA (3.6%), subsequently permeabilized (Permeabilization Buffer, Invitrogen, Thermo Fischer Scientific) and blocked in PBS+10% FCS for 1 hour at room temperature. Cells were incubated overnight at 4 °C with or without anti-TSP2 (1:20,000) (Rabbit IgG, polyclonal, kind gift from Prof. Alex Loukas, James Cook University, Australia). After four PBS washes, cells were incubated for 1 hour with an AlexaFluor-594-Donkey-anti-rabbit IgG (1:500) (Invitrogen) in PBS+10% FCS. Cells were washed again for 3 times followed by 30 minutes incubation with Hoechst (1:200)(33342, Sigma-Aldrich), one washing step, and 30 minutes CellBrite green (1:100) (Biotium, Fremont, CA, USA). Both Hoechst and Cellbrite were diluted in PBS+2% FCS. After a final wash, cells were transferred to a confocal 96 wells plate and spun briefly to sediment the cells. Images were taken using an Andor Dragonfly 500 spinning disk confocal system (Oxford Instruments, Abingdon, UK) with a 60 $\times$  or 100 $\times$  objective. For flow cytometry, cells were treated similar, but including a 20 minutes Aqua live/dead staining (Invitrogen) before fixation, and after the secondary antibody and washing steps, the cells were resuspended in a buffer for flow cytometry and measured on a BD LS1Fortessa (BD Biosciences).

## Isolation and stimulation of human B cells

Isolated peripheral blood mononuclear cells (PBMCs) from venous whole blood of healthy volunteers (as described in <sup>26</sup>) were cryopreserved as described<sup>27</sup> till further use. B cells from thawed PBMCs were purified by using a human Pan B Cell Isolation Kit (Miltenyi Biotec) following the manufacturer's protocol. B cell purity was checked by flow cytometry (CD19, clone HIB19, BioLegend) and was >90%. B cells were seeded in a 96-wells U bottom plate, 300,000 cells per well, in RPMI 1640 supplemented with 10% FCS, penicillin and streptomycin as described above, and L-glutamine (2 mM)/pyruvate (1 mM) (Sigma-Aldrich). After 44 hours of stimulation with 50  $\mu$ g/ml adult worm ES, adult worm EVs, adult worm EV-depleted supernatant, or PBS control (all equal volume as ES), supernatant was collected and stored at -20 °C till cytokine measurements.

## ELISA

Culture supernatants from the B cells were thawed and cytokines were quantified by commercial ELISA kits (mouse IL-6, mouse IL-10, human IL-6, human IL-10; BD OptEIA™, BD Biosciences) according to the manufacturer's instructions. Technical duplicates were averaged and statistic analysis was performed on data from three or more independent experiments in Graphpad Prism (version 9, GraphPad Software Inc., La Jolla, CA, United States).

## Results

### Adult worm ES induces IL-10 release by mouse splenic B cells

We first investigated the effects of adult worm secretions (ES) on the activation of mouse splenic B cells. For this, isolated splenic CD19<sup>+</sup> cells from a naïve mouse were incubated with either SEA or adult worm ES. Both stimuli induced the release of IL-10, but not IL-6, by the B cells and the response by the worm ES was dose dependent (Figure 2A). Next, we questioned whether there are specific molecules present in ES that harbor the IL-10-inducing capacity. For this, ES was fractionated by size-exclusion FPLC (Supplementary Figure S1B), in which it was expected that similar to other size exclusion chromatography methods<sup>24</sup>, EVs will elute in the first fraction after the void volume. Mouse splenic B cells were subsequently incubated with the collected fractions and showed that IL-10 production was most pronounced after stimulation with fractions 1, 2, 7, 8, and 9 (Figure 2B). These results indicate that in these fractions there is an enrichment of specific ES components that induce IL-10 release by mouse splenic B cells.

To investigate whether the IL-10 inducing fractions of adult worm ES contain possible regulatory proteins, the most abundant SDS-PAGE protein bands in these fractions (Supplementary figure S1B) were processed for in-gel trypsin digestion and protein identification by mass spectrometry (results are summarized in the supplementary datasheet). This selection of proteins was compared to the recently published proteome of the complete secretome of cultured male and female adult worms<sup>28</sup> and showed an >80% overlap in detected proteins (Figure 2C). Among these proteins were regulatory proteins from the 14-3-3 family<sup>29</sup>, and heat shock proteins (HSP)<sup>30</sup> but also other proteins with immunomodulatory potential such as glyceraldehyde 3-phosphate dehydrogenase (GAPDH)<sup>31</sup>, cathepsin<sup>32</sup>, malate dehydrogenase<sup>33</sup>, and calmodulin<sup>34</sup>. Interestingly, 14-3-3 and HSP are often found in eukaryotic extracellular vesicles (EVs)<sup>5</sup>. Two tetraspanins (G4VS95: TSP-1<sup>35</sup> and AOA5K4F8N6: TSP-2<sup>28</sup>), a family of proteins commonly associated to EVs<sup>7</sup> and known to be present on adult worm EVs<sup>9,24</sup>, were also among the detected proteins. Next, we compared our proteomic data set to proteins that

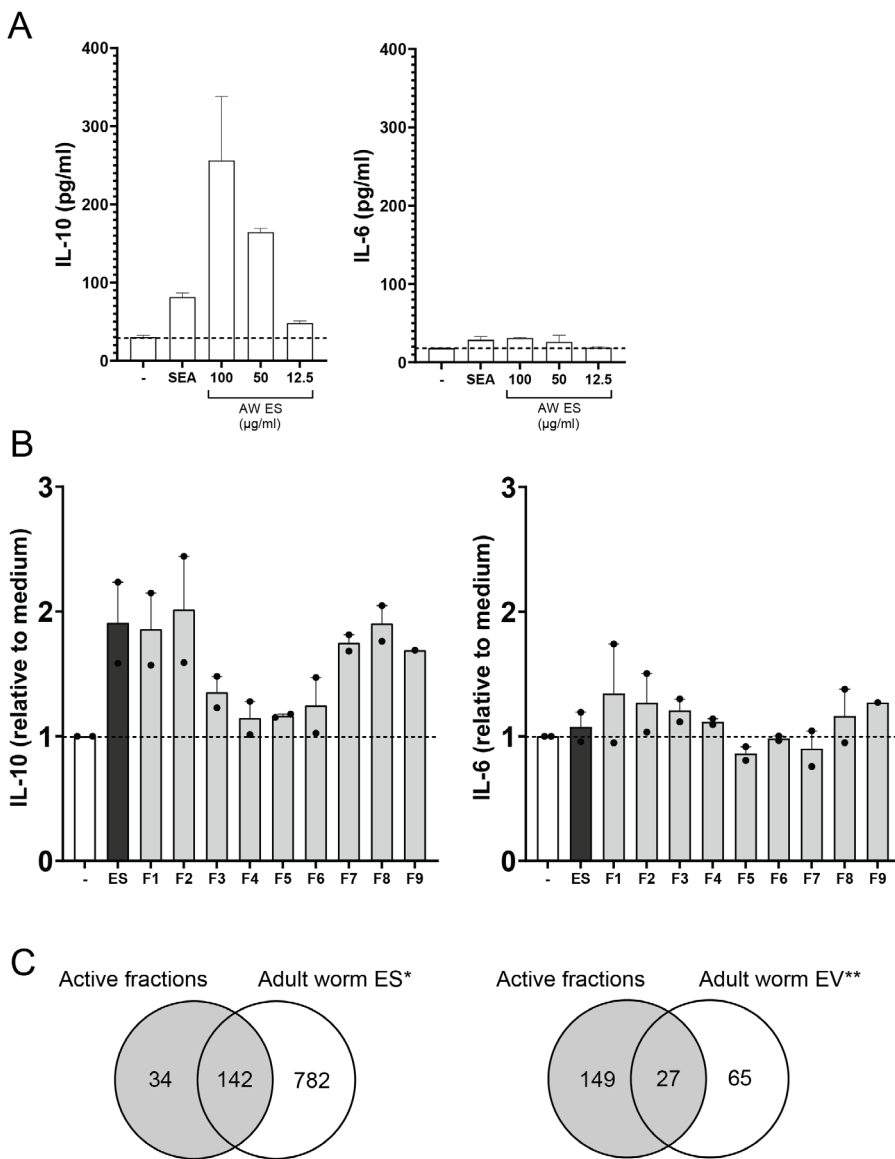


**Figure 2. Adult worm ES induces IL-10 production by murine splenic B cells**

A: IL-10 and IL-6 release by 3 day stimulated mouse splenic B cells. SEA concentration is 20 µg/ml. Data from 2 replicates, but representative for 2 independent experiments. Mean±SD

B: Similar as in A, with stimulations of 50 µg/ml complete ES or 50 µg/ml of indicated fractions of ES, previously collected by size fractionation. Data of 2 independent experiments. Mean±SEM

C: Proteins from proteomic analysis in combined active ES fractions F1 and F7 as compared to published proteins in adult worm ES\*<sup>28</sup> or EVs\*\*<sup>9,11,12</sup>.

were reported in at least 2 of the 3 current publications on *S. mansoni* adult worm EV protein content<sup>9,11,12</sup>. We found that 27 of the 176 (15%) proteins in the active fractions were previously reported to be EV-associated. This percentage increased to almost 45% when including proteins that have been reported once among the other studies (Table 1). Interestingly, the enrichment of EV-proteins was highest (40%) in FPLC fraction 1 compared to fraction 7 (21%) (Table 2). This first collected fraction contains large sized proteins but also includes molecular complexes and particles, such as EVs. These results suggest that the IL-10 inducing fractions were enriched for EV-associated proteins and that EVs among the ES products might influence mouse naïve splenic B cells.

### Adult worm EVs interact with mouse B cells

To investigate whether adult worm EVs indeed interact with B cells, complete adult worm ES and purified adult worm EVs from this ES were incubated with mouse splenic B cells which were subsequently stained with an *S. mansoni* tetraspanin-2 (TSP2)-specific antibody and analyzed by fluorescence microscopy and by flow

**Table 1. Overview of adult worm ES fraction proteins also reported as EV-associated in previous studies.**

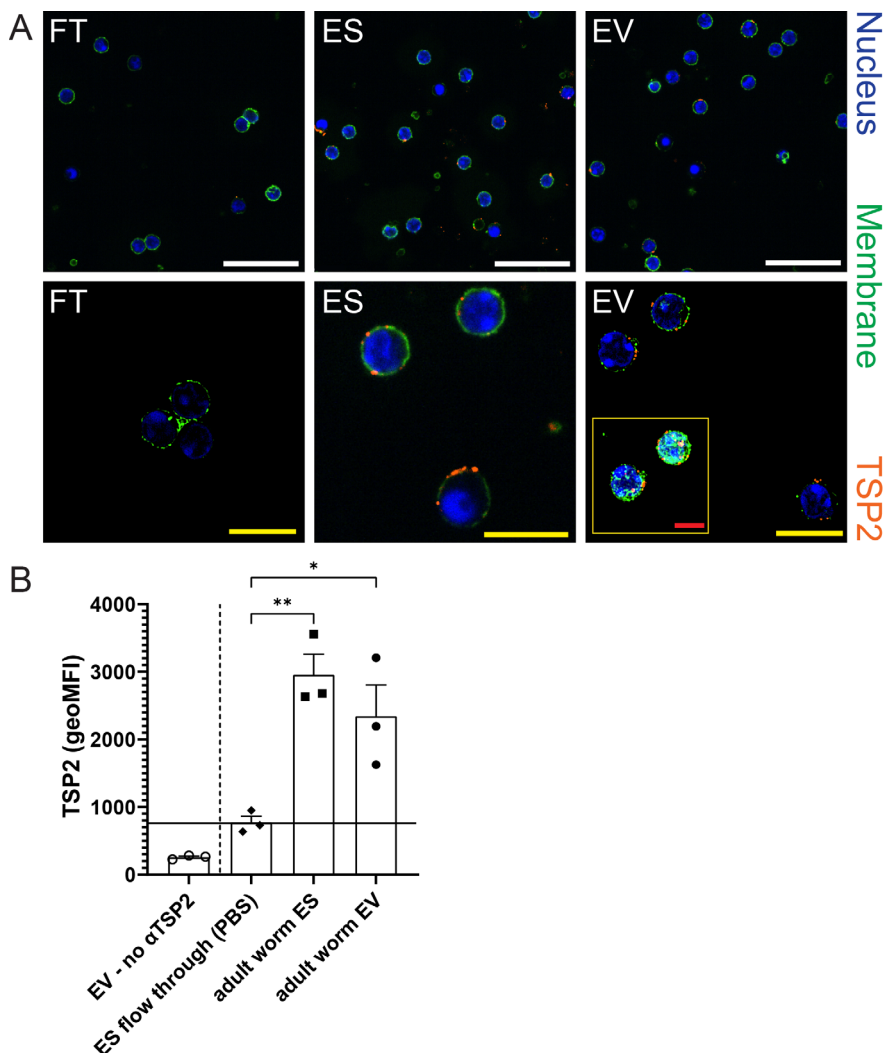
Comparison of EV-associated proteins detected in the combined proteomes of F1 and F7 with those published in the literature<sup>8,9,11,12</sup>. The more EV proteins were included, the more overlap with the ES fractions (most right column).

176 proteins detected in active ES fractions	# EV proteins in publications	# of proteins in both EV publications and detected in active worm ES fractions	# proteins only in EV publications	# proteins only found in active ES fractions	% of proteins detected in active ES fractions that are also reported as EV-associated proteins
EV-associated proteins reported in $\geq 2$ publications on adult worm EV	92	27	65	149	15.3
EV-associated proteins reported in $\geq 2$ publications on schistosome EV	118	38	80	138	21.6
EV-associated proteins reported in $\geq 1$ publications on adult worm EV	338	79	259	97	44.9

**Table 2. Enrichment of EV-associated proteins in first collected FPLC fraction of adult worm ES.**

Higher percentage of adult worm EV-associated proteins detected in fraction 1 from adult worm ES (most right column). Adult worm EV proteins included were reported in at least 2 adult worm EV publications<sup>9,11,12</sup>.

	# Total detected proteins	# Same proteins reported in adult worm EV	% EV-associated proteins detected in fraction
Fraction 1	37	15	40.5
Fraction 7	161	35	21.7



cytometry. B cells incubated with ES and with EVs showed the presence of TSP2 at the plasma membrane (Figure 3), suggesting that both purified EVs and EVs in total adult worm ES interacted with the cells. Interaction of EVs with the B cells seemed unaffected by pre-incubating the cells with EGTA or pre-incubating the EVs with the TSP2 targeting antibody (Supplementary Figure 2). From these data we can conclude that the EVs in ES released by adult worms interact with mouse B cells *in vitro*.

### **EVs released by adult worms increase IL-10 production by mouse B cells**

Since it was previously shown that additional CD40 ligation enhanced IL-10 release by mouse splenic B cells in response to SEA<sup>20</sup>, we tested whether the same applies to adult worm ES. Indeed, CD40 co-stimulation increased cytokine responses in response to adult worm ES (Figure 4A). Since a dose of 0.5 µg/ml of the CD40 co-stimulatory antibody (as compared to 1 and 2 µg/ml) resulted in the highest IL-10 release with minimal increase in IL-6 production (Figure 4A), we continued with this dose  $\alpha$ CD40 in following experiments.

To study the contribution of EVs within the adult worm ES on B cell responses, equal volume of worm ES, EVs purified from ES, and EV-depleted ES were added to naïve splenic B cells. After 48 hours, both purified EVs and the EV-depleted ES increased IL-10 release by stimulated B cells, but to a lower extent than total adult worm ES (Figure 4B). This may suggest that IL-10 inducing signals are present both within EVs and non-EV components. However, we observed that a residual amount of EV-associated TSP2 protein could still be purified from the

#### **← Figure 3. Schistosoma adult worm EVs interact with mouse B cells**

Mouse splenic B cells were incubated with ES flow through (FT, equal to PBS), worm ES, or worm EVs, all to the same amount as 50 µg/ml ES, for 18 hours. Presence of schistosome EVs is shown by a *Schistosoma*-specific TSP2 targeting antibody.

**A:** Confocal microscopy shows the presence of EV marker TSP2 (anti-TSP2, orange) around the membranes (Cellbrite, green) of the B cells (Hoechst, nuclei are blue) after ES and EV incubation. Scale bars: white= 30 µm; yellow=10 µm; red= 5 µm. Pictures are either a section of the cells or z-stack projections (insert).

**B:** Average TSP2 geometric mean fluorescent intensity (geoMFI) of the incubated B cells measured by flow cytometry. The signal in PBS stimulated B cells represents unspecific binding of the TSP2 antibody. Cells incubated with EVs but no TSP2 antibody excluded binding from the secondary antibody alone. Data from 3 independent experiments. Mean±SEM One-way ANOVA with Dunnett's multiple comparisons test; \*p < 0.05, \*\*p < 0.01

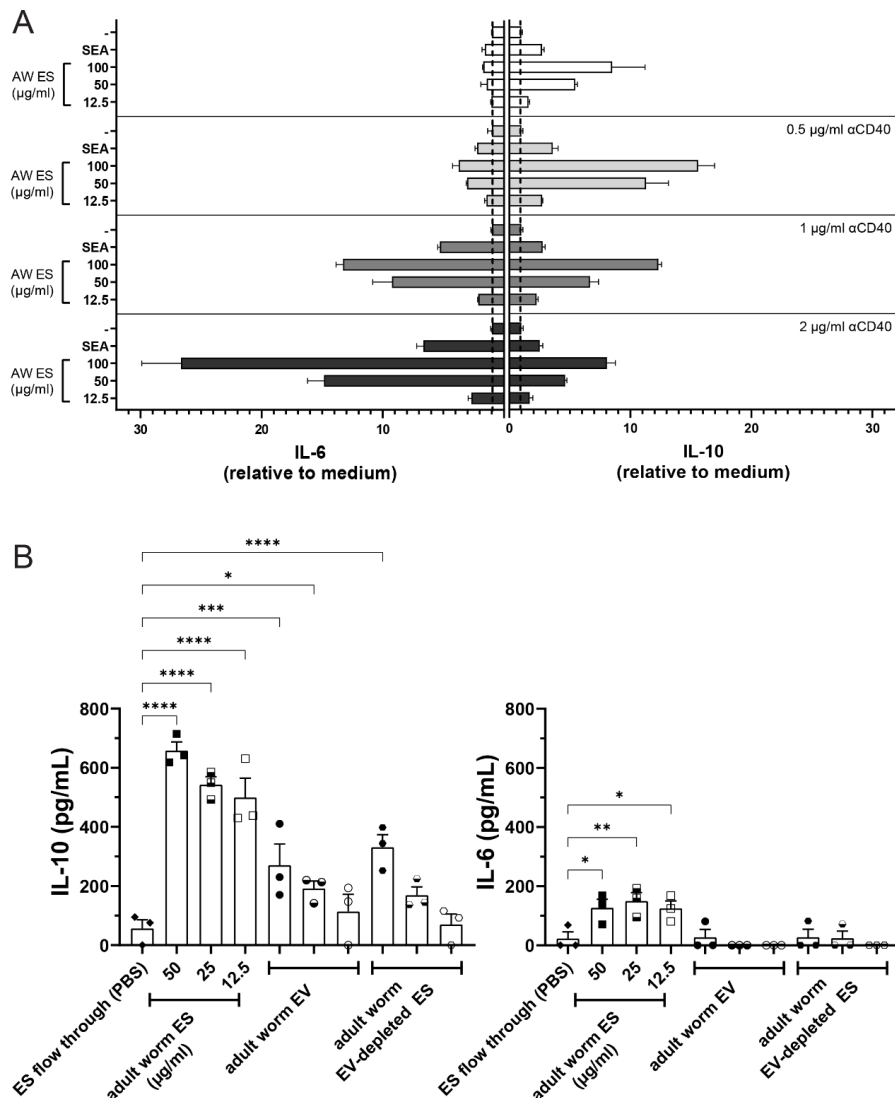
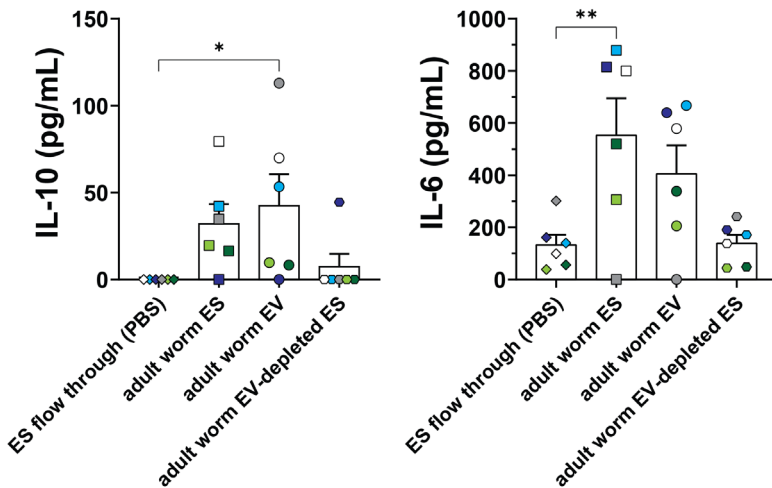


Figure 4. Adult worm EVs induce IL-10 production by murine splenic B cells

**A:** Cytokine production of mouse splenic B cells stimulated with ES for 3 days increased with additional CD40 stimulation. SEA concentration is 20  $\mu$ g/ml. Data from 2 replicates and representative for 2 independent experiments. Mean  $\pm$  SD

**B:** Cytokine release by mouse splenic B cells stimulated with ES, EVs of EV-depleted ES for 2 days. The volumes of resuspended purified EVs and EV-depleted ES added were equal to the ES. All conditions were in the presence of 0.5  $\mu$ g/ml  $\alpha$ CD40. Data points are averaged technical duplicates from 3 independent experiments. Mean $\pm$ SEM One-way ANOVA with Dunnett's multiple comparisons test \* $p$  < 0.05, \*\* $p$  < 0.01, \*\*\* $p$  < 0.001, \*\*\*\* $p$  < 0.0001



**Figure 5. Cytokine production of adult worm ES and EVs stimulated human B cells**

IL-10 and IL-6 release by human B cells isolated from peripheral blood of 6 healthy individuals after 2 days of stimulation with adult worm ES, EVs, or EV-depleted ES. Equal volume of EV and EV-depleted ES was used as for the 50  $\mu$ g/mL ES stimulation. Each individual donor corresponds to one and the same color. Mean $\pm$ SEM One-way ANOVA with Dunnett's multiple comparisons test \* $p$  < 0.05, \*\* $p$  < 0.01

'EV-depleted' adult worm ES fraction (Supplementary Figure 1D). Thus, it cannot be excluded that contaminating EVs in the EV-depleted adult worm ES influenced the cytokine production by B cells exposed to this material. In contrast to complete adult worm ES, the EVs and EV-depleted ES did not induce IL-6 release by mouse splenic B cells. Combined, these results show that adult worm EVs can induce IL-10 release by mouse B cells.

### Adult worm EVs stimulate cytokine responses by human B cells

Finally, we questioned whether adult worm ES and EVs could also activate human peripheral blood B cells. B cells were isolated from PBMCs from six healthy individuals and exposed to complete adult worm ES, adult worm EVs or EV-depleted ES. Complete ES and purified EVs both induced an increase in IL-10 and IL-6 release, while the EV-depleted ES did not seem to induce (strong) cytokine responses (Figure 5). Not all donors showed the same responses to the adult worm released products, which point at some heterogeneity in the responses between donors. Nevertheless, these data indicate that adult worm ES and their purified EVs can induce both IL-6 and IL-10 responses in human peripheral blood B cells.

## Discussion

Schistosome secretions modulate host immune responses to enable parasite survival<sup>5</sup>, in part through the activation of immune tolerance and increased IL-10 producing B cells<sup>18</sup>. Here we showed that schistosome adult worm ES induces IL-10 release by both murine splenic B cells and human peripheral B cells. Both adult worm EVs as well as non-EV-associated factors seem to harbor this activity.

The finding that highly purified adult worm EVs can modulate B cell immune responses contributes to a limited number of studies on immunoregulatory effects of (mammalian) EVs on B cells<sup>36-38</sup>. For example, EVs from mesenchymal stromal/stem cells (MSC) can inhibit B cell proliferation and activation via miRNA transfer<sup>39</sup>, while mast cell-derived EVs increased IL-10 competent murine B cells via EV-associated CD40L<sup>40</sup> or attenuated pro-inflammatory cytokine expression by B cells via prostaglandins<sup>36</sup>. While it seems unlikely that worm-derived EVs contain (host-derived) CD40L, prostaglandins have been found in adult worm ES<sup>41</sup>. However, it is unknown whether prostaglandins are also present in worm EVs.

Proteomic analysis of the IL-10 inducing fractions (Supplementary datasheet) revealed the presence of EV-associated proteins such as Sm29, Sm22.6, tetraspanins, 14-3-3 protein, L-lactate dehydrogenase, and enolase<sup>9,12</sup>. Recombinant versions of Sm29, Sm22.6, and tetraspanin (namely TSP2) have been tested as potential vaccine candidates against schistosomes, of which Sm29 and TSP2 showed reduced egg and worm burden after immunization<sup>42,43</sup>. Interestingly, Sm29 and Sm22.6 also seem to have regulatory functions: e.g. Sm29 increased IL-10 production in human monocyte-derived dendritic cells<sup>44</sup> and both Sm29 and Sm22.6 increased IL-10 production in murine splenic cells<sup>45,42</sup>. The mammalian 14-3-3 protein was able to enhance B cell survival, proliferation and expansion<sup>46</sup>, while its 14-3-3 $\epsilon$  isoform has anti-inflammatory properties as part of the TNF receptor-associated factor 2<sup>47</sup>. The 14-3-3 $\epsilon$  protein of *S. mansoni* can bind to human type 1 TGF $\beta$  receptor<sup>48</sup>. Intriguingly, targeting mammalian TGF $\beta$  receptors to stimulate tolerance was demonstrated for Treg cell inducing protein *Hp-TGM* released by *Heligmosomoides polygyrus*<sup>49</sup>. The TGF $\beta$  receptor is also present on B cells<sup>50</sup>, but whether *S. mansoni* or *H. polygyrus* induces IL-10 release from B cells via this route is currently unknown.

Enolase and L-lactate dehydrogenase (LDH) are both important in the cell metabolism pathway towards lactate production. Schistosomes depend on glucose metabolism for their survival, which also results in increased lactate levels<sup>51</sup>. Lactate as immunomodulator is well known within the tumor field, as e.g. Tregs thrive in a lactate-rich environment and their proliferation and immunosuppressive capacity highly depend on lactate consumption as fuel source<sup>52</sup>. Invasive tumors

are known to increase LDH and which has subsequent immunosuppressive effects<sup>53</sup>. Interestingly, there seems a role for B cell-expressed LDH in expansion of IL-10 producing Breg cells<sup>54</sup>. Furthermore, lactate can bind to G-protein coupled receptor (GPR)65 (TDAG8) that is present on human and mouse B cells, and was shown to reduce pro-inflammatory cytokine production, such as IL-6, in mouse bone marrow-derived macrophages<sup>55</sup>. Whether the EV-associated adult worm ES proteins we detected by mass spectrometry are actually taken up by B cells and contribute to IL-10 induction is unknown.

A possible component with immunomodulatory potential in adult worm ES is hemozoin<sup>56</sup>. This crystal form of the otherwise toxic blood digestion product heme was taken up by B cells as shown for hemozoin from *Plasmodium falciparum* and was stimulating TLR9 in B cells via its bound malarial DNA<sup>57,58</sup>. Here, we have used an optimized EV isolation protocol for adult worm EVs to exclude hemozoin<sup>24</sup>, so we argue that the majority of EV-mediated IL-10 B cell responses are hemozoin-independent. Other possible IL-10-inducing contaminants within worm ES to consider are products released by eggs that are laid by female worms during the 48 hours culture<sup>20,59</sup>. However, the number of eggs produced in these cultures is limited (<300) and previous studies showed that 20 µg/mL SEA was needed to induce IL-10 production in B cells<sup>20</sup>, therefore a significant contribution of egg material in adult worm ES and EV preparations seems unlikely.

Despite the fact that we do not know which individual EV molecule(s) stimulate(s) B cell IL-10 production, we provide strong evidence that the adult worm EVs interact with B cells (Figure 3). We used schistosome specific TSP2-targeting antibodies to detect EV-B cell interaction. However, this detection does not reveal whether it was the whole EV population or a subpopulation that interacted with the B cells, since information on TPS2 expression on EV-subsets from schistosomes is still lacking. It is known for mammalian EVs that the tetraspanin profile on EVs can differ per *in vitro* or *in vivo* source<sup>60</sup>. This also raises the question which of the isolated adult worm EVs were released by males or females in our mixed worm cultures, as both sexes have a different protein expression profile with potentially different immunomodulatory consequences<sup>28,61</sup>. IL-10 producing B cells have been identified in male only infections and in mixed-sex infections<sup>19,22</sup>, but the effect of female only secretions on immune cells has not been reported. Whether the EVs remain present at the B cell surface or are internalized by the cells or fuse with the membrane is something we could not evaluate by our TSP2 detection assay. Studying the fate of the worm EVs after interaction with the B cells will also provide directions for which molecules (surface or cargo) are most likely involved in the immune modulation.

The adult worm EVs may interact with B cells via a receptor or a receptor-in-

dependent mechanism. We know that these EVs are highly glycosylated<sup>14</sup> and that schistosome EVs can bind to antigen presenting cells via EV-associated glycans<sup>14,15</sup>. However, initial tests of pre-treating the B cells with EGTA to block glycan-lectin interactions or pre-treating the adult worm EV with the  $\alpha$ TSP2 antibody did not reduce interaction of the EVs with the B cells (Supplementary Figure S2). This suggests that C-type lectin receptors and TSP2 on the EVs are not essential for EV-B cell interaction and the putative downstream IL-10 induction. B cells express only few CLRs compared to myeloid cells and the B cell CLRs seem to have a bigger role in self-recognition and homeostasis<sup>62</sup> and only little is reported on their role in pathogen recognition<sup>63</sup>. However, since anti-glycan antibodies targeting schistosome glycans have been reported in naïve individuals<sup>64</sup>, there is a possibility that adult worm EVs and their associated glycans interact with B cell receptors recognizing those glycans. Future studies should address whether this putative interaction exists.

The differences in IL-6 response between the mouse (Figure 4) and human B cells (Figure 5) might be attributed to the fact that the B cell species and sources are different (spleen versus peripheral blood) and may represent different populations. For example, unstimulated human B cells lack TLR3 and TLR4 expression while mouse splenic B cells do express those receptors<sup>65</sup>. Furthermore, human peripheral blood B cells produce both IL-10 and IL-6 in response to various TLR stimulations, with or without additional CD40 ligation or added cytokines, while those B cell populations still exerted immune suppressive effects<sup>66</sup>. However, it is unclear to which extent IL-10 producing human peripheral blood and mouse splenic B cells induced by adult worm EVs have similar regulatory capacities.

This study shows that *Schistosoma*-derived EVs can target and affect B cells. This emphasizes that these blood-residing parasites have developed diverse and complex survival mechanisms via host immune modulation in which schistosome EV-host cell interactions should be considered as an important factor. *Schistosoma* EVs should therefore be taken into account in the design of novel vaccination strategies and/or strategies to target hyperinflammatory disorders.

## Acknowledgements

The authors would like to express their gratitude to Jan de Best and the other members of the life-cycle team for maintaining the availability of the parasites, Professor Alex Loukas from James Cook University, Queensland (Australia), for providing the TSP-2-targeting antibodies, Joyce Lam for assisting with the worm cultures, and Dr. Angela van Diepen for tracing back methods information.

## Funding

This work was supported by the Nederlandse Organisatie voor Wetenschappelijk Onderzoek (NWO) Graduate School Program (022.006.010) (to MK) and the Dutch Lung Foundation AWWA Consortium (5.1.15.015) (to HS).

## References

1. McManus, D. P. *et al.* Schistosomiasis. *Nature Reviews Disease Primers* **4**, (2018).
2. Hambrook, J. R. & Hanington, P. C. Immune Evasion Strategies of Schistosomes. *Front Immunol* **11**, 624178 (2020).
3. Acharya, S., Da'dara, A. A. & Skelly, P. J. Schistosome immunomodulators. *PLoS Pathog* **17**, e1010064 (2021).
4. Maizels, R. M., Smits, H. H. & McSorley, H. J. Modulation of Host Immunity by Helminths: The Expanding Repertoire of Parasite Effector Molecules. *Immunity* **49**, 801–818 (2018).
5. Skelly, P. J. & Da'dara, A. A. Schistosome secretomes. *Acta Trop* **236**, 106676 (2022).
6. White, R. *et al.* Special considerations for studies of extracellular vesicles from parasitic helminths: A community-led roadmap to increase rigour and reproducibility. *J Extracell Vesicles* **12**, e12298 (2023).
7. Théry, C. *et al.* Minimal information for studies of extracellular vesicles 2018 (MISEV2018): a position statement of the International Society for Extracellular Vesicles and update of the MISEV2014 guidelines. <https://doi.org/10.1080/20013078.2018.1535750> **7**, (2018).
8. Nowacki, F. C. *et al.* Protein and small non-coding RNA-enriched extracellular vesicles are released by the pathogenic blood fluke *Schistosoma mansoni*. *J Extracell Vesicles* **4**, 28665 (2015).
9. Sotillo, J. *et al.* Extracellular vesicles secreted by *Schistosoma mansoni* contain protein vaccine candidates. *Int J Parasitol* **46**, 1–5 (2016).
10. Zhu, L. *et al.* Molecular characterization of *S. japonicum* exosome-like vesicles reveals their regulatory roles in parasite-host interactions. *Sci Rep* **6**, 25885 (2016).
11. Samoil, V. *et al.* Vesicle-based secretion in schistosomes: Analysis of protein and microRNA (miRNA) content of exosome-like vesicles derived from *Schistosoma mansoni*. *Sci Rep* **8**, 3286 (2018).
12. Kifle, D. W. *et al.* Proteomic analysis of two populations of *Schistosoma mansoni*-derived extracellular vesicles: 15k pellet and 120k pellet vesicles. *Mol Biochem Parasitol* **236**, 111264 (2020).
13. Dagenais, M. *et al.* Analysis of *Schistosoma mansoni* extracellular vesicles surface glycans reveals potential immune evasion mechanism and new insights on their origins of biogenesis. *Pathogens* **10**, (2021).
14. Kuipers, M. E. *et al.* Life stage-specific glycosylation of extracellular vesicles from *Schistosoma mansoni* schistosomula and adult worms drives differential interaction with C-type lectin receptors DC-SIGN and MGL. *Frontiers in Molecular Biosciences* **10**, (2023).
15. Kuipers, M. E. *et al.* DC-SIGN mediated internalisation of glycosylated extracellular vesicles from *Schistosoma mansoni* increases activation of monocyte-derived dendritic cells. *J Extracell Vesicles* **9**, 1753420 (2020).
16. Meningher, T. *et al.* Schistosomal extracellular vesicle-enclosed miRNAs modulate host T helper cell differentiation. *EMBO Rep* **21**, e47882 (2020).
17. Ray, A., Wang, L. & Dittel, B. N. IL-10-independent regulatory B-cell subsets and mechanisms of action. *Int Immunol* **27**, 531–536 (2015).
18. Hussaarts, L., van der Vlugt, L. E., Yazdanbakhsh, M. & Smits, H. H. Regulatory B-cell induction by helminths: implications for allergic disease. *J Allergy Clin Immunol* **128**, 733–739 (2011).

19. van der Vlugt, L. E. P. M. *et al.* Schistosomes induce regulatory features in human and mouse CD1d(hi) B cells: inhibition of allergic inflammation by IL-10 and regulatory T cells. *PLoS One* **7**, e30883 (2012).
20. Haeberlein, S. *et al.* Schistosome egg antigens, including the glycoprotein IPSE/alpha-1, trigger the development of regulatory B cells. *PLoS Pathog* **13**, e1006539 (2017).
21. Obieglo, K. *et al.* Type I interferons provide additive signals for murine regulatory B cell induction by *Schistosoma mansoni* eggs. *Eur J Immunol* **49**, 1226–1234 (2019).
22. Mangan, N. E. *et al.* Helminth infection protects mice from anaphylaxis via IL-10-producing B cells. *J Immunol* **173**, 6346–6356 (2004).
23. Käll, L., Canterbury, J. D., Weston, J., Noble, W. S. & MacCoss, M. J. Semi-supervised learning for peptide identification from shotgun proteomics datasets. *Nat Methods* **4**, 923–925 (2007).
24. Kuipers, M. E. *et al.* Optimized Protocol for the Isolation of Extracellular Vesicles from the Parasitic Worm *Schistosoma mansoni* with Improved Purity, Concentration, and Yield. *J Immunol Res* **2022**, 5473763 (2022).
25. Van Deun, J. *et al.* EV-TRACK: transparent reporting and centralizing knowledge in extracellular vesicle research. *Nat Methods* **14**, 228–232 (2017).
26. Hussaarts, L. *et al.* Rapamycin and omega-1: mTOR-dependent and -independent Th2 skewing by human dendritic cells. *Immunol Cell Biol* **91**, 486–489 (2013).
27. Mouwenda, Y. D. *et al.* Characterization of T cell responses to co-administered hookworm vaccine candidates Na-GST-1 and Na-APR-1 in healthy adults in Gabon. *PLOS Neglected Tropical Diseases* **15**, e0009732 (2021).
28. Kenney, E. T. *et al.* Differential Excretory/Secretory Proteome of the Adult Female and Male Stages of the Human Blood Fluke, *Schistosoma mansoni*. *Frontiers in Parasitology* **1**, (2022).
29. Kaplan, A., Bueno, M. & Fournier, A. E. Extracellular functions of 14-3-3 adaptor proteins. *Cell Signal* **31**, 26–30 (2017).
30. Binder, R. J. Functions of heat shock proteins in pathways of the innate and adaptive immune system. *J Immunol* **193**, 5765–5771 (2014).
31. Sahoo, S. *et al.* Glyceraldehyde-3-phosphate dehydrogenase of the parasitic nematode *Haemonchus contortus* binds to complement C3 and inhibits its activity. *Parasite Immunol* **35**, 457–467 (2013).
32. Donnelly, S. *et al.* Helminth cysteine proteases inhibit TRIF-dependent activation of macrophages via degradation of TLR3. *J Biol Chem* **285**, 3383–3392 (2010).
33. Montes, C. L., Zuñiga, E. I., Vazquez, J., Arce, C. & Gruppi, A. Trypanosoma cruzi mitochondrial malate dehydrogenase triggers polyclonal B-cell activation. *Clin Exp Immunol* **127**, 27–36 (2002).
34. Houston, D. S., Carson, C. W. & Esmon, C. T. Endothelial cells and extracellular calmodulin inhibit monocyte tumor necrosis factor release and augment neutrophil elastase release. *J Biol Chem* **272**, 11778–11785 (1997).
35. Buro, C. *et al.* Transcriptome Analyses of Inhibitor-treated Schistosome Females Provide Evidence for Cooperating Src-kinase and TGF $\beta$  Receptor Pathways Controlling Mitosis and Eggshell Formation. *PLoS Pathog* **9**, e1003448 (2013).

36. Kato, T., Fahrmann, J. F., Hanash, S. M. & Vykoukal, J. Extracellular Vesicles Mediate B Cell Immune Response and Are a Potential Target for Cancer Therapy. *Cells* **9**, 1518 (2020).

37. Xie, M. *et al.* Immunoregulatory Effects of Stem Cell-Derived Extracellular Vesicles on Immune Cells. *Frontiers in Immunology* **11**, (2020).

38. Buzas, E. I. The roles of extracellular vesicles in the immune system. *Nat Rev Immunol* **23**, 236–250 (2023).

39. Adamo, A. *et al.* Extracellular Vesicles Mediate Mesenchymal Stromal Cell-Dependent Regulation of B Cell PI3K-AKT Signaling Pathway and Actin Cytoskeleton. *Frontiers in Immunology* **10**, (2019).

40. Mion, F. *et al.* Mast Cells Control the Expansion and Differentiation of IL-10-Competent B Cells. *The Journal of Immunology* **193**, 4568–4579 (2014).

41. Giera, M. *et al.* The *Schistosoma mansoni* lipidome: Leads for immunomodulation. *Analytica Chimica Acta* **1037**, 107–118 (2018).

42. Alves, C. C. *et al.* Sm29, but Not Sm22.6 Retains its Ability to Induce a Protective Immune Response in Mice Previously Exposed to a *Schistosoma mansoni* Infection. *PLoS Negl Trop Dis* **9**, e0003537 (2015).

43. Eyayu, T., Zeleke, A. J. & Worku, L. Current status and future prospects of protein vaccine candidates against *Schistosoma mansoni* infection. *Parasite Epidemiol Control* **11**, e00176 (2020).

44. Lopes, D. M. *et al.* *Schistosoma mansoni* rSm29 Antigen Induces a Regulatory Phenotype on Dendritic Cells and Lymphocytes From Patients With Cutaneous Leishmaniasis. *Front Immunol* **9**, 3122 (2019).

45. Cardoso, F. C. *et al.* *Schistosoma mansoni* Tegument Protein Sm29 Is Able to Induce a Th1-Type of Immune Response and Protection against Parasite Infection. *PLOS Neglected Tropical Diseases* **2**, e308 (2008).

46. Munier, C. C., Ottmann, C. & Perry, M. W. D. 14-3-3 modulation of the inflammatory response. *Pharmacol Res* **163**, 105236 (2021).

47. Fu, W. *et al.* 14-3-3 epsilon is an intracellular component of TNFR2 receptor complex and its activation protects against osteoarthritis. *Ann Rheum Dis* **80**, 1615–1627 (2021).

48. McGonigle, S., Beall, M. J., Feeney, E. L. & Pearce, E. J. Conserved role for 14-3-3 $\epsilon$  downstream of type I TGF $\beta$  receptors. *FEBS Letters* **490**, 65–69 (2001).

49. White, M. P. J. *et al.* The parasite cytokine mimic Hp-TGM potently replicates the regulatory effects of TGF- $\beta$  on murine CD4+ T cells. *Immunol Cell Biol* **99**, 848–864 (2021).

50. Tamayo, E., Alvarez, P. & Merino, R. TGF $\beta$  Superfamily Members as Regulators of B Cell Development and Function—Implications for Autoimmunity. *Int J Mol Sci* **19**, 3928 (2018).

51. Howe, S. *et al.* Lactate as a novel quantitative measure of viability in *Schistosoma mansoni* drug sensitivity assays. *Antimicrob Agents Chemother* **59**, 1193–1199 (2015).

52. Watson, M. J. *et al.* Metabolic support of tumour-infiltrating regulatory T cells by lactic acid. *Nature* **591**, 645–651 (2021).

53. Miholjcic, T. B. S. *et al.* Rationale for LDH-targeted cancer immunotherapy. *Eur J Cancer* **181**, 166–178 (2023).

54. Meng, X. *et al.* Hypoxia-inducible factor-1 $\alpha$  is a critical transcription factor for IL-10-producing B cells in autoimmune disease. *Nat Commun* **9**, 251 (2018).

55. Manosalva, C. *et al.* Role of Lactate in Inflammatory Processes: Friend or Foe. *Front Immunol* **12**, 808799 (2021).

56. Xiao, S. hua & Sun, J. Schistosoma hemozoin and its possible roles. *International Journal for Parasitology* **47**, 171–183 (2017).

57. Torgbor, C. *et al.* A Multifactorial Role for *P. falciparum* Malaria in Endemic Burkitt's Lymphoma Pathogenesis. *PLOS Pathogens* **10**, e1004170 (2014).

58. Parroche, P. *et al.* Malaria hemozoin is immunologically inert but radically enhances innate responses by presenting malaria DNA to Toll-like receptor 9. *Proceedings of the National Academy of Sciences* **104**, 1919–1924 (2007).

59. Chayé, M. A. M., Tontini, C., Ozir-Fazalalikhan, A., Voskamp, A. L. & Smits, H. H. Use of Toll-Like Receptor (TLR) Ligation to Characterize Human Regulatory B-Cells Subsets. *Methods Mol Biol* **2270**, 235–261 (2021).

60. Mizenko, R. R. *et al.* Tetraspanins are unevenly distributed across single extracellular vesicles and bias sensitivity to multiplexed cancer biomarkers. *Journal of Nanobiotechnology* **19**, 250 (2021).

61. Winkelmann, F. *et al.* Comparative proteome analysis of the tegument of male and female adult *Schistosoma mansoni*. *Sci Rep* **12**, 7569 (2022).

62. Brown, G. D., Willment, J. A. & Whitehead, L. C-type lectins in immunity and homeostasis. *Nat Rev Immunol* **18**, 374–389 (2018).

63. Ali, M. F., Driscoll, C. B., Walters, P. R., Limper, A. H. & Carmona, E. M.  $\beta$ -Glucan-Activated Human B Lymphocytes Participate in Innate Immune Responses by Releasing Proinflammatory Cytokines and Stimulating Neutrophil Chemotaxis. *J Immunol* **195**, 5318–5326 (2015).

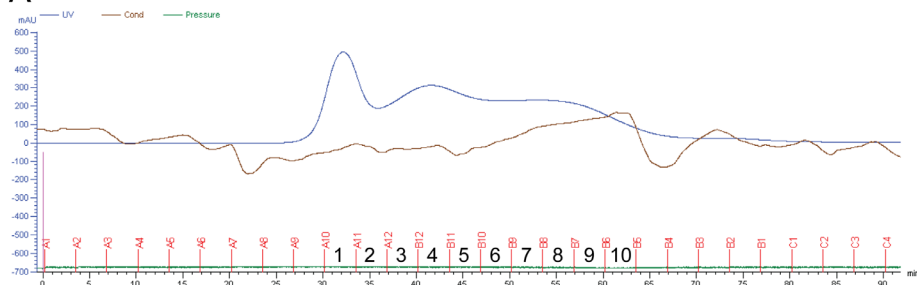
64. Kildemoes, A. O. *et al.* Identification of CAA as highly specific and sensitive antibody target for acute schistosomiasis diagnostics. 2023.03.07.23286891 Preprint at <https://doi.org/10.1101/2023.03.07.23286891> (2023).

65. Stögerer, T. & Stäger, S. Innate Immune Sensing by Cells of the Adaptive Immune System. *Frontiers in Immunology* **11**, (2020).

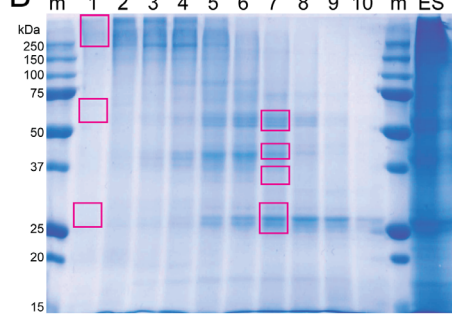
66. Glass, M. C. *et al.* Human IL-10-producing B cells have diverse states that are induced from multiple B cell subsets. *Cell Rep* **39**, 110728 (2022).

## Supplementary figures

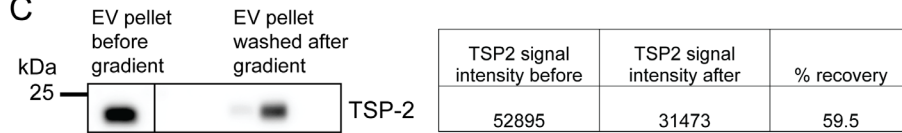
A



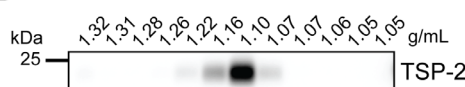
B



C

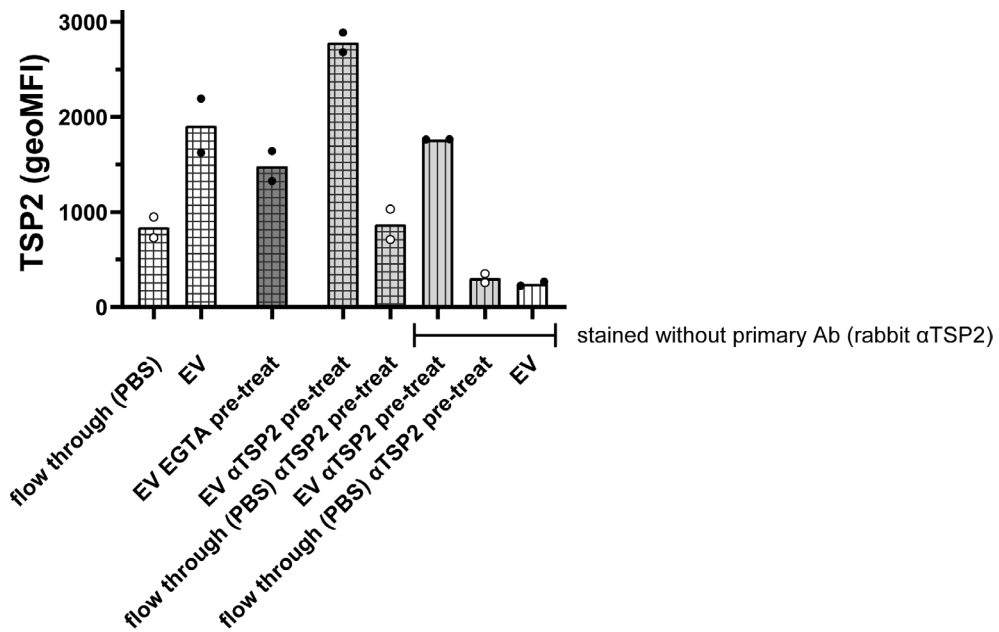


D



← **Supplement Figure S1. Representative chromatogram fractions of adult worm ES and adult worm EV isolation by density gradients**

**A:** Representative gel filtration chromatograph of one run of complete adult worm ES on a Sephadex S-300 HR column. Collected fractions are indicated as 1-10. **B:** SDS-PAGE coomassie staining of chromatogram fractions 1-10 and total ES. Pink squares indicate the areas that were cut for in-gel-digestion and proteomics analysis. m, marker. **C:** EVs in a  $100,000 \times g$  pellet were equally split and one half was subjected to an iodixanol density gradient purification step after which the EV containing fractions were pooled and EVs re-pelleted and resuspended in the same volume as the other half. EVs before and after the gradient were checked for the marker TSP2 by western blotting and signals intensities were determined with ImageJ. Loss of EVs is >40%. **D:** The  $100,000 \times g$  EV-depleted ES was ultracentrifuged at  $200,000 \times g$  and the pelleted material was subjected to iodixanol density gradient centrifugation, after which 12 density fractions were collected. Western blot of TSP2 shows that adult worm EVs are still present in the EV-depleted ES.



**Supplement Figure S2. No effect of pre-incubation of EVs with αTSP2 or pre-incubation of cells with EGTA on EV-B cell interaction**

EVs and ES flow through (FT, equal to PBS) were or were not pre-incubated for 30 minutes with αTSP2 (1:500) (αTSP2 pre-treat). Splenic B cells from mice were pre-incubated with or without EGTA (10 mM) for 30 minutes before incubation with adult worm EVs (EGTA pre-treat). EVs and ES flow through including their pre-treatments were added in similar amount as 50 µg/ml ES and incubated with the B cells for 18 hours. Cells were washed and stained for TSP2 (primary rabbit-αTSP2) and a secondary antibody with fluorochrome (donkey αrabbit) to indicate EV binding. Average TSP2 geometric mean fluorescent intensity (geoMFI) of the incubated B cells was measured by flow cytometry. Data from 2 independent experiments.

Supplementary Data Sheet can be viewed here →







# Chapter 6

## DC-SIGN mediated internalisation of glycosylated extracellular vesicles from *Schistosoma* *mansonii* increases activation of monocyte-derived dendritic cells

Marije E. Kuipers, Esther N.M. Nolte-’t Hoen, Alwin J. van der Ham, Arifa Ozir-Fazalalikhan, D. Linh Nguyen, Clarize M. de Korne, Roman I. Koning, John J. Tomes, Karl F. Hoffmann, Hermelijn H. Smits\*, Cornelis H. Hokke\*  
\*These authors contributed equally

Journal of Extracellular Vesicles, 2020

PMID: 32489529

DOI: [10.1080/20013078.2020.1753420](https://doi.org/10.1080/20013078.2020.1753420)

## Abstract

Helminths like *Schistosoma mansoni* release excretory/secretory (ES) products that modulate host immunity to enable infection. Extracellular vesicles (EVs) are among these ES products, yet molecular mechanisms and functionality of *S. mansoni* EV interaction with host immune cells is unknown. Here we demonstrate that EVs released by *S. mansoni* schistosomula are internalised by human monocyte-derived dendritic cells (moDCs). Importantly, we show that this uptake was mainly mediated via DC-SIGN (CD209). Blocking DC-SIGN almost completely abrogated EV uptake, while blocking mannose receptor (MR, CD206) or dendritic cell immunoreceptor (DCIR, CLEC4A) had no effect on EV uptake. Mass spectrometric analysis of EV glycans revealed the presence of surface N-glycans with terminal  $\text{Gal}\beta 1\text{-}4(\text{Fuc}\alpha 1\text{-}3)\text{GlcNAc}$  (Lewis X or  $\text{Le}^x$ ) motifs, and a wide array of fucosylated lipid-linked glycans, including  $\text{Le}^x$ , a known ligand for DC-SIGN. Stimulation of moDCs with schistosomula EVs led to increased expression of costimulatory molecules CD86 and CD80 and regulatory surface marker PD-L1. Furthermore, schistosomula EVs increased expression of IL-12 and IL-10 by moDCs, which was partly dependent on the interaction with DC-SIGN. These results provide the first evidence that glycosylation of *S. mansoni* EVs facilitates the interaction with host immune cells and reveals a role for DC-SIGN and EV-associated glycoconjugates in parasite-induced immune modulation.

## Introduction

*Schistosoma mansoni* is one of the major helminth parasites of humans with over 200 million people infected<sup>1,2</sup>. In the initial phase of infection, schistosome larvae (cercariae) penetrate the skin of the host and transform into schistosomula. These schistosomula larvae will migrate to the circulatory system, develop into adult worms that mate and lay eggs<sup>3</sup>. *S. mansoni* can live up to 10 years in its host because it has developed successful mechanisms to evade immune responses. To establish this immune evasion, the parasite releases excretory/secretory (ES) products that act on the host immune system<sup>4</sup>. Among these ES products are extracellular vesicles (EVs) and evidence is accumulating that parasite-derived EVs contribute to parasite-host interaction<sup>5</sup>. The molecular composition of EVs from *S. mansoni* larvae and adult worms life stages has been partially characterized<sup>6-8</sup>, but the interaction of their EVs with host cells remains unexplored.

For schistosomes to initiate and maintain infection, modulating host innate and adaptive immune responses is crucial<sup>9</sup>. Mouse models have shown that cercarial penetration triggers migration of innate antigen presenting cells (APCs), such as macrophages and dendritic cells (DCs), towards the skin draining lymph nodes<sup>10</sup>. These APCs have upregulated costimulatory molecules, like CD86 and major histocompatibility complex (MHC) class II, which are important for initiating adaptive immune responses. *In vitro* stimulation of mouse bone marrow-derived DCs (BMDCs) with ES from schistosomula shows a similar pattern: increased costimulatory molecules and MHC class II expression and increased pro-inflammatory cytokine release (IL-6, IL-12, and TNF- $\alpha$ )<sup>11</sup>. Furthermore, cercarial secretions can upregulate the expression of IL-10 and programmed death ligand (PD-L)1 and 2 in human monocyte-derived (mo)DCs, suggesting that the parasite additionally utilizes regulatory pathways to dampen adaptive immune responses<sup>12</sup>. Relatively little is known about the exact molecular or structural components derived from schistosomula that induce immunomodulatory effects. Thus far, it has been shown that recombinant tetraspanins, transmembrane proteins associated to adult worm EVs<sup>13</sup>, induce IL-10 and Th1 cytokine responses by peripheral blood mononuclear cells<sup>14</sup>. Whether schistosomula EVs have similar effects on human DCs has not been investigated.

Studies exploring the molecular content of schistosomula ES have shown that part of the cytokine responses by mouse macrophages and whole blood of infected individuals is induced by glycosylated antigens in the ES<sup>15,16</sup>. Schistosome glycoconjugates can be recognized by host pathogen recognition receptors (PRRs) on APCs, in particular the C-type lectin receptors (CLRs) such as the mannose receptor (MR, CD206)<sup>17</sup>, dectin-1/2<sup>18</sup>, dendritic cell immunoreceptor (DCIR, CLEC4A, CD367)<sup>19</sup>, and dendritic cell-specific ICAM-3-grabbing nonintegrin (DC-SIGN,

CD209)<sup>20</sup>. A well-known immunogenic glycan-motif, Gal $\beta$ 1-4(Fuc $\alpha$ 1-3)GlcNAc or Lewis X (Le $x$ ), is present on glycoproteins in schistosomula and egg ES and can be recognized by DC-SIGN<sup>21</sup> as well as MR<sup>22</sup>, leading to different effects depending on the structural context of the Le $x$  motif. Pathogen-associated molecular patterns (PAMPs) containing high-mannose (oligomannose) structures, which form ligands for MR and DC-SIGN<sup>23</sup> have also been found on glycoproteins in ES from schistosomes<sup>24</sup>. This raises the question whether schistosomula EVs expose glycans instrumental in targeting to host immune cells and whether these EV-associated glycans play a role in modifying subsequent immune responses. While it is known that mammalian EVs contain glycoconjugates, publications on the structure and function of EV glycans are very limited so far<sup>25-29</sup>.

In order to gain insights into the interaction of schistosome EVs with the immune system we studied the interaction of schistosomula EVs with human moDCs and found that the EVs are internalised mainly via DC-SIGN. We show that N-glycans on the surface and glycolipids of the EVs contain DC-SIGN ligands, including Le $x$ . Furthermore, we demonstrate that these EV preparations increase the activation status of moDCs, affecting both immunostimulatory and immunoregulatory pathways which were partly dependent on the interaction with DC-SIGN. Our study provides evidence for a specific CLR-mediated uptake of EVs that substantiates the importance of EV-associated glycoconjugates in pathogen-host interaction.

## Materials and Methods

### Schistosomula culture

Infected *Biomphalaria glabrata* snails were incubated in water at 30 °C for 2 h to shed cercariae of the Puerto Rican-strain of *S. mansoni* by exposure to light. The collected cercariae in water were stored on ice for 1.5 h to immobilize them and were subsequently pelleted by centrifugation at 440 × g. After removal of the supernatant, 12 ml of pre-warmed (37 °C) DMEM (Dulbecco's Modified Eagle Medium, high glucose with L-glutamine, Lonza, Basel, Switzerland) supplemented with 200 U/ml penicillin and 200 µg/ml streptomycin (Sigma-Aldrich, St. Louis, MO, USA), was added to transform the cercariae to schistosomula by providing mechanical force via pipetting and incubating for 20 min at 37 °C<sup>30</sup>. Cercarial bodies were separated from their tails using an orbital shaker. The collected schistosomula were resuspended in DMEM at a concentration of 7,500 schistosomula/ml and cultured in 25 cm<sup>2</sup> polystyrene flasks (Greiner Bio-One, Alphen a/d Rijn, The Netherlands) at 37 °C and 5% CO<sub>2</sub> for 72 h.

## EV isolation and staining

Schistosomula ES products were enriched for EVs by differential centrifugation as previously described, with minor modifications<sup>6</sup>. Briefly, the collected culture supernatant (9–34 ml per culture, 7,500 schistosomula/ml) was centrifuged in 15 ml tubes (Greiner Bio-One) twice at 500 × *g* (k-factor 115,790.8) for 2 min (4 °C) (SX4750A rotor and an Allegra X-15R centrifuge) (Beckman Coulter, Brea, CA, USA) with low brake to remove remaining parasites. To remove any residual debris, the supernatant was subsequently centrifuged at 700 × *g* (k-factor 82,764.4) for 20 min (4 °C, low brake). Next, an EV-enriched pellet was obtained by centrifugation of the supernatant at 31,000 rpm (average around 120,000 × *g*, k-factor 216.3) for 80 min at 4 °C (max. acceleration and brake), followed by three wash steps with cold phosphate buffered saline (PBS) (B. Braun, Melsungen, Germany) in thinwall polypropylene tubes using an SW41 Ti rotor and an Optima XE-90 ultracentrifuge (Beckman Coulter). For binding/uptake experiments, EVs were stained with PKH26 (Sigma-Aldrich) after the first ultracentrifugation step by addition of 80 µl Diluent C to the resuspended EV-enriched pellet and incubation of 93 µl diluted PKH26 (1.5 µl in 100 µl Diluent C) for 3 min at RT before addition of 11 ml PBS. Unconditioned culture medium incubated without parasites was processed (and stained) following the same procedures and was used as (dye) control. EV-enriched pellets (from 66,300–253,200 schistosomula) for *in vitro* experiments were resuspended in 510 µl PBS, for transmission electron microscopy (TEM) and glycan analysis in 100 µl PBS, and for cryo EM in 40 µl PBS. All were stored at -80 °C until further use except for 1 cryo EM sample, which was processed directly after EV isolation. We have submitted all relevant data of our experiments to the EV-TRACK knowledgebase (EV-TRACK ID: EV190032)<sup>31</sup>.

## Transmission electron microscopy

EV preparations were generated in Leiden and visualized by TEM at Aberystwyth University, as described previously<sup>6</sup>. Briefly, 10 µl of EV-enriched sample was fixed with an equal volume of 4% glutaraldehyde, adsorbed onto Formvar/carbon-coated copper grids (Agar scientific, Stansted, UK) for 40 min, and subsequently contrast stained with 2% uranyl acetate (pH 4) for 10 min. Processed samples were then visualized on a Jeol 1010 transmission electron microscope operated at 80 kV. Images were recorded with a Kodak MegaPlus camera Model 1.4i, other than the addition of scale bars, no further image processing was done. Sizes were measured by hand using Fiji/ImageJ software<sup>32</sup>.

## Nanoparticle tracking analysis (NTA)

EV-enriched suspensions were diluted 1:100 in PBS (to obtain 25–100 particles per frame at camera level 16) before analysing the concentration and size distribution by nanoparticle tracking analysis (NTA) using a NanoSight NS500 (Malvern Panalytical, Malvern, UK) equipped with an sCMOS camera. For each EV-enriched pellet, three videos of 30 seconds were recorded on three different camera levels: 12, 14, and 16. The analysis was done with NTA3.3 software and a detection threshold of 5. The average particle concentration of nine videos per EV-enriched sample, after subtraction of the NTA background data from PBS alone, was used for further experiments. We additionally measured the protein concentration of the EV-enriched pellets with microBCA according to the manufacturers protocol (Pierce, Thermo Fisher Scientific, Waltham, MA, USA).

## Cryo electron microscopy

Previously frozen or freshly isolated EV preparations (EV from 86,00–112,00 schistosomula in 40 µl PBS) were visualized by cryo EM. Copper EM grids supporting a carbon film with regularly spaced 2 micron holes (R2/2, Quantifoil, Jena, Germany) were glow-discharged in air at 0.2 mbar for 2 min at 20 mA (EMITECH K950X with glow discharger unit). A 3 µl drop of sample was applied to the grid and transferred into the environmental chamber of a Leica EM grid plunger (Leica Microsystems, Wetzlar, Germany) operating at RT and between 92% and 94% humidity. Excess sample was blotted away for 1 second using filter paper (Whatman no.1) and without waiting plunged into a mixture of ethane/propane (63/37 v/v) cooled with liquid nitrogen to -193 °C. After vitrification, grids were stored under liquid nitrogen and transferred into a cryo holder (type 626, Gatan, Germany). In total 238 cryo-EM projection images were recorded by 1 second exposures at spot 5 on a FEI Tecnai F12 at 120 kEV on a 4k × 4k CCD camera (Eagle, Thermo Fisher Scientific) at a magnification of 13,500 × (0.85 nm pixel size) and a defocus value ~ -8 microns. Size measurement was performed by hand using Fiji/ImageJ software<sup>32</sup>. After removing double images and images with no EVs, 233 images were used to measure a total of 1056 EVs, which were subsequently quantified in segments of 20 nm (i.e. 21–40 nm, 41–60 nm, 61–80 nm...861–880 nm, 881–900 nm).

## Human monocyte-derived dendritic cells (moDCs)

Venous blood of healthy volunteers who provided informed consent, approved by the Institutional Review Board of Leiden University Medical Centre, was used to isolate monocytes and differentiate to moDCs as previously described<sup>33</sup>. Immature DCs were harvested on day 5 or 6, counted, seeded at 5 × 10<sup>4</sup> cells/well in a 96

well flat-bottom plate, and rested overnight at 37 °C and 5% CO<sub>2</sub>. Subsequently, cells were stimulated with or without a pre-incubation of 30 min with 10 mM EGTA (Sigma-Aldrich), 20 µg/ml αDC-SIGN/CD209 (clone AZN-D1, custom order without sodium-azide) (Beckman Coulter), 20 µg/ml αMR/CD206 (clone 15-2) (BioLegend, San Diego, CA, USA), 20 µg/ml αDCIR/CLEC4A (clone 111F8.04, Dendritics, Novus Biologicals, Centennial, CO, USA), and 20 µg/ml mouse IgG1 isotype control (clone P3.6.2.8.1) (Invitrogen, Thermo Fisher Scientific) in the presence of αFcγR-binding inhibitor (eBioscience, Invitrogen) and in the presence or absence of the maturation factors IL-1β (25 ng/ml) (BioLegend) and TNF-α (50 ng/ml) (Sino Biological, Beijing, P.R. China) or LPS (100 ng/ml) (InvivoGen, San Diego, CA, USA). As a positive control for the αMR, PF-647-labelled recombinant omega-1 was used<sup>22,34</sup>. EV-enriched pellets were thawed only once and several EV batches were pooled before incubation with the cells (6 × 10<sup>9</sup> EV/ml or mentioned otherwise). To investigate the effect of surface de-N-glycosylation, EVs were incubated with or without peptide N-glycosidase F (PNGase F) (4 U/100 µl, Roche Diagnostics, Almere, The Netherlands) at 37 °C for 20 h before moDC incubation. Supernatants were collected from >85% CD1a<sup>+</sup> cell cultures after 24 h stimulation and IL-6 (Sanquin, Amsterdam, The Netherlands), IL-10 (BioLegend), and IL-12p70 (BD Biosciences, Franklin Lakes, NJ, USA) cytokine production was determined with ELISA according to the manufacturers protocols. Stimulated moDCs were washed, stained, and measured by flow cytometry on a FACSCanto II (BD Bioscience) and using the following antibodies: CD1a-BV421 (clone HI149) (BioLegend), HLA-DR-APC-eF780 (clone LN3) (eBioscience), PD-L2/CD273-FITC (clone MIH18) (Miltenyi Biotec, Bergisch Gladbach, Germany), CD86-FITC (clone 2331 (FUN-1)), CD40-APC (clone 5C3), CD80-V450 (clone L307.4), PD-L1/CD274-PE-Cy7 (clone MIH1) (all BD Bioscience) with the addition of Fc receptor binding inhibitor (eBioscience) and Aqua live/dead staining (Invitrogen). Flow cytometric measurements were analysed with FlowJo (version 10, BD Bioscience).

## Confocal microscopy

5 × 10<sup>4</sup> moDCs/chamber were seeded onto poly-L-lysine (Sigma-Aldrich) coated coverslips of a 4 chamber glass bottom dish (ø35mm; Greiner Bio-One) for 24 h. Cells were pre-incubated with EGTA or αDC-SIGN+αFcγR-binding inhibitor as described above, incubated with PKH-labelled schistosomula EV-enriched pellets for 5 h, subsequently washed, and treated with Hoechst (Sigma-Aldrich). Images were taken at 37 °C and 5% CO<sub>2</sub> on a Leica TCS (true confocal scanning SP8 WLL (white light laser) microscope (Leica Microsystems). The sequential scanning mode was applied to image Hoechst (excitation: 405 nm, emission: 420–470 nm) and PKH26 (excitation: 561 nm, emission: 570–630 nm). For imaging the uptake of

EVs, a 63× objective (Leica HC PL APO 63×/1.40na OIL CS2) was used. The z-stacks were recorded and maximum projections of the recorded z-stacks were generated using the Leica software (LAS X version 1.1.0.12420; Leica Microsystems).

### N-glycan and glycolipid-glycan analysis

For the N-glycan analysis, EV-enriched pellets (in PBS) from >100,000 cultured schistosomula were lyophilized, resuspended in 100  $\mu$ l milliQ water, sonicated and subsequently reduced and denatured for 10 min at 95 °C with the addition of SDS and  $\beta$ -mercaptoethanol which were neutralized by adding NP-40 (Sigma-Aldrich). Full details on N-glycan isolation has been described previously<sup>35</sup>. N-glycans were released by PNGase F (4 U/100  $\mu$ l) incubation for 24 h at 37 °C and cleaned up by collection in the flow through of reversed phase (RP) C18-cartridges (JT Baker, Phillipsburg, NJ, USA) followed by isolation on carbon cartridges (Supelclean ENVI-carb SPE, Sigma-Aldrich). In addition, directly after isolation, intact EV preparations in PBS were treated with PNGase F for 24 h at 37 °C to release directly accessible N-glycans (surface glycans). The total suspension was subsequently transferred to a thinwall polypropylene tube and topped up with PBS. The EVs were pelleted by ultracentrifugation at 42,000 rpm (average around 120,000  $\times g$ , k-factor 85.4) for 65 min at 4 °C (max. acceleration and brake) using a TLS-55 rotor and an Optima TLX (Beckman Coulter). Next, the supernatant containing the PNGase F released N-glycans was collected and these N-glycans were isolated with C18- and carbon-cartridges. The EV-enriched pellet without PNGase F accessible surface N-glycans was resuspended in PBS, lyophilized, sonicated, reduced, denatured, and treated with PNGase F to isolate remaining N-glycans as above.

For glycolipid-glycans analysis, EV-enriched pellets were lyophilized, resuspended in milliQ water, sonicated, and subjected to extraction with chloroform and methanol (MeOH). The upper phase was collected after sonication and centrifugation. Similar volume as collected was replaced with 50% MeOH and the previous steps were repeated twice. All collected upper phases of the extraction were applied to an RP C18-cartridge and flow-through and wash fractions were combined and applied to another C18-cartridge. Glycolipids were eluted from the cartridges with chloroform/MeOH/water and dried under a flow of nitrogen. The glycolipids were subsequently dissolved in 200  $\mu$ l 50 mM sodium acetate with 0.1% sodium taurodeoxycholate hydrate (Sigma-Aldrich), sonicated, and heated to 60 °C for 10 min. 2 mU of recombinant endoglycoceramidase II (*Rhodococcus* sp.) (rEGCase II) (Takara-bio, Kusatsu, Shiga, Japan) was added to release the lipid-bound glycans. After 24 h at 37 °C, another 2 mU was added and the sample was incubated at 37 °C for another 24 h. The purification of released

lipid-glycans was performed as described for the N-glycans using RP C18- and carbon cartridges.

To support glycan structure assignments, part of the isolated N-glycans and glycolipid-glycans were additionally treated with hydrofluoric acid (HF), which removes labile substitutions including  $\alpha$ 1-3 linked fucoses. All isolated glycans were labelled with 2-aminobenzoic acid and purified by Biogel P10 (Bio-Rad, Hercules, CA, USA). The labelled glycans were measured by MALDI-TOF-MS with 2,5-dihydroxybenzoic acid (Bruker Daltonics, Bremen, Germany) as matrix using UltrafleXtreme mass spectrometers (Bruker Daltonics) in the negative-ion reflectron mode. When necessary, samples were cleaned up with ZipTip C18 (Merck Millipore, Burlington, MA, USA) before MALDI-TOF-MS. The obtained mass spectra were smoothed and the base-line was subtracted using FlexAnalysis (version 3.4, Bruker Daltonics). Glycan compositions were identified from the peak lists using GlycoWorkbench (Version 3)<sup>36</sup>. Peaks with a signal to noise ratio below 2 were excluded and masses are registered as deprotonated  $[M-H]^-$ . 2-AA was taken into account as a fixed reducing-end modification. For the interpretation of the relative most abundant signals for spectral assignments we used (when available) previously published structural data from *S. mansoni* glycans<sup>35</sup>. In the spectra, the structure of the most likely or most abundant isomer of the composition is indicated.

## RNA extraction and qPCR analysis

Human moDCs were pre-incubated with or without  $\alpha$ DC-SIGN,  $\alpha$ MR, or IgG1 isotype and stimulated with IL-1 $\beta$  and TNF- $\alpha$  and schistosomula EV-enriched preparations as described above. After 6 h stimulation at 37 °C and 5% CO<sub>2</sub>, cells were stored on ice for 10 min, harvested, washed with cold PBS, snap frozen, and stored at -80 °C till RNA extraction. RNA was extracted with the RNeasy Kit (Qiagen, Hilden, Germany) according to the manufacturer's protocol. RNA was quantified using NanoDrop 1000 Spectrophotometer (Thermo Fisher Scientific) and cDNA synthesis was performed on 0.2  $\mu$ g RNA according to standard procedures. Primer Express (Applied Biosystems, Waltham, MA, USA) was used to design primers that were synthesized by Biolegio (Nijmegen, The Netherlands). Sequences of the primers were:  $\beta$ -actin\_Foward(F): 5'- GCTACGAGCTGCCTGACGG-3';  $\beta$ -actin\_Reverse(R): 5'- CAGCGAGGCCAGGATGGAGCC-3';  $\beta$ -2-M\_F: 5'- TGCCGTGTGAACCATGTGA-3';  $\beta$ -2-M\_R: 5'-CCAAATGCGGCATCTCAA-3'; RPLPO\_F: 5'-GGCGACCTGGAAGTCCAAT-3'; RPLPO\_R: 5'-CCATCAGCAC-CACAGCCTTC-3'; IL-10\_F: 5'-ACCTGCCTAACATGCTTCGAG-3'; IL-10\_R: 5'-CCAGCTGATCCTTCATTGAAAG-3'; TNF- $\alpha$ \_F: 5'-TCTTCTCGAACCCCGAGTGA-3'; TNF- $\alpha$ \_R: 5'-CCTCTGATGGCACCACCAAG-3'; IL-12p35\_F: 5'-CTCCTGGACCACCT-

CAGTTTG-3'; IL-12p35\_R: 5'-TTGTCTGGCCTCTGGAGCA-3'. Quantitative real-time PCR (qPCR) was performed using CFX96 instruments (Bio-Rad Laboratories) and CFX Maestro (Bio-Rad) software. Technical duplicates with  $<1$   $C_q$  value difference were averaged and gene expression was calculated with the  $\Delta\Delta C_q$  method using the average  $C_q$  of the reference genes  $\beta$ -actin,  $\beta$ -2-M, and RPLPO to normalize<sup>37</sup>.

## Statistical analyses

All data were analysed using a paired student t-test or repeated measures One-way ANOVA (P-values  $<0.05$  were considered significant) with Tukey's or Dunnett's Multiple Comparison Test in GraphPad Prism 5.0 (GraphPad Software, Inc., La Jolla, CA, USA).

## Results

### Cryo electron microscopy reveals ultrastructural characteristics of schistosomula EVs

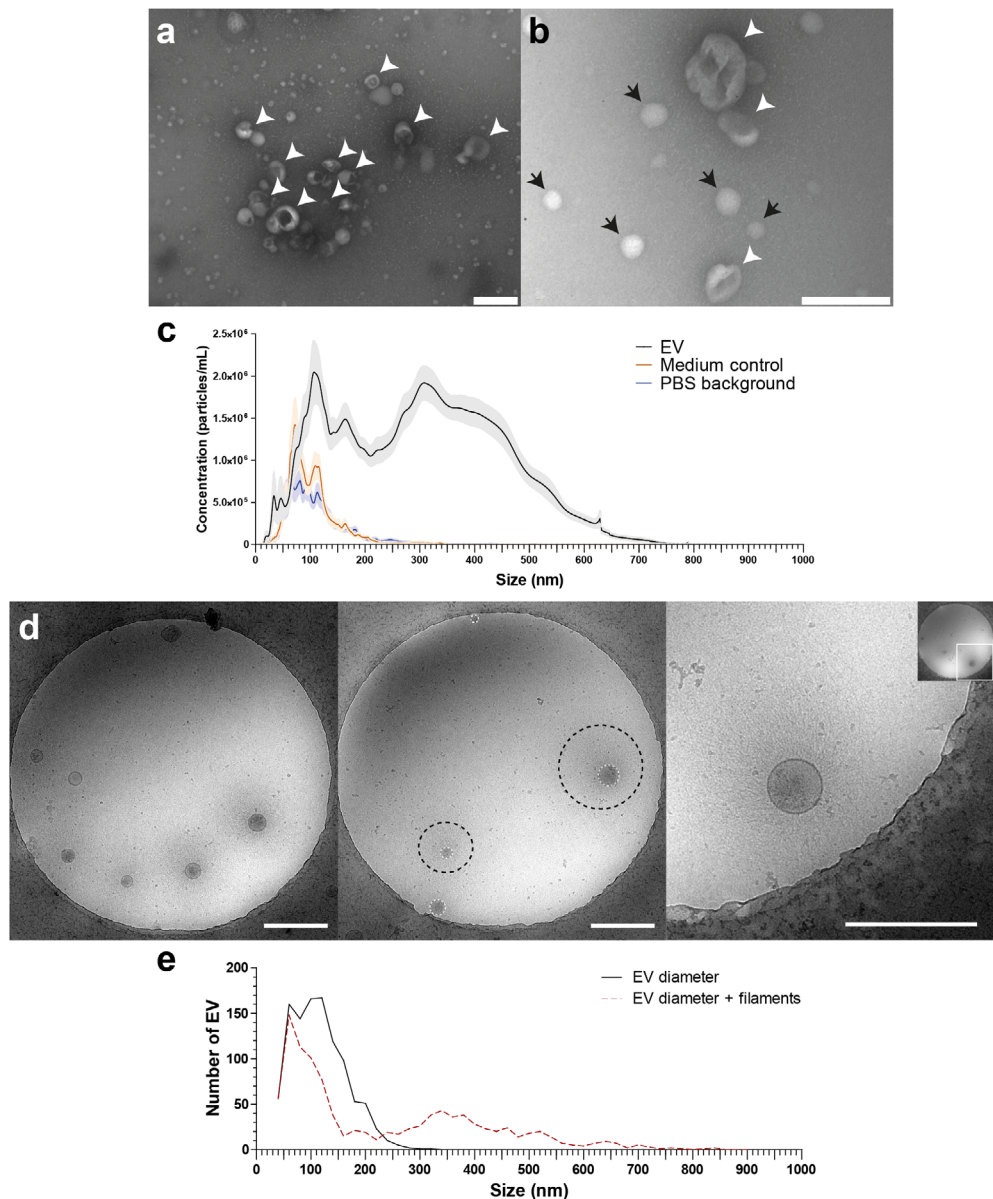
Schistosomula were cultured for 72 h and EV-enriched preparations were obtained from schistosomula ES by sequential (ultra)centrifugation steps. TEM confirmed isolation of vesicles in the size-range between 35 and 190 nm (Figure 1a-b). NTA analysis showed a size-range of 30–650 nm with a minor peak around 40 nm and three major peaks around 110, 160, and 350 nm (Figure 1c). Culture medium without parasites that was processed similarly (medium control) and PBS alone only showed minor peaks between 60 and 150 nm as NTA background (Figure 1c).

#### → Figure 1. TEM, NTA and cryo EM measurement of schistosomula EVs

EV-enriched preparations analysed by transmission electron microscopy at 60,000  $\times$  (a) and 120,000  $\times$  magnification (b). Scale bars are 200 nm. EVs are pointed out with arrow heads, the small ( $<60$  nm) structures (black arrows) in (b) are artefacts and were also observed in PBS only. In addition, EVs were analysed by nanoparticle tracking analysis (NTA) (c). The graph shows the average of 17 schistosomula EV-enriched preparations (black line), 10 medium controls (dark orange line), and 15 PBS (background) in which the preparations were resuspended (blue line), averages are shown with SEM (lighter areas). Cryo EM of EVs at 13,500  $\times$  magnification (d). Scale bars are 500 nm. The EV membrane and stretch of the filamentous structures are indicated in the middle pane with white dashed circles and black dashed circles, respectively. Right pane shows a close up of one EV with filaments. Quantification of the EV sizes excluding (EV diameter) or including (EV diameter + filaments) the thin filaments from a total of 1056 EVs (e). EM pictures are representative for four biological replicates.

The average particle concentration measured with NTA was  $2.33E^{10}/100,000$  schistosomula and the average protein concentration of EV-enriched preparations was  $6 \mu\text{g}/100,000$  schistosomula.

Although the TEM images corresponded with previous observations<sup>6</sup>, there was a discrepancy in the sizes measured with the TEM and NTA. Therefore, we



additionally analysed the EV preparations with cryo EM to visualise the near native state of the EVs and measure their size (Figure 1d). Interestingly, the cryo EM revealed thin filament-like structures covering the EV surface in 45.5% of all measured EV and in >70% of EVs when excluding EVs smaller than 100 nm. The filamentous structures ranged from 10 to 340 nm in length (average length of 128.5 nm) additional to the size of the EV diameter to the EV membrane (Figure 1e). These surface structures were most likely lost during the sample preparation for negative stained TEM (Figure 1a) and thus not observed, while NTA size measurement did include these structures as shown by similar size ranges between NTA and cryo EM.

### **Internalisation of schistosomula EV by human moDCs is calcium dependent**

To investigate the interaction of schistosomula EVs with human moDCs, EVs were first labelled with the fluorescent dye PKH26. MoDCs ( $0.25E^6$  moDC/ml) were incubated with a maximum of  $6E^9$  EV/ml, which is equivalent to approximately 10 moDCs receiving the number of EVs released by one schistosomulum during three days of culture. After 2 h of incubation, there was a dose-dependent increase in EV binding/uptake by the CD1a<sup>+</sup> moDCs indicated by an increased geometric mean fluorescence intensity (geoMFI) relative to cells in medium only (Figure 2). Furthermore, the fluorescence of cells incubated with dye control was unchanged, indicating that the increase in MFI was due to binding/uptake of labelled EVs and not due to dye aggregates<sup>38</sup>. EV binding/uptake by moDCs did not change due to stimulation of the cells with LPS or in the presence of IL-1 $\beta$ +TNF- $\alpha$ . Incubation at 4 °C instead of 37 °C did not lead to binding/uptake of EVs by the moDCs (Figure 2), suggesting that the interaction with and uptake of the schistosomula EVs by target cells are active processes. We visually confirmed that EVs were internalised by moDCs with confocal microscopy (Figure 2c).

MoDCs are known to express C-type lectin receptors that bind glycan motifs present on schistosome ES components in a calcium dependent manner<sup>39</sup>. To investigate whether moDCs also recognise schistosomula EVs via CLR-glycan motif interactions, moDCs were incubated with fluorescently labelled EVs in the presence of the calcium chelator EGTA and subsequently analysed by flow cytometry and confocal microscopy (Figure 2d-e). Pre-incubation of EGTA almost completely abrogated the fluorescence signal and EV internalisation of moDCs compared to EV-exposed moDCs without EGTA pre-incubation, indicating calcium dependent interaction with moDCs such as CLRs. Next, when EGTA was added after incubation with EVs in order to remove EVs bound to CLRs, this resulted in

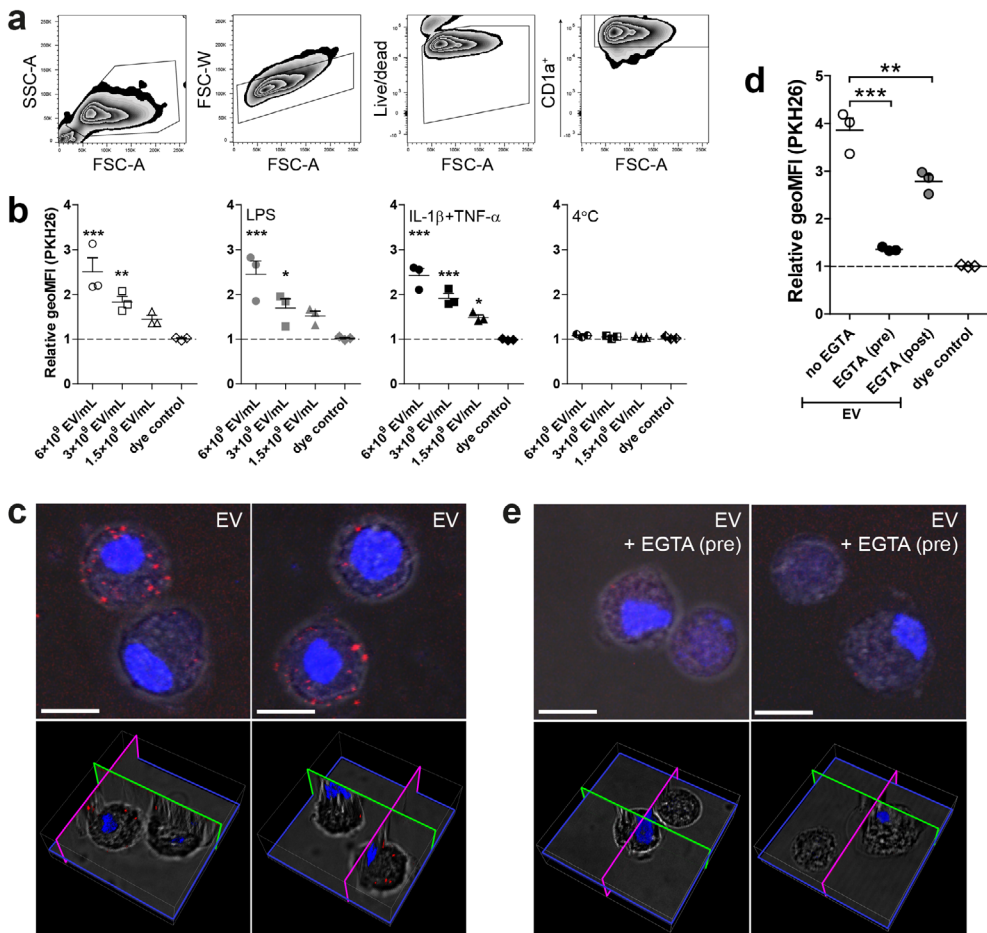


**Figure 2. Dose dependent uptake of schistosomula EVs by human moDC is temperature and calcium dependent**

Measured PKH26 fluorescence (PKH26 labelled EVs) of CD1a<sup>+</sup> cells was obtained via gating as pictured in (a). The geoMFI (geometric mean fluorescent intensity) of PKH26 is shown relative to unstimulated cells (b). MoDC from three donors. EV uptake visualized by confocal microscopy (c). Images show maximum projections (top panels) and 3D visualizations (bottom panels) of recorded z-stacks of two different fields. PKH26-labelled EVs are stained in red and the nuclei in blue (Hoechst). Selected pictures are representative for three donors. Human moDC incubated with EVs with either EGTA added pre- or post-incubation (d). Confocal images of moDC pre-treated with EGTA followed by EV incubation (e). Scale bars are 10  $\mu$ m. Mean  $\pm$  SEM \*p < 0.05, \*\*p < 0.01, \*\*\*p < 0.001, using repeated measures ANOVA with Dunnett's Multiple Comparison Test compared to cells in medium only (b) or repeated measures ANOVA with Tukey's Multiple Comparison Test (d). SSC-A, side-scatter; FSC-A, forward-scatter

only a minor reduction of fluorescence signal (Figure 2d), confirming that most of the EVs were internalised by moDCs rather than bound to the surface.

### Schistosomula EVs contain CLR ligands on their surface

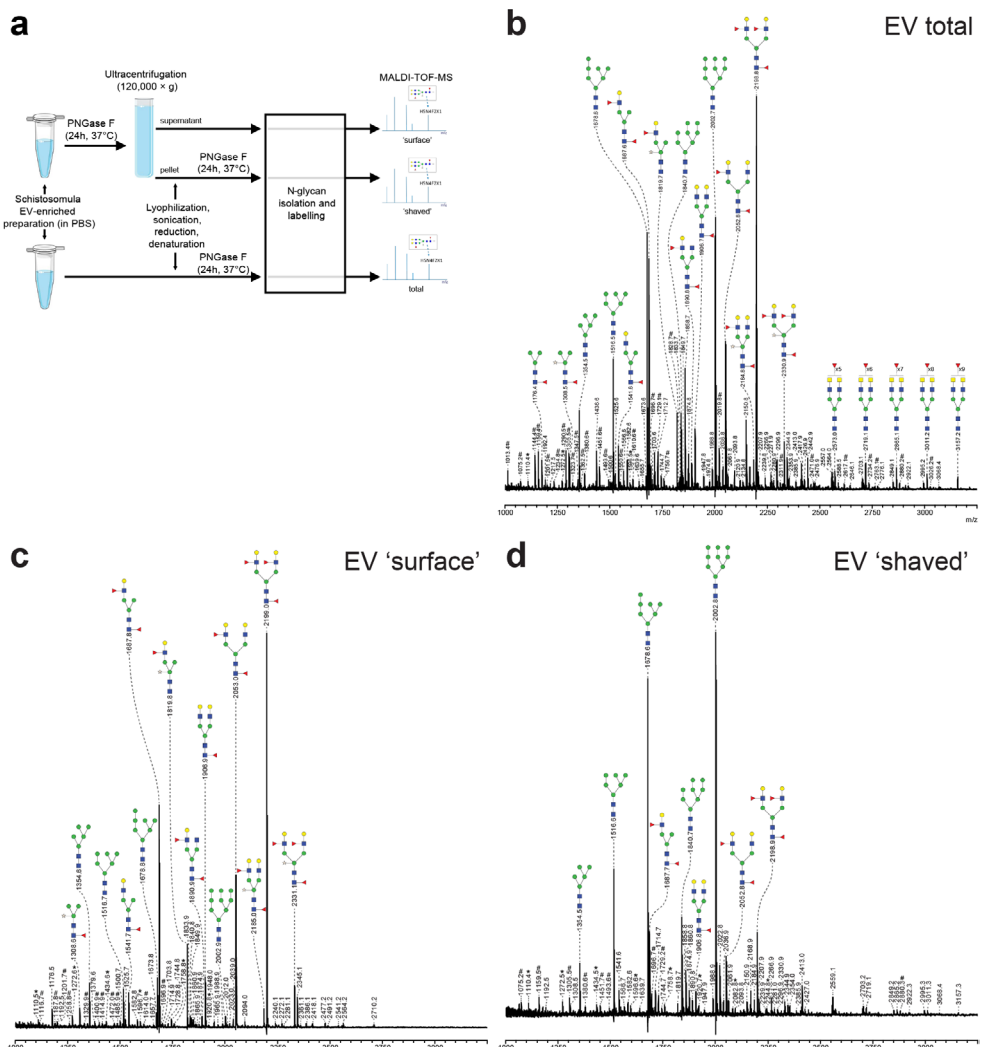
We next analysed the glycosylation of schistosomula EVs to assess whether ligands for CLRs were present. First, the overall N-glycan content of the EV-enriched preparations was determined by mass spectrometry (Figure 3a). MALDI-TOF mass spectra of PNGase F released N-glycans were assigned based on the detailed glycan structure descriptions available for overall N-glycan preparations of *S. mansoni* schistosomula<sup>35</sup>. Interestingly, the spectrum of N-glycans from the EV preparation was highly similar to previously published spectra of total extracts of three-day cultured schistosomula<sup>24,35</sup>. The major signals are from oligomannosidic structures of complex glycans with a core(α6)-fucose and one or two antennae consisting of Galβ1-4GlcNAc (LacNAc, LN) and/or Le<sup>x</sup>. Structures with a core-xylose modification or GalNAcβ1-4GlcNAc (LacDiNAc or LDN) antennae with five to nine fucose residues were observed at relatively low levels (Figure 3b). These results show that schistosomula EVs contain similar N-glycans as previously found in total schistosomula extracts, including Le<sup>x</sup> and oligomannose motifs, which are both ligands for DC-SIGN and MR<sup>21,23</sup>.

To identify specific N-glycans that might be available for interaction with CLRs on the surface of EVs, we treated intact EVs with PNGase F to release all ('surface') N-glycans that were accessible to the enzyme. MALDI-TOF-MS analysis was performed on both the released 'surface' N-glycans as well as on the remaining N-glycans of the PNGase F-treated ('shaved') EVs (Figure 3c-d), which likely represent glycans on the inside of the EVs. Interestingly, the most

#### → Figure 3. Schistosomula EV-surface N-glycans include DC-SIGN ligands

Basic scheme of the protocol for obtaining the N-glycan spectra (images adjusted from Servier Medical Art) (a), details can be found in the materials and methods. PNGase F released N-glycans measured by MALDI-TOF-MS from total (b), intact (PGNase F accessible N-glycans, 'surface') (c), and PNGase F treated (PGNase F non-accessible N-glycans on either surface or inside of the EV, 'shaved') (d) EV-enriched preparations. Signals are labelled with monoisotopic masses. Putative structural assignments were deduced from these masses based on hydrofluoric acid (HF) treatment (data not shown) and published data of schistosomula glycans<sup>35</sup>. Spectra shown are representative for three biological replicates. Red triangle, fucose; yellow circle, galactose; green circle, mannose; blue square, N-acetylglucosamine; yellow square, N-acetylgalactosamine; white star, xylose; \*, signals corresponding to a hexose oligomer of unknown origin; #, non-glycan signals

abundantly detected N-glycans on the EV surface contained one or two  $\text{Le}^x$  antennae (Figure 3c) while the major glycans of the 'shaved' EVs were the oligomannosidic structures (Fig 3d). These results show that the glycoproteins on the surface of schistosomula EVs carry a specific subset of N-glycans with  $\text{Le}^x$  motifs, which are potential ligands for DC-SIGN or MR in the context of pathogen-host interactions<sup>19,40,41</sup>.



## EVs are internalized via DC-SIGN but not MR or DCIR

To investigate whether DC-SIGN or MR on moDCs were involved in uptake of schistosomula EVs via glycan motifs on these EVs, moDCs were pre-incubated with antibodies blocking DC-SIGN or MR and subsequently incubated with labelled schistosomula EVs for 2 h (Figure 4a-b). In addition we investigated EV binding after blocking DCIR, a receptor expressed on moDCs that does not bind  $\text{Le}^x$  containing glycans but has been shown to bind *S. mansoni* cercarial extract<sup>19</sup>. Blocking DC-SIGN led to almost complete inhibition of EV uptake while blocking the MR, DCIR, or pre-incubation with the isotype control did not reduce EV internalisation. Inhibition of EV internalisation after DC-SIGN block was confirmed by confocal microscopy (Figure 4c). This reveals that schistosomula EVs were internalised by moDCs via DC-SIGN.

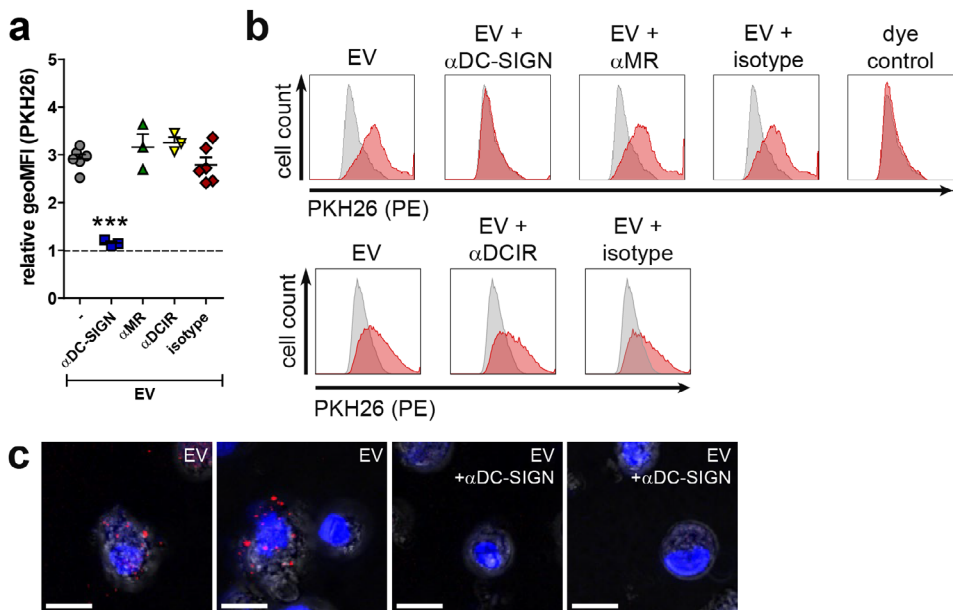


**Figure 4. Schistosomula EVs are internalised via interactions with CLR DC-SIGN**  
 PKH26 fluorescence of CD1a<sup>+</sup> cells with indicated pre-incubations (x-axis). The geoMFI (geometric mean fluorescent intensity) is shown relative to cells in medium only (a). MoDC from three to six donors. Representative histograms of two donors from same data plotted in a (b). Confocal microscopy visualisation of EV uptake and inhibition of EV uptake when DC-SIGN was blocked (c). Images show maximum projections of recorded z-stacks. PKH26-labelled EVs are stained in red and the nuclei in blue (Hoechst). Scale bar is 10  $\mu\text{m}$ . Selected images are representative for three donors. Mean $\pm$ SEM \*\*\*p < 0.001, using repeated measures ANOVA with Tukey's Multiple Comparison Test. MR, mannose receptor

## EV-associated glycolipid-glycans include DC-SIGN ligands

Given that the EV surface contained DC-SIGN ligands, including the  $\text{Le}^x$  motif, we investigated whether EV deprived from surface N-glycans by PNGase F treatment would still be internalised by moDCs. Interestingly, the PNGase F-treated EVs showed a minor but not significant reduction in internalisation, and the EV uptake could still be inhibited by blocking DC-SIGN (Figure 5a). Since it has been shown that cercariae produce glycolipid-glycans that contain  $\text{Le}^x$  and other potential DC-SIGN ligands<sup>35,42</sup>, we additionally determined the total lipid-derived glycan profile of the schistosomula EVs (Figure 5b). Here we detected a heterogeneous set of highly  $\alpha 3$ -fucosylated glycolipid structures, mostly similar to the glycolipid-glycans found in total schistosomula extract<sup>35</sup>. Interestingly, these lipid-glycans had terminal motifs that contained  $\text{Le}^x$ ,  $\text{Fuc}\alpha 1-3\text{Gal}\beta 1-4(\text{Fuc}\alpha 1-3)\text{GlcNAc}$  (pseudo-Lewis Y( $\text{Le}^y$ )) and  $\text{GalNAc}\beta 1-4(\text{Fuc}\alpha 1-3)\text{GlcNAc}$  (LDN-F) (Figure 5b insert), which are all previously described ligands of DC-SIGN<sup>42,43</sup>. These data suggest that additional to surface N-glycans, EV-associated lipid-glycans play a role in interaction with DC-SIGN.

## Schistosomula EVs induced increased cytokine release and costimulatory molecule expression on moDCs

Next, we investigated whether incubation of moDCs with schistosomula EVs affect their activation status and cytokine production. We first incubated human moDCs for 24 h with EV-enriched preparations but observed no or very low release of cytokines. Therefore, in addition to EVs, moDCs were co-cultured with IL-1 $\beta$  and TNF- $\alpha$ , cytokines that are released by immune cells upon schistosome infection<sup>3</sup>, allowing us to further investigate whether EVs could change the activation status of moDCs. Under these conditions, schistosomula EVs significantly increased IL-6, IL-10 and IL-12 secretion by moDCs (Figure 6a).

Furthermore, a significant upregulation of the costimulatory molecules CD80, CD86 and regulatory surface molecule PD-L1 was observed, while there was no significant effect on CD40, HLA-DR and PD-L2 expression (Figure 6b). These data suggest that the EV-enriched preparations were mostly synergizing or augmenting other inflammatory signals.

## Role for DC-SIGN in EV-augmented immune responses

Since schistosomula-derived EVs were mainly internalised via DC-SIGN, we hypothesized that inhibiting this receptor would alter the observed augmented immune responses of moDCs by the EVs. Blocking DC-SIGN during a 24 h EV stimulation, however, did not show a significant effect on IL-6, IL-10 and IL-12 release (Figure 7a) nor on the expression of the co-stimulatory surface markers CD80,

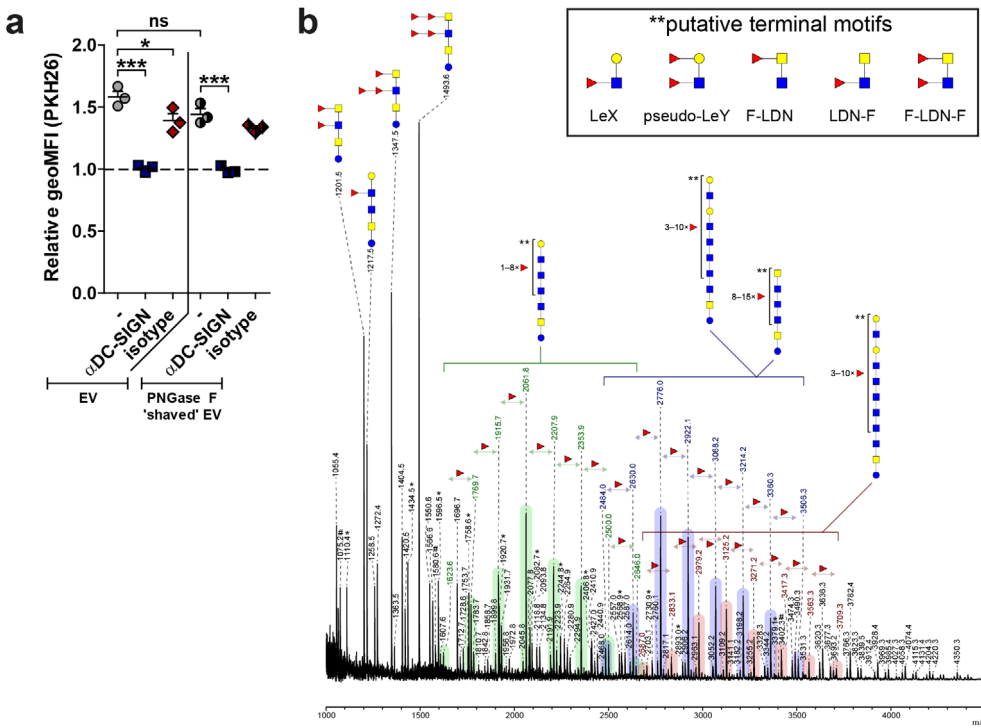


**Figure 5. Internalisation of schistosomula EVs without surface N-glycans via DC-SIGN and EV-associated glycolipid-glycans**

The geoMFI (geometric mean fluorescent intensity) of PKH26 relative to unstimulated moDC after 2 h incubation with labelled EVs that were treated without or with PNGase F (a). Pre-incubations are indicated on the x-axis. MoDC from 3 donors. Mean $\pm$ SEM \* $p < 0.05$ , \*\*\* $p < 0.001$ , using repeated measures ANOVA with Tukey's Multiple Comparison Test. EV-derived glycolipid-glycans measured by MALDI-TOF-MS (b). Signals are labelled with monoisotopic masses. Putative structural assignments were deduced from these masses based on published data of schistosomula glycans<sup>35</sup> and on hydrofluoric acid (HF) data (not shown). Coloured bars indicate the corresponding core structure with varying numbers of fucose substitutions. Putative terminal motifs formed by these fucoses are indicated in the insert. The spectrum shown is representative for three biological replicates. Red triangle, fucose; yellow circle, galactose; blue square, N-acetylglucosamine; yellow square, N-acetyl-galactosamine; Le<sup>X</sup>, Lewis X; Le<sup>Y</sup>, Lewis Y; F-LDN/LDN-F/F-LDN-F, fucosylated LacDiNAC \*, signals corresponding to a hexose oligomer of unknown origin; #, non-glycan signals

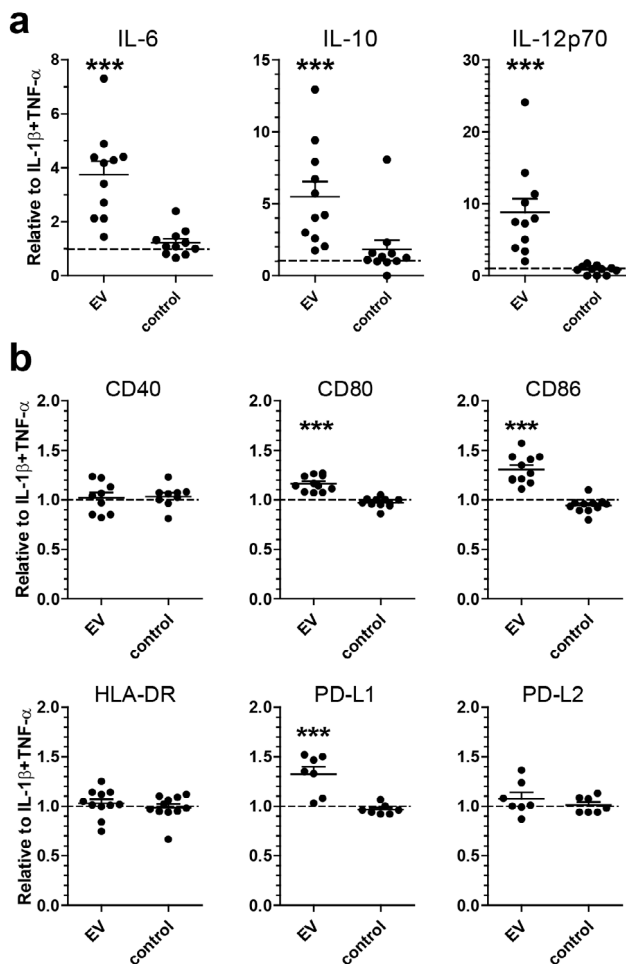


**Figure 6. Schistosomula EVs augment moDC immune responses**

Released cytokines (a) and surface marker expression (b) of moDC incubated with EVs. The control is medium without parasites that has been cultured and processed exactly like the schistosomula EVs. Data points are shown as fold change relative to moDC with IL-1 $\beta$  and TNF- $\alpha$  for that specific donor. MoDC from 7 to 11 donors. Mean $\pm$ SEM \*\*\*p < 0.001, using repeated measures ANOVA with Dunnett's Multiple Comparison Test

CD86, HLA-DR, PD-L1 and PD-L2 after 48 h stimulation (Figure 7b). To understand why the blocking of DC-SIGN did not consistently influence the enhanced immune responses of moDCs by the EVs whereas it almost completely blocked EV internalisation after 2 h, we studied EV uptake in the presence of DC-SIGN blocking antibodies after 48 h of incubation. Blocking of DC-SIGN significantly

**→ Figure 7. Role for DC-SIGN in augmented immune responses by schistosomula EVs**

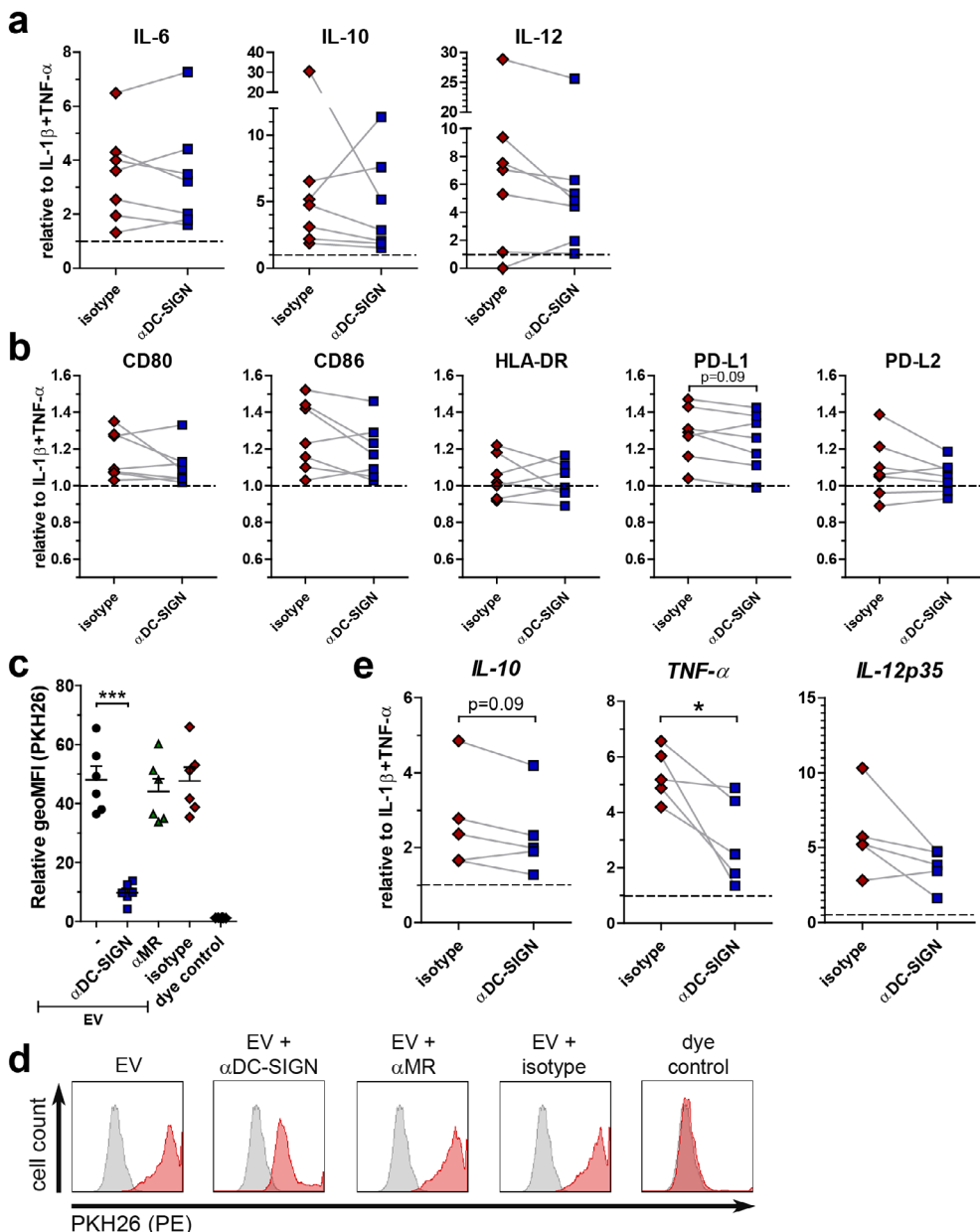
Released cytokines (a) and surface marker expression (b) of moDC with indicated pre-incubations (x-axes) before EV incubation. Linked points represent data from one donor. Data is shown as fold change relative to moDC with IL-1 $\beta$  and TNF- $\alpha$  from that specific donor (n=7). Summary of geometric mean fluorescent intensity (geoMFI) of moDC incubated with PKH26-labelled EVs for 48 h, relative to medium control (c) (n=6). Histograms of moDC from one representative donor from data plotted in c (d). Relative expression of mRNA from moDC after 6 h EV incubation and indicated pre-incubations (x-axes) (e) (n=5). \*p < 0.05, \*\*\*p < 0.001, using repeated measures ANOVA with Tukey's Multiple Comparison Test (c) or paired student t-test (a, b, e)

reduced EV internalisation after 48 h (Figure 7c). However, the vast majority of the moDCs were still positive for the fluorescent dye, although the fluorescent intensity was lower when DC-SIGN was blocked (Figure 7d). Possibly other mechanisms than those mediated by DC-SIGN play a role in EV internalisation by moDCs after prolonged exposure. To investigate whether blocking of DC-SIGN does interfere with moDC function during shorter incubations with schistosomula-derived EVs, moDCs were stimulated with EVs in the absence or presence of blocking antibodies for 6 h, after which cytokine mRNA expression was determined. Indeed, at this time point, the effect of blocking DC-SIGN was more prominent with a significant reduction in TNF- $\alpha$  mRNA and a trend for lower IL-10 mRNA expression (Figure 7e). IL-12p35 mRNA levels were also reduced in most donors, though not significant. These results show that, within the first hours of exposure but not at a longer timescale, the moDC immune profile is influenced by schistosomula EVs through internalisation via DC-SIGN.

## Discussion

Schistosome parasites are master regulators of host immune responses and they release various molecules and products to achieve this. Here we demonstrate that *S. mansoni* schistosomula release EVs that contain Le<sup>x</sup> antigens on their surface. Interaction of the glycosylated EVs with DC-SIGN on moDCs lead to internalisation and enhanced expression of both immunostimulatory and regulatory effector molecules. Thus, schistosome EVs appear to contribute to immune modulation by the parasite.

Schistosomula are multicellular organisms, having various organs and cells as potential sources of their released EVs. It has been shown that micron-sized vesicles are released from their acetabular glands<sup>11,44</sup> and it is suggested that EVs can also derive from the tegument<sup>6</sup>. Since multicellular organisms release



heterogeneous populations of EVs, it is likely that the moDCs can internalise these EVs via various receptors and/or routes<sup>13</sup>. The schistosomula-derived EV populations described here were heterogeneous in size, which we analysed with NTA (Figure 1c) and cryo EM (Figure 1e). The size of EVs may influence uptake

routes, as has been shown for *Helicobacter pylori* outer membrane vesicles (OMVs): small OMVs were taken up via caveolin-mediated endocytosis and bigger OMVs via micropinocytosis and endocytosis<sup>45</sup>. The major population of EVs >300 nm we observed have not been described before for *S. mansoni* schistosomula<sup>6</sup>. Although we used a similar schistosomula EV isolation protocol as Nowacki *et al*<sup>6</sup>, the isolated EVs in that paper were only visualised by TEM of negatively stained EVs and not by NTA. With this same technique, our isolated schistosomula EVs also showed similar sizes <200 nm (Figure 1a-b) but only with the NTA and cryo EM the EV population >300 nm was detectable. EVs >300 nm have not been found among adult worms EVs<sup>7,8,46</sup>. Schistosomes are organisms with a complex life cycle and the schistosomula and adult worm life stages differ in size, shape, molecular, and cellular make up, and interaction with the host and its immune system<sup>2,47</sup>. Therefore, it is likely that different life stages of the parasite produce different EV populations regarding molecular content<sup>6,48</sup> as well as size. Furthermore, the adult worm EVs published have been isolated by different protocols which may further explain differences between the observed sizes of EVs derived from various schistosome different life stages.

Interestingly, our cryo EM data showed that around half of the schistosomula-derived EVs were covered with thin filament-like structures (Figure 1d). These structures have not been described for eukaryotic EVs so far. It remains to be explored what the molecular composition of these EV-associated structures is and whether these structures are specific for *S. mansoni* and/or specifically related to the schistosomula life stage. These thin filaments resemble the electron-dense surface layer of extracellular proteins and LPS or glycocalyx on some bacteria<sup>49,50</sup> and their released OMVs<sup>51</sup>. We hypothesize that the structures on schistosomula EVs are composed of large, complex glycoconjugates and/or include proteins with attached glycan polymers, similar to the mammalian glycocalyx consisting of proteoglycans with attached glycosaminoglycans<sup>25</sup>. Altogether, the EM analyses emphasize that cryo EM provides improved visualisation of the near native state of isolated EVs compared to TEM of negatively stained EVs.

EVs released by *S. mansoni* schistosomula were internalised by human moDCs (Figure 2). Previous studies have demonstrated that *S. japonicum* EVs derived from adult worms and eggs are also internalised by host cells<sup>46,52-54</sup>. This indicates, together with our data, that at least three lifecycle stages of *Schistosoma* in humans release EVs that interact with the host. By chelating extracellular calcium with EGTA, schistosomula EV could not bind to or be taken up by the moDC (Figure 2d-e). This suggests that the interaction of the EVs with the moDC was via the ligation of glycoconjugates to CLRs, which is calcium dependent, and not via protein-protein interaction. By inhibiting specific CLRs we show that

internalisation of schistosomula EVs by moDCs is primarily facilitated by DC-SIGN (Figure 4). This CLR is known to bind schistosome egg<sup>21</sup>, cercarial<sup>43</sup>, and worm antigens<sup>55</sup>, via glycan motifs including mannotriose, Le<sup>x</sup>, LDN-F, and pseudo-Le<sup>y</sup><sup>19,42,43</sup>. In contrast, CLR DCIR mainly binds Le<sup>B</sup> (Lewis B) and sulpho-Le<sup>A</sup> (Lewis A) motifs<sup>19</sup>, and indeed, blocking this receptor did not reduce EV uptake by the moDC. Previously, it was shown that the egg-derived glycoprotein omega-1, which carries Le<sup>x</sup> containing N-glycans highly similar to those found here on the EVs (Figure 3), is mainly internalised by moDCs via the MR<sup>22</sup>. However, when blocking the MR, EV internalisation was not inhibited. This difference of internalisation routes between omega-1 and EVs could be explained by the characteristics of the two CLRs: DC-SIGN has one carbohydrate recognition domain (CRD), is present as tetramers, and it clusters in (lipid raft) nanodomains that are distributed on the cell membrane. Clustering increases the avidity of low affinity glycan-lectin interactions and allows this receptor to interact at multiple sites with pathogens that differ greatly in size<sup>56</sup>. On the other hand, the MR consists of multiple CRDs, which results in binding of multivalent or repetitive ligands to a single MR monomer<sup>57</sup>. Considering these aspects, larger particles such as EVs would favour DC-SIGN mediated uptake while smaller glycosylated proteins are more likely to be internalised via other receptors, such as the MR. A very recent publication substantiates this theory by showing that tumour-derived apoptotic EVs with high-mannose glycans on their surface were mainly internalized via interaction with DC-SIGN and not the MR<sup>58</sup>. Furthermore, it suggests that, together with our findings, DC-SIGN mediated EV uptake may be a widely occurring mechanism, across a broad spectrum of species and may not be exclusive to schistosomula-derived EVs. Of note is that helminths, including *S. mansoni*, lack sialic acid in their glycan repertoire, which is a fundamental difference with mammalian glycans. It was recently found that EVs released by human glioblastoma cells had complex sialic acid-capped N-glycans on their surface that mainly bound to Siglec-9 on moDCs<sup>59</sup>. When sialic acids on the EV surface were enzymatically removed and Le<sup>y</sup> was inserted, EV uptake by moDC and binding of the EVs to DC-SIGN were increased. Furthermore, EVs from murine hepatic cell lines expose sialyl-Le<sup>x</sup> on the EV surface and removing the sialic acids with neuraminidase significantly increased EV uptake by M1 cell lines<sup>28</sup>. However, no DC-SIGN blocking experiments were performed in these studies. Thus, the question remains whether EV internalisation via DC-SIGN is specific for schistosomula EVs, or whether it is a more general mechanism via which EVs from both pathogens and mammalian cells are internalized. However, we cannot exclude the possibility that internalisation of schistosomula EVs may be facilitated via different CLRs in a different host. For example, the murine macrophage galactose-type lectin (MGL-1)<sup>60</sup> can bind to Le<sup>x</sup>

while the human MGL cannot<sup>61</sup>. Human MGL binds to LDN motifs, which were absent in our schistosomula EV glycan analyses.

So far, most research on glycosylation of pathogen-derived EVs focussed on lipopolysaccharides of bacterial OMVs<sup>62–65</sup>. Only very recently, the presence of glycoconjugates on the surface of EVs released by the helminth *Fasciola hepatica* was studied using lectin microarrays<sup>66</sup>. Here we performed a more detailed structural analysis of glycans associated with EVs released by a helminth parasite. Using mass spectrometry we showed the presence of mainly complex type N-glycans with Le<sup>x</sup> motifs as well as oligomannose and high mannose glycans (Figure 3b) and the presence of lipid-linked glycans with Le<sup>x</sup>, pseudo-Le<sup>y</sup>, and other  $\alpha$ 3-fucosylated glycan motifs (Figure 5b). The EV N-glycan profile was qualitatively very similar to that of whole schistosomula<sup>35</sup>. The overall glycosylation pattern associated with this particular schistosome life stage was reflected in the EVs, however, with differences in relative abundances of the glycans. Biological replicates of the parasite culture and EV isolation generated at two different laboratories (Leiden and Aberystwyth) showed similar N-glycan profiles, confirming the reproducibility of the EV isolation protocol and glycan patterns<sup>6</sup>. Mostly complex glycans with Le<sup>x</sup> motifs were cleaved from intact EVs by incubation with PNGase-F (Figure 3c), implicating that these structures were on the EV surface. Glycoconjugates on the EV surface can influence their cellular internalisation, as was shown for bacterial OMV<sup>65</sup>, murine hepatic cell line EVs<sup>28</sup>, tumour-derived EVs<sup>58,59</sup>, and *F. hepatica* adult worm EVs<sup>66</sup>. Interestingly, PNGase F treated EVs were still internalised by moDC via DC-SIGN (Figure 5a). This indicates that other glycans with DC-SIGN ligands such as the fucosylated lipid-linked glycans play a role in this process, either specifically or in addition to the N-glycans. Mass spectrometry analysis showed the presence of EV-associated glycolipid-glycans (Figure 5b) containing several structures that were reported previously for schistosomula<sup>35</sup>, but with more extended higher molecular weight structures. Our data indicate that many of the EV lipid-derived glycans contain motifs such as Le<sup>x</sup>, pseudo-Le<sup>y</sup>, and other  $\alpha$ 3-linked fucose containing motifs that can bind to DC-SIGN<sup>42,43</sup>, which may explain why PNGase-F treated EVs could still be internalised via DC-SIGN. Furthermore, *S. mansoni* produce various O-glycans<sup>35</sup>, which are possibly also present on EVs and contribute to EV-CLR interaction. We therefore suggest that both N-glycans and glycolipid-glycans, and possibly O-glycans, contribute to the interaction of the EVs with DC-SIGN. This interaction is most likely via Le<sup>x</sup> motifs, which are abundant in these glycan types, with the possible contribution of other  $\alpha$ 3-fucosylated lipid-glycans.

Interestingly, the complex type N-glycans on the EV surface and many of the glycolipids of the schistosomula EVs contain antigenic glycan motifs that

were previously shown to be the target of antibodies of various isotypes during schistosome infection. These motifs include N-glycan core-xylose, Le<sup>X</sup>, and the various fucosylated glycolipid motifs<sup>67-69</sup>. It is therefore tempting to speculate that EVs can either elicit these antibodies and/or that EVs are targeted by antibodies generated against other, similarly glycosylated, antigens produced by schistosomes during an infection. Antibodies that recognize and bind molecules on the EV surface can facilitate internalisation by APCs, for example via Fc receptors. Antibody-bound EVs can be targeted to different intracellular compartments compared to EVs without antibodies. This has been observed for EVs from the helminth *Heligmosomoides polygyrus*<sup>70</sup>. *H. polygyrus* EVs pre-incubated with antisera were targeted to lysosomes. However, lysosome targeting has also been observed for antigens internalised by DC-SIGN<sup>71</sup>. Another possibility is that EV uptake is enhanced after incubation with antisera, which was observed for *F. hepatica* EVs and RAW264.7 macrophages<sup>66</sup>. Differences in route of uptake can possibly alter the fate of the EVs and thus possibly influence EV-induced immunomodulation.

Cross-species communication via EVs that contributes to modulation of host immune responses has been described previously for helminths, including *H. polygyrus*<sup>70</sup> and *Nippostrongylus brasiliensis*<sup>72</sup>. In this study, we observed that *S. mansoni* schistosomula EVs are capable of augmenting activation-induced cytokine secretion and surface molecule expression by human moDCs, including both immunostimulatory and regulatory factors (Figure 6). It has been suggested that a delicate balance between benefit for the host and benefit for the parasite contributes to overall survival of the parasite within the host with limited pathology<sup>3</sup>. The induction of pro-inflammatory cytokines is a natural response of the host to the skin-invading pathogen, however, this response is transient. Priming of a protective adaptive immune response is hampered, probably via the induction of regulatory responses by the parasite, such as increased IL-10 release and PD-L1 expression<sup>12</sup>, allowing the parasite to develop into mature worms and start egg laying. Different molecules present in the heterogenous EV population may have contributed to the observed augmented immune responses. It is known that DC-SIGN signalling via fucose ligands, which are motifs found on the N-glycan and lipid-glycan structures of the EVs, mainly increases IL-10 and decreases pro-inflammatory responses<sup>73</sup>. In contrast, we observed that blocking DC-SIGN actually decreased pro-inflammatory TNF- $\alpha$  and IL-12 mRNA and did not fully reduce the responses to baseline (Figure 7e). Thus, it is likely to assume that schistosomula EVs contain a mix of various (glycosylated) proteins and RNAs (amongst other biological molecules, such as lipids<sup>74</sup>) that all may contribute to a combined effect on host immunity<sup>6</sup>. Indeed, the NTA data as well as the cryo-EM show at least a variation in EV size and with or without the thin filaments,

and it is tempting to speculate that these different EVs may show variation in their surface glycan profile and may have specific activities on host immunity. Interestingly, since total ES from schistosomula increases IL-12, IL-6 and IL-10 release as well as CD86 expression by mouse BMDCs<sup>11</sup>, it is tempting to suggest that part of the effects of the ES are mediated by the EVs in that secretion.

In contrast to the strong blocking effect of anti-DC-SIGN antibodies on EV internalisation (Figure 4 and Figure 7c), however, blocking DC-SIGN did not significantly alter EV-augmented immune responses during prolonged stimulation (Figure 7a-b). The variation we detected among donors in reduction or increase of IL-10 release in the presence of blocking DC-SIGN (Figure 7a) was also observed in another study that examined glycan-mediated effects by larval ES<sup>75</sup>. These donor-specific variances could be associated with intrinsic DC-SIGN levels, which vary highly between and within donors<sup>76</sup>. Furthermore, residual uptake of EVs via other processes such as (macro-)pinocytosis or protein–protein interaction could still have affected the immune activation of moDCs upon prolonged culture (Figure 7d). Shorter incubation, however, showed that part of the augmented immune profile of moDCs by schistosomula EVs was indeed dependent on interaction with DC-SIGN (Figure 7e) and provides evidence that interaction of glycans on the EV surface with DC-SIGN does play a role in immune modulation of host responses.

In conclusion, our study demonstrates that *S. mansoni* schistosomula release glycosylated EVs that carry Le<sup>x</sup>, pseudo-Le<sup>y</sup>, and other fucosylated motifs, and we reveal a distinct role for DC-SIGN in glycan-mediated internalisation of EVs by host immune cells. This interaction contributes to increased pro- and anti-inflammatory responses, substantiating that EVs play a role in host immune regulation by helminths to establish and control infection. Future studies on how EV-associated molecules contribute to immune modulation will further our understanding of parasite–host interactions and may provide insights for vaccine development.

## Authors' contributions

M.E.K. contributed to conceiving the study, performed the schistosomula cultures, EV isolations, NTA, cryo EM measurements, moDC isolations/stimulations, ELISAs, flow cytometry, RNA extraction, qPCR, data analysis, and drafting of the manuscript. A.J.H. assisted with moDC isolations/differentiation and constructing flow cytometry panels. A.O.F. performed shedding of snails to obtain cercariae and assisted with moDC isolations. D.L.N. performed the N-glycan characterization and assisted with the analysis of the spectra. C.M.K. performed the confocal microscopy and generated the confocal images. R.I.K. performed the cryo EM imaging and assisted with the subsequent analysis. J.J.T. performed the TEM

imaging and contributed to the TEM analysis. K.F.H. contributed to the design of experiments, interpretation of the results and correcting the manuscript. E.N.-'tH. contributed to conceiving the study, the design of the experiments, overseeing the EV isolation, interpretation of the results and drafting of the manuscript. H.H.S. and C.H.H. both participated in conceiving the study, the design of the experiments, interpretation of the results and drafting of the manuscript. All authors read and approved the final manuscript.

## Acknowledgements

We would like to thank Jan de Best, Frank Otto and the rest of the *S. mansoni* life-cycle team for maintaining the availability of *S. mansoni* parasites, Pieter Vader from the University Medical Center Utrecht (The Netherlands) for using the NanoSight, Thiago Patente, Anna Zawistowska-Deniziak, Leonard Pelgrom, Roos van Schijlenburg, Nikolas Duszenko, and Eline Brombacher for assisting with cell isolation/differentiation and feedback on the moDC model, the staff from the LUMC Flow Cytometry Core Facility for maintaining the flow cytometer used, Fanny Nowacki for providing EVs from Aberystwyth, Mr Alan Cookson of the Aberystwyth University Advanced Microscopy and Bio-imaging Laboratory for his help and support with TEM, Lisa Koornneef, Bruno Guigas, and Tom Driedonks for discussing qPCR analysis, and Koen Stam for feedback on the statistical analysis.

## Disclosure of interest

The authors report no conflict of interest.

## Funding

This work was supported by grants from NWO Graduate School Program 022.006.010 (to M.E.K.); ZonMW-Vidi 20972 (to H.H.S.); the European Research Council under the European Union's Seventh Framework Programme [FP/2007–2013]/ERC Grant Agreement No. 337581 (to E.N.-'tH.).

## References

1. Colley, D. G., Bustinduy, A. L., Secor, W. E. & King, C. H. Human schistosomiasis. *The Lancet* **383**, 2253–2264 (2014).
2. Maizels, R. M., Smits, H. H. & McSorley, H. J. Modulation of Host Immunity by Helminths: The Expanding Repertoire of Parasite Effector Molecules. *Immunity* **49**, 801–818 (2018).
3. Mountford, A. P. & Trottein, F. Schistosomes in the skin: a balance between immune priming and regulation. *Trends Parasitol* **20**, 221–226 (2004).
4. Maizels, R. M. & McSorley, H. J. Regulation of the host immune system by helminth parasites. *Journal of Allergy and Clinical Immunology* **138**, 666–675 (2016).
5. Wu, Z. *et al.* Extracellular Vesicle–Mediated Communication Within Host–Parasite Interactions. *Front Immunol* **9**, 3066 (2018).
6. Nowacki, F. C. *et al.* Protein and small non-coding RNA-enriched extracellular vesicles are released by the pathogenic blood fluke *Schistosoma mansoni*. *J Extracell Vesicles* **4**, 28665 (2015).
7. Sotillo, J. *et al.* Extracellular vesicles secreted by *Schistosoma mansoni* contain protein vaccine candidates. *Int J Parasitol* **46**, 1–5 (2016).
8. Samoil, V. *et al.* Vesicle-based secretion in schistosomes: Analysis of protein and microRNA (miRNA) content of exosome-like vesicles derived from *Schistosoma mansoni*. *Sci Rep* **8**, 3286 (2018).
9. Maizels, R. M. & Yazdanbakhsh, M. Immune Regulation by helminth parasites: cellular and molecular mechanisms. *Nature Reviews Immunology* **3**, 733–744 (2003).
10. Hogg, K. G., Kumkate, S., Anderson, S. & Mountford, A. P. Interleukin-12 p40 secretion by cutaneous CD11c+ and F4/80+ cells is a major feature of the innate immune response in mice that develop Th1-mediated protective immunity to *Schistosoma mansoni*. *Infect Immun* **71**, 3563–3571 (2003).
11. Paveley, R. A., Aynsley, S. A., Cook, P. C., Turner, J. D. & Mountford, A. P. Fluorescent imaging of antigen released by a skin-invading helminth reveals differential uptake and activation profiles by antigen presenting cells. *PLoS Negl Trop Dis* **3**, e528 (2009).
12. Winkel, B. M. F. *et al.* Early Induction of Human Regulatory Dermal Antigen Presenting Cells by Skin–Penetrating *Schistosoma mansoni* Cercariae. *Front Immunol* **9**, 2510 (2018).
13. van Niel, G., D’Angelo, G. & Raposo, G. Shedding light on the cell biology of extracellular vesicles. *Nat Rev Mol Cell Biol* **19**, 213–228 (2018).
14. Egesa, M. *et al.* *Schistosoma mansoni* schistosomula antigens induce Th1/Pro-inflammatory cytokine responses. *Parasite Immunol* **40**, e12592 (2018).
15. Jenkins, S. J., Hewitson, J. P., Ferret-Bernard, S. & Mountford, A. P. Schistosome larvae stimulate macrophage cytokine production through TLR4-dependent and -independent pathways. *Int Immunol* **17**, 1409–1418 (2005).
16. Paveley, R. A. *et al.* The Mannose Receptor (CD206) is an important pattern recognition receptor (PRR) in the detection of the infective stage of the helminth *Schistosoma mansoni* and modulates IFNgamma production. *Int J Parasitol* **41**, 1335–1345 (2011).
17. van Die, I. & Cummings, R. D. The Mannose Receptor in Regulation of Helminth–Mediated Host Immunity. *Front Immunol* **8**, 1677 (2017).

18. Kaisar, M. M. M. *et al.* Dectin-1/2-induced autocrine PGE2 signaling licenses dendritic cells to prime Th2 responses. *PLoS Biol* **16**, e2005504 (2018).
19. Bloem, K. *et al.* DCIR interacts with ligands from both endogenous and pathogenic origin. *Immunol Lett* **158**, 33–41 (2014).
20. van Liempt, E. *et al.* Schistosoma mansoni soluble egg antigens are internalized by human dendritic cells through multiple C-type lectins and suppress TLR-induced dendritic cell activation. *Mol Immunol* **44**, 2605–2615 (2007).
21. van Die, I. *et al.* The dendritic cell-specific C-type lectin DC-SIGN is a receptor for Schistosoma mansoni egg antigens and recognizes the glycan antigen Lewis x. *Glycobiology* **13**, 471–478 (2003).
22. Everts, B. *et al.* Schistosome-derived omega-1 drives Th2 polarization by suppressing protein synthesis following internalization by the mannose receptor. *J Exp Med* **209**, 1753–67, S1 (2012).
23. Geijtenbeek, T. B. & Gringhuis, S. I. C-type lectin receptors in the control of T helper cell differentiation. *Nat Rev Immunol* **16**, 433–448 (2016).
24. Jang-Lee, J. *et al.* Glycomics analysis of Schistosoma mansoni egg and cercarial secretions. *Mol Cell Proteomics* **6**, 1485–1499 (2007).
25. Gerlach, J. Q. & Griffin, M. D. Getting to know the extracellular vesicle glycome. *Mol Biosyst* **12**, 1071–1081 (2016).
26. Williams, C. *et al.* Glycosylation of extracellular vesicles: current knowledge, tools and clinical perspectives. *J Extracell Vesicles* **7**, 1442985 (2018).
27. Freitas, D. *et al.* Different isolation approaches lead to diverse glycosylated extracellular vesicle populations. *J Extracell Vesicles* **8**, (2019).
28. Williams, C. *et al.* Assessing the role of surface glycans of extracellular vesicles on cellular uptake. *Scientific Reports* **9**, (2019).
29. Shimoda, A., Sawada, S., Sasaki, Y. & Akiyoshi, K. Exosome surface glycans reflect osteogenic differentiation of mesenchymal stem cells: Profiling by an evanescent field fluorescence-assisted lectin array system. *Scientific Reports* **9**, (2019).
30. Colley, D. G. & Wikle, S. K. Schistosoma mansoni: simplified method for the production of schistosomules. *Exp Parasitol* **35**, 44–51 (1974).
31. Van Deun, J. *et al.* EV-TRACK: transparent reporting and centralizing knowledge in extracellular vesicle research. *Nat Methods* **14**, 228–232 (2017).
32. Schindelin, J. *et al.* Fiji: an open-source platform for biological-image analysis. *Nat Methods* **9**, 676–682 (2012).
33. Hussaarts, L. *et al.* Rapamycin and omega-1: mTOR-dependent and -independent Th2 skewing by human dendritic cells. *Immunol Cell Biol* **91**, 486–489 (2013).
34. Wilbers, R. H. P. *et al.* Production and glyco-engineering of immunomodulatory helminth glycoproteins in plants. *Scientific Reports* **7**, (2017).
35. Smit, C. H. *et al.* Glycomic Analysis of Life Stages of the Human Parasite Schistosoma mansoni Reveals Developmental Expression Profiles of Functional and Antigenic Glycan Motifs. *Mol Cell Proteomics* **14**, 1750–1769 (2015).

36. Ceroni, A. *et al.* GlycoWorkbench: a tool for the computer-assisted annotation of mass spectra of glycans. *J Proteome Res* **7**, 1650–1659 (2008).

37. Bustin, S. A. *et al.* The MIQE guidelines: minimum information for publication of quantitative real-time PCR experiments. *Clin Chem* **55**, 611–622 (2009).

38. Simonsen, J. B. Pitfalls associated with lipophilic fluorophore staining of extracellular vesicles for uptake studies. *J Extracell Vesicles* **8**, 1582237 (2019).

39. Hokke, C. H. & van Diepen, A. Helminth glycomics – glycan repertoires and host–parasite interactions. *Mol Biochem Parasitol* **215**, 47–57 (2017).

40. van Kooyk, Y. & Geijtenbeek, T. B. DC-SIGN: escape mechanism for pathogens. *Nat Rev Immunol* **3**, 697–709 (2003).

41. Everts, B. *et al.* Omega-1, a glycoprotein secreted by *Schistosoma mansoni* eggs, drives Th2 responses. *J Exp Med* **206**, 1673–1680 (2009).

42. Meevissen, M. H. J. *et al.* Specific glycan elements determine differential binding of individual egg glycoproteins of the human parasite *Schistosoma mansoni* by host C-type lectin receptors. *Int J Parasitol* **42**, 269–277 (2012).

43. Meyer, S. *et al.* DC-SIGN mediates binding of dendritic cells to authentic pseudo-LewisY glycolipids of *Schistosoma mansoni* cercariae, the first parasite-specific ligand of DC-SIGN. *J Biol Chem* **280**, 37349–37359 (2005).

44. Dorsey, C. H., Cousin, C. E., Lewis, F. A. & Stirewalt, M. A. Ultrastructure of the *Schistosoma mansoni* cercaria. *Micron* **33**, 279–323 (2002).

45. Turner, L. *et al.* Helicobacter pylori Outer Membrane Vesicle Size Determines Their Mechanisms of Host Cell Entry and Protein Content. *Front Immunol* **9**, 1466 (2018).

46. Liu, J. *et al.* *Schistosoma japonicum* extracellular vesicle miRNA cargo regulates host macrophage functions facilitating parasitism. *PLoS Pathog* **15**, e1007817 (2019).

47. Dunne, D. W. & Cooke, A. Opinion – A worm's eye view of the immune system: consequences for evolution of human autoimmune disease. *Nature Reviews Immunology* **5**, 420–426 (2005).

48. Kifle, D. W. *et al.* Proteomic analysis of two populations of *Schistosoma mansoni*-derived extracellular vesicles: 15k pellet and 120k pellet vesicles. *Mol Biochem Parasitol* **236**, 111264 (2020).

49. Hunter, R. C. & Beveridge, T. J. High-resolution visualization of *Pseudomonas aeruginosa* PAO1 biofilms by freeze–substitution transmission electron microscopy. *J Bacteriol* **187**, 7619–7630 (2005).

50. Liu, Y., Hidaka, E., Kaneko, Y., Akamatsu, T. & Ota, H. Ultrastructure of *Helicobacter pylori* in human gastric mucosa and *H. pylori*-infected human gastric mucosa using transmission electron microscopy and the high-pressure freezing–freeze substitution technique. *J Gastroenterol* **41**, 569–574 (2006).

51. Gui, M. J., Dashper, S. G., Slakeski, N., Chen, Y. Y. & Reynolds, E. C. Spheres of influence: *Porphyromonas gingivalis* outer membrane vesicles. *Molecular Oral Microbiology* **31**, 365–378 (2016).

52. Wang, L. *et al.* Exosome-like vesicles derived by *Schistosoma japonicum* adult worms mediates M1 type immune-activity of macrophage. *Parasitol Res* **114**, 1865–1873 (2015).

53. Zhu, L. *et al.* Molecular characterization of *S. japonicum* exosome-like vesicles reveals their regulatory roles in parasite–host interactions. *Sci Rep* **6**, 25885 (2016).

54. Zhu, S. *et al.* Release of extracellular vesicles containing small RNAs from the eggs of *Schistosoma japonicum*. *Parasit Vectors* **9**, 574 (2016).

55. van Stijn, C. M. *et al.* *Schistosoma mansoni* worm glycolipids induce an inflammatory phenotype in human dendritic cells by cooperation of TLR4 and DC-SIGN. *Mol Immunol* **47**, 1544–1552 (2010).

56. Garcia-Vallejo, J. J. & van Kooyk, Y. The physiological role of DC-SIGN: a tale of mice and men. *Trends Immunol* **34**, 482–486 (2013).

57. Gazi, U. & Martinez-Pomares, L. Influence of the mannose receptor in host immune responses. *Immunobiology* **214**, 554–561 (2009).

58. Horrevorts, S. K. *et al.* Glycan-Modified Melanoma-Derived Apoptotic Extracellular Vesicles as Antigen Source for Anti-Tumor Vaccination. *Cancers (Basel)* **11**, (2019).

59. Dusoswa, S. A. *et al.* Glycan modification of glioblastoma-derived extracellular vesicles enhances receptor-mediated targeting of dendritic cells. *J Extracell Vesicles* **8**, 1648995 (2019).

60. Eriksson, M. *et al.* Biological evaluation of multivalent lewis X-MGL-1 interactions. *Chembiochem* **15**, 844–851 (2014).

61. Marcelo, F. *et al.* Identification of a secondary binding site in human macrophage galactose-type lectin by microarray studies: Implications for the molecular recognition of its ligands. *Journal of Biological Chemistry* **294**, 1300–1311 (2019).

62. Kaparakis, M. *et al.* Bacterial membrane vesicles deliver peptidoglycan to NOD1 in epithelial cells. *Cell Microbiol* **12**, 372–385 (2010).

63. Stevenson, T. C. *et al.* Immunization with outer membrane vesicles displaying conserved surface polysaccharide antigen elicits broadly antimicrobial antibodies. *Proc Natl Acad Sci U S A* **115**, E3106–E3115 (2018).

64. Kuipers, M. E., Hokke, C. H., Smits, H. H. & Hoene, E. N. M. N. <sup>1</sup>. Pathogen-Derived Extracellular Vesicle-Associated Molecules That Affect the Host Immune System: An Overview. *Frontiers in Microbiology* **9**, 2182 (2018).

65. O'Donoghue, E. J. *et al.* Lipopolysaccharide structure impacts the entry kinetics of bacterial outer membrane vesicles into host cells. *PLoS Pathog* **13**, e1006760 (2017).

66. de la Torre-Escudero, E. *et al.* Surface molecules of extracellular vesicles secreted by the helminth pathogen *Fasciola hepatica* direct their internalisation by host cells. *PLoS Negl Trop Dis* **13**, e0007087 (2019).

67. Nkurunungi, G. *et al.* Microarray assessment of N-glycan-specific IgE and IgG profiles associated with *Schistosoma mansoni* infection in rural and urban Uganda. *Sci Rep* **9**, 3522 (2019).

68. van Diepen, A. *et al.* Differential anti-glycan antibody responses in *Schistosoma mansoni*-infected children and adults studied by shotgun glycan microarray. *PLoS Negl Trop Dis* **6**, e1922 (2012).

69. Yang, Y. Y. *et al.* Specific anti-glycan antibodies are sustained during and after parasite clearance in *Schistosoma japonicum*-infected rhesus macaques. *PLoS Negl Trop Dis* **11**, e0005339 (2017).

70. Coakley, G. *et al.* Extracellular Vesicles from a Helminth Parasite Suppress Macrophage Activation and Constitute an Effective Vaccine for Protective Immunity. *Cell Rep* **19**, 1545–1557 (2017).

71. Engering, A. *et al.* The dendritic cell-specific adhesion receptor DC-SIGN internalizes antigen for presentation to T cells. *J Immunol* **168**, 2118–2126 (2002).
72. Eichenberger, R. M. *et al.* Hookworm Secreted Extracellular Vesicles Interact With Host Cells and Prevent Inducible Colitis in Mice. *Front Immunol* **9**, 850 (2018).
73. Gringhuis, S. I., Kaptein, T. M., Wevers, B. A., Mesman, A. W. & Geijtenbeek, T. B. Fucose-specific DC-SIGN signalling directs T helper cell type-2 responses via IKKepsilon- and CYLD-dependent Bcl3 activation. *Nat Commun* **5**, 3898 (2014).
74. Giera, M. *et al.* The *Schistosoma mansoni* lipidome: Leads for immunomodulation. *Analytica Chimica Acta* **1037**, 107–118 (2018).
75. Turner, J. D. *et al.* Schistosome infection is associated with enhanced whole-blood IL-10 secretion in response to cercarial excretory/secretory products. *Parasite Immunol* **35**, 147–156 (2013).
76. Baribaud, F., Pohlmann, S., Leslie, G., Mortari, F. & Doms, R. W. Quantitative Expression and Virus Transmission Analysis of DC-SIGN on Monocyte-Derived Dendritic Cells. *Journal of Virology* **76**, 9135–9142 (2002).





# Chapter 7

## Summarizing discussion and future perspectives

## Introduction

Parasites evolved together with their hosts over millions of years. Some of them, like *Schistosoma mansoni*, have gained ways to survive within the venous system of the host for prolonged times. Part of the survival strategies of schistosomes have evolved to combat or evade the innate and adaptive immune responses deployed by the host. Elucidating how these developed immunomodulatory mechanisms work can aid the understanding of our immune system. By studying how parasites evade the immune system, we might discover how we can steer immune responses for our own benefit in immunological diseases<sup>1,2</sup>.

Decades of research on *S. mansoni* substantiated that these organisms release products, so called 'excretory/secretory products' (ES), that can influence host immunity<sup>3</sup>. Each life stage: schistosomula larvae, adult worms, and eggs, release a different set of ES products, each with different effects on host immune responses<sup>4</sup>. ES contains various types of molecules such as metabolites, peptides, lipids, proteins, including glycoconjugates thereof, with a unique glycosylation profile linked to each life stage<sup>5</sup>. And it is known that these glycans play an important part in immune recognition and regulation<sup>6</sup>.

A little over 10 years ago, extracellular vesicles (EVs) were first described to be part of helminth parasites' released products<sup>7,8</sup>. The first publications of EVs released by *S. mansoni* schistosomula and adult worms followed soon and reported on their protein and RNA content<sup>9,10</sup>. During this time, when the field of helminth-derived EVs was still in its infancy, our research group started the ground work on EVs released by schistosomes that led to the work described in this thesis. Here, the aim was to explore the glycosylation of *S. mansoni* EVs and their interactions with and effects on host immune cells. In this discussion, I will reflect on the results obtained along this explorative journey and on the missing links that can be the focus for future endeavors.

### ***Schistosoma mansoni* EVs: what is their cellular source?**

Schistosomes are multicellular organisms and thus far, the exact cellular source(s) of the EVs isolated from *in vitro* cultured helminths remains unknown<sup>11</sup>. As described in Chapter 2, release of vesicle-like structures by *Schistosoma* parasites has been visualized well before EVs became a main focus of research<sup>12,13</sup>. Since then, only limited studies have shown or suggested possible origins for helminth released EVs, such as the adult worm tegument (its outer layer)<sup>8</sup> and their intestinal lumen<sup>14</sup>. For *Schistosoma* larvae, the EV-associated protein SmLEV1 was detected in high concentration in the pre-acetabular glands and on the parasites' surface<sup>15</sup>, suggesting that these are potential sites of origin for schistosomula EVs. Our findings on the EV-associated glycans that are presented in this thesis

(Chapter 4 and 6) provide additional information on the possible EV-releasing source in the parasites.

The GalNAc $\beta$ 1-4GlcNAc $\beta$ 1 (LacDiNAc / LDN) structure that was substantially present on the adult worm EVs has been reported to be present in or on the worms' tegument and excretory system<sup>16</sup>. Additionally, lectin staining suggested that the O-linked  $\alpha$ -GalNAc (Tn antigen), which is another glycan we expect to be present on the EV surface, is also found in or on the tegument<sup>17</sup>. Through visualisation by monoclonal antibodies, fucosylated LDN variants, including GalNAc $\beta$ 1-4(Fuc $\alpha$ 1-3)GlcNAc $\beta$ 1 (LDN-F), Fuc $\alpha$ 1-3GalNAc $\beta$ 1-4GlcNAc $\beta$ 1 (F-LDN) and Fuc $\alpha$ 1-3GalNAc $\beta$ 1-4(Fuc $\alpha$ 1-3)GlcNAc $\beta$ 1 (F-LDN-F) have been found in the parenchyma (F-LDN, LDN-F, F-LDN-F)<sup>16,18</sup>, the excretory system (LDN-F, F-LDN-F), and in the gut (LDN-F)<sup>16</sup> of adult worms. The detection of these structures partly depended on whether the worms were frozen or fixed. Detection in the gut and secretory system of LDN-F was only visible in frozen sections and not when fixed with a solution that contained ethanol<sup>16</sup>. Furthermore, the F-LDN and F-LDN-F traced in parenchymal ducts disappeared after chloroform/methanol treatment<sup>18</sup>. The disappearance of glycans after such treatments suggests that these fucosylated LDNs are most likely attached to lipids. Indeed, mass spectrometry of adult worm extracts show exclusively fucosylated LDN motifs in the glycolipid profile<sup>5</sup>. Interestingly, however, we could not detect any glycolipids in worm EVs and also western blots of the EVs gave no signal for F-LDN and F-LDN-F. We could detect LDN-F by western blot in highly weight bands, but the LDN-F motif was not among the abundant peaks in the N-glycan spectra. Concluding from these data, the majority of the adult worm EVs would be most likely released from their tegument and not the parenchyma surrounding the gut. This is also substantiated by high abundance of the EV-associated protein Tetraspanin-2 (TSP2)<sup>10</sup> in the surface tegument of adult worms<sup>19</sup>.

Glycan motifs we detected on the schistosomula EVs, mainly Gal $\beta$ 1-4(Fuc $\alpha$ 1-3)GlcNAc (Lewis X or Le $X$ ) and highly fucosylated glycolipids, have also been detected on cercariae and schistosomula<sup>16,20</sup>. Le $X$  was mostly localized to the oral sucker in cercariae<sup>16</sup> and in the oral sucker area of schistosomula 3 hour post-transformation. Expression of Le $X$  became visible in the whole schistosomula 24 hours or later after cercarial transformation<sup>20</sup>. Additionally, detection of fucosylated LDNs or mono- and multifucosylated GlcNAc with monoclonal antibodies showed these motifs on the whole surface of both cercariae and schistosomula. One antibody that binds F-LDN, LDN-F, and F-LDN-F showed presence of these glycan structures on the whole schistosomula surface in both fixed and live parasites. In contrast, an antibody that was more specific for LDN-F only detected this motif on fixed parasites, suggesting that fixation might have

exposed underlying glycans<sup>20</sup>. Interestingly, the same LDN-F targeting antibody showed limited LDN-F presence in schistosomula EVs. These data suggest that isolated EVs from schistosomula are most likely released from their tegument surface. However, we cannot exclude that the cercarial oral sucker and acetabular glands release EVs that contributed to the complete EV pool isolated from the medium after 72 hours culture. To study this further, one can utilize the fact that cercarial acetabular gland atrophies between 48–72 hours post infection (e.g. transformation)<sup>21</sup>. If a substantial amount of EVs are released by the acetabular gland, its atrophy may lead to a reduction of these EVs released in culture. Thus, comparing the glycosylation profile of isolated EVs from <24 hours cultured schistosomula versus EVs released between 72 to 96 hours post transformation will illustrate what proportion was acetabular gland-derived in our 0–72 hours collected EVs. This information is important to further understand in which stage of transformation and development the schistosomula release EVs with the immunomodulatory effects that we have observed for our isolated schistosomula EVs on monocyte-derived dendritic cells (moDCs).

Our data supports that adult worm and schistosomula EVs originate from the parasites' tegument. For the adult worm EVs, this is substantiated by the presence of specific glycans (e.g., LDN and the Tn antigen) and the abundance of TSP2 on the tegument surface, which we also found on the EVs. Schistosomula EVs are likely released from their tegument surface because of the EV-association of many fucosylated glycans, including Le<sup>x</sup>, that is similar to the glycans on the surface of cercariae and schistosomula. However, further evidence is required since the tegument as EV source remains under debate<sup>22</sup>. Here I will propose and illustrate three methodologies for exploration. The first would be to incubate live worms or schistosomula with a TSP2 or glycan-targeting antibody and isolate their released EVs at different time points for detection. Most ideally, the antibody is conjugated to a fluorescent molecule, so that the presence of the antibody on the EV can be shown easily either by high resolution flow cytometry<sup>23</sup> or super resolution microscopy<sup>24</sup>. The possibilities for this labeling will expand with the availability of glycan targeting nanobodies<sup>25</sup>. Nanobodies are small fragments of heavy-chain-only antibodies of camelids. Because they are smaller than intact immunoglobulins, they allow for a higher spatial resolution<sup>26</sup> and reduce multiplex bias when aiming to detect more than one target<sup>27</sup>. The second approach extends the use of labeling molecules by targeting differentially expressed proteins or glycans along the parasites' anatomy. Subsequent single EV measurements could point towards a more detailed localization of EV releasing cells. These regions could then be further examined by (cryo) transmission electron microscopy (TEM), targeting the same molecules with gold-nanobodies<sup>28</sup> to identify the true origin

of schistosome released EVs. Thirdly, the location of EV release may be studied by taking advantage of the use of host lipids by helminths for the construction of lipid membranes<sup>29,30</sup>. It has been shown that when feeding fluorescent lipid analogues to *Anisakis* spp. and *Trichuris suis* larvae in culture, they integrated this lipid in their released EVs<sup>31</sup>. Previous lipid staining of schistosomes also showed that there was specificity of labeled phosphatidylcholine analogues to the surface, gut and acetabulum<sup>32</sup>, but these experiments have not been done in relation to released EVs. Using different lipid formulations that are incorporated in different cellular locations within the parasite, one could study which EV is derived from which location based on EV fluorescence.

Knowing the exact cellular source of the EVs can provide valuable insights in how schistosomes employ EVs in the host. For example, if EVs are released from the schistosomula acetabular glands, it might suggest that these EVs are involved in enzymatic digestion of extracellular matrix components during skin penetration<sup>33</sup>. And when EVs are released from the tegument, either from schistosomula or adult worms, these might contribute to disable host defense mechanisms as complement and immunoglobulins<sup>21</sup>. In addition, EVs from the adult worm tegument might play a role in the inhibition of blood coagulation, since ecto-enzymes as alkaline phosphatase are present on the tegument surface<sup>34</sup> and have been detected in adult worm EVs<sup>10,35</sup>. Furthermore, uncovering which cells of schistosomes release EVs that can modulate host immune responses might also direct us to the cells that release well-known immunomodulatory ES components<sup>36</sup>. In future perspective when helminth derived (stem) cell lines will become available, which would overcome many challenges in helminth EV research<sup>37</sup>, it would be advantageous that collected EVs from the cell cultures are close to identical to the EVs released by the whole organism. For this, we need to know the cell source of which the EVs in whole parasite cultures derive from. Ultimately, deep understanding of helminth EV release may reveal possible new therapeutic targets to combat schistosome infections.

### **Surface structures on schistosome EVs: unique, helminth specific, or common across species?**

One of the characteristic features of the EVs isolated from the schistosomula were their long hair-like surface structures (Chapter 6). To date, the specific molecular makeup of these structures is still unclear. Hence, I want to emphasize that the comparisons in this paragraph will be based on visual features. Similar surface protruding structures have been reported on adult worm EVs released by *Hymenolepis diminuta*, *Ascaris suum*, *H. polygyrus bakeri*, and *Oesophagostomum dentatum*<sup>37</sup>, but they seem different from the ones on schistosomula EVs since

the structures on the EVs from these other parasites are less “fluffy” and much shorter in length. In Chapter 4 we mentioned that the presence of EV surface protrusions, as we also observed for *S. mansoni* adult worms, may be a hallmark for pathogen-derived EVs, because they have mainly been reported for EVs from helminths<sup>37</sup>, bacteria<sup>38,39</sup>, fungi<sup>40</sup>, and EVs from mammalian cells transfected with nematode or viral membrane proteins<sup>41</sup>. However, short protruding surface structures have also been detected on EVs from human primary tracheobronchial cell cultures<sup>42,43</sup> and BEAS-2B lung epithelial cells<sup>44</sup>. It is possible that more mammalian or pathogen-derived EVs contain similar filamentous structures as those present on the schistosomula EVs. This characteristic may be easily missed, as the only way to clearly visualize them is by high quality cryo TEM, which is not available in all laboratories. We were prompted to use cryo TEM, as we observed a discrepancy in size measurements between classic TEM and Nanoparticle Tracking Analysis (NTA) (Chapter 6). Of note, only half of the schistosomula EVs we analyzed by cryo TEM contained the hair-like structures. This could imply a difference in cell type or cell compartment origin of the EVs (from multivesicular body or from plasma membrane). Considering the clear morphological differences between the two schistosomula EV populations with or without the surface structures, it is tempting to assume that these EVs have distinct functional roles within the host. For now, it seems that the schistosomula EV hair-like surface structure is outstanding in their “fluffy” morphology and extended length, but not completely unique. This raises the question about their biological significance. Since we isolated EVs from 0–72 hours cultured schistosomula post-transformation, and schistosomula have been reported to leave the skin 48 to 72 hours post infection<sup>21</sup>, their EVs might play a role during the skin stage and/or the lung stage. Below, I will briefly discuss how these structures could be connected to schistosomula survival strategies in both the skin and the lung and describe two experimental directions in which these structures could be further elucidated.

In the first three hours after invading the skin, the schistosomula will shed its cercarial glycocalyx. This layer of proteins and glycans protected the cercariae against osmotic pressure when it was still in water<sup>21</sup>. In the skin, however, it is a prime target for the complement system<sup>45</sup>. Interestingly, this glycocalyx looks very similar to the EV surface structures<sup>13</sup>. Thus, it seems likely that some of the EVs and their structures serve as decoys to attract complement until the schistosomula has reorganized its membrane, which expresses various molecules that can disarm complement and immunoglobulins<sup>46</sup>. This could be examined by incubating schistosomula EVs with normal human serum (NHS) or heat-inactivated NHS and subsequent detection of activated complement component C9<sup>47</sup>. Actual binding of complement to the structures could subsequently be explored by TEM

and gold-labelled anti-C9. Checking complement binding of EVs released by schistosomula after different timepoints following cercarial transformation will provide additional knowledge on whether it is the glycocalyx like structure that serves as this scavenger function on the EVs.

From the skin, the schistosomula will migrate to the lungs where they reside for several days<sup>21</sup>. Here, the visual similarity between the schistosomula EV structures and the airway epithelial EV structures offers an interesting case for assessment of functionality. The airway EVs are highly enriched in mucins, which are known to be heavily O-glycosylated<sup>48</sup>. Within the airways, mucins are part of the innate immune defense system to protect against pathogens and environmental toxins<sup>44</sup>. Part of these toxins are reactive oxygen species (ROS). ROS plays an important role in the lung stage of *Schistosoma* infections<sup>49,50</sup>, where schistosomula switch to anaerobic metabolism and scavenger molecule release to survive<sup>21</sup>. Another molecule that can scavenge ROS are proteoglycans, which are similarly heavy glycosylated proteins as mucins. Glycosaminoglycans have been shown to be modified or degraded by several ROS species after direct contact<sup>51</sup>. Thus, it might be that the long hair-like structures we observe on the surface of schistosomula EVs are similar scavenger glycans. Whether these are actually mucins is currently unknown, as there are no reports on mucin expression by schistosomula<sup>21</sup>. However, based on the many glycans we found in schistosomula EV preparations, we do assume that these surface structures consist of glycans, with or without a protein backbone. One way to test if the schistosomula EV structures would be relatively similar to proteoglycans, is to check by TEM whether the structures are degraded after incubating the EVs with ROS, such as H<sub>2</sub>O<sub>2</sub><sup>52</sup>. Another interesting factor in the lungs that combats pathogens are surfactants, which include C-type lectin receptors (CLRs) from the collectin family<sup>53</sup>. One of these, surfactant protein (SP)-D, has been shown to bind to the oral sucker of *S. mansoni* cercariae and the complete surface of the schistosomula, most likely via F-LDN and F-GlcNAc<sup>54</sup>. We detected similar glycan structures on the schistosomula EVs (Chapter 4 and 6), which suggest another molecular scavenger function of released schistosomula EVs. Whether SP-D binds to schistosomula EVs and whether this would colocalize with fucosylated glycans on the surface could be examined using super resolution microscopy.

My suggestions thus far mainly included the possible scavenger functions of the EV hair-like structures to protect the schistosomula from harmful host defense molecules. However, both in the skin and in the lung, immunomodulation by the parasite is crucial for its survival<sup>55,56</sup>. Therefore, we should also consider that these surface structures increase the interaction with host antigen presenting

cells, like DCs and macrophages, either by itself or via a scavenged host molecule. There are two experimental directions to get more information on these unique EV structures and their function in immune modulation: determining their exact composition or trying to separate EVs with the structures from EVs without. Hereafter, examples for both options will be further elaborated.

To determine the structures' molecular makeup, we already performed an initial experiment where schistosomula EVs were treated with PNGase F (to release N-glycans) or very briefly with proteases. However, no differences in the structures were observed by cryo TEM after both treatments (unpublished data). This experiment should be repeated with longer treatments and various proteases to really exclude the presence of a protein backbone. In addition, albeit technically challenging<sup>57</sup>, more effort can be made to investigate the presence or absence of O-glycans, as the larval stage of schistosomes expresses various O-glycans<sup>6,58</sup>. To examine whether the highly abundant glycolipids are part of these hair-like structures, one could culture the schistosomula in presence of different lipid formulations to possibly alter the EV glycolipid composition. When the composition of the structures is known, subsequent functional experiments can be performed in which EVs with removed or altered surface structures can be compared to the 'original' EVs. These could be a repetition of the moDC experiments presented in Chapter 6 to study the role of these structures in the observed dependence on DC-SIGN interaction and the enhancement of pro- and anti-inflammatory cytokines. However, with this approach, there will still be the contribution of the EVs without the structures, as they remain most likely unaltered. Addressing this issue seamlessly transitions us towards the second experimental direction: separate the two population of EVs.

To separate EVs with and without the hair-like surface structures we can utilize the possible difference in biochemical characteristics between the two. Our density gradient experiments presented in Chapter 3 show that schistosomula EVs float to a higher equilibrium density in a sucrose gradient compared to EVs from adult worms, but both life stage EVs behave similar in iodixanol gradients. This different behavior in a high- (sucrose) or isosmotic (iodixanol) solutions may be due to different interaction of the schistosomula surface structures with surrounding solutions. Factors to consider for separation, besides size, include surface charge<sup>59</sup> and hydrophobicity<sup>60</sup>. For example, to separate negatively charged plasma EVs from positively charged lipoprotein particles, researchers applied a dual-mode chromatography based on size and ion exchange<sup>61</sup>. Additionally, a hybrid chromatography with separation on charge, size and glycan-binding has been illustrated<sup>62</sup>. Logically, when knowing a specific ligand (protein or glycan motif) that is exclusively expressed on the surface structures, or exclusively on

the surface of the EVs without structures, one can easily remove this population by an affinity-based method<sup>63</sup>. Once separation succeeds, the isolated EV population can be tested for their immunomodulatory effects on host cells. Unraveling the function and molecular configuration of the schistosomula EV structures may increase our understanding of how schistosomes deploy their vesicles during the initial stage of infection, either as scavengers and/or immunomodulators. Furthermore, we might be able to use this knowledge by adding similar structures to therapeutic nanoparticles<sup>64</sup>.

### **Host molecules associated with schistosome EVs: absent, overlooked, or culture condition dependent?**

To be able to attribute molecular characteristics or functions to EVs, the populations of isolated EVs must be free from contaminating molecules (Chapter 2). These can include EVs that are present in cell culture supplements such as FCS, large (nucleo)protein complexes that are co-isolated in size-based methods, or lipoprotein particles that end up at similar gradient densities<sup>65</sup>. Schistosomes can be kept alive in culture for a few days in medium without red blood cells or FCS. This limits the extent to which EV isolates of cultured schistosomes contain contaminants and EVs derived from these mammalian sources. Still, we needed to separate EVs from non-EV molecules released by the parasite. In Chapter 3, we presented an optimized density gradient separation protocol to minimize EV loss of the limited schistosome material and to reliably characterize and study the effect of these EVs. However, it could be that some host materials that are not present in culture would be normally utilized by the parasite for its metabolism, development, and immune evasion. These host molecules could also end up in their released EV and possibly affect their interaction with host cells. Furthermore, there is a recent interest and growing body of evidence in the EV field that mammalian EVs in the blood spontaneously adsorb proteins from the protein-rich blood matrix<sup>66-69</sup>. This 'protein corona' around the EV, either strongly or loosely bound to the surface, can contain lipoproteins, immunoglobulins, enzymes, and larger protein complexes and aggregates and can affect the bioavailability and bio-distribution of EVs<sup>66</sup>. Since schistosomes reside in the blood, similar interaction of the EV surface with blood components would be conceivable. In case host molecules are incorporated in the EVs and/or bind to the EVs after their release, both could have an impact on the EVs' characteristics and function. This raises the question whether the EV populations we studied are similar to the *in vivo* situation in terms of EV-associated glycans, the cellular interaction of the EVs with host cells, and immune responses induced by schistosome EVs. In the following two paragraphs I will discuss what is currently documented on host

molecules associated to or interacting with schistosome EVs and what should be considered in follow-up investigations. In the final two paragraphs of this section, I will describe the current information regarding *in vivo* released *Schistosoma* EVs and give suggestions on how this field can move forward.

Within our glycomics data presented in Chapter 4 and 6, we did not detect any sialic acids. The presence of sialylated glycans would automatically indicate the presence of glycans from the host, as the molecular machinery essential for their biosynthesis is absent in schistosomes<sup>6</sup>. Contradictory, another research group did detect host derived sialic acids in their *S. mansoni* adult worm EV preparations<sup>70</sup>. A likely explanation for this difference is that the other group cultured their worms in the presence of EV-depleted FCS, which is shown never to be fully EV-free<sup>71</sup>. Indeed, the authors reported in a subsequent publication that the majority of sialic acid glycans were linked to bovine proteins<sup>72</sup>. However, it remains unknown whether these bovine proteins were present in or on the adult worm EVs or on co-isolated bovine EVs that remained in the EV-depleted FCS. In addition, studies on the proteome of adult worm EVs did<sup>73</sup> or did not<sup>10</sup> detect host proteins in their EV preparations, but it is unknown whether this was depending on culture conditions. A third proteomics study did not report whether they searched their data for host proteins in adult worm EVs<sup>35</sup>. There is sufficient data on adsorption of host proteins in the worm's tegument as one of their survival strategies<sup>21</sup>, mainly via its own surface receptors that can bind host antigens<sup>74</sup>. This could suggest that if EVs are collected from adult worms briefly after perfusion, there is a higher chance of finding possible host molecules associated to the EVs than in prolonged cultures in absence of host material. To study this, one could repeat the experimental design described for exploring the tegument as EV source, and incubate freshly obtained adult worms with anti- or nanobodies targeting host molecules, such as IgG or complement components<sup>74,75</sup> or lectins targeting sialylated glycans<sup>70,76</sup>. This approach is preferred over host molecule detection after EV isolation, to avoid the contribution of possible host molecules on EVs in regurgitated gut material<sup>77</sup>. Subsequent EV isolations will inform on the presence of these host molecules on the EV surface. By collecting EVs over time, both with and without re-incubating the worms with host-derived blood, we can better understand the dynamics of host proteins associated with released EVs. When host proteins on EVs subside over time in blood and serum free cultures, it would be worth to incubate immune cells with the early and the late released EVs to study differences in immune responses in presence or absence of EV-associated host proteins. However, this approach only provides answers when the rest of the *Schistosoma* EV composition does not change over time.

An additional element of interest would be to compare the interaction of

schistosome EVs with blood components or serum of uninfected versus infected animals/individuals. It has been reported that *S. mansoni* adult worm EVs can elicit a humoral response in mice<sup>72</sup>. Furthermore, pre-incubation of adult worm EVs with serum from rabbits immunized with recombinant *Schistosoma* specific TSP2 and TSP4 inhibited their uptake by endothelial and monocytic cell lines<sup>78</sup>. However, in our experiments where we preincubated adult worm EVs with antibodies targeting TSP2, we did not observe any reduction in interaction with B cells (Chapter 5). Finally, anti-sera from rats immunized with *H. polygyrus* EVs were reported to increase the uptake of EVs in murine bone marrow derived macrophages<sup>79</sup>. The authors additionally showed that incubation with anti-sera directed internalized EVs more towards degradation in lysosomes, thereby reducing the immunomodulatory ability of these EVs. Altogether, these data suggest that host components in blood may very well interact with schistosome released EVs. However, changes in EV capacity for immune modulation upon interaction with host molecules might be cell type dependent and should be further explored. Eventually, the ideal goal would be to have isolated schistosome EVs from parasite cultures for *in vitro* stimulations that are like those presented to the host cells *in vivo*. For that we need to know how to optimize parasite culture conditions and most of all what the surface molecules and molecular cargo are of *in vivo* released EVs.

Thus far, only a few research groups searched for schistosome-derived EVs in blood of infected patients<sup>80</sup>, hamsters<sup>81</sup>, and mice<sup>73</sup>. However, these studies did not report the detection of parasite-derived EVs (or separation from mammalian EVs) and it remains unclear whether the parasite molecules isolated from the blood is EV-associated. This is in part due to the absence of confirmation that the detected schistosome-derived miRNAs are EV-associated and that the EVs are parasite derived<sup>73,80</sup>. Hence, solid evidence of *Schistosoma* EVs released *in vivo* is, to the best of my current understanding, still lacking. There is, however, one study that compared *in vitro* released *Echinococcus granulosus* EVs to *in vivo* EVs in fluid from parasite harboring cysts in infected people<sup>82</sup>. Results showed major differences in protein amount and content between the two EV sources, which is not surprising considering that the cyst fluid is surrounded by a parasite-derived germinal layer and its fluid also contained many host-derived materials, including lipoprotein particles, immunoglobulins, and complement<sup>82</sup>. This example demonstrates how difficult it can be to separate parasite EVs from host EVs from host body fluids. Yet, there might be an overlooked solution to discriminate parasite EVs from host EVs. As presented in Chapter 5, adult worm EVs could be detected in contact with mouse and human B cells by targeting them with an antibody against *S. mansoni* TSP2. This antibody did not bind to the host tetraspanins, indicating that

the existence of schistosome EVs *in vivo* can be supported by detection of worm specific proteins that are enriched in EVs, such as TSP2<sup>10</sup> or SmLEV1<sup>15</sup>. Antibodies against these proteins should be tested for their suitability to trace parasite EVs in blood cells or tissue sections of infected animals. Another strategy could be to use these antibodies to immunocapture schistosome EVs from plasma of infected individuals. These immunocaptured EVs could subsequently be characterized and compared with similarly isolated EVs from parasite cultures to further understand possible differences between *in vitro* and *in vivo* released EVs. It is important to keep in mind that potential differences between *in vitro* and *in vivo* isolated EV populations may be caused by differences in (re-)uptake of selective EV subsets by host cells and parasites *in vitro* or *in vivo*. Additional *in vitro* studies from cultured parasites should be performed to show that there are indeed specific schistosome EV subsets that target distinct cell types.

A more challenging, yet promising approach to trace EVs released *in vivo* is the use of gene manipulation or transgenesis of schistosomes<sup>83</sup>. Interference RNA (via double stranded DNA) or mRNA addition via electroporation have been shown effective to transiently alter schistosomula and adult worms genetically in culture<sup>84-86</sup>. Moreover, with the rise of CRISPR-Cas as gene editing tool, schistosomes can now be genetically modified<sup>87,88</sup>. This is heritable when done in the egg zygote, but so far there are no reports on this being implemented. Hence, there could be an opportunity to generate a genetically modified *S. mansoni* strain that expresses TSP2 and/or smLEV1 coupled to a fluorescent molecule like GFP. If multiple colors could be linked in one transgenic parasite, and each color linked to a different EV-associated molecule that is enriched in a specific stage of schistosome development, this would greatly enhance our understanding of EV targeting by schistosomes *in vivo*. While it may still take a long time before we succeed in generating such transgenic parasites, it is surprising that the approach of targeting parasite-specific molecules is not utilized more often and pursued in the helminth research. Overall, the molecular differences of proteins between parasite and host is a huge advantage over the mammalian EV field when aiming to detect EVs derived from a specific source *in vivo*<sup>89</sup>.

## 7

### Cellular targets of schistosome EVs: more than immune cells?

One objective in this thesis was to study the interaction of *Schistosoma* EVs with host immune cells. We have shown in Chapter 4 that EVs from adult worms and schistosomula can interact *via* EV-associated glycans with CLRs MGL and DC-SIGN on CLR-expressing cell lines, respectively. In Chapter 5 we provided evidence of interaction between adult worm EVs and mouse and human B cells. Lastly, in Chapter 6 we demonstrated that the internalization of schistosomula

EVs by human moDCs is mostly DC-SIGN dependent. Other research has shown that *S. mansoni* adult worm EVs can be internalized by primary mouse CD4 T cells<sup>90</sup> and THP1 monocytes<sup>78</sup> and *S. japonicum* adult worm EVs can interact with mouse peripheral blood monocytes and T cells<sup>91</sup>. However, none of these studies have investigated possible EV-receptor interaction. There are various CLRs on monocytes, macrophages, DCs, neutrophils, and B cells<sup>92</sup>, and all these cells are worth investigating to see whether they can interact with schistosome EVs via their associated glycans. However, for this part of the discussion, I want to shift the reflection to cells beyond blood immune cells that the parasites may also encounter in the host, as they might be equally important targets for the parasite EVs. Other cells that have been shown to be affected during a schistosome infection, or when stimulated with ES material, include keratinocytes<sup>93</sup>, lung endothelial cells<sup>94</sup>, and liver cells<sup>95</sup>. EVs from *Echinostoma caproni*<sup>8</sup>, *Heligmosomoides polygyrus*<sup>14</sup>, *Nippostrongylus brasiliensis*<sup>96</sup>, and *Trichuris muris*<sup>97</sup>, all interact with intestinal epithelial cells, and *Opisthorchis viverrini* EVs can interact with cholangiocytes (cells of the bile duct)<sup>98</sup>. However, studies on the interaction of schistosome EVs with host cells other than phagocytes and lymphocytes is limited. Thus far, there is one study showing interaction of *S. mansoni* adult worm EVs with an endothelial cell line<sup>78</sup>, one study on *S. japonicum* adult worm EVs that interacted with murine liver cells (NCTC cell line)<sup>99</sup> and two studies on *S. japonicum* egg-derived EVs that were suggested to be internalized by murine liver cells (HEPA1-6 cell line)<sup>100</sup> and human liver stellate cells (LX-2 cell line)<sup>101</sup>. I hereafter will further discuss cells in the liver and endothelial cells as potential target cells for schistosome EVs and use our current understanding of the EV-associated glycans as starting point to future directions to explore.

Adult worms reside in the portal vein, meaning that almost everything they will release will travel to or through the liver. In Chapter 4, we described that adult worm released EVs mainly contain LDN motifs on their surface N-glycans, but also contain the O-glycan Tn antigen. Using CRL expressing cell lines, we discovered that these EVs mainly interacted with the MGL receptor and not so much with DC-SIGN. The MGL receptor is exclusively expressed on tolerogenic DCs and macrophages and it mainly recognizes GalNAc residues, which includes sialylated and non-sialylated Tn antigen and LDN<sup>102</sup>. The alternative name for the MGL is DC-ASGPR, as the MGL gene is in the same cluster as the asialoglycoprotein receptor (ASGPR)<sup>103</sup>. The ASGPR is nearly exclusively expressed on hepatocytes in the liver and recognizes N-glycans terminating in  $\beta$ Gal or  $\beta$ GalNAc<sup>103</sup>. Thus, based on our findings that the surface glycans on the adult worm EVs contain terminal  $\beta$ GalNAc, the ASGPR is a potential receptor for these EVs in the liver. In the next paragraph, I will hypothesize how targeting of the ASGPR by worm EVs

can be linked to current *in vivo* data and what *in vitro* studies can be performed to investigate this interaction.

The general function of ASGPR in the liver is to clear proteins, lipoprotein particles<sup>104</sup>, and mammalian EVs after they are desialylated, leading to exposed  $\beta$ Gal<sup>105</sup>. The ASGPR also takes up senescent, desialylated platelets which subsequently leads to increased numbers of platelet producing megakaryocytes<sup>106</sup> and impairment of this platelet clearance reduces the levels of platelet activity<sup>106</sup>. During human schistosome infections, increased levels of HDL particles can be observed in plasma<sup>107</sup> as well as lower platelet levels, and the blood needs longer time to coagulate<sup>108</sup>. It is tempting to suggest that competitive binding of worm EVs to the ASGPR plays a role in these HDL and platelet changes. Altering the lipoprotein particle levels might be a strategy of the parasite to obtain the lipids it cannot synthesize itself<sup>29,30</sup>. And reduced amounts of platelets that do not coagulate quickly, benefit both the adult worms and its host, as this lowers the chance on thrombotic complications induced by the worms' presence<sup>109</sup>. One initial experiment should first confirm the interaction of adult worm EVs with the ASGPR on cultured hepatocytes. Thereafter, the subsequent effect on levels of lipoprotein particles or senescent platelets left in the medium can be studied<sup>110,111</sup>. The next step would be to inject the EVs in liver organoids<sup>112</sup> to study the amount of EVs that interact with each individual cell type within the liver. Since the liver resident macrophages (Kupffer cells) also express an LDN binding CLR<sup>113</sup>, there might be a functional significance when adult worm EVs have a preferential targeting to the hepatocytes *via* ASGPR or to the liver Kupffer cells.

In addition to the liver, the interaction of schistosome EVs with endothelial cells are worth exploring further<sup>78</sup>. Endothelial cells not only modulate metabolic homeostasis, vascular permeability, coagulation, and cell extravasation, they also participate in both innate and adaptive immune responses<sup>114</sup>. They express several TLRs, can upregulate MHC II and co-stimulatory molecules as OX40 ligand, CD80 and CD86, and release pro- and anti-inflammatory cytokines and chemokines. Kifle *et al*, have shown that incubation of HUVECs with adult worm EVs led to differential expression of genes associated with intravascular parasitism, such as increased IL-6 and chemokines and downregulation of coagulation<sup>78</sup>. They suggested a role for schistosome TSP2 and TSP4 in the adult worm EV uptake by blocking these EV-associated proteins with antibodies<sup>78</sup>. Still, this might not be the only interaction these EVs can have with endothelial cells. There are currently two CRLs described that can be found in endothelial cells: CLEC1A and CLEC8A. These receptors are actually C-type Lectin-Like receptors (CTLRs) and do not need calcium to interact with glycans and can also bind proteins and/or lipids<sup>115</sup>. It might be that EV-glycosylation is redundant for the EVs to interact

with endothelial cells. Yet, both receptors might still play a role in targeting and/or affecting endothelial cells, which I will elaborate on next.

CLEC1A (or CLEC-1) in endothelial cells is mainly present intracellularly, but expression is increased upon IL-10 and TGF $\beta$  stimulation<sup>116</sup>. Once activated, it can dampen Th17 responses, however, the exact ligand for this effect remains unreported<sup>115</sup>. Th17 responses play a role in the development of severe schistosomiasis pathology<sup>117</sup>, thus reduction of these responses *via* CLEC1A activation would benefit the host and thus the parasite. In human lung transplants, decreased expression of CLEC1A is a predictive marker for the development of graft rejection<sup>118</sup>. I speculate that increased and activated CLEC1A could benefit tolerance to the “non-self” parasites in the blood. For future experiments, the possible interaction with CLEC1A could be studied by incubation of EVs in the presence or absence of IL-10 and TGF $\beta$  to increase CLEC1A expression on the endothelial cells. Subsequent changes in mRNA of the CTLR overexpressing cells may also indicate whether uptake of the EVs effects endothelial functions.

The other CTLR, CLEC8A, also called lectin-like oxidized low-density lipoprotein receptor-1 (LOX-1) recognizes oxidized and acetylated LDL and is mainly studied in the context of atherosclerosis<sup>115</sup>. LOX-1 belongs to the ‘scavenger receptor’ family<sup>119</sup> and it has been shown that scavenger receptors on endothelial cells mediate EV uptake *in vivo*<sup>24,120</sup>. However, it remains unknown whether glycosylation is essential for this scavenger receptor-mediated uptake, and there is currently no mention in the literature on interaction of *Schistosoma* secretions with scavenger receptors. Of note, *Schistosoma* adult worm EVs contain their own scavenger receptor, namely the CD36-like class B scavenger receptor<sup>35</sup>. It has been reported that *S. japonicum* eggs use the CD36-like protein to bind and internalize HDL to get essential cholestryl esters for egg embryo development<sup>121</sup>. Schistosome adult worm CD36-like receptor has been shown to bind human LDL<sup>122</sup>, and LDL binding has also been observed on the worms’ tegument<sup>123</sup>. It is therefore possible that the CD36-like scavenger receptor on adult worm released EVs bind to LDL and facilitate uptake by LOX-1 on endothelial cells *via* the scavenged LDL. This seems likely as also mammalian EVs are reported to be prone for binding to LDL<sup>110</sup>. For involvement of LOX-1, schistosome EVs can be pre-incubated with various lipoprotein particles that have been oxidized or not to see whether this influences their interaction with endothelial cells. Finally, we should consider that uptake of adult worm EVs by endothelial cells can happen *via* their TSPs, their associated glycans, or indirectly by scavenging host (lipoprotein) particles, which all may lead to subsequent different downstream effects and this should be explored further.

The survival of schistosomes in the host depends not only on their

immunomodulatory strategies. The interaction with or mimicking of host molecules, modulation of complement, and prevention of blood coagulation, all contribute to a prolonged infection without death of the parasite or killing of its host<sup>124</sup>. Cells in the liver and endothelial cells play a role in pathogen recognition and forward this information towards the immune system. Schistosomes need to restrict these signals to mask their presence, possibly by their released EVs. Increasing our knowledge on how schistosome EVs affect these host cells, could reveal how to uncloak them and make them more visible to the immune system, which could be beneficial for future vaccination strategies<sup>125</sup>.

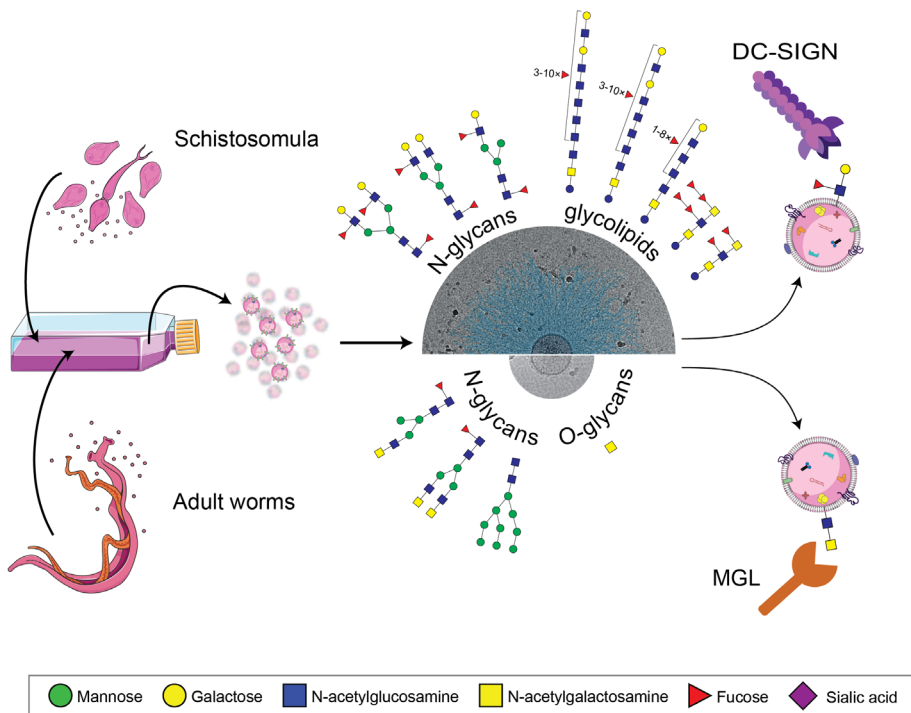
## **Schistosome induced immune responses: what is the significance of EVs and their cargo?**

*Schistosoma spp.* are master regulators of their hosts' immune system, which is partly achieved through targeted release of specific immunomodulatory components<sup>1,21,36</sup>. We and others have provided evidence that schistosome released EVs can affect host immune responses<sup>80,91,126</sup>, which adds up to the reports on other helminth EVs with similar capacity<sup>127</sup>. In Chapter 5, we showed that highly purified adult worm EVs are able to induce the release of IL-10 by mouse splenic B cells and IL-6 and IL-10 by peripheral blood B cells from humans. This corresponds with the observation that single sex male infections in absence of eggs, which are strong inducers of B cell IL-10 release<sup>128</sup>, also led to increased IL-10 producing B cells<sup>129</sup>. In Chapter 6 we demonstrated that EVs released by the schistosomula augment moDC activation, leading to more CD86, CD80, and PD-L1 expression and increased IL-12 and IL-10 release. These findings corresponded with previous publications on responses in the skin upon cercarial infection and *in vitro* stimulations with schistosomula ES<sup>56,130,131</sup>. However, many of these induced immune responses cannot be exclusively appointed to EVs, because other ES components<sup>132-135</sup> and EV depleted ES (Chapter 5) show similar capacities. Furthermore, it remains unknown whether observed immune responses are depending on EV-receptor interaction or that the delivery of the EV luminal cargo plays a significant role. In the next two paragraphs, I will propose some experimental approaches to investigate the functional differences between EVs and non-EV ES components on immune responses and to study the contribution of EV-surface molecules versus their luminal cargo.

One benefit of EVs would be that EVs allow the parasite to deliver a complete set of molecules to recipient cells all at once, and this combination could have more effect on immune responses than just one molecule present in the ES. In addition, as shown for DC-SIGN, some receptors preferentially interact with bigger particles compared to smaller single proteins<sup>136-138</sup>, which may eventually

lead to a different uptake route and effect of EVs compared to smaller ES components. So how to study the difference of immune responses between EVs and non-EV ES components released by the parasite? In chapter 5, we found that it is very difficult to completely deplete the ES from EVs using differential ultracentrifugation. Therefore, it might be an option to use a trans-well system, where parasites will be placed on the top and cells in the bottom, with a Matrigel or PEGDA hydrogel instead of a permeable membrane. Parasites release their products in the top well, and depending on the type of gel, EVs can (Matrigel) or cannot (PEGDA hydrogel) pass through, while the smaller ES products can still pass both gel types<sup>139</sup>. This way, the effect of ES without EVs and ES with EVs can be examined. Another strategy would be to put more effort in separating the EVs from the ES<sup>63</sup>, for example by immunocapture of EVs. However, for this, it is important to know which EV-associated molecule (protein or glycan) is not present as non-EV ES component. Although proteomics have been performed on schistosome ES<sup>140</sup> (containing EVs) and EVs<sup>10,73,35</sup> separately, there are no reports on comparative analysis of the protein content or glycosylation profile between EV-enriched and EV-depleted ES from the same preparation. In addition, it would also be worth investigating overlapping proteins detected in both EV preparation and as non-EV-associated proteins in the ES. When making these as recombinant proteins<sup>132,141</sup>, they could be added to immune cells as extracellular protein, or be incorporated in an EV mimic<sup>142</sup> to study whether the association with EV-like particles influences the downstream effects.

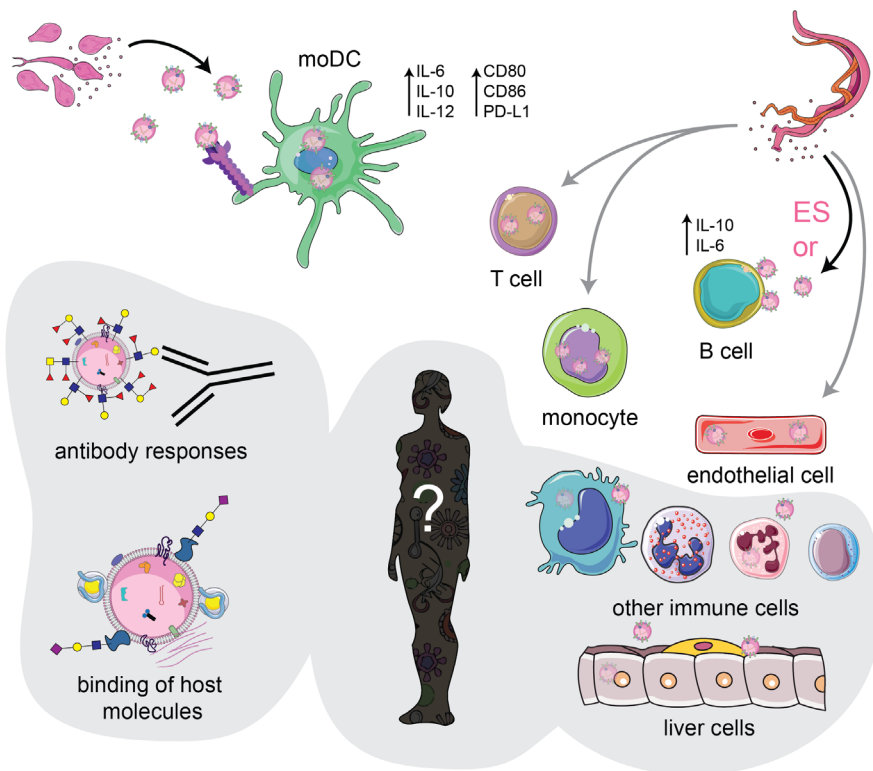
Another potential benefit for schistosomes to release EVs in addition to other ES components is the protection of luminal EV cargo, like RNAs, from degrading enzymes. Several studies have proposed that micro(mi)RNA associated with schistosome EVs have an effect on immune responses<sup>90,91,99-101</sup>. However, these studies often showed immune effects by cells that were transfected with miRNAs that were previously detected in unpurified EV preparations. Together with the helminth EV community, we have proposed the proper controls for the assessment of EV-associated molecules, including nucleic acids, in a recent position paper<sup>37</sup>. In addition to RNAs, luminal proteins have been described for adult worm EVs, but their importance in EV function was not investigated<sup>35</sup>. Thus, there is currently no solid evidence that immune effects are induced by EV surface molecules interacting with cellular receptors, by their luminal cargo that is delivered into the cell, or both. Investigating this, however, is currently hampered by technical difficulties. For example, altering EV cargo with either biogenesis inhibitors or disruption techniques also changes other EV characteristics that influence cellular interaction<sup>143,144</sup>. It may be easier to investigate the role of the EV surface, in our case its surface glycans interacting with CLRs, and their downstream effect on



### Main findings presented in this thesis

- Adult worm EVs can be separated from non-EV ES components using density gradients (Chapter 3)
- Schistosomula and adult worm EVs both have a glycosylation profile that corresponds with their own life stage, yet show different enrichments (Chapter 4 and 6)
- Adult worm EVs interact with the MGL receptor and schistosomula EVs with DC-SIGN (Chapter 4)
- Adult worm EVs interact with B cells and induce cytokine release by these cells (Chapter 5)
- Schistosomula EVs interact specifically with DC-SIGN on human moDCs (Chapter 6)
- Schistosomula EVs increase immune responses by human moDCs (Chapter 6)

**Summarizing overview of current understanding of the glycosylation of EVs from *S. mansoni* schistosomula and adult worms, the interaction of these EVs with host cells and EV-induced immune responses**



### Follow up questions

- What are the cellular sources of the schistosome EVs?
- What are the structures on the schistosome EV surface, and are these structures common for EVs across species?
- Can host molecules bind to schistosome EVs and what would be its impact on the function of these EVs?
- What other host cells can schistosome EVs interact with?
- What is the role of EVs within ES induced immune responses by schistosomes?
- Are schistosome EVs released *in vivo* and do they share characteristics with *ex vivo* released EVs?
- Can schistosomula EVs induce antibody responses within the host?

Text boxes describe the main findings presented in this thesis and the follow up questions. More details in text. Uptake of adult worm EVs by T cells, monocytes, and endothelial cells have been presented elsewhere<sup>78,90</sup>.

immune cells without the presence of other EV-associated molecules (e.g. luminal cargo). For this, we can utilize systems like *Nicotiana benthamiana* plants, that are already used to reconstruct native helminth glycoproteins<sup>145</sup>. In addition, it has been shown that EVs can be isolated from *N. tabacum*<sup>146</sup>. It would be interesting to examine the possibilities of generating plant EVs containing the surface glycans we found on schistosomula or adult worms. With these transgenic plant EVs it might be possible to reveal whether immune cell targeting and effector functions by schistosome EVs are depending on their associated surface glycans or their additional cargo.

Elucidating the role of EVs for schistosome induced immune responses will tell us whether it is useful to focus research efforts towards EVs or whether we should keep including the non-EV released ES components in future studies on immune regulation by this parasite. Furthermore, when the parasite seems to depend largely on these vesicles, either for immune evasion, immune modulation, and/or anti-coagulation, they would offer a new target for drug treatments and vaccines.

## **Schistosome EVs and host immunity: inspiration for vaccine development**

Schistosomiasis still affects hundreds of millions of people. Annual mass drug administration in affected communities provides treatment, but does not prevent reinfection<sup>147</sup>. Therefore, researchers are aiming to develop a vaccine against schistosomes for decades, with four candidates now on clinical trials, but it might still be a long way till a safe and sufficiently effective vaccine against schistosomes becomes available<sup>148</sup>. One of these vaccines that is currently being tested is recombinant smTSP2<sup>149</sup>, a protein highly present on schistosomula and adult worm EVs<sup>10</sup> (Chapter 3). EVs are already explored as vaccine candidates against cancer, viral infections, and non-viral infections such as bacteria and parasites<sup>150</sup>. Several studies in mice have shown that administration of EVs isolated from *ex vivo* helminth cultures, often in presence of an adjuvant, can reduce infection readouts upon parasite challenge<sup>79,151-154</sup>. Only one of these studies included *S. mansoni* EVs, which was a subcutaneous injection of a crude preparation of egg-derived EVs that reduced worm and egg counts and granuloma formation upon cercarial challenge<sup>154</sup>. Interestingly, unpublished data on administration of isolated *S. mansoni* adult worm EVs did not affect subsequent infection challenge and readouts in mice, despite the presence of TSP2 in these EVs<sup>155</sup>. It is tempting to suggest that this might be because of the LDN and Tn antigen containing glycan motifs on adult worm EVs that favor tolerance via MGL activation. Thus far, there are no reports on schistosomula EVs and their *in vivo* effect on host

immunity. Therefore, in this final section of the discussion, I will advocate that the unexplored glycosylated schistosomula EVs can be an inspiration for future vaccine development.

In a recent study, researchers extensively tested 96 recombinant antigens found in proteomics and transcriptional data from the schistosomula stage<sup>156</sup>. These antigens included surface proteins as well as various secreted proteins. They tested all 96 as vaccine candidates in a mouse infection model, however, none showed strong protection against subsequent schistosome infection<sup>156</sup>. However, since the recombinant proteins were generated in human embryonic kidney (HEK) cells, these antigens missed one important native feature: helminth glycosylation. Studies in “self-curing” rhesus macaques have shown that these macaques generate high IgG titers against (multi-)fucosylated terminal LDN and Le<sup>x</sup> motifs upon schistosome infection<sup>157</sup>. Furthermore, baboons, which are natural hosts for schistosomes like humans, develop protective anti-glycan antibody responses when vaccinated with radiation-attenuated cercariae<sup>158</sup>. The developed antibodies by the vaccinated baboons mainly targeted multi-fucosylated motifs on O-glycans and glycosphingolipid glycans<sup>159</sup>. We have found Le<sup>x</sup> and multi-fucosylated motifs to be associated with schistosomula EVs (Chapter 6). Thus, these data suggests that schistosomula EV-associated glycans could induce a (protective) humoral response.

One approach to study the influence of schistosomula EV-associated glycans on antibody responses is to vaccinate an animal model with isolated schistosomula EVs. A second approach is to generate *N. benthamiana* plant EVs exposing N-glycans consisting of multifucosylated LDN and Le<sup>x</sup> motifs and test these as vaccine strategy in animal models. An additional important factor for these types of studies is the choice of adjuvant. It has been shown that synthetic nanoparticles provide additional adjuvant properties and can enhance immunity<sup>160,161</sup>. For example, soluble worm antigens loaded into mesoporous silica nanoparticles stimulated a stronger immune response than worm antigens in combination with a more conventional aluminum salt adjuvant<sup>162</sup>. Membrane-encapsulated nanoparticles are currently explored as therapeutic agents<sup>163</sup>, such as coating nanoparticles with bacterial outer membrane vesicles<sup>164</sup>. Thus, a similar nanoparticle coating could be explored using schistosomula EVs or the plant EVs with specific schistosomula glycans, thereby providing a stronger adjuvant to stimulate immunity. Finally, this could also be combined with loading a specific mRNA within the nanoparticles, a novel vaccine technology that has advanced rapidly in the past years<sup>165</sup>. The mRNA could code for one of the receptors expressed on the worm surface that plays a role in binding to or inactivating host molecules<sup>22,74</sup>. When these worm proteins can be targeted by antibodies, thereby inhibiting their function, this

could potentially make the worm less capable to evade host immune responses and increase parasite killing.

Native EVs release by the parasite might not yield the required immunity to offer full protection. However, utilization of EVs to deduce the exact molecules needed for a strong humoral response against the parasite may bring us closer to developing an effective vaccine against schistosomes.

## In conclusion

The work presented in this thesis lays the foundation for deepening our fundamental knowledge on EV isolation methods, EV-glycosylation, and EV-mediated host immune responses by schistosomes. The current age is represented by technological advances for EV isolation of EV subsets<sup>63</sup>, single EV measurement techniques<sup>166–168</sup>, more sensitive omics approaches<sup>169</sup>, and *in vivo* EV tracking<sup>120</sup>. Combining these advancements with the development of transgenic parasites<sup>88</sup> and controlled human *Schistosoma* infection trials<sup>170,171</sup> will open up a range of future possibilities to uncover the true function of schistosome released EVs. With the increasing amount of data and a rise of machine learning tools<sup>172–174</sup>, and the realization that there is common ground between helminths and cancer (glycan) mediated immunotolerance<sup>175</sup>, multidisciplinary collaborations are crucial to accelerate novel discoveries that will benefit the health of many individuals.

## References

1. Angeles, J. Ma. M., Mercado, V. J. P. & Rivera, P. T. Behind Enemy Lines: Immunomodulatory Armamentarium of the Schistosome Parasite. *Frontiers in Immunology* (2020) doi:10.3389/fimmu.2020.01018.
2. Li, J. *et al.* The Potential Role of Schistosome-Associated Factors as Therapeutic Modulators of the Immune System. *Infection and Immunity* (2020) doi:10.1128/iai.00754-19.
3. Pearce, E. J. & MacDonald, A. S. The immunobiology of schistosomiasis. *Nat Rev Immunol* **2**, 499–511 (2002).
4. Acharya, S., Da'dara, A. A. & Skelly, P. J. Schistosome immunomodulators. *PLoS Pathog* **17**, e1010064 (2021).
5. Smit, C. H. *et al.* Glycomic Analysis of Life Stages of the Human Parasite *Schistosoma mansoni* Reveals Developmental Expression Profiles of Functional and Antigenic Glycan Motifs. *Mol Cell Proteomics* **14**, 1750–1769 (2015).
6. Hokke, C. H. & van Diepen, A. Helminth glycomics – glycan repertoires and host-parasite interactions. *Mol Biochem Parasitol* **215**, 47–57 (2017).
7. Silverman, J. M. & Reiner, N. E. Leishmania exosomes deliver preemptive strikes to create an environment permissive for early infection. *Front Cell Infect Microbiol* **1**, 26 (2011).
8. Marcilla, A. *et al.* Extracellular vesicles from parasitic helminths contain specific excretory/secretory proteins and are internalized in intestinal host cells. *PLoS One* **7**, e45974 (2012).
9. Nowacki, F. C. *et al.* Protein and small non-coding RNA-enriched extracellular vesicles are released by the pathogenic blood fluke *Schistosoma mansoni*. *J Extracell Vesicles* **4**, 28665 (2015).
10. Sotillo, J. *et al.* Extracellular vesicles secreted by *Schistosoma mansoni* contain protein vaccine candidates. *Int J Parasitol* **46**, 1–5 (2016).
11. Abou-El-Naga, I. F. Emerging roles for extracellular vesicles in *Schistosoma* infection. *Acta Trop* **232**, 106467 (2022).
12. Wilson, R. A. & Barnes, P. E. The formation and turnover of the membranocalyx on the tegument of *Schistosoma mansoni*. *Parasitology* **74**, 61–71 (1977).
13. Samuelson, J. C. & Caulfield, J. P. The cercarial glycocalyx of *Schistosoma mansoni*. *J Cell Biol* **100**, 1423–1434 (1985).
14. Buck, A. H. *et al.* Exosomes secreted by nematode parasites transfer small RNAs to mammalian cells and modulate innate immunity. *Nat Commun* **5**, 5488 (2014).
15. Gasan, T. A. *et al.* *Schistosoma mansoni* Larval Extracellular Vesicle protein 1 (SmLEV1) is an immunogenic antigen found in EVs released from pre-acetabular glands of invading cercariae. *PLOS Neglected Tropical Diseases* **15**, e0009981 (2021).
16. Remoortere, A. van *et al.* Various stages of *Schistosoma* express Lewisx, LacdiNAc, GalNAc $\beta$ 1-4 (Fuc $\alpha$ 1-3)GlcNAc and GalNAc $\beta$ 1-4(Fuc $\alpha$ 1-2Fuc $\alpha$ 1-3)GlcNAc carbohydrate epitopes: detection with monoclonal antibodies that are characterized by enzymatically synthesized neoglycoproteins. *Glycobiology* **10**, 601–609 (2000).

17. Schmidt, J. Glycans with N-acetyllactosamine type 2-like residues covering adult *Schistosoma mansoni*, and glycomimesis as a putative mechanism of immune evasion. *Parasitology* **111** (Pt 3), 325–336 (1995).

18. Robijn, M. L. M. *et al.* Mapping fucosylated epitopes on glycoproteins and glycolipids of *Schistosoma mansoni* cercariae, adult worms and eggs. *Parasitology* **130**, 67–77 (2005).

19. Tran, M. H. *et al.* Tetraspanins on the surface of *Schistosoma mansoni* are protective antigens against schistosomiasis. *Nat Med* **12**, 835–840 (2006).

20. Smit, C. H. *et al.* Surface expression patterns of defined glycan antigens change during *Schistosoma mansoni* cercarial transformation and development of schistosomula. *Glycobiology* **25**, 1465–1479 (2015).

21. Hambrook, J. R. & Hanington, P. C. Immune Evasion Strategies of Schistosomes. *Front Immunol* **11**, 624178 (2020).

22. Wilson, R. A. & Jones, M. K. Fifty years of the schistosome tegument: discoveries, controversies, and outstanding questions. *International Journal for Parasitology* **51**, 1213–1232 (2021).

23. Welsh, J. A. *et al.* MIFlowCyt-EV: a framework for standardized reporting of extracellular vesicle flow cytometry experiments. *Journal of Extracellular Vesicles* **9**, 1713526 (2020).

24. Hyenne, V. *et al.* Studying the Fate of Tumor Extracellular Vesicles at High Spatiotemporal Resolution Using the Zebrafish Embryo. *Developmental Cell* **48**, 554–572.e7 (2019).

25. Khilji, S. K. *et al.* Generation of glycan-specific nanobodies. *Cell Chem Biol* **29**, 1353–1361.e6 (2022).

26. Virant, D. *et al.* A peptide tag-specific nanobody enables high-quality labeling for dSTORM imaging. *Nat Commun* **9**, 930 (2018).

27. Mizenko, R. R. *et al.* Tetraspanins are unevenly distributed across single extracellular vesicles and bias sensitivity to multiplexed cancer biomarkers. *Journal of Nanobiotechnology* **19**, 250 (2021).

28. Kijanka, M. *et al.* A novel immuno-gold labeling protocol for nanobody-based detection of HER2 in breast cancer cells using immuno-electron microscopy. *Journal of Structural Biology* **199**, 1–11 (2017).

29. Bexkens, M. L. *et al.* *Schistosoma mansoni* does not and cannot oxidise fatty acids, but these are used for biosynthetic purposes instead. *International Journal for Parasitology* **49**, 647–656 (2019).

30. Giera, M. *et al.* The *Schistosoma mansoni* lipidome: Leads for immunomodulation. *Analytica Chimica Acta* **1037**, 107–118 (2018).

31. Boysen, A. T. *et al.* Fluorescent Labeling of Helminth Extracellular Vesicles Using an In Vivo Whole Organism Approach. *Biomedicines* **8**, 213 (2020).

32. Furlong, S. T., Thibault, K. S., Morbelli, L. M., Quinn, J. J. & Rogers, R. A. Uptake and compartmentalization of fluorescent lipid analogs in larval *Schistosoma mansoni*. *J Lipid Res* **36**, 1–12 (1995).

33. Fishelson, Z. *et al.* *Schistosoma mansoni*: Cell-specific expression and secretion of a serine protease during development of cercariae. *Experimental Parasitology* **75**, 87–98 (1992).

34. Bhardwaj, R. & Skelly, P. J. Characterization of Schistosome Tegumental Alkaline Phosphatase (SmAP). *PLOS Neglected Tropical Diseases* **5**, e1011 (2011).

35. Kifle, D. W. *et al.* Proteomic analysis of two populations of *Schistosoma mansoni*-derived extracellular vesicles: 15k pellet and 120k pellet vesicles. *Mol Biochem Parasitol* **236**, 111264 (2020).

36. Skelly, P. J. & Da'dara, A. A. Schistosome secretomes. *Acta Trop* **236**, 106676 (2022).

37. White, R. *et al.* Special considerations for studies of extracellular vesicles from parasitic helminths: A community-led roadmap to increase rigour and reproducibility. *J Extracell Vesicles* **12**, e12298 (2023).

38. Gui, M. J., Dashper, S. G., Slakeski, N., Chen, Y. Y. & Reynolds, E. C. Spheres of influence: *Porphyromonas gingivalis* outer membrane vesicles. *Molecular Oral Microbiology* **31**, 365–378 (2016).

39. Cecil, J. D. *et al.* Outer Membrane Vesicle–Host Cell Interactions. *Microbiology Spectrum* **7**, 7.1.06 (2019).

40. Rizzo, J. *et al.* Revisiting *Cryptococcus* extracellular vesicles properties and their use as vaccine platforms. *bioRxiv* **2020.08.17.253716** (2021) doi:10.1101/2020.08.17.253716.

41. Zeev-Ben-Mordehai, T., Vasishtan, D., Siebert, C. A., Whittle, C. & Grünewald, K. Extracellular Vesicles: A Platform for the Structure Determination of Membrane Proteins by Cryo-EM. *Structure* **22**, 1687–1692 (2014).

42. Kesimer, M. *et al.* Characterization of exosome-like vesicles released from human tracheobronchial ciliated epithelium: a possible role in innate defense. *FASEB J* **23**, 1858–1868 (2009).

43. Kesimer, M. & Gupta, R. Physical characterization and profiling of airway epithelial derived exosomes using light scattering. *Methods* **87**, 59–63 (2015).

44. Fujita, Y., Kosaka, N., Araya, J., Kuwano, K. & Ochiya, T. Extracellular vesicles in lung microenvironment and pathogenesis. *Trends Mol Med* **21**, 533–542 (2015).

45. Marikovsky, M., Levi-Schaffer, F., Arnon, R. & Fishelson, Z. *Schistosoma mansoni*: killing of transformed schistosomula by the alternative pathway of human complement. *Exp Parasitol* **61**, 86–94 (1986).

46. Hockley, D. J. & McLaren, D. J. *Schistosoma mansoni*: changes in the outer membrane of the tegument during development from cercaria to adult worm. *Int J Parasitol* **3**, 13–25 (1973).

47. Da'dara, A. A. & Krautz-Peterson, G. New insights into the reaction of *Schistosoma mansoni* cercaria to the human complement system. *Parasitol Res* **113**, 3685–3696 (2014).

48. Hallal, S., Túzesi, Á., Grau, G. E., Buckland, M. E. & Alexander, K. L. Understanding the extracellular vesicle surface for clinical molecular biology. *Journal of Extracellular Vesicles* **11**, e12260 (2022).

49. Shen, J. *et al.* Nitric oxide blocks the development of the human parasite *Schistosoma japonicum*. *Proc Natl Acad Sci U S A* **114**, 10214–10219 (2017).

50. El Ridi, R., Tallima, H., Mahana, N. & Dalton, J. P. Innate immunogenicity and in vitro protective potential of *Schistosoma mansoni* lung schistosomula excretory–secretory candidate vaccine antigens. *Microbes and Infection* **12**, 700–709 (2010).

51. Khoder-Agha, F. & Kietzmann, T. The glyco-redox interplay: Principles and consequences on the role of reactive oxygen species during protein glycosylation. *Redox Biology* **42**, 101888 (2021).

52. Moseley, R. & Waddington, R. J. Modification of gingival proteoglycans by reactive oxygen species: potential mechanism of proteoglycan degradation during periodontal diseases. *Free Radic Res* **55**, 970–981.

53. Ochs, M. *et al.* On Top of the Alveolar Epithelium: Surfactant and the Glycocalyx. *International Journal of Molecular Sciences* **21**, 3075 (2020).

54. van de Wetering, J. K. *et al.* Surfactant Protein D Binding to Terminal  $\alpha$ 1-3-Linked Fucose Residues and to *Schistosoma mansoni*. *Am J Respir Cell Mol Biol* **31**, 565–572 (2004).

55. Coulson, P. S. The radiation-attenuated vaccine against schistosomes in animal models: paradigm for a human vaccine? *Adv Parasitol* **39**, 271–336 (1997).

56. Mountford, A. P. & Trottein, F. Schistosomes in the skin: a balance between immune priming and regulation. *Trends Parasitol* **20**, 221–226 (2004).

57. Martins, Á. M., Ramos, C. C., Freitas, D. & Reis, C. A. Glycosylation of Cancer Extracellular Vesicles: Capture Strategies, Functional Roles and Potential Clinical Applications. *Cells* **10**, (2021).

58. Collins, J. J., King, R. S., Cogswell, A., Williams, D. L. & Newmark, P. A. An atlas for *Schistosoma mansoni* organs and life-cycle stages using cell type-specific markers and confocal microscopy. *PLoS Negl Trop Dis* **5**, e1009 (2011).

59. Midekassa, G. *et al.* Zeta Potential of Extracellular Vesicles: Toward Understanding the Attributes that Determine Colloidal Stability. *ACS Omega* **5**, 16701–16710 (2020).

60. Paganini, C. *et al.* High-Yield Separation of Extracellular Vesicles Using Programmable Zwitterionic Coacervates. *Small* **19**, 2204736 (2023).

61. Van Deun, J. *et al.* Integrated Dual-Mode Chromatography to Enrich Extracellular Vesicles from Plasma. *Adv Biosyst* **4**, e1900310 (2020).

62. Kaddour, H., Tranquille, M. & Okeoma, C. M. The Past, the Present, and the Future of the Size Exclusion Chromatography in Extracellular Vesicles Separation. *Viruses* **13**, 2272 (2021).

63. Liangsupree, T., Multia, E. & Riekkola, M.-L. Modern isolation and separation techniques for extracellular vesicles. *Journal of Chromatography A* **1636**, 461773 (2021).

64. Mehta, P. & Shende, P. Evasion of opsonization of macromolecules using novel surface-modification and biological-camouflage-mediated techniques for next-generation drug delivery. *Cell Biochem Funct* (2023) doi:10.1002/cbf.3880.

65. Théry, C. *et al.* Minimal information for studies of extracellular vesicles 2018 (MISEV2018): a position statement of the International Society for Extracellular Vesicles and update of the MISEV2014 guidelines. <https://doi.org/10.1080/20013078.2018.1535750> **7**, (2018).

66. Singh, P. *et al.* Removal and identification of external protein corona members from RBC-derived extracellular vesicles by surface manipulating antimicrobial peptides. *Journal of Extracellular Biology* **2**, e78 (2023).

67. Buzas, E. I. Opportunities and challenges in studying the extracellular vesicle corona. *Nat Cell Biol* **24**, 1322–1325 (2022).

68. Tóth, E. Á. *et al.* Formation of a protein corona on the surface of extracellular vesicles in blood plasma. *J Extracell Vesicles* **10**, e12140 (2021).

69. Wolf, M. *et al.* A functional corona around extracellular vesicles enhances angiogenesis, skin regeneration and immunomodulation. *J Extracell Vesicles* **11**, e12207 (2022).

70. Dagenais, M. *et al.* Analysis of *schistosoma mansoni* extracellular vesicles surface glycans reveals potential immune evasion mechanism and new insights on their origins of biogenesis. *Pathogens* **10**, (2021).

71. Lehrich, B. M., Liang, Y., Khosravi, P., Federoff, H. J. & Fiandaca, M. S. Fetal Bovine Serum-Derived Extracellular Vesicles Persist within Vesicle-Depleted Culture Media. *International Journal of Molecular Sciences* **19**, 3538 (2018).

72. Dagenais, M., Gerlach, J. Q., Geary, T. G. & Long, T. Sugar Coating: Utilisation of Host Serum Sialoglycoproteins by *Schistosoma mansoni* as a Potential Immune Evasion Mechanism. *Pathogens* **11**, 426 (2022).

73. Samoil, V. *et al.* Vesicle-based secretion in schistosomes: Analysis of protein and microRNA (miRNA) content of exosome-like vesicles derived from *Schistosoma mansoni*. *Sci Rep* **8**, 3286 (2018).

74. Loukas, A., Jones, M. K., King, L. T., Brindley, P. J. & McManus, D. P. Receptor for Fc on the Surfaces of Schistosomes. *Infect Immun* **69**, 3646–3651 (2001).

75. Tarleton, R. L. & Kemp, W. M. Demonstration of IgG-Fc and C3 receptors on adult *Schistosoma mansoni*. *J Immunol* **126**, 379–384 (1981).

76. Crocker, P. R., Paulson, J. C. & Varki, A. Siglecs and their roles in the immune system. *Nat Rev Immunol* **7**, 255–266 (2007).

77. Skelly, P. J., Da'dara, A. A., Li, X. H., Castro-Borges, W. & Wilson, R. A. Schistosome Feeding and Regurgitation. *PLoS Pathogens* **10**, e1004246 (2014).

78. Kifle, D. W. *et al.* Uptake of *Schistosoma mansoni* extracellular vesicles by human endothelial and monocytic cell lines and impact on vascular endothelial cell gene expression. *Int J Parasitol* **50**, 685–696 (2020).

79. Coakley, G. *et al.* Extracellular Vesicles from a Helminth Parasite Suppress Macrophage Activation and Constitute an Effective Vaccine for Protective Immunity. *Cell Rep* **19**, 1545–1557 (2017).

80. Meningher, T. *et al.* Schistosomal MicroRNAs Isolated From Extracellular Vesicles in Sera of Infected Patients: A New Tool for Diagnosis and Follow-up of Human Schistosomiasis. *J Infect Dis* **215**, 378–386 (2017).

81. Bexkens, M. L. *et al.* *Schistosoma mansoni* infection affects the proteome and lipidome of circulating extracellular vesicles in the host. *Molecular and Biochemical Parasitology* **238**, (2020).

82. Zhou, X. *et al.* Extracellular vesicles derived from *Echinococcus granulosus* hydatid cyst fluid from patients: isolation, characterization and evaluation of immunomodulatory functions on T cells. *International Journal for Parasitology* **49**, 1029–1037 (2019).

83. Lalawmpuui, K. & Lalrinkima, H. Genetic manipulations in helminth parasites. *J Parasit Dis* **47**, 203–214 (2023).

84. Skelly, P. J., Da'dara, A. & Harn, D. A. Suppression of cathepsin B expression in *Schistosoma mansoni* by RNA interference. *International Journal for Parasitology* **33**, 363–369 (2003).

85. Correnti, J. M., Brindley, P. J. & Pearce, E. J. Long-term suppression of cathepsin B levels by RNA interference retards schistosome growth. *Molecular and Biochemical Parasitology* **143**, 209–215 (2005).

86. Rinaldi, G. *et al.* Development of Functional Genomic Tools in Trematodes: RNA Interference and Luciferase Reporter Gene Activity in *Fasciola hepatica*. *PLOS Neglected Tropical Diseases* **2**, e260 (2008).

87. Ittiprasert, W. *et al.* Programmed genome editing of the omega-1 ribonuclease of the blood fluke, *Schistosoma mansoni*. *Elife* **8**, e41337 (2019).

88. Ittiprasert, W. *et al.* Targeted insertion and reporter transgene activity at a gene safe harbor of the human blood fluke, *Schistosoma mansoni*. *Cell Reports Methods* **3**, 100535 (2023).

89. van Niel, G. *et al.* Challenges and directions in studying cell-cell communication by extracellular vesicles. *Nat Rev Mol Cell Biol* **23**, 369–382 (2022).

90. Meningher, T. *et al.* Schistosomal extracellular vesicle-enclosed miRNAs modulate host T helper cell differentiation. *EMBO Rep* **21**, e47882 (2020).

91. Liu, J. *et al.* *Schistosoma japonicum* extracellular vesicle miRNA cargo regulates host macrophage functions facilitating parasitism. *PLoS Pathog* **15**, e1007817 (2019).

92. Geijtenbeek, T. B. H. & Gringhuis, S. I. Signalling through C-type lectin receptors: shaping immune responses. *Nat Rev Immunol* **9**, 465–479 (2009).

93. Bourke, C. D. *et al.* Epidermal keratinocytes initiate wound healing and pro-inflammatory immune responses following percutaneous schistosome infection. *Int J Parasitol* **45**, 215–224 (2015).

94. Trottein, F. *et al.* *Schistosoma mansoni* schistosomula reduce E-selectin and VCAM-1 expression in TNF-alpha-stimulated lung microvascular endothelial cells by interfering with the NF- $\kappa$ B pathway. *Eur J Immunol* **29**, 3691–3701 (1999).

95. Sombetzki, M. *et al.* A one-year unisexual *Schistosoma mansoni* infection causes pathologic organ alterations and persistent non-polarized T cell-mediated inflammation in mice. *Frontiers in Immunology* **13**, (2022).

96. Eichenberger, R. M. *et al.* Hookworm Secreted Extracellular Vesicles Interact With Host Cells and Prevent Inducible Colitis in Mice. *Front Immunol* **9**, 850 (2018).

97. Eichenberger, R. M. *et al.* Characterization of *Trichuris muris* secreted proteins and extracellular vesicles provides new insights into host-parasite communication. *J Extracell Vesicles* **7**, 1428004 (2018).

98. Chaiyadet, S. *et al.* Carcinogenic Liver Fluke Secretes Extracellular Vesicles That Promote Cholangiocytes to Adopt a Tumorigenic Phenotype. *J Infect Dis* **212**, 1636–1645 (2015).

99. Zhu, L. *et al.* Molecular characterization of *S. japonicum* exosome-like vesicles reveals their regulatory roles in parasite-host interactions. *Sci Rep* **6**, 25885 (2016).

100. Zhu, S. *et al.* Release of extracellular vesicles containing small RNAs from the eggs of *Schistosoma japonicum*. *Parasit Vectors* **9**, 574 (2016).

101. Wang, L. *et al.* Sja-miR-71a in Schistosome egg-derived extracellular vesicles suppresses liver fibrosis caused by schistosomiasis via targeting semaphorin 4D. *Journal of Extracellular Vesicles* **9**, 1785738 (2020).

102. van Kooyk, Y., Ilarregui, J. M. & van Vliet, S. J. Novel insights into the immunomodulatory role of the dendritic cell and macrophage-expressed C-type lectin MGL. *Immunobiology* **220**, 185–192 (2015).

103. van Vliet, S. J., Saeland, E. & van Kooyk, Y. Sweet preferences of MGL: carbohydrate specificity and function. *Trends in Immunology* **29**, 83–90 (2008).

104. Rensen, P. C. *et al.* Determination of the upper size limit for uptake and processing of ligands by the asialoglycoprotein receptor on hepatocytes in vitro and in vivo. *J Biol Chem* **276**, 37577–37584 (2001).

105.Yang, C. *et al.* Desialylated Mesenchymal Stem Cells-Derived Extracellular Vesicles Loaded with Doxorubicin for Targeted Inhibition of Hepatocellular Carcinoma. *Cells* **11**, 2642 (2022).

106.Igdoura, S. A. Asialoglycoprotein receptors as important mediators of plasma lipids and atherosclerosis. *Curr Opin Lipidol* **28**, 209–212 (2017).

107.Fonseca, C. S. M. da *et al.* Human Plasma Lipid Modulation in Schistosomiasis Mansoni Depends on Apolipoprotein E Polymorphism. *PLoS One* **9**, e101964 (2014).

108.Bisetegn, H. *et al.* A Comparative Cross-Sectional Study of Coagulation Profiles and Platelet Parameters of *Schistosoma mansoni*-Infected Adults at Haik Primary Hospital, Northeast Ethiopia. *Interdisciplinary Perspectives on Infectious Diseases* **2022**, e5954536 (2022).

109.Da'dara, A. A. & Skelly, P. J. Schistosomes versus platelets. *Thrombosis Research* **134**, 1176–1181 (2014).

110.Lozano-Andrés, E. *et al.* Physical association of low density lipoprotein particles and extracellular vesicles unveiled by single particle analysis. 2022.08.31.506022 Preprint at <https://doi.org/10.1101/2022.08.31.506022> (2022).

111.Sørensen, A. L. *et al.* Role of sialic acid for platelet life span: exposure of  $\beta$ -galactose results in the rapid clearance of platelets from the circulation by asialoglycoprotein receptor-expressing liver macrophages and hepatocytes. *Blood* **114**, 1645–1654 (2009).

112.Olgasi, C., Cucci, A. & Follenzi, A. iPSC-Derived Liver Organoids: A Journey from Drug Screening, to Disease Modeling, Arriving to Regenerative Medicine. *International Journal of Molecular Sciences* **21**, 6215 (2020).

113.van den Berg, T. K. *et al.* LacdiNAc-Glycans Constitute a Parasite Pattern for Galectin-3-Mediated Immune Recognition1. *The Journal of Immunology* **173**, 1902–1907 (2004).

114.Mai, J., Virtue, A., Shen, J., Wang, H. & Yang, X.-F. An evolving new paradigm: endothelial cells – conditional innate immune cells. *Journal of Hematology & Oncology* **6**, 61 (2013).

115.Chiffolleau, E. C-Type Lectin-Like Receptors As Emerging Orchestrators of Sterile Inflammation Represent Potential Therapeutic Targets. *Frontiers in Immunology* **9**, (2018).

116.Thebault, P. *et al.* The C-Type Lectin-Like Receptor CLEC-1, Expressed by Myeloid Cells and Endothelial Cells, Is Up-Regulated by Immunoregulatory Mediators and Moderates T Cell Activation1. *The Journal of Immunology* **183**, 3099–3108 (2009).

117.Mbow, M. *et al.* T-Helper 17 Cells Are Associated With Pathology in Human Schistosomiasis. *J Infect Dis* **207**, 186–195 (2013).

118.Lopez Robles, M. D. *et al.* Cell-surface C-type lectin-like receptor CLEC-1 dampens dendritic cell activation and downstream Th17 responses. *Blood Advances* **1**, 557–568 (2017).

119.Chen, M., Masaki, T. & Sawamura, T. LOX-1, the receptor for oxidized low-density lipoprotein identified from endothelial cells: implications in endothelial dysfunction and atherosclerosis. *Pharmacology & Therapeutics* **95**, 89–100 (2002).

120.Verweij, F. J. *et al.* Live Tracking of Inter-organ Communication by Endogenous Exosomes In Vivo. *Developmental Cell* **48**, 573–589.e4 (2019).

121.Okumura-Noji, K. *et al.* CD36-related protein in *Schistosoma japonicum*: candidate mediator of selective cholestryl ester uptake from high-density lipoprotein for egg maturation. *FASEB J* **27**, 1236–1244 (2013).

122.Dingirard, N. & Yoshino, T. P. Potential role of a CD36-like class B scavenger receptor in the binding of modified low-density lipoprotein (acLDL) to the tegumental surface of *Schistosoma mansoni* sporocysts. *Molecular and Biochemical Parasitology* **146**, 219–230 (2006).

123.Tempone, A. J., Bianconi, M. L. & Rumjanek, F. D. The interaction of human LDL with the tegument of adult *Schistosoma mansoni*. *Mol Cell Biochem* **177**, 139–144 (1997).

124.Dagenais, M. & Tritten, L. Hidden in plain sight: How helminths manage to thrive in host blood. *Frontiers in Parasitology* **2**, (2023).

125.Wilson, R. A. Models of Protective Immunity against Schistosomes: Implications for Vaccine Development. *Pathogens* **12**, 1215 (2023).

126.Wang, L. *et al.* Exosome-like vesicles derived by *Schistosoma japonicum* adult worms mediates M1 type immune-activity of macrophage. *Parasitol Res* **114**, 1865–1873 (2015).

127.Drurey, C. & Maizels, R. M. Helminth extracellular vesicles: Interactions with the host immune system. *Mol Immunol* **137**, 124–133 (2021).

128.Haeberlein, S. *et al.* Schistosome egg antigens, including the glycoprotein IPSE/alpha-1, trigger the development of regulatory B cells. *PLoS Pathog* **13**, e1006539 (2017).

129.Mangan, N. E. *et al.* Helminth infection protects mice from anaphylaxis via IL-10-producing B cells. *J Immunol* **173**, 6346–6356 (2004).

130.He, Y.-X., Chen, L. & Ramaswamy, K. *Schistosoma mansoni*, *S. haematobium*, and *S. japonicum*: early events associated with penetration and migration of schistosomula through human skin. *Exp Parasitol* **102**, 99–108 (2002).

131.Winkel, B. M. F. *et al.* Early Induction of Human Regulatory Dermal Antigen Presenting Cells by Skin-Penetrating *Schistosoma Mansoni* Cercariae. *Front Immunol* **9**, 2510 (2018).

132.Sanin, D. E. & Mountford, A. P. Sm16, a major component of *Schistosoma mansoni* cercarial excretory/secretory products, prevents macrophage classical activation and delays antigen processing. *Parasit Vectors* **8**, 1 (2015).

133.Ramaswamy, K., Kumar, P. & He, Y. X. A role for parasite-induced PGE2 in IL-10-mediated host immunoregulation by skin stage schistosomula of *Schistosoma mansoni*. *J Immunol* **165**, 4567–4574 (2000).

134.L S Alves, C. *et al.* Immunomodulatory properties of *Schistosoma mansoni* proteins Sm200 and SmKI-1 in vitro and in a murine model of allergy to the mite *Blomia tropicalis*. *Mol Immunol* **124**, 91–99 (2020).

135.Alves, C. C. *et al.* Sm29, but Not Sm22.6 Retains its Ability to Induce a Protective Immune Response in Mice Previously Exposed to a *Schistosoma mansoni* Infection. *PLoS Negl Trop Dis* **9**, e0003537 (2015).

136.Garcia-Vallejo, J. J. & van Kooyk, Y. The physiological role of DC-SIGN: a tale of mice and men. *Trends Immunol* **34**, 482–486 (2013).

137. Gazi, U. & Martinez-Pomares, L. Influence of the mannose receptor in host immune responses. *Immunobiology* **214**, 554–561 (2009).

138. Horrevorts, S. K. *et al.* Glycan-Modified Melanoma-Derived Apoptotic Extracellular Vesicles as Antigen Source for Anti-Tumor Vaccination. *Cancers (Basel)* **11**, (2019).

139. Mason, H. G., Bush, J., Agrawal, N., Hakami, R. M. & Veneziano, R. A Microfluidic Platform to Monitor Real-Time Effects of Extracellular Vesicle Exchange between Co-Cultured Cells across Selectively Permeable Barriers. *International Journal of Molecular Sciences* **23**, 3534 (2022).

140. Kenney, E. T. *et al.* Differential Excretory/Secretory Proteome of the Adult Female and Male Stages of the Human Blood Fluke, *Schistosoma mansoni*. *Frontiers in Parasitology* **1**, (2022).

141. Lopes, D. M. *et al.* *Schistosoma mansoni* rSm29 Antigen Induces a Regulatory Phenotype on Dendritic Cells and Lymphocytes From Patients With Cutaneous Leishmaniasis. *Front Immunol* **9**, 3122 (2019).

142. Liu, X., Xiao, C. & Xiao, K. Engineered extracellular vesicles-like biomimetic nanoparticles as an emerging platform for targeted cancer therapy. *Journal of Nanobiotechnology* **21**, 287 (2023).

143. Mir, B. & Goetsch, C. Extracellular Vesicles as Delivery Vehicles of Specific Cellular Cargo. *Cells* **9**, 1601 (2020).

144. Nizamudeen, Z. A. *et al.* Low-Power Sonication Can Alter Extracellular Vesicle Size and Properties. *Cells* **10**, 2413 (2021).

145. Wilbers, R. H. P. *et al.* Production and glyco-engineering of immunomodulatory helminth glycoproteins in plants. *Scientific Reports* **7**, (2017).

146. Kocholata, M., Prusova, M., Auer Malinska, H., Maly, J. & Janouskova, O. Comparison of two isolation methods of tobacco-derived extracellular vesicles, their characterization and uptake by plant and rat cells. *Sci Rep* **12**, 19896 (2022).

147. Egesa, M., Hoffmann, K. F., Hokke, C. H., Yazdanbakhsh, M. & Cose, S. Rethinking Schistosomiasis Vaccine Development: Synthetic Vesicles. *Trends in Parasitology* **33**, 918–921 (2017).

148. Siddiqui, A. J. *et al.* A Critical Review on Human Malaria and Schistosomiasis Vaccines: Current State, Recent Advancements, and Developments. *Vaccines* **11**, 792 (2023).

149. Jia, X. *et al.* Solution structure, membrane interactions, and protein binding partners of the tetraspanin Sm-TSP-2, a vaccine antigen from the human blood fluke *Schistosoma mansoni*. *J Biol Chem* **289**, 7151–7163 (2014).

150. Santos, P. & Almeida, F. Exosome-Based Vaccines: History, Current State, and Clinical Trials. *Frontiers in Immunology* **12**, (2021).

151. Shears, R. K., Bancroft, A. J., Hughes, G. W., Grencis, R. K. & Thornton, D. J. Extracellular vesicles induce protective immunity against *Trichuris muris*. *Parasite Immunology* **40**, e12536 (2018).

152. Treliis, M. *et al.* Subcutaneous injection of exosomes reduces symptom severity and mortality induced by *Echinostoma caproni* infection in BALB/c mice. *International Journal for Parasitology* **46**, 799–808 (2016).

153. Chaiyadet, S. *et al.* Vaccination of hamsters with *Opisthorchis viverrini* extracellular vesicles and vesicle-derived recombinant tetraspanins induces antibodies that block vesicle uptake by cholangiocytes and reduce parasite burden after challenge infection. *PLOS Neglected Tropical Diseases* **13**, e0007450 (2019).

154. Mossallam, S. F., Abou-El-naga, I. F., Bary, A. A., Elmorsy, E. A. & Diab, R. G. *Schistosoma mansoni* egg-derived extracellular vesicles: A promising vaccine candidate against murine schistosomiasis. *PLoS neglected tropical diseases* **15**, (2021).

155. Kifle, D. W. *Schistosoma mansoni* extracellular vesicles: immunobiology and vaccine efficacy. *College of Public Health, Medical and Veterinary Sciences Centre for Molecular Therapeutics Australian Institute of Tropical Health and Medicine* (James Cook University, 2020). doi:10.25903/fhzh-2h14.

156. Crosnier, C. *et al.* Systematic screening of 96 *Schistosoma mansoni* cell-surface and secreted antigens does not identify any strongly protective vaccine candidates in a mouse model of infection [version 1; peer review: 3 approved]. *Wellcome Open Research* **4**, (2019).

157. Yang, Y. Y. *et al.* Specific anti-glycan antibodies are sustained during and after parasite clearance in *Schistosoma japonicum*-infected rhesus macaques. *PLoS Negl Trop Dis* **11**, e0005339 (2017).

158. Soisson, L. A., Reid, G. D., Farah, I. O., Nyindo, M. & Strand, M. Protective immunity in baboons vaccinated with a recombinant antigen or radiation-attenuated cercariae of *Schistosoma mansoni* is antibody-dependent. *J Immunol* **151**, 4782–4789 (1993).

159. Yang, Y. Y. M. *et al.* Micro Array-Assisted Analysis of Anti-Schistosome Glycan Antibodies Elicited by Protective Vaccination With Irradiated Cercariae. *The Journal of Infectious Diseases* **219**, 1671–1680 (2019).

160. Poon, C. & Patel, A. A. Organic and inorganic nanoparticle vaccines for prevention of infectious diseases. *Nano Ex.* **1**, 012001 (2020).

161. Seré, S. *et al.* Proof of Concept Study: Mesoporous Silica Nanoparticles, From Synthesis to Active Specific Immunotherapy. *Frontiers in Nanotechnology* **2**, (2020).

162. Oliveira, D. C. de P. *et al.* Mesoporous silica nanoparticles as a potential vaccine adjuvant against *Schistosoma mansoni*. *Journal of Drug Delivery Science and Technology* **35**, 234–240 (2016).

163. Lin, Q. *et al.* Recent progress in cancer cell membrane-based nanoparticles for biomedical applications. *Beilstein J. Nanotechnol.* **14**, 262–279 (2023).

164. Naskar, A., Cho, H., Lee, S. & Kim, K. Biomimetic Nanoparticles Coated with Bacterial Outer Membrane Vesicles as a New-Generation Platform for Biomedical Applications. *Pharmaceutics* **13**, 1887 (2021).

165. You, H. *et al.* The mRNA Vaccine Technology Era and the Future Control of Parasitic Infections. *Clin Microbiol Rev* **36**, e0024121 (2023).

166. Riazanski, V. *et al.* Real time imaging of single extracellular vesicle pH regulation in a microfluidic cross-flow filtration platform. *Commun Biol* **5**, 1–13 (2022).

167. Dechantsreiter, S. *et al.* Heterogeneity in extracellular vesicle secretion by single human macrophages revealed by super-resolution microscopy. *J Extracell Vesicles* **11**, e12215 (2022).

168.Hilton, S. H. & White, I. M. Advances in the analysis of single extracellular vesicles: A critical review. *Sensors and Actuators Reports* **3**, 100052 (2021).

169.Shaba, E. *et al.* Multi-Omics Integrative Approach of Extracellular Vesicles: A Future Challenging Milestone. *Proteomes* **10**, 12 (2022).

170.Langenberg, M. C. C. *et al.* A controlled human *Schistosoma mansoni* infection model to advance novel drugs, vaccines and diagnostics. *Nat Med* **26**, 326–332 (2020).

171.Koopman, J. P. R. *et al.* Safety and infectivity of female cercariae in *Schistosoma*-naïve, healthy participants: a controlled human *Schistosoma mansoni* infection study. *eBioMedicine* **97**, (2023).

172.Waury, K. *et al.* Proteome encoded determinants of protein sorting into extracellular vesicles. 2023.02.01.526570 Preprint at <https://doi.org/10.1101/2023.02.01.526570> (2023).

173.Greenberg, Z. F., Graim, K. S. & He, M. Towards artificial intelligence-enabled extracellular vesicle precision drug delivery. *Advanced Drug Delivery Reviews* **199**, 114974 (2023).

174.Paproski, R. J., Pink, D., Sosnowski, D. L., Vasquez, C. & Lewis, J. D. Building predictive disease models using extracellular vesicle microscale flow cytometry and machine learning. *Mol Oncol* **17**, 407–421 (2023).

175.Narasimhan, P. B. *et al.* Similarities and differences between helminth parasites and cancer cell lines in shaping human monocytes: Insights into parallel mechanisms of immune evasion. *PLoS Negl Trop Dis* **12**, e0006404 (2018).



The purpose of life is to discover your gift. The work of life is to develop it. The meaning of life is to give your gift away.  
- David S. Viscott, Finding your strength at difficult times: a book of meditations, 1993

# Appendices

**Popular science summary (English & Dutch)**

**Nederlandse samenvatting voor niet-ingewijden**

**Curriculum Vitae**

**List of publications**

**Dankwoord / acknowledgements**

## **Popular science summary (English)**

The research in this thesis explores the interaction between the parasitic worm *Schistosoma mansoni* and the immune system. The co-evolution of these worms with the human host has enabled them to develop optimal strategies to influence the immune system. The studies presented focus on extracellular vesicles (EVs) released by the worms and the role of glycans (sugar molecules) in this interaction. Both adult worm and larval EVs contain glycans and have different effects on immune cells, such as B-lymphocytes and dendritic cells, stimulating the release of signaling molecules. The glycans on the EVs appear to be crucial for interacting with specific receptors on immune cells. This research contributes to understanding the communication between parasites and their hosts and could potentially lead to the development of new therapies for immune-related diseases.

## **Populair-wetenschappelijke samenvatting (Nederlands)**

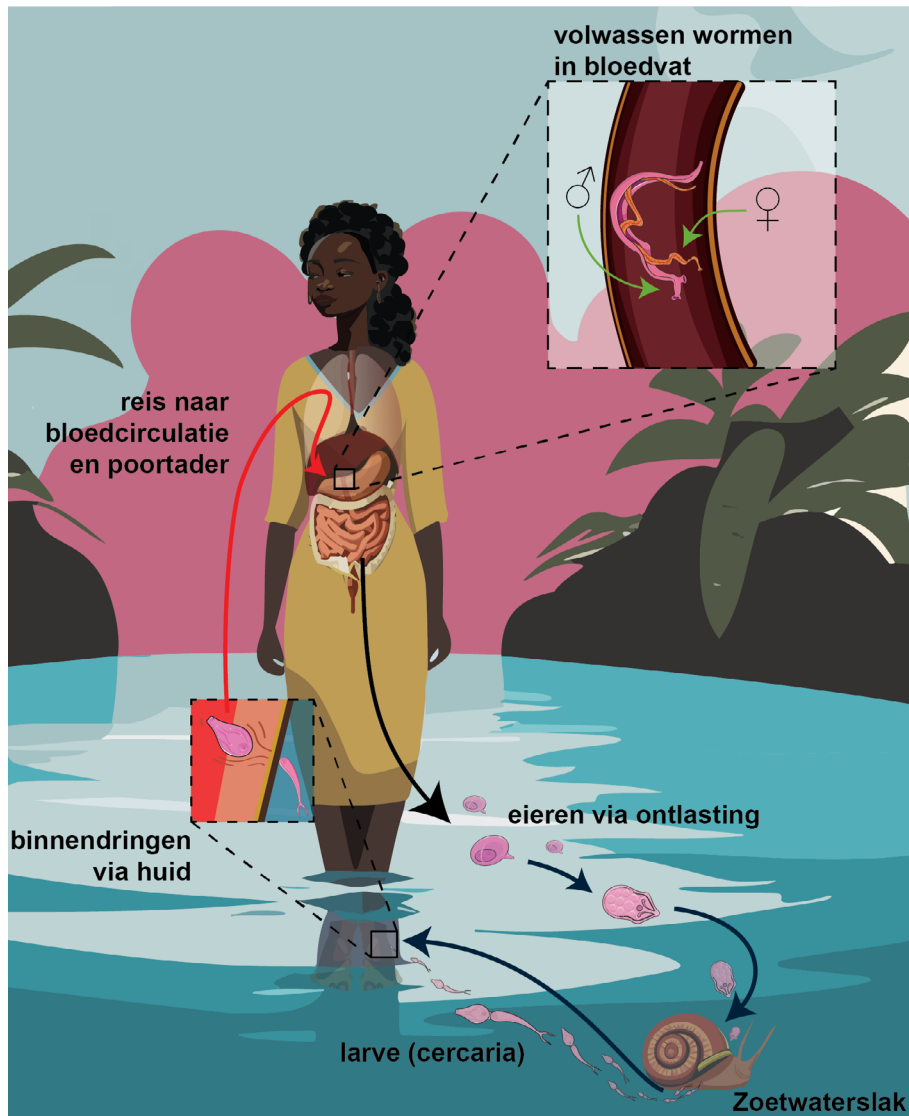
Dit proefschrift behandelt de interactie tussen de parasitaire worm *Schistosoma mansoni* en het immuunsysteem. De evolutie van deze wormen samen met de menselijke gastheer heeft hen in staat gesteld optimale strategieën te ontwikkelen om het immuunsysteem te beïnvloeden. De beschreven studies richten zich op extracellulaire blaasjes (genaamd "extracellular vesicles" (EVs)) die door de wormen worden uitgescheiden en de rol van glycanen (suikermoleculen) in deze interactie. De EVs van zowel volwassen wormen als larven bevatten glycanen en hebben verschillende effecten op immuuncellen, zoals B-lymfocyten en dendritische cellen, waarbij ze afgifte van signaalmoleculen stimuleren. De glycanen op de EVs lijken belangrijk te zijn voor de interactie met specifieke receptoren op immuuncellen. Dit onderzoek draagt bij aan het begrijpen van de communicatie tussen parasieten en hun gastheer en kan mogelijk leiden tot de ontwikkeling van nieuwe therapieën voor immuunziekten.

## Nederlandse samenvatting voor niet-ingewijden

*Samenvatting van dit proefschrift getiteld: 'Extracellulaire Vesikels van Schistosoma mansoni en hun Impact op het Immuunsysteem: Geglycosyleerde Boodschappers in de Communicatie tussen Gastheer en Ziekteverwekker'*

Parasitaire wormen bestaan al langer dan de mensheid. Gedurende de ontwikkeling van de mens, en ook ons afweersysteem, zijn de wormen meegeëvolueerd. Ons afweersysteem is essentieel om ziekmakende binnendringers (zoals parasieten, bacteriën en schimmels) te ontdekken en onschadelijk te maken. Door de co-evolutie van worm en mens hebben parasieten optimale strategieën ontwikkeld om ons afweersysteem te kunnen sturen en/of af te remmen om zo te overleven in ons lichaam. Één van deze parasitaire wormen is *Schistosoma mansoni*. Volgens de Wereldgezondheidsorganisatie zijn er wereldwijd zo'n 250 miljoen mensen geïnfecteerd met *Schistosoma*-wormen. Aangezien de worm afhankelijk is van een slak als tussengastheer (zie Figuur 1), en deze slak alleen leeft in tropisch zoet water, wordt de overlast van infecties met deze parasiet enkel in tropische gebieden van de wereld ervaren. Waar goed sanitair ontbreekt, zullen de eieren via de ontlasting in het water terechtkomen waar het diertje uit het ei de slak in het water kan infecteren. De larven (genaamd cercariae) die zich in de geïnfecteerde slak ontwikkelen, komen in hetzelfde water terecht en kunnen daarna weer een mens infecteren door zich door de huid te wurmen. Eenmaal in de huid heet de larve dan een schistosomulum en deze gaat in de menselijke gastheer op zoek naar een bloedvat. De volwassen wormen (mannetjes en vrouwtjes), waar deze schistosomula zich tot ontwikkelen, leven voornamelijk in de poortader bij de lever en in de bloedvaten rondom de darmen en voeden zich met rode bloedcellen. Het vrouwtje van de wormparen produceert eieren die in de darmen moeten worden uitgescheiden (en via de ontlasting buiten het lichaam terecht komen) om de levenscyclus rond te maken. Echter, de eieren kunnen ook meegesleept worden in de bloedbaan en komen dan vast te zitten in het eerste vaatbed (met kleine bloedvaten) dat ze tegenkomen. Dit eerste vaatbed dat de eieren tegenkomen is de lever en hier kunnen ze een enorm sterke afweerreactie opwekken. Bij een langdurige, onbehandelde infectie met veel wormen kan dit leiden tot littekenvorming in de lever, leverfalen en uiteindelijk de dood van de gastheer.

Toch is een infectie met deze parasiet niet alleen maar slecht. *Schistosoma*-parasieten zijn in staat om ons afweersysteem zodanig te sturen dat ze tientallen jaren in ons bloed kunnen leven. Door het sturen en dempen van het afweersysteem van de gastheer heeft dit als neveneffect dat ook andere afweerreacties bijgestuurd worden. Dit is met name te zien in het lage aantal mensen dat allergieën en

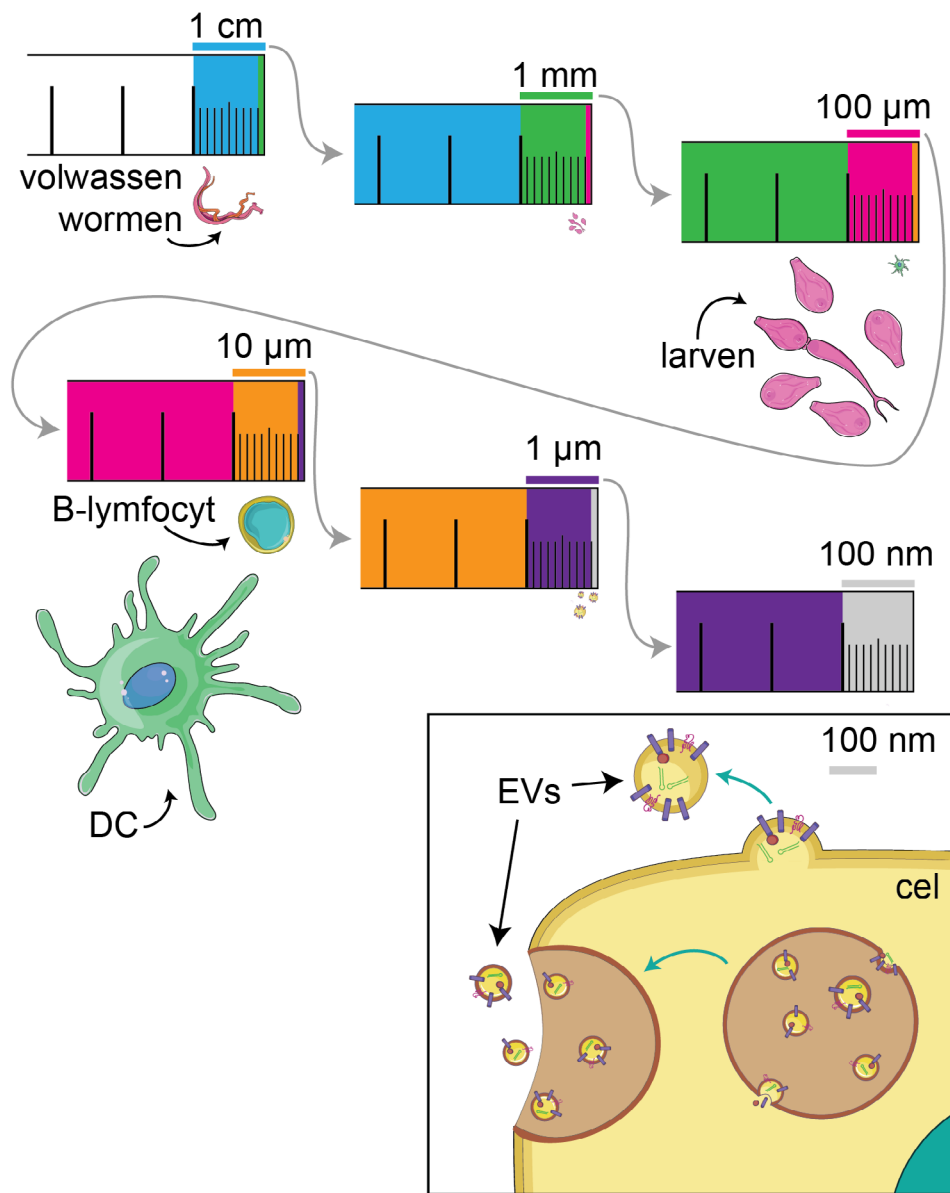


**Figuur 1. Levenscyclus van *Schistosoma mansoni* parasiet.**

De larven (cercariae) dringen de huid van de gastheer binnen en reizen via bloedvaten naar de poortader bij de lever waar ze ontwikkelen tot volwassen wormen. Een mannelijke en vrouwelijke worm vormen een paar waarbij de vrouwtjes de eieren leggen. Dit doen ze met name in de bloedvaten rond de darm omdat de eieren via de ontlassing het lichaam verlaten. Bij contact met water komt een miracidium uit het ei die een tropische zoetwaterslak kan infecteren. In deze slak ontwikkelt één miracidium zich tot vele nieuwe larven. De larven komen uit de slak weer vrij in het water en kunnen mensen infecteren die zich in het water bevinden.

auto-immuunziektes heeft in gebieden waar veel parasitaire wormen voorkomen in vergelijking tot mensen uit een Westerse samenleving. De hypothese is dat een wormeninfestatie vroeg in het leven helpt bij het trainen van ons afweersysteem, wat bijdraagt aan de optimale demping van afweerreacties, iets waar het bij mensen met allergieën of autoimmuniteit aan schort. Een vraag binnen wetenschappelijk onderzoek is: kunnen we begrijpen hoe de wormen ons afweer sturen en/of remmen, en kunnen we dit nabootsen met moleculen? Dan kunnen we de ontwikkeling van immuunziektes zoals allergieën en auto-immuniteit verminderen of voorkomen zonder dat mensen met parasieten geïnfecteerd hoeven te zijn (geweest). Daarnaast kan kennis over de overlevingsstrategieën van de parasiet ook helpen bij het vinden van nieuwe behandelingen tegen de parasiet zelf. Een infectie met *Schistosoma* kan tegenwoordig goed behandeld worden met medicatie, maar mensen kunnen opnieuw geïnfecteerd raken omdat ze zelden afdoende immuniteit ontwikkelen en er nog geen vaccin is. Er wordt al veel onderzoek gedaan naar de losse moleculen die de *Schistosoma* parasieten uitscheiden en wat voor effect ze hebben op onze afweer, maar dit heeft nog niet geleid tot een therapie tegen afweerziektes. Meer recent is ontdekt dat de parasieten ook hele pakketjes met moleculen uitscheiden en hier is nog maar beperkt onderzoek naar gedaan.

Alle cellen in ons lichaam communiceren met elkaar. Dit kan door middel van direct cel-cel contact, bijvoorbeeld hoe een afweercel checkt of een andere cel nog gezond, juist ziek of geïnfecteerd is. Een tweede manier van communicatie tussen cellen is via uitgescheiden losse (signaal)moleculen, zoals bijvoorbeeld hormonen. Een derde manier van communicatie tussen cellen is via extracellulaire (uitgescheiden) blaasjes ("extracellular vesicles" in het Engels, afgekort EVs). Deze EVs zijn hele pakketjes met moleculen die worden omringd door eenzelfde membraan als een cel, en ze kunnen op twee verschillende manieren door een cel worden uitgescheiden. vergeleken met een cel zijn ze nog 100 keer kleiner: tussen de 50 en 200 nanometer (Figuur 2). Hun kleine omvang maakt het uitdagend om er onderzoek naar te doen want er zijn speciale technieken nodig om ze te isoleren en te meten. Het voordeel van communicatie tussen cellen via EVs is dat er in één keer veel informatie van de ene cel naar de andere cel kan worden doorgegeven. Je zou het kunnen vergelijken met het opsturen van een pakketje via de post in plaats van een kaart: met het pakketje kun je veel meer delen met de ontvanger. En net als postpakketjes zijn EVs heel verschillend in omvang en lading, zelfs als ze van dezelfde cel afkomstig zijn. Deze EVs worden door cellen van bijna alle organismen uitgescheiden, van zoogdieren tot planten. En we weten dus sinds een tiental jaren dat parasieten ook dit soort EVs uitscheiden.



**Figuur 2. Een indicatie van afmeting van de organismen, cellen en extracellulaire blaasjes (EVs) onderzocht in dit proefschrift.**

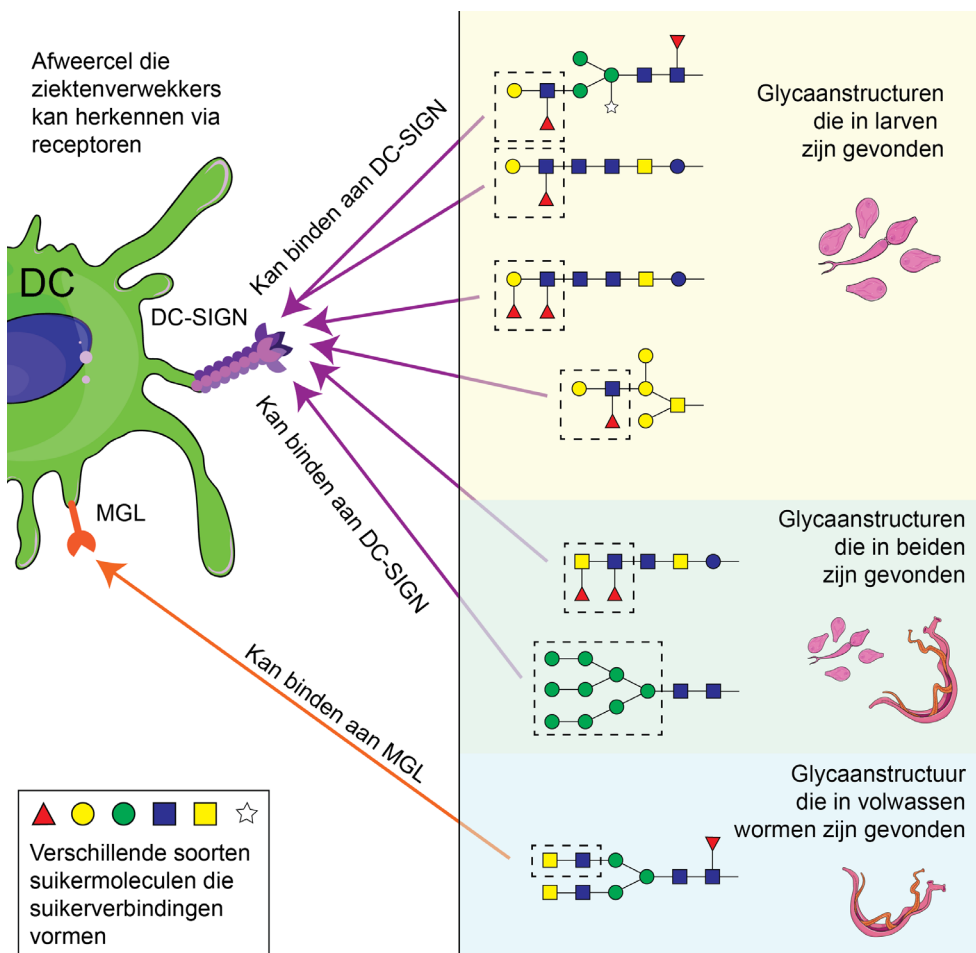
Volwassen *Schistosoma*-wormen zijn tussen de 6 en 17 mm en de larven tussen de 100 en 250 µm. Menselijke afweercellen, zoals een B-lymfocyt en dendritische cel (DC) zijn respectievelijk 8-10 µm en 10-15 µm. EVs worden door cellen uitgescheiden en zijn tussen de 50-200 nm.

Maar er is nog weinig bekend over de communicatie van de parasieten EVs naar onze afweercellen en wat voor effecten ze teweegbrengen op deze cellen.

Voor het verdere begrijpen van het onderzoek in dit proefschrift is ook nog de introductie van glycosylering en glycanen nodig. Glycosylering is het proces waarbij suikerketens worden gebonden aan eiwitten of lipiden (vetzuren). Deze suikerketens (glycanen) spelen een belangrijke rol in veel biologische processen en zijn essentieel voor de structuur en functie van veel moleculen in levende organismen. Ook moleculen van parasieten, bacteriën en schimmels bevatten glycanen. De afweercellen die een grote rol spelen bij het opsporen van indringers hebben vele verschillende receptoren (dat zijn moleculen, vaak op het celoppervlak, die specifieke andere moleculen herkennen via een 'sleutel-slot' principe) die glycanen van eigen cellen of van ziekteverwekkers kunnen herkennen. Het type receptor dat wordt geactiveerd heeft uiteindelijk invloed op de afweerreactie die volgt. Er zijn receptoren die de reactie activeren (om ziekteverwekkers te vernietigen) maar ook receptoren die een afweerreactie afremmen. Voor *Schistosoma*-parasieten weten we dat elk levensstadium (larven, volwassen wormen en eieren) een eigen samenstelling heeft van de glycanen die ze produceren (Figuur 3). We weten ook welke receptoren deze glycanen mogelijk kunnen herkennen en het is ook bekend dat elk levensstadium weer andere afweerreacties in de gastheer teweegbrengt. Maar er is amper kennis over de glycosylering van de EVs van de parasiet en of deze glycanen een rol spelen in de interactie van deze pakketjes met receptoren op de afweercellen.

In dit proefschrift is onderzoek gedaan naar de EVs van de *Schistosoma mansoni* parasiet, welke glycanen deze pakketjes bevatten, en wat voor invloed de EVs van deze parasiet hebben op afweercellen. De introductie (**hoofdstuk 1**) geeft een korte inleiding van de onderwerpen en hoofdstukken in dit proefschrift. **Hoofdstuk 2** geeft een overzicht van wetenschappelijk gepubliceerde onderzoeken over specifieke moleculen die gevonden zijn in EVs van bacteriën, parasieten en schimmels waarbij een effect op het afweersysteem is aangetoond.

In **hoofdstuk 3** beschrijven we een geoptimaliseerde methode om de EVs die gekweekte *Schistosoma*-parasieten uitscheiden te isoleren. Om iets te kunnen zeggen over een effect van EVs is het belangrijk deze te scheiden van andere losse moleculen die tegelijkertijd uitgescheiden worden door de parasiet, zoals groepen 'losse' eiwitten. Voor de scheiding zijn twee methodes vergeleken: scheiden op grootte en scheiden op dichtheid. Hierbij kwamen we erachter dat een afbraakproduct van de bloedconsumptie van de wormen even klein kan zijn als de EVs zelf, dus dat we deze niet konden scheiden op grond van grootte. Met behulp van een dichtheidsgradiënt konden de EVs wel gescheiden worden van de bloedproducten en andere losse eiwitten, omdat de EVs een andere dichtheid



**Figuur 3. Glycanen die gevonden zijn in volwassenen wormen en larven van *Schistosoma mansoni* en door welke receptor ze herkend kunnen worden.**

De larven en volwassenen verschillen in glycanen profiel. De structuren hier rechts weergegeven zijn slechts een klein deel van alle structuren die eerder gerapporteerd zijn. De glycaanstructuren (suikerbindingen) die herkend worden door de desbetreffende receptor staan binnen de gestreepte vakjes. DC-SIGN en MGL zijn receptoren die op cellen van het afweersysteem zitten die een belangrijke functie hebben in het herkennen van ziekteverwekkers. De dendritische cel (DC) is zo'n afweercel.

hadden. Hierbij zijn twee soorten dichtheidsgradiënten vergeleken, waarvan er één was die zowel EVs van volwassen wormen als de EVs van de larven goed kon scheiden van hun niet-EV-materiaal. Vervolgens hebben we de dichtheidsgradiënt verder geoptimaliseerd naar een kleiner volume om zo het gebruik van laboratoriumproducten en verwerkingstijd te verminderen. We laten zien dat dit uiteindelijk zorgt dat er minder EVs verloren gaan tijdens de isolatie. Hierdoor kunnen we uiteindelijk meer experimenten doen met hetzelfde kweekmateriaal van de parasieten. Omdat voor het behoud van de levenscyclus van de parasiet een gastheer essentieel is en hiervoor proefdieren noodzakelijk zijn, is het dus een grote winst dat we met onze geoptimaliseerde methode meer EVs overhouden om onderzoek mee te doen.

In **hoofdstuk 4** laten we zien dat de EVs van de volwassen *Schistosoma*-wormen glycanen bevatten. De glycanen van zowel de buiten- als binnenkant van deze worm EVs zijn in detail in kaart gebracht. Bij het vergelijken van een aantal glycaanstructuren op/in EVs van volwassen wormen en de larven zagen we dat er duidelijke verschillen waren tussen de twee levensstadia. De glycanen aan de buitenkant van de volwassen wormen EVs gaven de suggestie dat ze met een specifieke receptor, de MGL, zouden kunnen binden. Dit hebben we getest met behulp van cellen die genetisch gemodificeerd zijn en daardoor veel van deze MGL-receptor op hun celoppervlak hebben. We hebben de interactie van de volwassen wormen EVs met deze cellen vergeleken met cellen die een andere receptor, DC-SIGN, op hun celoppervlak hebben. De DC-SIGN-receptor bindt aan een andere glycaanstructuur dan de MGL-receptor. Deze vergelijking liet zien dat de EVs van de volwassen wormen inderdaad veel meer interactie hadden met de cellen die de MGL-receptor hadden dan de cellen met de DC-SIGN-receptor. Deze studie laat dus zien dat er glycanen op het oppervlak van de parasiet EVs zitten en dat deze glycanen een belangrijke rol kunnen spelen voor de interactie met gastheercellen.

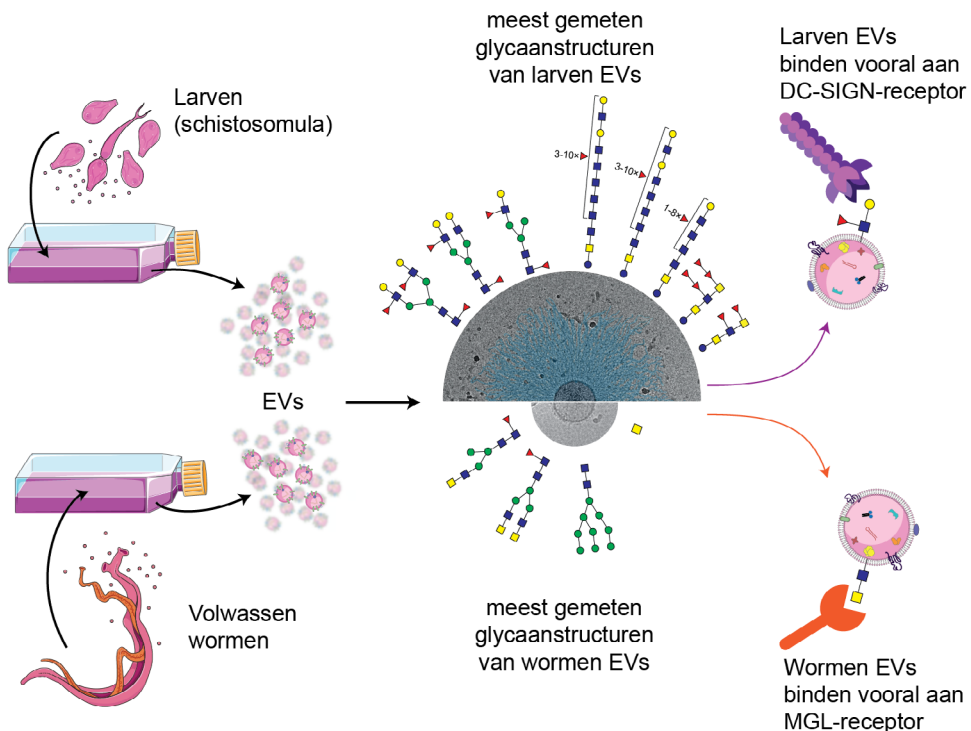
Vervolgens hebben we in **hoofdstuk 5** onderzocht wat voor effect de EVs van de volwassen wormen hebben op een specifieke afweercel, de B-lymfocyt. Deze cel zorgt voornamelijk voor de uiteindelijke productie van antistoffen tegen ziekteverwekkers, maar kan ook een rol spelen in het versterken of dempen van afweerreacties door signaalmoleculen uit te scheiden. Een van deze signaalmoleculen, genaamd cytokines, vertellen andere afweercellen om in de aanval te gaan of juist niet. Een voorbeeld van cytokines die aanzetten tot een sterkere afweerreactie zijn IL-6 en IL-12 en een cytokine die juist een afweerreactie kan dempen is IL-10. In dit hoofdstuk laten we zien dat wat de volwassen wormen uitscheiden in het kweekmedium (hun gehele secretemateriaal) zorgt voor het aanmaken en uitscheiden van IL-10 door B-lymfocyten van muizen. Geïsoleerde

EVs van de wormen konden ook een IL-10-reactie in deze cellen stimuleren. Daarnaast hebben we ook gekeken naar de effecten op B-lymfocyten die uit bloed van gezonde mensen zijn geïsoleerd. Hierbij zagen we zowel IL-10 als IL-6 productie door de cellen als we deze cellen samen kweekten met worm EVs. Deze studie laat zien dat de wormen zowel EVs als andere moleculen uitscheiden die beiden een effect hebben op B-lymfocyten. We laten zien dat er interactie is van de worm EVs met de B-lymfocyten en dat dit mogelijk een dempende rol op afweerreacties heeft.

**Hoofdstuk 6** beschrijft de studie waarin we de EVs van de larven van *Schistosoma mansoni* onderzoeken. Hierbij hebben we, net als voor de volwassen wormen in hoofdstuk 4, de glycanen aan de buiten- en binnenkant in kaart gebracht. Waar we voor de worm EVs alleen glycanen aan eiwitten hebben kunnen detecteren, vinden we voor de larven EVs ook veel glycanen aan lipiden. Verder hebben we ontdekt dat de EVs van de larven lange haarachtige structuren op hun oppervlak hebben. Dit hebben we met een elektronenmicroscoop in beeld kunnen brengen. Wat deze structuren precies zijn en wat hun rol is, dat moet nog verder worden onderzocht. De glycaanstructuren die we het meeste vonden op de EVs van de larven binden met name aan de DC-SIGN-receptor. Deze receptor wordt veel tot expressie gebracht op dendritische cellen (DCs). De DC is belangrijk voor de herkenning van ziekteverwekkers, het communiceren met andere afweercellen en het aanzetten of afremmen van verschillende afweerreacties. De DCs hebben we verkregen door monocyten (een ander type witte bloedcel) uit bloed van gezonde mensen te isoleren en in het laboratorium zodanig te veranderen dat ze op DCs lijken. We zagen dat deze monocyte-afkomstige DCs (ofwel moDCs) na interactie met EVs van larven meer signaalstoffen (de cytokines) gingen uitscheiden, zoals IL-6, IL-12 en IL-10. Na het blokkeren van de DC-SIGN receptor op de moDCs veranderde de afgifte van deze cytokines als reactie op de EVs, maar deze verandering (meer of minder) was anders tussen de verschillende bloeddonoren. Uit deze studie kunnen we concluderen dat de EVs die de *Schistosoma*-larven uitscheiden een versterkend effect hebben op afweerreacties, maar dat dit zowel activerend als dempend zou kunnen zijn. Dit is mogelijk een mechanisme waarmee de parasiet voorkomt dat er een hele sterke afweerreactie tot stand komt zodra de larve de huid binnendringt. De glycanen op de EVs en de interactie met de DC-SIGN-receptor spelen hoogstwaarschijnlijk een belangrijke rol hierbij.

Tot slot wordt in de discussie (**hoofdstuk 7**) een samenvatting gegeven van het onderzoek beschreven in dit proefschrift. Daarnaast worden in dit hoofdstuk ook suggesties gedaan voor toekomstig onderzoek naar *Schistosoma* EVs om uiteindelijk meer te weten te komen over hoe de parasieten met hun gastheer communiceren via EVs.

In conclusie: het onderzoek beschreven in dit proefschrift laat zien dat EVs uitgescheiden door volwassen wormen en larven van de parasiet *Schistosoma mansoni* glycanen bevatten. Deze glycanen spelen een rol in de interactie van de EVs met afweercellen van de gastheer. Het is aannemelijk dat deze EVs een belangrijke functie hebben tijdens een infectie van de (menselijke) gastheer, maar dit zal verder onderzocht moeten worden. Uiteindelijk kan de verkregen informatie ons helpen bij het ontwikkelen van nieuwe therapieën voor de preventie en behandeling van immuunziektes.



**Figuur 4. Visuele samenvatting van een selectie bevindingen die worden gepresenteerd in dit proefschrift.**

Geïsoleerde extracellulaire blaasjes (EVs) van *Schistosoma*-larven en volwassen wormen zijn gemeten op hun bevattende glycanenstructuren. De EVs van de verschillende levensstadia verschillen in glycanen en ook in uiterlijk (morfologie): de elektronenmicroscoop plaatjes in het midden laten zien dat larven EVs haarachtige structuren bevatten (handmatig blauw ingekleurd) die niet zichtbaar zijn voor de wormen EVs. Tot slot hebben we laten zien dat de glycanenstructuren bepalend zijn voor de interactie met receptoren. De EVs van de larven binden vooral aan de DC-SIGN-receptor, terwijl de volwassen wormen EVs vooral binden aan de MGL-receptor.

## Curriculum Vitae

Marije Erline Kuipers was born on May 23, 1986, in Haarlem, the Netherlands. In 2004, she graduated from pre-university education (VWO) at the Coornhert Lyceum, also in Haarlem. Although she had an interest in biology and chemistry, her drive to be creative led her to apply to the Royal Academy of Arts in The Hague, where she was accepted to study Fine Art. She obtained her bachelor's degree (BA) in 2008 with digital artwork revealing how we rely on our memories when interpreting new and unknown images. Three years after her graduation, Marije realized she had untapped potential and wanted to contribute more to society. In 2011, she eagerly began a bachelor's in Biomedical Sciences at the Leiden University Medical Center (LUMC).

In 2013, she did an internship at the Center for Proteomics and Metabolomics in collaboration with the Department of Rheumatology at the LUMC, supervised by Dr. M.A. Giera and Dr. A. Ioan. The project involved studying the polyunsaturated fatty acid adrenic acid as a possible pro-resolving lipid mediator. For her second bachelor's internship (2014), Marije studied EVs released by *Schistosoma mansoni* supervised by Dr. H.H. Smits from the Department of Parasitology at the LUMC in collaboration with Dr. E.N.M. Nolte-'t Hoen at the Department of Biochemistry and Cell Biology at the Faculty of Veterinary Medicine of Utrecht University (UU). Marije worked in both laboratories during this internship, and her enthusiasm for EVs and parasites has persisted since. After obtaining her bachelor's degree (BSc) *cum laude* at the LUMC and her honors academy certificate from Leiden University, she continued with a master's in Biomedical Sciences in September 2014, also at the LUMC.

For her first master's internship, Marije went to Cambridge (UK) to work in the lab of Prof. Dr. R.C. Hardie at the Department of Physiology, Development, and Neuroscience at the University of Cambridge. There, she generated *Drosophila* mutants to study the role of phosphatidylinositol in phototransduction. For her internship report, Marije received the award for Best Student Biomedical Sciences 2015. At the end of 2015, Marije began her second internship, continuing the project on *S. mansoni*-derived EVs, supervised by Dr. H.H. Smits at the Department of Parasitology at the LUMC. During this year, Marije further developed EV isolation protocols, optimized parasite cultures, tested the interaction of EVs with immune cells, and started exploring EV glycosylation. She secured funding to continue the Schistosome EV project for her PhD through the personal BW-plus/excellent student MSc-PhD program grant (LUMC, Board of Directors) and the Immunity, Infection, and Tolerance graduate program grant (NWO/LUMC). After graduating with her master's (MSc) *cum laude* at the end of 2016, Marije continued the EV project as a PhD student under the joint supervision of Dr. C.H. Hokke and Dr.

H.H. Smits at the LUMC and Dr. E.N.M. Nolte-‘t Hoen at the department of Biomolecular Health Sciences at UU, resulting in the research described in this thesis.

Since the summer of 2021, Marije is a post-doctoral researcher in the lab of Dr. E.N.M. Nolte-‘t Hoen at UU. As part of the MIMIC-KeY consortium (A KEY to the Understanding of Extracellular Vesicles and Rational Design of MIMICKING Nanoparticles), she studies specific cellular targeting by cancer EV subsets. Since 2024, she also participates in the FlaviVaccine project, which aims to develop a pan-flavivirus vaccine candidate.

## List of publications

### Publications related to this thesis

1. **Kuipers ME**, Nguyen DL, van Diepen A, Mes L, Bos E, Koning RI, Nolte-'t Hoen ENM, Smits HH\*, Hokke CH\*. Life stage-specific glycosylation of extracellular vesicles from *Schistosoma mansoni* schistosomula and adult worms drives differential interaction with C-type lectin receptors DC-SIGN and MGL. *Front Mol Biosci.* 2023 Mar 15;10:1125438.  
(\* shared senior authorship)
2. **Kuipers ME**, Koning RI, Bos E, Hokke CH, Smits HH, Nolte-'t Hoen ENM. Optimized Protocol for the Isolation of Extracellular Vesicles from the Parasitic Worm *Schistosoma mansoni* with Improved Purity, Concentration, and Yield. *J Immunol Res.* 2022 Apr 8;2022:5473763.
3. **Kuipers ME**, Nolte-'t Hoen ENM, van der Ham AJ, Ozir-Fazalalikhan A, Nguyen DL, de Korne CM, Koning RI, Tomes JJ, Hoffmann KF, Smits HH\*, Hokke CH\*. DC-SIGN mediated internalisation of glycosylated extracellular vesicles from *Schistosoma mansoni* increases activation of monocyte-derived dendritic cells. *J Extracell Vesicles.* 2020 Apr 30;9(1):1753420.  
(\* shared senior authorship)
4. **Kuipers ME**, Hokke CH, Smits HH, Nolte-'t Hoen ENM. Pathogen-Derived Extracellular Vesicle-Associated Molecules That Affect the Host Immune System: An Overview. *Front Microbiol.* 2018 Sep 12;9:2182.

## Publications outside this thesis

5. Wang F, Veth T, **Kuipers M**, Altelaar M, Stecker KE. Optimized Suspension Trapping Method for Phosphoproteomics Sample Preparation. *Anal Chem.* 2023 Jun 27;95(25):9471-9479.
6. White R, Sotillo J, Ancarola ME, Borup A, Boysen AT, Brindley PJ, Buzás EI, Cavallero S, Chaiyadet S, Chalmers IW, Cucher MA, Dagenais M, Davis CN, Devaney E, Duque-Correa MA, Eichenberger RM, Fontenla S, Gasan TA, Hokke CH, Kosanovic M, **Kuipers ME**, Laha T, Loukas A, Maizels RM, Marcilla A, Mazanec H, Morphew RM, Neophytou K, Nguyen LT, Nolte-'t Hoen E, Povelones M, Robinson MW, Rojas A, Schabussova I, Smits HH, Sungpradit S, Tritten L, Whitehead B, Zakeri A, Nejsum P, Buck AH, Hoffmann KF. Special considerations for studies of extracellular vesicles from parasitic helminths: A community-led roadmap to increase rigour and reproducibility. *J Extracell Vesicles.* 2023 Jan;12(1):e12298.
7. Gasan TA, **Kuipers ME**, Roberts GH, Padalino G, Forde-Thomas JE, Wilson S, Wawrzyniak J, Tukahebwa EM, Hoffmann KF, Chalmers IW. Schistosoma mansoni Larval Extracellular Vesicle protein 1 (SmLEV1) is an immunogenic antigen found in EVs released from pre-acetabular glands of invading cercariae. *PLoS Negl Trop Dis.* 2021 Nov 18;15(11):e0009981.
8. Brouwers H, Jónasdóttir HS, **Kuipers ME**, Kwekkeboom JC, Auger JL, Gonzalez-Torres M, López-Vicario C, Clària J, Freysdottir J, Hardardottir I, Garrido-Mesa J, Norling LV, Perretti M, Huizinga TWJ, Kloppenburg M, Toes REM, Binstadt B, Giera M, Ioan-Facsinay A. Anti-Inflammatory and Proresolving Effects of the Omega-6 Polyunsaturated Fatty Acid Adrenic Acid. *J Immunol.* 2020 Nov 15;205(10):2840-2849.
9. Bollepalli MK, **Kuipers ME**, Liu CH, Asteriti S, Hardie RC. Phototransduction in Drosophila Is Compromised by Gal4 Expression but not by InsP3 Receptor Knockdown or Mutation. *eNeuro.* 2017 Jun 26;4(3):ENEURO.0143-17.2017.

## Dankwoord/acknowledgements

Never a dull moment... Het is een enorme reis geweest, zowel wetenschappelijk als persoonlijk, en ik had het niet tot hier gered zonder de mensen om mij heen. Ik wil iedereen daarvoor enorm bedanken, met een aantal mensen in het bijzonder.

Allereerst, mijn promotor en copromotoren. Ik heb zo geboft met jullie wetenschappelijke kennis, enthousiasme en goede begeleiding! Ron, ik haalde altijd weer nieuwe ideeën uit onze discussies. Dankjewel voor de no-nonsense en directheid waarmee je communiceert en dat je mij hebt laten inzien dat niet per se ieder detail relevant is. Hermelijn, je hebt mij kalm en geduldig door al mijn (persoonlijke) worstelingen heen begeleid. Dankjewel voor het altijd bereikbaar zijn en voor het inzicht dat rust nemen net zo belangrijk is als hard werken. Esther, zoals jij je inzet voor anderen op het werk en daarbuiten is inspirerend. Ik leer altijd veel van onze gesprekken en je openheid over je eigen uitdagingen.

To my office mates: Bruno, thank you so much for all the nice talks we had over the years, whether it was about science or not. Jacqueline, ik ben dankbaar voor de steun die we aan elkaar hebben gehad op goede en slechte dagen. Simon, jammer dat we door alle lockdowns maar kort samen het kantoor deelden.

Een grote dank gaat uit naar de analisten Arifa, Linh, Alwin, Yvonne, Frank, Janneke en Jan. Jullie hebben mij alle fijne kneepjes van het labwerk geleerd en mij enorm geholpen met experimenten. Clarize, Angela, Nicole en Simone, dank jullie wel voor jullie bijdrage aan mijn projecten. Maria Y., Bart, Fabrizio, Meta and Blandine, thank you all for sharing your scientific knowledge with me during these years. Lynn en Joyce, bedankt dat jullie bij mij stage wilden lopen, mijn labwerk iets verlicht hebben en dat ik op jullie mocht oefenen met begeleiden. En dank aan het secretariaat, met name Corrie, Jantien, Suzanne en Gerdien, voor alle administratieve hulp.

A huge shout out THANKS to all my other PARA colleagues. There were so many in those seven years I was there, I'm sorry I cannot name you all here. I cherish all the good talks, laughs, and lab outings with all of you. You have broadened my horizon.

Dank aan iedereen waarmee ik heb samengewerkt: Paul, Peter en George voor hulp en advies bij de proteomics, Henk en Yavuz voor het RNA-werk, en Roman en Erik voor de elektronenmicroscopie. Thank you Karl and John for your input and work on the schistosomula EVs. Also thanks to all others along the way that let me be part of their projects.

My appreciation to everyone in Utrecht, you were my EV-to-go-to people. I always felt welcome when I showed up at the B&C department. To my current EV/IB colleagues, thank you for supporting me to the finish line. Xinyi and Bram,

thank you for sharing stories and struggles in the office.

Mijn paranimfen/vrienden, Lisa en Leonard, dank voor al jullie steun. Lisa, ik had mijn studie niet zonder jou willen doen. We vullen elkaar perfect aan. Je begrijpt al mijn problemen in de wetenschap en daarbuiten. Leonard, wat was het fijn jou bij de PARA te ontmoeten. Ik waardeer je eerlijkheid en kan altijd bij jou terecht, wat er ook is.

De volgende alinea geldt ook voor jullie.

To my friends: Elise, Saskia, Thierry, and Brooke. You are always there for me. You are my safety net and my mirrors. With you I share the moments that make life worth living. I love you.

Eddy, zonder jou had ik dit avontuur nooit kunnen starten. Ik ben dankbaar voor alle jaren die we samen waren, de kansen die je mij hebt gegeven en dat we los van elkaar opnieuw ons geluk hebben gevonden zonder elkaar te verliezen.

Mam, dank je wel voor alles, ik ben dankbaar dat jij en papa mij de vrijheid en het vertrouwen hebben gegeven mijn eigen (om)weg te gaan. Je onvoorwaardelijke liefde is van onschatbare waarde. Elmer, broer, dank voor je hulp met het bijspijken van mijn middelbare schoolkennis toen ik weer ging studeren. Robert en Marloes, dank voor de support naar mij en mijn familie. Jytte, Sido en Linna, dank dat ik jullie toffe tante mag zijn. Doris, Freddi, Wolf, Thomas, Silke, Stephan und Paul, Ich bin dankbar, dass Sie mich in Ihre Familie aufgenommen haben.

Lieve Martin, wij zijn vanaf 2013 al het 'Dream Team'. Eerst op het lab, daarna als vrienden, en nu als geliefden. Je weet hoe het is om in de wetenschap te werken, en toch geef je mij regelmatig het advies om minder lang door te werken. Ik zal vanaf nu (proberen) beter naar je luisteren ;) Dank je wel voor alles dat je voor mij doet en voor je inspirerende productiviteit en moed. Jij brengt altijd een glimlach op mijn gezicht.



Behind every late diagnosed woman  
is a little girl  
who knew this world  
was never made for her  
but could never explain why  
-Jessica Jocelyn, Girl (remastered), 2023

